UNIVERSITÀ DI PARMA

Università degli Studi di Parma

DIPARTIMENTO DI SCIENZE CHIMICHE, DELLA VITA E DELLA SOSTENIBILITÀ AMBIENTALE

Corso di Dottorato di Ricerca in Biologia Evoluzionistica ed Ecologia

XXXIV CICLO

in co-tutela con Univesità di Klaipėda (LT)

New experimental data to implement Ecological Network Analysis of Nitrogen and Phosphorus in two eutrophic lagoons

Candidata:
Monia Magri

Coordinatore:
Prof. Pierluigi Viaroli

Tutori:
Prof. Marco Bartoli
Prof. Antonio Bodini
Prof. Artūras Razinkovas-Baziukas

Anni Accademici 2018/2019 - 2020/2021

KLAIPĖDA UNIVERSITY

Monia MAGRI

NEW EXPERIMENTAL DATA TO IMPLEMENT ECOLOGICAL NETWORK ANALYSIS OF NITROGEN AND PHOSPHORUS IN TWO EUTROPHIC LAGOONS

DOCTORAL DISSERTATION

NATURAL SCIENCES,
ECOLOGY AND ENVIRONMENTAL SCIENCES (N 012)

Klaipėda, 2022

Doctoral dissertation was prepared in the period 2019–2022 at Klaipėda University and at University of Parma, based on Agreement No. JDS - 11 for co-tutored PhD degree thesis undersigned by the parties on 2019 March 14, based on the conferment a doctorate right which was granted for Klaipėda University, by the order of the Minister of Education, Science and Sport (Republic of Lithuania) No. V-160, signed on 22 February, 2019.

Academic advisors:

Prof. dr. Marco BARTOLI (University of Parma, Italy, Natural Sciences, Ecology and Environmental Sciences – N 012);

Prof. dr. Antonio BODINI (University of Parma, Italy, Natural Sciences, Ecology and Environmental Sciences – N 012);

Prof. dr. Artūras RAZINKOVAS-BAZIUKAS (Klaipėda University, Lithuania, Natural Sciences, Ecology and Environmental Sciences – N 012).

The doctoral dissertation is defended at the public meeting of the Board of University of Parma in Evolutionary Biology and Ecology and the Board of Klaipėda University in Ecology and Environmental Sciences.

Chairman:

Prof. dr. Pierluigi VIAROLI (University of Parma, Italy, Natural Sciences, Ecology and Environmental Sciences – N 012);

Members:

Prof. dr. Daniele NIZZOLI (University of Parma, Italy, Natural Sciences, Ecology and Environmental Sciences – N 012);

Prof. dr. Cristina MENTA (University of Parma, Italy, Natural Sciences, Zoology – N 014);

Prof. dr. Ali ERTÜRK (Istanbul University, Turkey, Natural Sciences, Ecology and Environmental Sciences – N 012);

Prof. dr. Sergej OLENIN (Klaipeda University, Lithuania, Natural Sciences, Ecology and Environmental Sciences – N 012).

The dissertation will be defended on May 26, 2022, 10:30 a.m. Address: Department of Chemistry, Life Sciences and Environmental Sustainability, Parco Area delle Scienze 11/A, I-43124 Parma, Italy, Bioscience building, Room 5. The doctoral dissertation was sent out on 26$^{\text{th}}$ April 2022. The doctoral dissertation is available for review at the Library of the Klaipėda University.

KLAIPĖDOS UNIVERSITETAS

Monia MAGRI

AZOTO IR FOSFORO VIRSMŲ VERTINIMAS DVIEJOSE EUTROFINĖSE LAGŪNOSE TAIKANT EKSPERIMENTINIUS DUOMENIS IR EKOLOGINIO TINKLO ANALIZĘ

DAKTARO DISERTACIJA

GAMTOS MOKSLAI,
EKOLOGIJA IR APLINKOTYRA (N 012)

Klaipėda, 2022

Mokslo daktaro disertacija rengta 2019–2022 metais Klaipėdos universitete ir Parmos universitete pagal Klaipėdos universitetui Lietuvos Respublikos švietimo ir mokslo ministro 2019 m. vasario 22 d. įsakymu Nr. V-160 suteiktą doktorantūros teisę bei dvišalio bendradarbiavimo sutartį Nr. JDS - 11 tarp Klaipėdos ir Parmos universitetų, pasirašytą 2019 m. kovo 14 d.

Vadovai:

Prof. dr. Marco BARTOLI (Parmos universitetas, Italija, gamtos mokslai, ekologija ir aplinkotyra – N 012);

Prof. dr. Antonio BODINI (Parmos universitetas, Italija, gamtos mokslai, ekologija ir aplinkotyra – N 012);

Prof. dr. Artūras RAZINKOVAS-BAZIUKAS (Klaipėdos universitetas, Lietuva, gamtos mokslai, ekologija ir aplinkotyra – N 012).

Daktaro disertacija ginama viešame Klaipėdos universiteto Ekologijos ir aplinkotyros mokslo krypties tarybos bei Parmos universiteto Evoliucinės biologijos ir ekologijos mokslo krypties tarybos posėdyje.

Pirmininkas:

Prof. dr. Pierluigi VIAROLI (Parmos universitetas, Italija, gamtos mokslai, ekologija ir aplinkotyra – N 012);

Nariai:

Prof. dr. Daniele NIZZOLI (Parmos universitetas, Italija, gamtos mokslai, ekologija ir aplinkotyra – N 012);

Prof. dr. Cristina MENTA (Parmos universitetas, Italija, gamtos mokslai, zoologija – N 014);

Prof. dr. Ali ERTÜRK (Stambulo universitetas, Turkija, gamtos mokslai, ekologija ir aplinkotyra – N 012);

Prof. dr. Sergej OLENIN (Klaipėdos universitetas, Lietuva, gamtos mokslai, ekologija ir aplinkotyra – N 012).

Daktaro disertacija bus ginama 2022 m. gegužės 26 d. 10:30 val. Adresas: Parco Area delle Scienze 11/A, I-43124 Parma, Italija, Biomokslų pastatas, 5 auditorija. Daktaro disertacija išsiųsta 2022 m. balandžio 26 d. Disertaciją galima peržiūrėti Klaipėdos universiteto bibliotekoje.

Contents

List of Figures

List of Tables

Abstract

The biogeochemical functioning of coastal lagoons is threatened by the interplay between eutrophication and climate change. In this study, the nitrogen and phosphorus dynamics were analysed in two eutrophic lagoons (the Goro Lagoon, North Adriatic Sea and the Curonian Lagoon, SE Baltic Sea) by combining experimental and modelling approaches aimed at investigating variations in their nutrient retention or removal capacity. The effects of climatic extremes, anoxia events, and the presence of different bioturbating organisms were tested with experimental activities carried out at the microscale. Detailed measurements on benthic processes have been implemented to construct networks depicting N and P circulation at the whole lagoon scale that were analysed via an integrative modelling tool. Results underline the high vulnerability of the analysed systems, mostly in summer and under heat waves and dry periods. Under these conditions the extent of internal recycling processes increase, largely exceeding external inputs and removal processes, with positive feedbacks on primary producers' activity. Vulnerable areas were identified, and they were characterized by low water circulation, muddy, organic-rich, and chemically reduced sediments, where the low oxygen concentration, and the accumulation of toxic compounds limit the presence of a biodiverse benthic community. In the perspective of nutrient stoichiometry, N and P cycling diverges in these vulnerable areas, especially during critical oxic-anoxic transitions, resulting in unbalanced regeneration and large P excess.

Keywords: Biogeochemistry, eutrophication, climate change, coastal filter, Ecological Network Analysis

Santrauka

Eutrofikacijos ir klimato kaitos sąveika kelia grėsmę pakrančių lagūnų biogeocheminiam funkcionavimui. Azoto ir fosforo dinamika buvo analizuojama dviejose eutrofinėse lagūnose: Sacco di Goro lagūnoje Šiaurės Adrijoje ir Kuršių mariose, pietrytinėje Baltijos jūros dalyje. Derinant eksperimentinius ir matematinio modeliavimo metodus buvo siekiama ištirti maistmedžiagių sulaikymo ir pašalinimo procesus. Klimato, ekstremalių įvykių, anoksijos ir skirtingų bioturbuojančių organizmų poveikis buvo tirtas in vitro eksperimentais. Siekiant sudaryti medžiagų tinklus, vaizduojančius N ir P apykaitą visoje lagūnoje, buvo atlikti išsamūs dugno nuosėdose vykstančių procesų matavimai, kurie buvo analizuojami naudojant apibendrinantį matematinio modeliavimo įrankį. Rezultatai išryškina didelį analizuojamų sistemų pažeidžiamumą, ypač vasarą ir esant itin aukštai temperatūrai bei sausringam laikotarpiui. Tokiomis sąlygomis didėja vidinė maistmedžiagių regeneracija, kuri gerokai viršija išorinės prietakos ir šalinimo procesus; tai, savo ruožtu, skatina fotosintetinančių organizmų vystymąsi. Buvo nustatytos jautrios zonos, kurioms būdinga lėta vandens apykaita, daug organinių medžiagų turinčios ir chemiškai redukuotos nuosėdos. Joms būdinga žema deguonies koncentracija ir nuodingų junginių kaupimasis riboja bentoso makrobestuburių bendrijos veiklą. Maistinių medžiagų stechiometrijos atžvilgiu, ypač kritinių oksinių-anoksinių virsmų metu, N ir P ciklai šiose zonose diverguoja, atsiranda nesubalansuota maistmedžiagių regeneracija ir didelis P perteklius.

Raktažodžiai: Biogeochemija, eutrofikacija, klimato kaita, priekrantės filtras, Ekologinio Tinklo Analizė

Chapter 1

Introduction

1.1 Relevance of the study

Coastal lagoons are highly dynamic ecosystems located at the interface between terrestrial and deep marine environments, which host a wide range of habitats and communities and provide ecosystems services of great environmental and economic values (Newton et al., 2014). Through a broad variety of biogeochemical processes, these coastal systems transform, retain, and remove terrigenous organic matter and nutrients from the watershed, before they reach the open sea, acting as "coastal filter" and reducing the anthropogenic impacts on deep marine environments (Asmala et al., 2017; Carstensen et al., 2020). The functioning of coastal lagoons is actually threatened by the interplay between eutrophication and climate change (Lloret et al., 2008). Eutrophication can be a naturally occurring process, but over the last decades, it has been dramatically increased by human activities, which through rocks mining, increased fertilizer production and combustion have more than doubled the amount of nitrogen (N) and phosphorous (P) to coastal areas (Nixon, 1995). The coastal fertilization impairs the balance between production and metabolism of organic matter and produces a cascade of indirect effects including the oxygen shortage and short-circuits of coupled adsorption-precipitation or oxidation-reduction processes, the accumulation of anaerobic end-products, the increase mortality of macrofauna, fish, and macrophytes meadows and a consequent loss of biodiversity and associated ecosystem services, the alteration of nutrient stoichiometric ratios (Cloern, 2001). In Europe, such risks have been contrasted with policies targeting nutrient loads reduction and based on the improvements of agricultural practices and wastewater treatment plants, whose effects may be delayed of decades due to the large accumulation of nutrient in soils and sediments (Bouraoui & Grizzetti, 2011; Viaroli et al., 2018). Coastal lagoons are extremely vulnerable to the effect of climate change (Anthony et al., 2009). Climate change, in particular in northern latitudes, will affect patterns of ice formation and melting, precipitation, and temperature regimes (Trenberth, 2005). Climatic extreme events are also expected to increase both in frequency and intensity, alternating high discharge, flash flood periods as well as phases with no precipitation and minimum river flow, resulting in sharp fluctuation of water supply (Lehner et al., 2006).

Climate change may have far reaching consequences on the nutrient dynamics and the ecological functioning of coastal lagoon ecosystems both by affecting the amount and composition of dissolved and particulate nutrient loads and by increasing the extent of internal recycling processes (Statham, 2012). These effects may further contrast the beneficial consequences of nutrient reduction policies at the watershed scale by stimulating primary production, system instability, and loss of biodiversity (Duarte, 2009).

The combined effects of eutrophication and climate change are therefore diverse, multifaceted, and difficult to forecasts. Experimental activities may get insight on biogeochemical processes which determine the nutrient retention capacity of these systems and on the main factors that increase or negatively affect their rates. However, they lack the possibility of the holistic evaluation of estuarine biogeochemical functioning and the assessment of the overall lagoon filter or source role. The evaluation of estuarine functioning could benefit from the application of integrative modelling tools (Wulff et al., 2012). One such modelling technique is the Ecological Network Analysis (ENA), a suite of algorithms developed to holistically analyse the ecosystem's structure and functioning (Kay et al., 1989; Ulanowicz, 1983, 2004). Network models map out the whole suite of material exchanges between biotic and abiotic components of a given ecosystem as they result from the transfer of energy and matter via feeding, biogeochemical and detrital pathways (Fath et al., 2007). The main limitation in the construction of phenomenological models derives from the lack of data or their poor quality (Scharler & Borrett, 2021). One possible solution resides in coupling an empirical sampling design based on high accuracy point measurements to the network construction.

The present study was carried out in two highly eutrophic coastal lagoons: the Goro Lagoon (Italy) and the Curonian Lagoon (Lithuania-Russia Federation). Both areas are characterized by intense algal blooms and recurring hypoxia/anoxia episodes in the warmer months, followed by occasional dystrophic events that affect the local economies (Bartoli et al., 2018; Viaroli et al., 2006). As most European lagoons, both the analysed systems are undergoing the direct and indirect impacts of climate change, including the increase in averages and maximum temperatures (Coppola & Giorgi, 2010; Dailidiene et al., 2011), and the shift in the timing of peak river discharge due to alteration in precipitation regime (Cozzi & Giani, 2011) or to the decrease in snow and ice cover (Cerkasova & Umgiesser, 2021; Idzelyte et al., 2019). Both systems have been extensively analysed in the last decades. These studies allowed a detailed assessment of the main hydrological features (Maicu et al., 2021; Marinov et al., 2006; Umgiesser et al., 2016; Zemlys et al., 2013), the nutrient loads (Castaldelli et al., 2013; Vybernaite-Lubiene et al., 2018), the seasonal dynamics of biogeochemical cycles (Bartoli, Castaldelli, Nizzoli & Viaroli, 2012; Bartoli et al., 2021; Nizzoli, Bartoli & Viaroli, 2006; Nizzoli et al., 2011; Petkuviene et al., 2016; Zilius, Bartoli, Daunys et al., 2012; Zilius et al., 2018), and of algal blooms (Bresciani et al., 2014; Naldi & Viaroli, 2002; Vaičiūtė et al., 2021; Viaroli et al., 2001) and of the main consequences of dystrophic events triggered by the decomposition of algal biomass (Azzoni et al., 2005; Giordani et al., 1997; Giordani et al., 1996; Vybernaite-Lubiene et al., 2017; Zilius et al., 2015; Zilius et al., 2014).

1.2 Aim and objectives of the study

The main aim of this study is to analyse the nitrogen (N) and phosphorous (P) dynamics in the Goro and the Curonian lagoons, by combining experimental and modelling approaches to understand how the filter functioning of these systems has been affected by the interplay between eutrophication and climate change.

The thesis consisted of several experimental activities carried out in both systems, each characterized by specific objectives and hypotheses. The collected information lay the foundation for the future implementation of updated ecological modelling (Goro Lagoon) or has been integrated with the bulk of available data on pelagic and sediment biological diversity and processes, to implement the Ecological Network Analysis of N and P at the whole lagoon scale (Curonian Lagoon).

The objectives of the specific experimental and modelling activities are:

1. To evaluate the effects of hydrological extremes (unusually heavy rainfall and high temperature) on the N filter action of the lagoon
2. To quantify the saturation threshold of the main N removal process and to identify the main factors regulating the equilibrium between removal and recycling
3. To evaluate the effects of bioturbating organisms on the sediment retention capacity of reactive P
4. To evaluate the reliability of data collected from experimental activities carried out via incubation of intact and reconstructed sediments
5. To evaluate the effects of transient anoxia events on the stoichiometry of benthic regeneration
6. To analyse the main factors impairing the biogeochemical cycling of N and P at the whole lagoon scale, and facilitating the blooms and persistence of cyanobacteria

1.3 Elements of novelty of the study

This study supplies new information on mechanisms that may represent new drivers or increase the extent of eutrophication phenomena in deeply impacted coastal lagoons. The Goro Lagoon was intensively studied in the 90's of the last century whereas limited experimental data are available for the last decade, after the intensification of clams farming. There was urgent need for this system to understand its biogeochemical response to climatic extremes, in order to forecast potential impact to the main economic activity. This study fills such knowledge gap as it provides new and original data from state of the art experimental work. New data reported in this thesis will allow to implement the ecological network constructed for N in the past (Christian et al., 1996) and compare past and present lagoon biogeochemical functioning. The effects of climatic extreme events on benthic nutrient dynamics have been analysed in environmental conditions

or simulated, and the nutrient retention capacity of the Goro Lagoon evaluated under different scenarios. The Curonian Lagoon has been intensively studied, particularly in the last decade, but for this system a holistic evaluation of the N and P biogeochemistry was missing. This study fills such gap as it couples detailed measurements of benthic processes carried out at the microscale with the application of a large-scale modelling tool, providing an integrated view of nutrient dynamics and quantitative evidences suggesting how differential N and P paths may be responsible of cyanobacteria blooms.

1.4 Scientific and practical significance of the results

Management actions implemented to contrast the eutrophication process in transitional waters acted mainly in two directions. Within watersheds they addressed the decrease in nutrient loads from agriculture and civil sources, often with limited success for N (Bouraoui & Grizzetti, 2011). Within lagoons they acted on water circulation, by digging canals or enlarging the lagoon-open sea mouths, or, more recently by covering highly reactive organic mud with sand deposits (García-Oliva et al., 2018; Svenja Oncken et al., 2022).

Results from this study underline the importance of sediment regeneration processes in lagoon ecosystems and demonstrate how they can be increased by the interplay between eutrophication and climate changes (Goro Lagoon) or between the above mentioned factors and the level of confinement of the lagoon, affecting hydrology, and water residence time (Curonian Lagoon). Different aspects have been deepened, including the biogeochemical consequences of unusually heavy rainfall or drought, transient anoxia events, and decreased benthic biodiversity. An integrated analysis of nutrient circulation at the lagoon scale has also been implemented and has proven to be a useful tool to identify key processes and vulnerable areas. These results help to shed light on the main mechanisms affecting the retention or removal capacity of the lagoon that can be of benefit for the implementation of effective management and restoration measurements, targeting the regulation of internal processes.

1.5 Scientific approval

The results of this study were presented at the following conferences:

1. XVI Meeting of Ph.D. Students And Young Researchers In Ecology And Sciences Of Aquatic Systems, Ostana, Italy, April 2019.
2. Scientific-practical conference “Sea and Coastal research–2019”, Klaipėda, Lithuania, May 2019.
3. XXIV Congress of the Italian Association of Oceanology and Limnology (A.I.O.L.), Bologna, Italy, June 2019.
4. XXIX Congress of the Italian Society of Ecology (S.It.E), Ferrara, Italy, September 2019.

5. XVII Meeting of Ph.D. Students And Young Researchers In Ecology And Sciences Of Aquatic Systems, Napoli, Italy (*Online event*), April 2021.

6. ECSA 58 - EMECS 13 Estuaries and coastal seas in the Anthropocene, Hull, UK (*Online event*), September 2021.

Publications on the dissertation topic:

1. **Magri, M.**, Benelli, S., Bonaglia, S., Zilius, M., Castaldelli, G., and Bartoli, M. (2020). The effects of hydrological extremes on denitrification, dissimilatory nitrate reduction to ammonium (DNRA) and mineralization in a coastal lagoon. *Science of The Total Environment*, 740, 140169.

2. Bartoli, M., Benelli, S., **Magri, M.**, Ribaudo, C., Moraes, P. C., and Castaldelli, G. (2020). Contrasting effects of bioturbation studied in intact and reconstructed estuarine sediments. *Water*, 12(11), 3125.

3. Bartoli, M., Benelli, S., Lauro, M., **Magri, M.**, Vybernaite-Lubiene, I., and Petkuviene, J. (2021). Variable oxygen levels lead to variable stoichiometry of benthic nutrient fluxes in a hypertrophic estuary. *Estuaries and Coasts*, 44(3), 689-703.

4. Vybernaite-Lubiene, I., Zilius, M., Bartoli, M., Petkuviene, J., Zemlys, P., **Magri, M.**, Giordani G. (2022). Biogeochemical budgets of nutrients and metabolism in the Curonian Lagoon (South East Baltic Sea): spatial and temporal variations. *Water*, 14,124.

5. **Magri, M.**, Benelli, S., Castaldelli, G., and Bartoli, M. (2022). The seasonal response of *in situ* denitrification and DNRA rates to increasing nitrate availability. *Estuarine, Coastal and Shelf Science*. (Simply modification asked after the first round of review)

6. **Magri, M.**, Bartoli, M., Bondavalli, C., Benelli, S., Zilius, M., Petkuviene, J., Vyberaite-Lubiene, I., Vaiciute, D., Griniene, E., Zemlys, P., Morkune, R., Daunys, D., Solovjova, S., Bucas, M., Baziukas-Razinkovas, A., and Bodini, A. (2022). Temporal and spatial differences of N and P biogeochemistry and estuarine functioning revealed via Ecological Network Analysis. (In Preparation)

7. Benelli, S., Janas, U., **Magri, M.**, and Bartoli, M. (2022). Burrowing macrofauna promotes reactive phosphorus recycling in an oxidised sedimentary environment. (In Preparation)

1.6 Volume and Structure of the thesis

This thesis consists of five main chapters. Besides the introduction (Chapter 1), the literature review (Chapter 2), and the general conclusions (Chapter 5), Chapter 3 and 4

focus on the results of the activities carried out in the Goro Lagoon and in the Curonian Lagoon, respectively. Chapter 6 provides a summary of the thesis in Lithuanian. The final chapter (Appendix) contains supplementary material that has not been included in the main sections. The dissertation volume is 211 pages, it contains 29 figures and 11 tables in the main sections and 7 tables in the appendix.

1.7 Abbreviation used in this study

Table 1.1: List of acronyms and symbols

C	Carbon
Chl-*a*	Chlorophyll *a*
CO_2	Carbon Dioxide
DIN	Dissolved Inorganic Nitrogen
DIP	Dissolved Inorganic Phosphorus
D_n	Coupled Nitrification-Denitrification
$DNRA_{tot}$	Total Dissimilatory Nitrate Reduction to Ammonium
DON	Dissolved Organic Nitrogen
DOP	Dissolved Organic Phosphorus
D_{tot}	Total Denitrification
D_w	Denitrification of Water Column Nitrate
ENA	Ecological Network Analysis
Fe^{3+}	Dissolved Oxidized Iron
Fe^{2+}	Dissolved Reduced Iron
Mn^{4+}	Dissolved Oxidized Manganese
Mn^{2+}	Dissolved Reduced Manganese
N	Nitrogen
N_2	Molecular Nitrogen
NCSP	Nitrogen network-Confined area-SPring season
NCSU	Nitrogen network-Confined area-SUmmer season
NH_4^+	Ammonium
NO_2^-	Nitrite
NO_3^-	Nitrate
NTSP	Nitrogen network-Transitional area-SPring season
NTSU	Nitrogen network-Confined area-SUmmer season
O_2	Dissolved Oxygen
P	Phosphorus
PO_4^{3-}	Phosphate
PCSP	Phosphorus network-Confined area-SPring season
PCSU	Phosphorus network-Confined area-SUmmer season
PIN	Particulate Inorganic Nitrogen
PIP	Particulate Inorganic Phosphorus
PON	Particulate Organic Nitrogen
POP	Particulate Organic Phosphorus
PTSP	Phosphorus network-Transitional area-SPring season
PTSU	Phosphorus network-Transitional area-SUmmer season
TDS	Total Dissolved Sulfides

Chapter 2

Literature Review

2.1 Nitrogen and phosphorus cycling in transitional ecosystems

Nitrogen (N) and phosphorus (P) are key elements for a variety of biological and chemical processes, both at the single organism level (N is a necessary element for protein synthesis, whereas P is needed for DNA and RNA) and at the ecosystem scale, since they are required to supply primary producers growth and are the limiting nutrients in most aquatic ecosystems (Herbert, 1999; Ryther & Dunstan, 1971; Sundby et al., 1992).

Nitrogen is present in the environment both in inorganic and organic forms as well as in different oxidation states. The redox reactions between the different compounds are mediated by a range of autotrophic and heterotrophic microorganisms and are strongly affected by environmental physico-chemical conditions and biological factors (e.g., temperature, salinity, pH, oxygen concentration, and macrofauna, microphytobenthos, and macrophytes activity) (Blackburn & Sorensen, 1988; Herbert, 1999). The complex nature of the N cycle is shown in Fig. 2.1. Via the N_2-fixation process, a group of specialized prokaryotes, ranging from strict anaerobes to obligate aerobes, transform the atmospheric molecular nitrogen (N_2), the major N reservoir, into ammonia (NH_3) (Vitousek et al., 2002). The process can be carried out both in the water column and into the sediments by a taxonomically diverse group of organisms that possess the enzyme nitrogenase. Since N atoms are linked by a very stable triple bond, the biological reduction of dinitrogen to ammonia is a high energy demanding process and the largest rates are reported in organic-rich environments, where suitable oxidizable organic carbon substrate is not a limiting factor (Postgate, 1987). The produced ammonium (NH_4^+) can be assimilated by primary producers and incorporated in organic compounds. These organic compounds are degraded by microorganisms or digested by animals and reconverted into inorganic compounds by the ammonification process (Blackburn & Henriksen, 1983). In shallow coastal environments, this process occurs both in the water column and into the sediment, but the latter plays a key role in receiving settled organic matter (Herbert, 1999). Benthic nutrient regeneration and metabolism are largely determined by the quantity and quality of the organic matter supplied to the sediments (Boynton et al., 1980). Depending on the

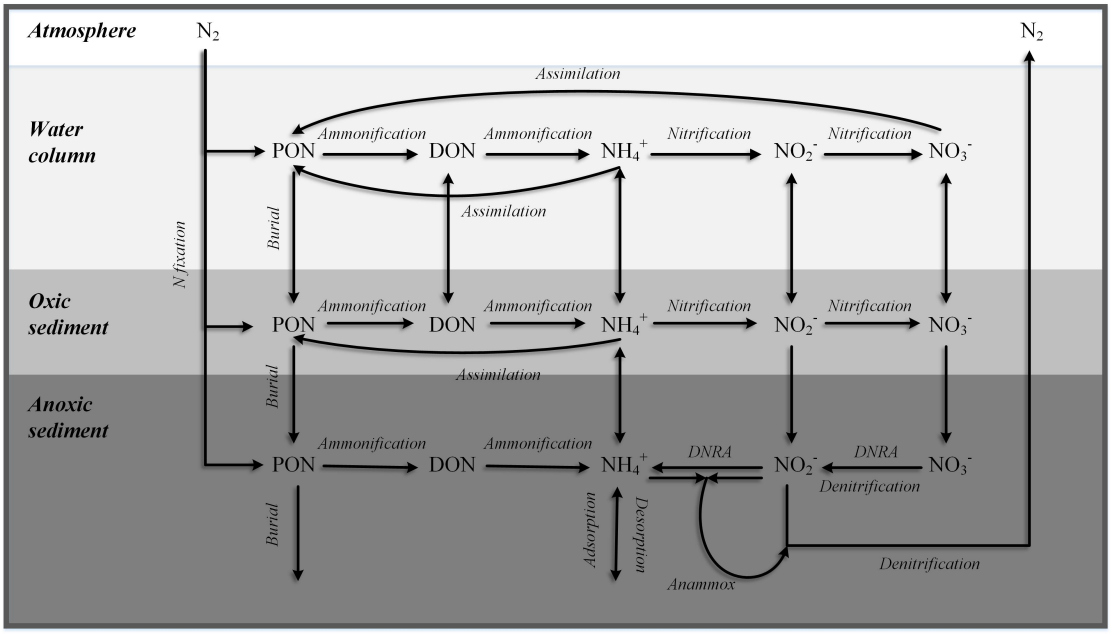

Figure 2.1: Schematic representation of N cycling in coastal sediments (modified from (Herbert, 1999))

complexity of the organic matter, ammonification can be a simple deamination reaction or a complex series of metabolic steps, leading to the production of intermediate organic products, constituting the dissolved organic nitrogen (DON) pool (e.g., ammino acids, short polypeptides, amines, urea), which will be subsequently degraded to NH_4^+ (Voss et al., 2012). Both the produced organic and inorganic N forms may diffuse from the water column to the sediment and vice versa, mainly driven by diffusion gradients. Ammonium can subsequently be permanently buried in deeper sediments, temporarily adsorbed to minerals, or can be oxidized, via nitrification process. Nitrification is carried out by a group of largely chemolithoautotrophic bacteria and is a strictly aerobic two-steps process leading to nitrite (NO_2^-) as intermediate and nitrate (NO_3^-) as the final product (Jickells & Weston, 2012). Nitrification within the sediments is restricted only to the first few millimetres of sediment, due to the reduced oxygen (O_2) penetration depth, which is affected mainly by sediment type, organic matter content, temperature, and presence of bioturbating organisms, microphytobenthos or rooted macrophytes (Ward, 2011). Bioturbating organisms through burrow ventilation transport O_2 downward to deep sediments, characterized by higher NH_4^+ concentration which together with excreted NH_4^+ provide high substrates availability for nitrification process (Moraes et al., 2018; Pelegrì & Blackburn, 1994). Primary producers via O_2 production and release can increase the thickness of the oxic layer and stimulate the nitrification process, but at the same time compete with nitrifiers for NH_4^+ availability (Bartoli et al., 2003; Risgaard-Petersen, 2003). Nitrate produced within the oxic sediment layer can be either assimilated or can diffuse to the overlying water or to the anoxic zone where it is reduced to N_2 by denitrifying bacteria

or to NH_4^+, by nitrate ammonifying bacteria. Denitrification is an anaerobic respiration process carried out by a group of heterotrophic bacteria using oxidized nitrogen as terminal electron acceptors (Cornwell et al., 1999). Denitrification is a key process since it decreases the amount of bioavailable N, reducing NO_3^- to inert gaseous end products (N_2O and N_2), which diffuse to the atmosphere. It mainly occurs in the anoxic sediment layer and involves NO_3^- diffusing into the sediment from the water column or produced into the oxic layer via nitrification. This process is regulated by a variety of factors including temperature, redox conditions, and NO_3^- and organic carbon availability (Seitzinger, 1988; Seitzinger et al., 2006). The presence of macrofauna can exert a profound influence on denitrification, both increasing the nitrification rates and the downward flux of NO_3^- to the anoxic zone via advective transport. Primary producers activity, conversely, can inhibit denitrifying bacteria due to the increased NO_3^- pathlength to reach the anoxic denitrification zone (Risgaard-Petersen, 2003). Denitrification is recognized as the dominant process of nitrate reduction in shallow coastal systems, but nitrate can be alternatively reduced by facultative anaerobic bacteria via dissimilatory nitrate reduction to ammonium (DNRA), fuelling the pool of bioavailable N (Burgin & Hamilton, 2007). The factors regulating the partitioning between these competitive processes are crucial and include salinity, temperature, and availability of NO_3^-, organic carbon and reductants as sulfides or dissolved iron (Fe^{2+}) (Burgin & Hamilton, 2007; Kessler, 2018; Nizzoli et al., 2010). DNRA has been demonstrated to out-compete denitrification in sulfidic and organic-rich sediments (An & Gardner, 2002). Despite denitrification dominates in removing fixed N in shallow systems, recent discoveries underlined the importance of anammox process, consisting in the anaerobic oxidation of ammonium coupled to nitrite reduction, that lead to N_2 production (Jickells & Weston, 2012). This process has been demonstrated to contribute from 0 to 20% of total N_2 production in estuarine and marsh sediments, but its importance increases in deeper, carbon (C) limited environment (Engström et al., 2005).

Phosphorous occurs in the aquatic environment mostly in particulate and to a lesser extent in dissolved forms, both inorganic and organic, whereas gaseous forms are negligible (Slomp, 2012). Compared to N, most of the processes constituting P cycling are chemical and not mediated by bacteria (Sundby et al., 1992). The P cycle is displayed in Fig. 2.2. The main source of P to aquatic systems is riverine runoff, where P is derived from weathering of sedimentary deposits and from leaching and decomposition of terrestrial organic materials. Most of P is delivered in particulate compounds, both inorganics (PIP, particulate inorganic phosphorus) and organics (POP, particulate organic phosphorus) (Seitzinger et al., 2005). Inorganic particulate forms are commonly associated with ions as Mg^{2+}, Ca^{2+}, Fe^{3+}, and Mn^{4+}. Among the most common and reactive forms, PIP includes orthophosphate easily adsorbed onto mineral particles (exchangeable P), P bounded to oxidized Fe and Mn ions (Fe/Mn-bound P), and different P bounded to Ca compounds (both *in situ* authigenically formed P, authigenic Ca-bound P, biogenic Ca-bound P derived from fish bones, and detrital Ca-bund P, derived from mechanical weathering) (Ruttenberg, 2004; Ruttenberg, 1992; Voss et al., 2011). Organic compounds represent the most reactive P forms and via bacteria mineralization processes,

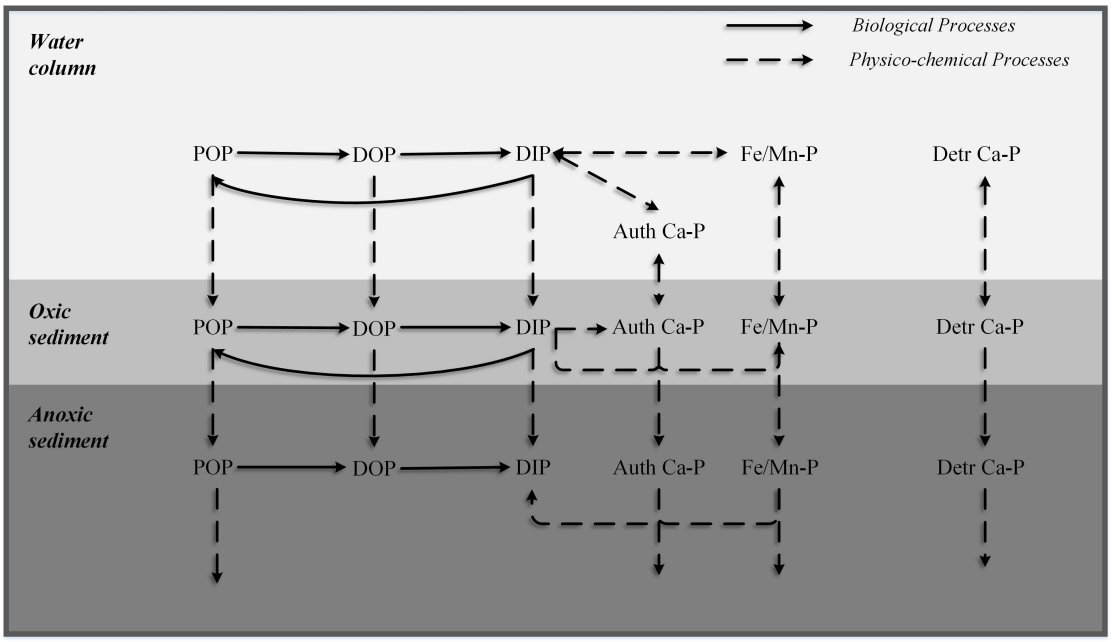

Figure 2.2: Schematic representation of P cycling in coastal sediments (modified from (Reddy et al., 2005))

both within the water column and into the sediments, are rapidly converted to intermediate dissolved organic phosphorus (DOP) compounds and finally to dissolved inorganic phosphorus (DIP), exclusively present as phosphate (PO_4^{3-}), available for primary producers assimilation (Sundby et al., 1992). Particulate inorganic P compounds are scarcely affected by microbially mediated processes, and their main transformations are related to geochemical diagenetic processes of adsorption/desorption or coprecipitation within different minerals, driven by environmental variables (e.g., oxygen, salinity, pH, and temperature) (Colman & Holland, 2000; Ruttenberg, 2004). In the coastal environment, the salinity increase determines the release of DIP from dissolved or particulate compounds, because of competition of anions in seawater with PO_4^{3-} for sorption sites (Van Der Zee et al., 2002). pH variations, mainly associated with anaerobic metabolism, may result in the release of reactive P from authigenic carbonate minerals (Ruttenberg, 2004). Redox transitions in bottom waters are of relevance mostly for Fe and Mn-bound P compounds because under oxygen shortage ferric and manganic oxide/hydroxide can be reduced and determine the release of reactive P (Canfield, 1994; Slomp et al., 1997). Besides this, an important control of sedimentary P cycling is provided by the rate of sulfate reduction, since the produced sulfides may reductively dissolve Fe oxides and release associated P (Roden & Edmonds, 1997). The sediment P cycle may be affected also by physical factors, as sediment resuspension, which can promote the rapid DIP efflux or conversely favour the sediment oxygenation stimulating sorption mechanisms (Sondergaard et al., 1992). In the same way, the enhanced oxygen penetration depth through macrofaunal or primary producers activities increase the volume of oxic sediment where P adsorption

and precipitation mechanisms take place (Karlson et al., 2007; Lewandowski & Hupfer, 2005).

2.2 Eutrophication: causes and consequences

Over the past century, world population, food production, and energy consumption have increased approximately by 2.5, 3, and 5 folds compared to the pre-industrial level (FAOSTAT, 2005). These changes resulted in a massive mobilization of bioavailable N and P, which greatly modified nutrients cycling worldwide (Nixon, 1995). The increase in fixed N was largely attributed to the production of fertilizer, fossil fuel emissions, and planting of N_2-fixing leguminous crops (Galloway et al., 2004; Galloway et al., 2008). In the same way, mining of rocks phosphate and its consequent use, mostly as fertilizer, increased the amount of bioavailable P as compared to the natural background derived from rocks weathering (Filippelli, 2008). It has been estimated that approximately $60\,\mathrm{Tg\,N\,y^{-1}}$ (Glibert, 2017) and $5\,\mathrm{Tg\,P\,y^{-1}}$ (Filippelli, 2008) mobilized in the watershed, reach the surface waters, and are transported to coastal ecosystems. At the global level, N is delivered equally as DIN and PN, whereas DON represents a minor portion (Seitzinger et al., 2005). In areas heavily impacted by anthropogenic activities, N is mainly exported as DIN via diffuse (non-point) sources, sustained by the approximately equal contributions of inorganic fertilizer, animal manure, and agricultural N_2 fixation (Harrison et al., 2005). Particulate forms dominate the export of P, but a lower PP:DIP ratio characterizes areas with more intense human activity (Seitzinger et al., 2005). Point-source derived P, mainly wastewater treatment plants, is the dominant source of DIP at the global scale, with diffuse agricultural sources accounting for less than 5% of total export (Harrison et al., 2005).

These increased nutrient load to coastal areas stimulates the autochthonous production of organic material by primary producers, resulting in a succession of direct and indirect system-level responses (Cloern, 2001; Nixon, 1995, 2009). The increase in phytoplankton growth determines an imbalance between algal production and consumption, followed by the enhancement of sedimentation of labile organic matter and the stimulation of microbial decomposition and oxygen consumption (Cloern, 2001). The latter determines the reduction of the depth of the oxic-anoxic interface within sediments and may result in a shift from aerobic to anaerobic metabolism in the upper sediment layer adjacent to bottom water and a dramatic change in dominant processes, affecting the sediment nutrient retention capacity (Jorgensen, 1996; Rabalais et al., 2009). As sediments become more chemically reduced, the phosphate bound to iron and manganese oxides can be released, determining a positive feedback that enhances the supply of P to the water column (Paerl et al., 2011). The reduction of the oxic layer thickness stimulates the denitrification by shortening the physical distance that NO_3^- must go through to reach the anoxic layer (Hietanen & Lukkari, 2007), but at the same time decreases the occurrence of nitrification and coupled nitrification-denitrification (Conley et al., 2007; Kemp et al., 2005; Roberts et al., 2012). If hypoxic or anoxic conditions persist, NO_3^- and oxidized Fe and Mn pools can be exhausted by microbes or chemically by the sulfides

produced by sulfate-reducing bacteria, leading to Fe^{2+} and Mn^{2+} precipitation and total dissolved sulfides (TDS) accumulation in the porewater (Thamdrup, 2000). High TDS concentrations further inhibit nitrification and denitrification processes and may favor DNRA (Burgin & Hamilton, 2007).

Direct and indirect eutrophication effects influence also living organisms. In the community of primary producers, fast-growing species, best adapted to high-nutrient conditions are selected at the expense of slower-growing vascular plants (Viaroli et al., 2008). As phytoplankton biomass increases, water transparency decreases, reducing the habitat for benthic autotrophic organisms (Jorgensen, 1996). The composition of primary producers' community is also affected the alteration of the Redfield reference ratios of nutrient stoichiometry (N:Si = 16:15, and N:P = 16:1 (Redfield, 1958)). The decrease in Si to N (or P) ratio, due to the human-induced selectively enhancement of N and P loads and the decrease in Si ones, prevents diatoms growth, favouring the dominance of alternative groups as flagellates/dinoflagellates (Jiang et al., 2010; Radach et al., 1990). The decrease in N:P ratio offers a competitive advantage to N-fixing cyanobacteria, due to their ability to use atmospheric and relatively inert molecular N_2 to satisfy their N requirements (Paerl et al., 2011). These shifts in primary producers community, enhance the rates of primary production and organic matter deposition. Under such circumstances, oxygen depletion can propagate and affect the heterotrophic organisms along with the food web (Diaz & Rosenberg, 1995). The increase in organic matter deposition and oxygen consumption affects the population of benthic macrofauna, determining a shift towards more tolerant and less biodiverse communities (Jorgensen, 1996). The disappearance of rooted macrophytes decreases the habitat and food availability (Egertson et al., 2004). The prevalence of large filamentous colonies and toxic forms of cyanobacteria, inhibits grazing by zooplankton and macrofauna (Ger et al., 2016). Changes in invertebrate communities may in turn indirectly affect higher trophic levels, reducing for example the abundance of prey for fishes or waterbirds (Ansell et al., 1998).

Since the beginning of the 1990s, the European Union has implemented different directives to control and reduce the nutrient load, targeting improvements of agricultural practices and wastewater treatment plants (e.g. Nitrate Directive, 91/676/EEC, Urban Waste Water Treatment Directive, 91/271/EEC, Water Framework Directive, 2000/60/EEC). These management policies have been more effective in regulating point nutrient sources as compared to diffuse ones and resulted in a general reduction of P loads (up to 30%), also due to the increased use of P-free detergents (Viaroli et al., 2018; Vybernaite-Lubiene et al., 2018). On the contrary, the total N exported to the sea has either stayed the same or even increased (Bouraoui & Grizzetti, 2011; Romero et al., 2013). This was attributed to the so-called *nitrogen heredity*, determined by the large N retention in groundwater and unsaturated zone and to the slow release to surface water (Ascott et al., 2017; Bartoli, Racchetti et al., 2012; Hansen et al., 2017; Van Meter et al., 2016). At the same time, in estuaries and lagoons characterized by cyanobacterial blooms, the significant reductions of external P loads should have decreased their intensity, but this did not happen. Conversely, they are persistent and tend to extend for longer periods, from the summer to the late autumn, raising new questions on an understudied

phosphorus heredity (Paerl et al., 2020; Randall et al., 2019; Vahtera et al., 2007; Vaičiūtė et al., 2021). The response of the coastal ecosystem to nutrient abatement may not be directly reversible and delayed by decades due to the accumulation of internal nutrient stocks, to slow changes that occurred at the community level, and to the combinations of multiple pressure, including climate changes (Duarte, 2009; Duarte et al., 2009).

2.3 The effect of climatic extremes on the functioning of transitional ecosystems

Eutrophication will continue to affect estuaries and transitional ecosystems, but superimposed to and interplaying with its impacts are those associated with climate changes, and the resulting interactions may be complex and non-linear (Lloret et al., 2008; Statham, 2012). Understanding the net effect of such changes in these systems is particularly important, as they play a crucial role in the retention and transformations of nutrients (Carstensen et al., 2020). At the global scale they remove up to 25% of the total reactive N and 20% of total reactive P delivered from the watersheds, mainly via denitrification and sediment burial (Asmala et al., 2017; Sharples et al., 2017). Climate changes, in particular in northern latitudes, are expected to affect patterns of ice formation and melting, precipitation, and temperature regimes (Lehner et al., 2006; Trenberth, 2005; Zhang et al., 2019). The effects of climatic extreme events, which are expected to increase both in frequency and intensity (IPCC, 2021), might be particularly significant, since they determine sharp fluctuation of hydrological conditions, alternating high discharge, flash flood periods as well as phases with no precipitation and minimum river flow (Lehner et al., 2006).

Extreme rainfall events are predicted to increase the amount and affect the composition and the timing of nutrients export from the watershed to transitional systems (Chen et al., 2018; Gao et al., 2014; Howarth et al., 2006). Floods associated with intense precipitation generate a large runoff and enhance N losses from intensively cultivated areas (Zheng et al., 2020). These losses have been demonstrated to largely increase after prolonged dry periods, which determine the expansion of the unsaturated soil volume and stimulate coupled processes of ammonification and nitrification (Ascott et al., 2017; Gómez et al., 2012; Klaus et al., 2020). Different studies demonstrated how few precipitation events can account for most of the particulate and dissolved P load delivered during the year (Carpenter et al., 1998; Carpenter et al., 2018). These events disproportionally mobilize P compared to N and contribute to the reduction in N:P loads (Correll et al., 1999; P. T. Kelly et al., 2019). The large pulses of nutrients may stimulate some processes, such as N removal through denitrification, whose rates increase with increasing NO_3^- in the water column, until saturating concentrations (Dong et al., 2000; Ogilvie et al., 1997). Following these events, however, the high river discharge leads to the decrease in water residence time, shortening the processing time during which nutrients can be repeatedly cycled through uptake by primary producers, sedimentation of organic matter, and mineralization or removal through burial or coupled nitrification-denitrification (Dettmann, 2001; Nixon et al., 1996; Seitzinger et al., 2006). High runoff increases water column

turbidity and reduces light penetration, affecting benthic primary producers' activity (Pratt et al., 2014) and their ability to regulate nutrient fluxes at the water-sediment interface (Risgaard-Petersen et al., 1994; Sundbäck et al., 2000). Enhanced transport of fluvial material may also alter significantly the structure and the functioning of the macrobenthic community, decreasing their biodiversity and the total biomass and favoring the establishment of opportunistic species (Cardoso et al., 2008; Ellis et al., 2002). The loss of specific functional groups strongly influences the ecosystem biogeochemistry because macrofauna, through bioturbation, feeding activity, excretion, and biodeposition of labile organic matter, significantly alter N and P benthic dynamics (Laverock et al., 2011; Stief, 2013).

At the opposite situation, low freshwater discharge after prolonged drought, seasonally decreases the amount of nutrients delivered to coastal areas and may decline the relative importance of external inputs compared to internal recycling (Feyen & Dankers, 2009; Howarth et al., 2000). Higher temperatures combined with low freshwater inflow, which characterize low rainfall periods, lead to the increase in water residence time and contribute to water stratification, which in turn increases the extent of hypoxia or anoxia (Du et al., 2018; Hallett et al., 2018; Statham, 2012). The decrease in O_2 concentration, as reported in the previous section, deeply affects biogeochemical processes and causes high mortality of macrofauna, fish, and seagrass/macrophyte meadows (Diaz & Rosenberg, 1995, 2008). Long periods of low river discharge and the increase in residence time result in salinity and sulfate reduction increase, both determining the enhancement of P release mechanisms and favoring DNRA over denitrification (An & Gardner, 2002; Gardner et al., 2006; Giblin et al., 2010; Rysgaard et al., 1999). In large, shallow estuaries that have retained and accumulated nutrients for long periods, such cascade events may mobilize from sediments large amounts of N and P, amplifying the relevance of internal nutrient recycling as compared to external sources (Conley et al., 2007). Such internal recycling has the potential to limit the beneficial effects of nutrient reduction policies at the watershed scale by stimulating primary production, system instability, and loss of biodiversity (Paerl et al., 2016).

2.4 The need for a holistic approach

Experimental activities aimed at analysing N and P dynamics usually focused on single processes and lack the possibility of estuarine biogeochemistry holistic assessments, due to the complexity of mechanisms and their multiple interactions and feedbacks. The evaluation of whole estuarine biogeochemical functioning, the estuarine filter or source role, and the metabolic shifts along environmental gradients and pressures can be only tackled with the application of integrative modelling tools (Christian et al., 2012; Wulff et al., 2012).

The Ecological Network Analysis (ENA) is a methodology that was developed to holistically analyse the ecosystem's structure and functioning (Fath & Patten, 1999; Fath et al., 2007; Finn, 1976; Hannon, 1973; Kay et al., 1989; Szyrmer & Ulanowicz, 1987; Ulanowicz, 2004). Network flow models are essentially steady-state ecological food webs,

which also includes non-feeding pathways, and represent a time-averaged snapshot of the system (Fath et al., 2007). The network models are constituted by nodes, which represent species, functional groups, or non-living resource pools and direct edges which indicate the transfer of thermodynamically conserved energy or matter between nodes via feeding, biogeochemical and detrital pathways (Ulanowicz, 2004). Through the application of a suite of different algorithms, ENA can be used to get insights on whole system structure, activity, and development, on the structure and magnitude of cycling, on the efficiency of energy transfer through trophic levels, and on the role of indirect interactions (Baird et al., 1995; Borrett et al., 2018; Ulanowicz, 1983). Despite most networks have been constructed to analyse food web interaction using energy or C as currency (Ulanowicz, 2012), several studies examined the behaviour of N in different freshwater and coastal ecosystems and at different spatial scales (Baird et al., 1995; Christian et al., 1996; Finn & Leschine, 1980; Hines et al., 2012; Magri et al., 2018; Small et al., 2014). There are fundamental differences between networks constructed to analyse nutrient and recycling dynamics and those based on food webs (Borrett et al., 2016). Most food-web networks are constituted by tens of compartments. Energy source (mainly solar light) is outside the network and is imported, whereas respiration causes the loss of usable energy (Borrett et al., 2006). Cycling is between living and dead organic forms, which are usually pooled in a single compartment. Biogeochemical networks are usually more aggregated. Cycling processes are minimally dissipative, they involve both particulate and dissolved organic and inorganic compounds, which are usually separated in different compartments, and the main focus is on bacterial processes (Christian et al., 2012). The nutrient required to sustain primary producers and biota are partly generated via internal mineralization processes and partly provided from the outside as external inputs. In this context nutrient models can be considered as relatively closed systems in which the external inputs and the recycling rates, impose limits on the standing stock of biomass and primary production (Baird et al., 2008).

Biogeochemical networks usually address some aspects of eutrophication and rely on a set of analyses that provide insights into how N flows through the systems and the direct and indirect influences of compartments on each other (Christian et al., 2012). For example, in (Christian & Thomas, 2003) the ENA was applied to understand how imported NO_3^- was transformed within the system, and which were the dominant processes in different seasons. They revealed the probable delay in ecosystem response to N loading reduction due to the high degree of internal recycling. (Christian et al., 1996; Christian et al., 2010) compared a series of simple networks for several coastal ecosystems to analyse the influence of primary producers growth forms, trophic status, and residence time on N cycling dynamics. The rapid turnover of phytoplankton and the longer residence time appeared to promote recycling and affect its pattern, resulting in an overall loss of ecosystem health in eutrophic systems compared to mesotrophic ones. Different studies underlined the central role of sediments as drivers of internal dynamics, alternatively sequestering and releasing reactive N (Small et al., 2014; Thomas & Christian, 2001; Whipple et al., 2014). A number of indicators, that respond to the level of growth, development, and resilience of the system, have been used to define the whole

system's health. Eutrophic systems for example were defined as systems characterized by an increase in the total flow or size, and a concurrent decrease in organization level (Christian et al., 2010). Comparatively, less attention has been given to the analysis of other elements such as P (Kaufman & Borrett, 2010) and even fewer studies simultaneously analysed N and P dynamics, usually compared to C (Baird et al., 1995; Baird et al., 2008, 2011; Scharler et al., 2015; Ulanowicz & Baird, 1999). These studies evidenced large differences in nutrients behaviour, with N and P displaying higher trophic transfer efficiency and higher recycling rates compared to C, and most of the recycling activities carried out through low trophic levels exchanges. In most of these studies, P exhibited the largest recycling over longer pathways than the other two elements and was characterized by the longer residence time (Baird et al., 2008; Scharler et al., 2015).

A key challenge for the success of network science lies in the quality of the data used for the models construction (Scharler & Borrett, 2021). The availability of suitable data influences how realistically the network model represents the system, for example affecting the number of compartments, and has consequences on the reliability of the outcomes. These networks are often constructed using a phenomenological approach that contrasts the more mechanistic approach based on the application of differential equations (Tennenbaum & Ulanowicz, 2006). Ecosystem networks constructed from empirical data require a large amount of information, which increases according to the extent of the model resolution. The data used for model construction often derive from a wide variety of sources spanning decades of experimental activities and include data with systematic differences in methodology, availability of information, and statistical variation (Thomas & Christian, 2001). Methodology rapidly evolves and earlier studies may not have involved techniques as accurate as later studies. Information on statistical error is not always available, therefore, these data are of varying and unknown degrees of reliability. Important data sources are those obtained by continuous data recorders, long-term government datasets (e.g., fisheries records), or open-access databases, whose reliability is not always guaranteed. When specific data from the analysed ecosystem are not available, they are implemented with literature data, that may not be representative. Metabolic rates for example are characterized by wide variations along with environmental parameters.

Historically, the network construction has been limited and guided by data availability. The first available ecological networks, like the Silver Springs (Odum, 1957) or Cone Springs (Tilly, 1968), were therefore rather small with a total of five highly aggregated nodes, including multiple species and resources grouped together. Recently, more detailed models have been constructed for systems that have been extensively studied, like the Chesapeake Bay (Baird et al., 1995; Ulanowicz & Baird, 1999) or the Neuse River Estuary (Borrett et al., 2006; Christian & Thomas, 2003; Schramski et al., 2006; Whipple et al., 2007). However, continuous datasets in time and over large spatial scale are rare for ecosystems. This should be especially important for ecosystems characterized by high areal and temporal heterogeneity, determined for example by wide hydrology variations, such as estuarine areas. An empirical sampling design that connects directly to network construction is a preferable approach to generating data, even if it is not always possible

or is not possible for all necessary parameters.

Chapter 3

Goro Lagoon

The Goro Lagoon is a shallow (average depth 1.5 m) and microtidal small lagoon (27 km^2) located in the southern part of the Po River Delta (Fig. 3.1, NE Italy). The lagoon receives freshwater inputs from two of the southernmost branches of the Po River, the Po di Volano in the western area and Po di Goro along the eastern boundary, and from three minor artificial channels (Collettore Giralda, Canal Bianco, Canale Bonello) (Viaroli et al., 2006). The freshwater discharge follows the seasonal pattern expected for temperate latitudes, with winter and spring peaks and summer minima (Viaroli et al., 2018). The lagoon is partially separated from the Adriatic Sea by two spits, the Scanno di Goro and the Scanno di Volano, whereas water exchanges with the sea occur through a 3 km wide mouth. The mouth is very shallow in the central area ($\sim$ 1 m depth) that constitutes the submerged part of the previous spit, whereas at its extremes two deeper channels are steadily dredged and maintained at about 5 m depth (Maicu et al., 2021). The lagoon is characterized by an estuarine water circulation, where freshwater discharge represents the main driving force and together with tides and winds determine a surface outflow and a bottom inflow of water, the latter mainly through the deep channels, and an average net transport of water out of the lagoon (annual average 37.8 $m^3 s^{-1}$, (Maicu et al., 2021)). The water renewal time ranges from few days to more than a week, with minimum values displayed in the marginal areas of the lagoon due to the Po di Volano and Po di Goro inlets, and close to the mouth, and maximum values in the northern corner and between the two sand spits of the Scanno di Goro. The salinity is highly variable due to fluctuations in freshwater and marine inflows (between $<$10 in the western corner and 25), with the widest daily variations in the area near the sea mouth, which can be up to 8 (Maicu et al., 2021). The hydrology affects the variable composition of sediments, a mosaic of sandy, silt and clayish zones. Sandy areas prevails close to the sea mouth, whereas muddy areas are more common in stagnant zones, as the eastern corner.

The Goro Lagoon is generally divided into three areas based on sedimentary and hydrological characteristics (Marinov et al., 2006). The western portion is located at the mouth of the Po di Volano and is characterized by the highest nutrients concentration and the lowest salinity; the sediments are muddy-clayish, with a high organic matter content and are highly bioturbated by surface and deep burrowers, such as *Corophium*

Figure 3.1: Map of the Goro Lagoon and location of the four sampling sites. The arrows indicate input from the Po di Volano and Po di Goro (solid arrrows) and from the minor tributaries (dashed arrows).

insidiosum and *Alitta succinea* (Bartoli, Castaldelli, Nizzoli & Viaroli, 2012; Politi et al., 2019). The eastern part, called Valle di Gorino, represents about half of the total surface, is very shallow (average depth 0.6 m), is characterized by muddy-sandy sediments and it receives freshwater inputs from different gates connecting the lagoon with the Po di Goro. This area is separated from the sea by the Scanno di Goro and is more shelter and characterized by slow water exchange and generally by higher temperature compared to the rest of the lagoon. The central portion is affected by tidal exchanges that determine more intense water circulation and prevent the organic matter accumulation.

The lagoon is intensively exploited for clam farming of the species *Ruditapes philippinarum* at present covering more than half of the bottom surface with densities higher than 1000 ind. m^{-2} (Bartoli et al., 2016). Clams were introduced in 1986 and farming become the main economic activity of this area, with an estimated crop of abut 15 000 t y^{-1}, which provide every year between 50 and 100 million euros to the local population (Bartoli et al., 2016; Viaroli et al., 2006). Since the mid-1980s the lagoon is exposed to blooms of nitrophilous macroalgae (*Ulva* sp., *Gracilaria* sp. and *Cladophora* sp.), which accumulated mainly in the sheltered Valle di Gorino, with estimated standing stocks that could reach 70 000 t as wet weight. The heavy loads of N generated in the Po River basin and delivered to the lagoon (1000-2000 t y^{-1}) have been considered the main cause of this phenomenon. Nitrate represents the dominant N forms and in the Po di Volano plume area it may reach concentration up to 200 µM. Besides external loads, different studies stressed the impact of high clam densities on internal nutrients recycling. Clams filtrate large water volumes and suspended particulate matter and deliver large amounts of labile organic matter on the sediment surfaces, as faeces and pseudofaeces. These labile substrata fuels microbial activity, increasing benthic O_2 uptake and nutrient recycling, and together with direct clams excretion, contributes to sustain primary producers activity (Bartoli et al., 1996; Bartoli et al., 2001; Naldi et al., 2020; Nizzoli, Bartoli & Viaroli, 2006; Nizzoli, Welsh, Fano et al., 2006). Moreover, the dominance of clams within the benthic community results in the overall loss of biodiversity and associated ecosystem services, as the stimulation of N removal processes (Nizzoli et al., 2002; Politi et al., 2019). During periods characterized by high temperature and low wind, macroalgal blooms can be followed by a collapse of their production, switching the metabolism from hypereutrophic to dystrophic. The decomposition of macroalgal mats leads to anoxia and may determine the onset of anaerobic processes and the release of sulfides to the water column, causing massive damage to the ecosystem and to the local economy (Giordani et al., 1997; Giordani et al., 1996).

The maximum spread of this phenomenon was observed in the early 1990s and stimulated a number of international and national research programs that have been realized until the early 2000s (Viaroli et al., 2006). They have explored many aspects including the water chemistry in the watershed and the quantification of the nutrient loads delivered from the main tributaries (Alvisi et al., 1991; Castaldelli et al., 2013; Viaroli et al., 2013), the hydrodynamic of the lagoon (Maicu et al., 2021; Marinov et al., 2008; Marinov et al., 2006), the dynamics of the macroalgal bloom (Naldi & Viaroli, 2002; Viaroli et al., 1995; Viaroli et al., 1996), the N and P benthic regeneration processes

(Bartoli, Castaldelli, Nizzoli & Viaroli, 2012; Bartoli et al., 1996), the main biogeochemical consequences of clam farming activities (Bartoli et al., 2003; Murphy et al., 2018; Nizzoli et al., 2007; Nizzoli, Bartoli & Viaroli, 2006; Nizzoli, Welsh, Fano et al., 2006; Nizzoli et al., 2011) and dystrophic events triggered by the decomposition of macroalgal biomass (Azzoni et al., 2005; Giordani et al., 1997; Giordani et al., 1996; Zilius et al., 2015). The dynamics of the lagoon have been analysed also via integrated modelling tools (Cattaneo et al., 2001; Zaldivar et al., 2003), including a 6-compartments model representing the N circulation that has been analysed via the Ecological Network Analysis (Christian et al., 1996; Christian et al., 2010).

In the last decades different management measurements have been implemented to increase the hydrodynamic of the lagoon, including the opening of the gates connecting the Po di Goro with the lagoon, mostly in the summer season, the dredging of a channel crossing the Scanno di Goro that increased the exchanges between the lagoon and the sea and the continuous dredging of canals within the Valle di Gorino (Marinov et al., 2006). Shallow and vulnerable areas are continuously capped with sand, to decrease their organic content and nutrient regeneration (Corbau et al., 2016). These actions, managed by local authorities, are likely one of the main causes of the decrease in blooms frequency, which has occurred in the last 20 years (Viaroli et al., 2006). They have been followed by a further extension of the farmed area, which in recent years moved from the eastern vulnerable and sheltered area to the more hydrodynamic mouth of the lagoon and actually extend up to the marine side of the Scanno di Goro.

In the next few decades, climate changes could have far reaching consequences on the dynamics of the Goro Lagoon. Since the Po di Volano watershed has large depressed areas, it may be very sensitive to marine intrusions and salinity increase due to the sea level rise (Antonioli et al., 2017). According to different climate changes projections the average temperatures are predicted to increase, with the maximum warming foreseen in the summer season, that could reach 3 °C in the next 50 years (Coppola & Giorgi, 2010). A general decline in precipitation and runoff (up to 40%) is expected and will result in an extension of the hydrological dry season (Coppola et al., 2014; Vezzoli et al., 2015). The frequency of extreme events will also enhance and lead to the overall increase in extremely dry and drought incline periods and very wet and flood incline periods (Coppola et al., 2014). As describe in detail in section 2.3 climate changes may represent a new, indirect driver of eutrophication by affecting the amount and composition of loads delivered to the coastal area, by increasing the extent of internal recycling processes and by altering the benthic community composition. Since the increase in the extension of the farmed area and the spread of these emerging environmental pressures, there is was an urgent need to characterize the biogeochemical functioning of this system, in order to forecast potential impact to the economic activities.

In this study some these aspects have been addressed in different experimental activities, whose summary is reported in Table 3.1. To represent and investigate the overall complexity of the lagoon, four different sedimentary environments have been selected based on different hydrodynamic, particle sorting, dominating macrofauna and average salinity. The first three sampling stations were selected to represent the three main areas

of the lagoon: Site 1 (44° 82′ 30″ N 12° 27′ 27″ E) is located in the western corner in the plume area of the Po di Volano, Site 2 (44° 79′ 47″ N 12° 32′ 38″ E) is located at the edge of the Valle di Gorino, and Site 3 is located near the sea mouth within a farmed area (44° 80′ 62″ N 12° 31′ 44″ E). A fourth site (Site 4, 44° 84′ 47″ N 12° 31′ 83″ E) was selected in the northern corner, an area characterized by low hydrodynamics, favoring the accumulation of macroalgal detritus and resulting in black, poorly bioturbated organic sediments (Politi et al., 2019; Zilius et al., 2015) (Fig. 3.1). These areas were alternatively analysed in the different experimental activities. Experiments were carried out in spring or summer via the traditional approach of dark incubation of intact or reconstructed sediments, and using of the ^{15}N isotope pairing technique (IPT) to quantify denitrification and DNRA rates. Water column and sediment parameters were also determined, as well as the riverine nutrient loads.

The response of N removal and recycling processes to recent climatic anomalies have been analysed in section 3.1. Benthic N fluxes, denitrification and DNRA rates have been measures in spring under unusually heavy rainfall and in summer following a dry period characterized by extremely high temperature. It has been hypothesized that both extreme events may affect the capacity of the lagoon to act as nutrient filter, decreasing the efficiency of removal processes. Particularly, in spring the high river discharge leads to high NO_3^- availability stimulating the denitrification activity but decreases the residence time, resulting in an overall decreased efficiency and in a large NO_3^- export to the sea. In summer, the dry period results in a salinity increase, a decrease in the abundance of bioturbating macrofauna that together with lower NO_3^- availability could determine a high recycling and export of NH_4^+ to the sea. Results from this study pointed out that the lagoon functioning may be extremely vulnerable to high nutrient pulse addition during flood events, which overwhelm the N removal capacity, due the saturation of the microbial enzymatic activity. The response of nitrate removal processes (denitrification and DNRA) to increasing NO_3^- availability have been therefore analysed with the aims to quantify their saturation thresholds and identify the main factors affecting the ration between the two processes (section 3.2). It is expected that the general dominance of denitrification (net removal) over DNRA (net recycling) can be altered in response to the accumulation of reductants in pore water and to the increase in salinity that characterize stagnant areas of the lagoon in the summer season. The effects of macrofauna on N have been deeply investigated whereas those on reactive P are understudied. In section 3.3 the effect of surface and deep bioturbating macrofauna on the dynamics of P and metals have been analysed to understand how these organisms affect the sediment retention capacity. It was assumed that bioturbating organisms may increase the release of reactive P due to the combined effect of excretion and advective transport but at the same time they increase the oxidation of sediments and their buffer capacity against massive, oxygen and redox-dependent DIP release under transient anoxia events. Since one of the purpose of this study was to collect information that will be upscaled to construct models representing the nutrient dynamics at the whole lagoon scale, the reliability of results obtained using different experimental approaches has been tested in section 3.4. Benthic fluxes have been analysed in intact and reconstructed sediments added with increasing densities of

Table 3.1: Summary of experimental activities carried out in the Goro Lagoon and of measured parameters.

Section	**Intact/Reconstructed sediments**	**Sites**	**Season**	**Activities**	**Parameters**
3.1	Intact	1,2,3	Spring, Summer	Water column Benthic fluxes IPT Sediments Inputs	Temperature, O_2, pH, Salinity, DIN O_2, N_2, DIN Denitrification, DNRA Density, porosity, C, N, $\delta^{13}C$, δ^{15}, NH_4^+ DIN
3.2	Intact	1,4	Spring, Summer	Water column IPT Sediments	Temperature, O_2, pH, Salinity, DIN Denitrification, DNRA Density, porosity, C, N, $\delta^{13}C$, $\delta^{15}N$, DIP, NH_4^+, TDS
3.3	Reconstructed	1	Spring	Water column Benthic fluxes Sediments	Temperature, O_2, pH, Salinity, DIN, DIP O_2, DIP, Fe^{2+}, Mn^{2+} Density, porosity, DIP, TDS, Fe^{2+}, Mn^{2+}
3.4	Intact and reconstructed	1,3	Summer	Water column Benthic fluxes IPT Sediments	Temperature, O_2, pH, Salinity, DIN, DIP O_2, N_2, DIN Denitrification, DNRA Density, porosity, C, N, Chl-*a*

bioturbating organisms to compare the degree of stimulation of benthic processes. It has been hypothesized that processes measured in intact sediments under *in situ* conditions may differ from those derived from reconstructed sediments, mostly due to the alteration of chemical gradients and oversimplification of the biological communities. The data collected in this thesis will allow to implement the ecological network constructed for N in the past (Christian et al., 1996) and compared the past and present functioning of the lagoon.

3.1 The effects of hydrological extremes on N removal and recycling[1]

Human activities, through increased fertilizer production and combustion, have more than doubled the load of bioavailable N to coastal areas, that have led to widespread eutrophication, hypoxia, and anoxia (Cloern, 2001; Diaz & Rosenberg, 2008; Nixon, 1995). Recent analyses suggest that in most European watersheds the total N exported to the sea has either stayed the same or even increased, despite the nitrate reduction directive which was established some 30 years ago (Viaroli et al., 2018; Vybernaite-Lubiene et al., 2018). This situation can be worsened by climate change, which affects the magnitude and the seasonal pattern of precipitation, increasing the frequency of high discharge, flash flood periods as well as phases with no precipitation and minimum river flow, with negative impacts on the ecosystem functioning (Lehner et al., 2006; Trenberth, 2005; Zhang et al., 2019). Different studies reported that the consequences of these sharp fluctuations of water supply, combined with increasing temperature and changes in the pattern of salinity due to sea level rise, may be amplified in transitional systems, such as estuaries and coastal lagoons (Anthony et al., 2009; Ferrarin et al., 2014). As reported in section 2.3 the effects of climatic extremes on benthic N cycling are diverse, site-specific and thus difficult to forecast, and affect both the amount of nutrient delivered to the transitional areas and their internal functioning (Najjar et al., 2010; Statham, 2012).

In this section, the variations in benthic N dynamics in response to the recent climatic anomalies of 2019 have been analysed in the Goro Lagoon. A spring sampling was conducted in May, which was characterized by unusually heavy rainfall with values of cumulative precipitation nearly 2.5 times higher compared to the past 20 years. A late-summer campaign was conducted at the beginning of September, following a period characterized by high temperature and low river discharge. Summer temperatures in the Po River basin show a clear increasing trend from the 1970s (Brunetti et al., 2006). In the Goro Lagoon, during summer 2019, water temperatures exceeded 30 °C for 8 days, whereas during the 2006 - 2018 period such threshold was exceeded for 3.5 days.

It has been hypothesized that: (1) low salinity and high NO_3^- availability, together with high densities of burrowing macrofauna lead to high denitrification efficiency and low N recycling during spring; (2) high salinities and low NO_3^- availability, together with low bioturbation lead to decreased denitrification efficiency and high N recycling during late-summer; (3) hydrological extremes lead to the loss of ecosystem services such as N removal.

[1]Results of this study have been published in: **Magri, M.**, Benelli, S., Bonaglia, S., Zilius, M., Castaldelli, G., and Bartoli, M. (2020). The effects of hydrological extremes on denitrification, dissimilatory nitrate reduction to ammonium (DNRA) and mineralization in a coastal lagoon. *Science of The Total Environment*, 740, 140169.

3.1.1 Material and methods

Sediments sampling and benthic flux measurements

Samplings were carried out on May 27th (spring campaign) and on September 2nd (summer campaign) 2019 at Sites 1, 2 and 3 (Fig. 3.1). At each site, 4 intact sediment cores (Plexiglass liners, i.d. 8.4 cm, length 30 cm) were randomly collected by hand for benthic fluxes and denitrification and DNRA measurements. Concurrently, 6 intact sediment cores (Plexiglass liners, i.d. 4.6 cm, length 20 cm) were collected at each site for the sediment characterization and the determination of pore water NH_4^+ concentration. Water column temperature, pH, salinity and O_2 concentration were measured at the three sites by means of a multiple probe (YSI Instruments, Mod 556). In addition, from each site, 80 L of water was collected for cores maintenance, pre-incubation, and incubation periods. The intact cores were immediately submerged with the top open in a box filled with *in situ* water, cooled with ice packs to slow microbial activity and transferred to the laboratory within a couple of hours. Once in the laboratory, the cores were placed into three large tanks, one for each site, filled with unfiltered water, maintained at *in situ* temperature and they were left to settle overnight (Dalsgaard et al., 2000). The water in the tanks was continuously aerated by aquarium pumps. Each core was equipped with a Teflon-coated magnet rotating at 40 rpm driven by a central magnet. Each magnet was suspended about 6 cm above the sediment surface to mix the water column, avoiding resuspension.

After overnight pre-incubations, the water within the tanks was replaced and the larger cores were incubated in the dark (Dalsgaard et al., 2000). Incubations for aerobic respiration and net N_2 and nutrient fluxes lasted 2-3 hours to keep O_2 concentration within 20% of initial values and started when gas-tight lids were positioned on the top of the cores (Dalsgaard et al., 2000). Dissolved O_2 concentration was measured with a microelectrode (OX-50, Unisense A/S, DK), whereas water samples were collected from the water phase of each core at the beginning and the end of the incubation. In both cases, an aliquot of water was transferred and flushed to 12-mL exetainers (Exetainer, Labco Limited, UK), and fixed with 100 µL of 7 M $ZnCl_2$ to stop microbial activity for N_2 determination. Another aliquot of 20 mL was filtered (Whatman GF/F glass fiber filters) and transferred to scintillation vials to analyze dissolved inorganic N compounds via standard spectrophotometric techniques. Samples for N_2 were analyzed to determine changes in N_2:Ar ratios via a membrane inlet mass spectrometer (MIMS) equipped with a copper reduction column maintained at 600 °C (Bay instrument, MD, USA) (Kana et al., 1994). Ammonium was determined using salicylate and hypochlorite in the presence of sodium nitroprussiate (Bower & Holm-Hansen, 1980). Nitrate was determined after reduction to NO_2^- in the presence of cadmium, and NO_2^- was determined using sulphanilamide and N-(1-naphthyl)ethylenediamine (APHA (American Public Health Association), 1992; Golterman et al., 1978). Gas and nutrient fluxes at the sediment-water interface were calculated according to the equation below:

$$F_x = \frac{(C_f - C_i)V}{At} \tag{3.1}$$

where F_x is the flux of the chemical species x expressed in µmol m^{-2} h^{-1} or mmol m^{-2} h^{-1}, C_i and C_f (µmol L^{-1} or mmol L^{-1}) are concentration values of the chemical species x at the beginning and at the end of incubation, respectively, V is the water column volume (L), A (m^2) is the sediment surface and t (h) is the incubation time.

Measurement of denitrification and DNRA rates

After the first incubation, the water in the tanks was renewed and the open cores were left submerged for 2 hours in *in situ* and well-mixed water. Thereafter, a second incubation was performed to quantify the denitrification rates with the isotope pairing technique (IPT, (Nielsen, 1992)). The water in the tanks was lowered just below the top of the cores and $^{15}NO_3^-$ from a stock solution of 20 mM ($Na^{15}NO_3^-$, Sigma Aldrich) was added to the water phase of each core to have a final ^{15}N atom % of 50%. A water sample was collected from each core before and after the $^{15}NO_3^-$ addition to determine the ^{15}N-enrichment of the NO_3^- pools. Thereafter, the cores were capped and incubated for 2-3 hours in dark conditions as described for nutrient flux measurements. At the end of the incubation, the whole sediment column was mixed with the water column and homogenized. An aliquot of the slurry was transferred to 12-mL exetainers, allowing abundant overflow and fixed with 200 µL of 7 M $ZnCl_2$ to stop the microbial activity. The abundance of $^{29}N_2$ and $^{30}N_2$ was determined via MIMS. The anammox contribution to N_2 production was considered negligible, as reported in previous denitrification measurements in the Goro Lagoon sediments (Moraes et al., 2018). Denitrification rates were calculated from the production of $^{29}N_2$ (*p29*) and $^{30}N_2$ (*p30*) as follows:

$$D_{15} = p29 + 2p30 \tag{3.2}$$

$$D_{14} = D_{15}(\frac{p29}{2p30}) \tag{3.3}$$

where D_{15} is the denitrification rate of the $^{15}NO_3^-$, whereas D_{14} is the denitrification rate of $^{14}NO_3^-$. From the total denitrification rate, the denitrification of nitrate diffusing to the anoxic layer from the water column (D_w) and the denitrification of nitrate produced within the sediments due to nitrification (D_n) were calculated as described by (Nielsen, 1992):

$$D_w = (\frac{^{14}NO_3^-}{^{15}NO_3^-})D_{15} \tag{3.4}$$

$$D_n = D_{14} - D_w \tag{3.5}$$

where $^{14}NO_3^-$ is the ambient nitrate concentration (µM) and $^{15}NO_3^-$ is the concentration of labelled nitrate added to the cores.

Within the same denitrification experiment, an additional aliquot of the slurred sediment (30 mL) was collected to determine the rates of DNRA. The samples were transferred to 50 mL falcon tubes and treated with KCl (2 M) for the determination of the

exchangeable ammonium pool and the $^{15}NH_4^+$ fraction. Briefly, tubes were shaken for 1 h, then centrifuged (1800 rpm for 15 min) and the supernatant was filtered into 20 mL scintillation vials for later analyses. These samples were purged with helium for 10 minutes, to eliminate $^{29}N_2$ and $^{30}N_2$ pools produced during the incubations. Samples were then transferred to exetainers and treated with alkaline hypobromite solution, to oxidize NH_4^+ to N_2 (Warembourg, 1993). The abundance of $^{29}N_2$ and $^{30}N_2$ was determined via MIMS. Assuming that DNRA occurs in the same sediment horizon as denitrification, total DNRA rates were calculated from the production of $^{15}NH_4^+$ ($p^{15}NH_4^+$), according to the equation reported in (Risgaard-Petersen & Rysgaard, 1995):

$$DNRA_{tot} = p^{15}NH_4^+(\frac{D_{14}}{D_{15}}) \tag{3.6}$$

Total DNRA rates were divided into direct DNRA of NO_3^- from the water column ($DNRA_w$) and coupled DNRA ($DNRA_n$) and were calculated as follows:

$$DNRA_w = (\frac{^{14}NO_3^-}{^{15}NO_3^-})p^{15}NH_4^+ \tag{3.7}$$

$$DNRA_n = DNRA_{tot} - DNRA_w \tag{3.8}$$

At the end of the incubation, sediments from all cores were sieved (0.5 mm mesh size) to retrieve the macrofauna. Organisms were sorted under a stereomicroscope (Leica S8 APO, amplification 8x), identified by dichotomous keys and by scientific papers (Wagele, 1981) to the lowest possible taxonomic level and counted. For each species, the dry weight was determined after drying at 80 °C for 48 h. For the clams, shells were removed, and only flesh weight was measured.

Sediment and pore water caracterization

The six additional sediment cores were extruded and sliced in five layers: 0-1, 1-2, 2-3, 3-5 and 5-10 cm for physical and chemical sediment characterization. Briefly, in half of the cores, the slices were rapidly homogenized and approximately 5 g of fresh sediment was collected by means of a cut-off 5-mL syringe, transferred to a pre-weighted tray, and dried at 70 °C for 48 h for density, water content, porosity and organic matter analyses. Bulk density was measured as the weight of a volume of 5 mL fresh sediment and porosity was calculated after drying at 70 °C until constant weight. Later, sediments were analyzed for C and N content and their isotopic composition in the upper 0-2 cm sediment layer with a mass spectrometer (Thermo Scientific Delta V) coupled with element analyzer (FlashEA 1112, Thermo Electron Corporation) at the Center for Physical Sciences and Technology (Lithuania). Before measurements samples were grinded and acidified with 1 N HCl in order to remove carbonates. The last three cores were sliced to analyze the vertical distribution of pore water NH_4^+ concentration. Water was extracted by centrifugation of wet sediment (1800 rpm for 15 min), the supernatant was then filtered and analyzed to determine NH_4^+ concentration as described in the section 3.1.1.

Rivers discharge and reactive N loadings

The Consorzio di Bonifica Pianura di Ferrara provided data on Po di Volano, Collettore Giralda, Canal Bianco, and Canale Bonello discharges. This authority continuously monitors the water discharge and provides daily or weekly average values. River discharges for Po di Goro were not available, then mean annual data derived from (Maicu et al., 2021) were used. It was assumed that other diffuse sources were negligible. At each tributary, water samples were collected in triplicates in May and September and immediately filtered into 20 mL vials for NH_4^+, NO_2^- and NO_3^- determination as described in the section 3.1.1. Sampling stations were located at a certain distance from the mouth of the canals to minimize the variability due to marine water intrusion. The daily load of dissolved inorganic N was obtained by multiplying the concentration measured at each sampling date by the mean daily discharge. The latter was calculated from monthly data of May and September.

Statistical analysis

Two-way analysis of variance (ANOVA) was used to assess the significance of sites and seasons in explaining differences among benthic net fluxes, denitrification and DNRA rates. The normality and the homogeneity of variance were checked using the Shapiro-Wilk test and the Levene median test, respectively. If significant heteroscedasticity was found, data were log-transformed. Pairwise multiple comparison of means was carried out using the Tukey's test for all the significant factors. Statistical significance was set at p level lower than 0.05. All statistical analyses were performed with R software v. 3.5.1 (R Core Team, 2018). Graphs were made with Sigma Plot 11.0.

3.1.2 Results

General features of water column, sediments and macrofauna at the sampling sites

The concentration of dissolved inorganic N, temperature and salinity displayed strong spatial and temporal variability influenced by different hydrological regimes. During spring the high freshwater discharge associated with unusually heavy rainfall, resulted in low salinity, low temperatures and high NO_3^- concentrations (Table 3.2). During summer drought, water temperatures increased by 3–6 °C as compared to spring, O_2 saturation decreased by 20% and NO_3^- concentrations decreased at all sites by a factor of 4. Salinities reflected limited riverine discharge with values close to marine measured at Site 2 and 3 (Table 3.2).

Sediment properties revealed sharp differences between Site 1 and the other two sites, mainly due to the riverine influence. This site was characterized by muddy-clayish sediments with higher porosity and higher C and N content, which decreased in summer. Particulate matter displayed more depleted $\delta^{13}C$ and $\delta^{15}N$ signatures and higher C:N compared to sites located closer to the sea entrance (Table 3.2).

Table 3.2: Main sediment and water column characteristics at the three sampling sites in spring and summer in the Goro Lagoon. Averages ± standard errors are reported.

Parameter	Season	Site 1	Site 2	Site 3
		Water column		
T (°C)	*Spring*	18	22	19
	Summer	23	25	25
Salinity	*Spring*	8	3	10
	Summer	5	28	29
O_2 (% sat)	*Spring*	82	87	90
	Summer	62	72	63
NH_4^+ (µM)	*Spring*	20.7 ± 0.1	4.2 ± 0.1	27.7 ± 0.3
	Summer	28.8 ± 0.9	9.9 ± 0.2	14.9 ± 0.4
NO_2^- (µM)	*Spring*	17.2 ± 0.1	4.7 ± 0.1	5.1 ± 0.1
	Summer	8.1 ± 0.4	1.8 ± 0.1	1.7 ± 0.1
NO_3^- (µM)	*Spring*	113.2 ± 2.7	84.6 ± 1.1	56.1 ± 2.4
	Summer	31.7 ± 3.2	22.6 ± 0.6	12.3 ± 0.6
		Sediments		
Type	*Spring*	Muddy-clayish	Muddy-sandy	Sandy
	Spring	Muddy-clayish	Muddy-sandy	Sandy
Porosity	*Spring*	0.71 ± 0.03	0.42 ± 0.01	0.43 ± 0.01
	Summer	0.82 ± 0.01	0.57 ± 0.03	0.53 ± 0.02
TN (%)	*Spring*	0.26 ± 0.01	0.01 ± 0.01	0.02 ± 0.01
	Summer	0.20 ± 0.01	0.04 ± 0.01	0.04 ± 0.01
$\delta^{15}N$ (‰)	*Spring*	4.56 ± 0.18	5.05 ± 0.38	5.83 ± 0.36
	Summer	4.16 ± 0.39	6.87 ± 0.58	5.30 ± 0.13
C_{org} (%)	*Spring*	2.81 ± 0.15	0.09 ± 0.01	0.15 ± 0.01
	Summer	1.79 ± 0.04	0.24 ± 0.08	0.35 ± 0.02
$\delta^{13}C$ (‰)	*Spring*	-26.79 ± 0.04	-21.64 ± 0.10	-24.73 ± 0.20
	Summer	-27.23 ± 0.01	-23.42 ± 0.30	-24.25 ± 0.10
C:N (mol:mol)	*Spring*	12.41 ± 0.50	7.85 ± 0.26	7.61 ± 0.16
	Summer	10.31 ± 0.19	7.82 ± 0.22	9.22 ± 0.18

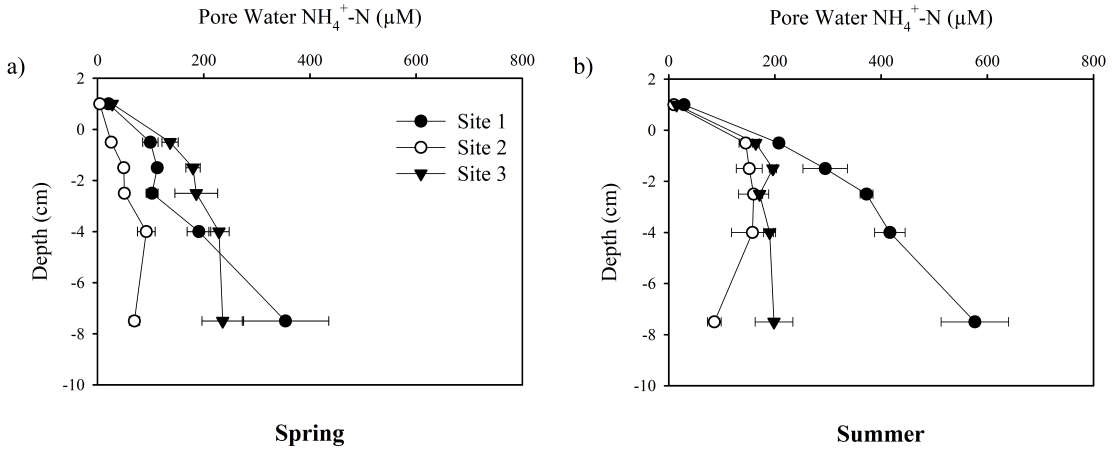

Figure 3.2: Vertical profiles of pore water NH_4^+-N concentration at the three sampling sites measured in spring (a) and summer (b) in the Goro Lagoon. Averages ± standard errors are reported.

At Site 1, vertical profiles of pore water NH_4^+ revealed an increasing trend, with the highest values observed in summer, when concentration peaked at about 600 µM at the 5–10 cm layer (Fig. 3.2). At the other sites, NH_4^+ concentration was less variable along the depth profiles, and increased from spring to summer at Site 2, whereas it showed similar seasonal values at Site 3. In both seasons, pore water NH_4^+ concentration exceeded that in the bottom water, suggesting upwards diffusive fluxes, generally increasing from spring to summer and with gradients peaking in the warmest season at the sediment-water interface (Fig. 3.2).

The abundance of dominating macrofaunal taxonomic groups differed among sites and seasons. In spring at Site 1 the sediments appeared heavily bioturbated, particularly by *C. insidiosum* and *A. succinea*, with densities of $7071 \pm 260\,\mathrm{ind.\,m^{-2}}$ and $2226 \pm 69\,\mathrm{ind.\,m^{-2}}$, respectively, which accounted on average for 80% of the total biomass. In summer the densities of these organisms drastically dropped to $105 \pm 10\,\mathrm{ind.\,m^{-2}}$ and $270 \pm 17\,\mathrm{ind.\,m^{-2}}$ for *C. insidiosum* and *A. succinea*, respectively. At Site 2 the biodiversity and the abundance of the macrobenthic community were relatively low and mainly dominated by *A. succinea* ($361 \pm 20\,\mathrm{ind.\,m^{-2}}$ in spring, $135 \pm 15\,\mathrm{ind.\,m^{-2}}$ in summer) and by the isopod *Cyathura carinata* ($180 \pm 30\,\mathrm{ind.\,m^{-2}}$ in spring and $1865 \pm 81\,\mathrm{ind.\,m^{-2}}$ in summer). At Site 3, located within the farmed area, *R. philippinarum* constituted more than 95% of the total macrofauna biomass, with densities of $768 \pm 56\,\mathrm{ind.\,m^{-2}}$ and $407 \pm 10\,\mathrm{ind.\,m^{-2}}$ in spring and summer, respectively.

Inorganic N fluxes at the sediment-water interface

Table A.1 reports the results of the two-way ANOVA to test the effects of seasons and sites on benthic fluxes. Inorganic N fluxes varied among sites depending on seasons ($p < 0.001$, Table A.1). In all three sites and both seasons, sediments were net NH_4^+ sources,

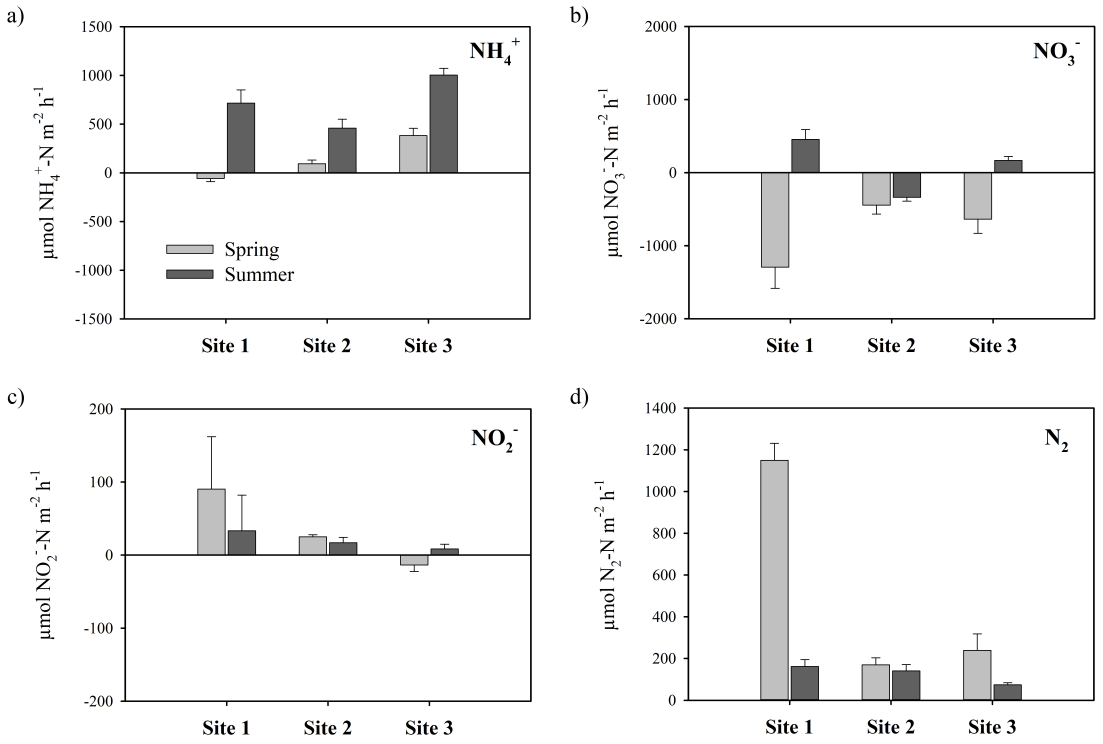

Figure 3.3: Benthic dark fluxes of NH_4^+-N (a), NO_3^--N (b), NO_2^--N (c), and N_2-N (d) measured at the three sampling sites in spring (light grey bars) and summer (dark grey bars) in the Goro Lagoon. Averages ± standard errors are reported. Fluxes are expressed in $\mu mol\,N\,m^{-2}\,h^{-1}$.

with Site 1 as exception during spring (Fig. 3.3a). At all sites NH_4^+ fluxes significantly increased (p <0.001, Table A.1) from spring (average rate 146 ± 59 $\mu mol\,N\,m^{-2}\,h^{-1}$) to summer (average rate 726 ± 73 $\mu mol\,N\,m^{-2}\,h^{-1}$), and Site 3 displayed the highest NH_4^+ recycling in both seasons.

Nitrite and NO_3^- were more erratic without clear patterns among sites and seasons (Table A.1). In spring, high water column NO_3^- concentrations resulted in large uptake (average rate $-730 \pm 150\,\mu mol\,N\,m^{-2}\,h^{-1}$) peaking at Site 1 (Tukey pairwise comparison, p <0.001; Fig. 3.3b). Site 1 and Site 3 in summer turned into net NO_3^- sources, with fluxes of $445 \pm 135\,\mu mol\,N\,m^{-2}\,h^{-1}$) and $168 \pm 55\,\mu mol\,N\,m^{-2}\,h^{-1}$, respectively, while Site 2 displayed values comparable to the spring season. Fluxes of NO_2^- were always nearly one order of magnitude lower than those of NO_3^-. In both seasons sediments from the three sites released NO_2^- to the overlying bottom water, with Site 3 as exception in spring (Fig. 3.3c).

Measured net N_2 fluxes were largely positive suggesting the dominance of denitrification over N_2-fixation (Fig. 3.3d). In spring sediment at Site 1 displayed the highest N_2 effluxes ($1150 \pm 81\,\mu mol\,N\,m^{-2}\,h^{-1}$), exceeding by a factor of 5 rates measured at Site 2 and Site 3. In summer there was a general decline in net N_2 production, in particular at

Site 1, which showed significant differences between seasons (Tukey pairwise comparison, p <0.001).

Aerobic respiration, denitrification and DNRA rates

Benthic O_2 uptake ranged from -1.74 to -8.77 mmol m^{-2} h^{-1} and significantly varied among the three sites in the two seasons (Fig. 3.4a, p <0.001, Table A.1). In spring, Site 1 displayed the highest O_2 uptake (-6.78 ± 0.32 mmol m^{-2} h^{-1}), which almost halved in summer despite the increase in temperature. Sites 2 and 3 were characterized by an opposite seasonal trend, with higher fluxes measured in summer, and peaking at Site 3 (-8.77 ± 0.87 mmol m^{-2} h^{-1}; Tukey pairwise comparison, p <0.001).

Total denitrification rates (D_{tot} = D_w + D_n) were more elevated in spring at all sites, with the highest rates measured at Site 1 (Tukey pairwise comparison, p <0.001, Fig. 3.4b). At this site denitrification was supported mainly by coupled nitrification-denitrification (625 ± 50 µmol N m^{-2} h^{-1}) and to a lesser extent by NO_3^- diffusing from the water column (442 ± 64 µmol N m^{-2} h^{-1}). Spring rates of D_n and D_w were about 5 times lower at Site 2 and 3 as compared to Site 1 (Tukey pairwise comparison, p <0.001). Despite the peak of denitrification matched with the peak of NO_3^- concentration in the water column, the D_n prevailed over the D_w in all the investigated sites, contributing nearly 60% of total denitrification (Fig. 3.4b). In summer at all three sites total denitrification rates decreased compared to spring (Tukey pairwise comparison, p <0.001 for Site 1 and 3). The greater change occurred at Site 1, where D_w and D_n rates dropped to 85 ± 18 µmol N m^{-2} h^{-1} and 132 ± 43 µmol N m^{-2} h^{-1}, respectively. The share of denitrification supported by nitrification was more variable in summer, ranging from 53 to 73% at Site 2 and 3, respectively (Fig. 3.4b). Total denitrification rates displayed a high accordance with N_2 fluxes measured via the N_2:Ar techniques, and values measured in the same core were significantly correlated (R^2=0.91, F=349.7, p<0.001), excluding the contribution of N-fixation (Robertson et al., 2019).

The highest rates of $DNRA_{tot}$ were found at Site 1 both in spring and summer (Fig. 3.4c). At all three sites values tended to increase in summer, but only at Site 2 seasonal differences were significant (Tukey pairwise comparison, p <0.001). In spring at Site 3 $DNRA_{tot}$ represented 10% of total NO_3^- reduction pathways, whereas at Site 1 and 2 it represented a minor portion. During summer the share of $DNRA_{tot}$ to NO_3^- reduction increased at all sites and reached nearly 33% at Site 1 and 3.

External loads versus internal removal and recycling

To compare the magnitude of external loads and internal processes, total DIN delivered from the lagoon watershed were normalized by the lagoon total surface, whereas removal and recycling rates were calculated by averaging denitrification rates and DIN effluxes measured at each sampling site. During spring the load of DIN was 27.25 ± 1.30 mmol m^{-2} d^{-1}. About 40% of the imported N was removed via denitrification (11.86 ± 1.02 mmol m^{-2} d^{-1}), whereas inorganic N recycling from sediments was negligible. In late-summer there was a steep decline in the riverine DIN load that decreased

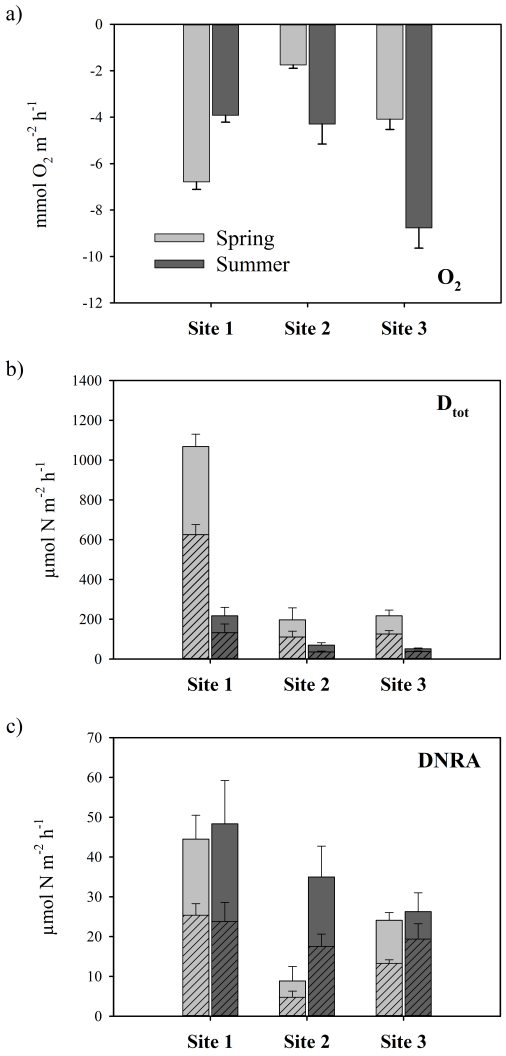

Figure 3.4: Benthic dark O_2 fluxes (a), denitrification (b) and DNRA rates (c) measured at the three sampling sites in spring (light grey bars) and summer (dark grey bars) in the Goro Lagoon. Total denitrification (D_{tot}) and DNRA rates include the portion coupled to nitrification, D_n and $DNRA_n$ (hatched bars) and the portion sustained by NO_3^- from the water column, D_w and $DNRA_w$ (solid bars). Averages ± standard errors are reported. Fluxes of O_2 are expressed in $\mathrm{mmol\,m^{-2}\,h^{-1}}$, whereas D_{tot} and $DNRA_{tot}$ rates are expressed in $\mu\mathrm{mol\,N\,m^{-2}\,h^{-1}}$.

by a factor of ∼3 (9.63±0.80 mmol m^{-2} d^{-1}), mainly due to lower discharge and decreased NO_3^- concentrations. The amount of inorganic N recycled from sediments increased and doubled the external inputs, averaging 20.18 ± 3.69 mmol m^{-2} d^{-1}, whereas N removal via denitrification accounted for 9% of total DIN load (sum of external input and internal recycling), corresponding to 2.70 ± 0.59 mmol m^{-2} d^{-1}.

3.1.3 Discussion

Temporal and spatial variability of N and O_2 dynamics in the Goro Lagoon

The obtained results indicate that the lagoon was predominantly removing N through benthic denitrification under high river discharge in spring, while it was recycling N via DNRA and remineralization under low discharge in late-summer. In spring, N-cycling was strongly influenced by the high freshwater discharge and the high NO_3^- load. The nutrient loads delivered from the Po River basin and from the Po di Volano sub-basin were monitored in different studies from the 1990s (Castaldelli et al., 2013; Castaldelli et al., 2020; Naldi et al., 2010; Viaroli et al., 2018). Dissolved inorganic nitrogen load displays a strong seasonality, with extremely high late-winter peaks and summer minimums. Nitrate, which represents on average more than 75% of total DIN load, is directly related to the water discharge, with wide inter-annual variations, from low values in dry years to peaks in wet years (Naldi et al., 2010; Viaroli et al., 2018). The spring load determined in this study was in the higher range of values previously reported for the same season (Castaldelli et al., 2013; Viaroli et al., 2013). Under these circumstances denitrification represented the leading process (Fig. 3.5), with total rates similar to values reported for other shallow estuarine systems in the wet season (Dong et al., 2000; Ogilvie et al., 1997; Seitzinger, 1988). Coastal lagoons act as benthic filters and regulate the supply of N both via denitrification and via the uptake of benthic primary producers (Risgaard-Petersen, 2003). Even though in this study only processes under dark conditions were analyzed, during spring photosynthetic activity of microphytobenthos and its nutrient uptake were likely suppressed by the enhanced water column turbidity, due to the delivery of suspended solid matter, and dissimilative processes represented the main pathway of N removal (Anderson et al., 2013). Despite the elevated NO_3^- availability in the water column, approximately 60% of denitrification was coupled to nitrification, indicating high sediment nitrification rates. At Site 1 the elevated nitrification is demonstrated to be associated with the high abundances of *C. insidiosum*, which via continuous ventilation of its 'U'-shaped burrows, pumps oxic water into the sediments, leading to the oxidation of pore water NH_4^+ in the upper sediment layers (Moraes et al., 2018; Pelegrì & Blackburn, 1994). Also, the presence of *A. succinea*, through the construction of dense burrow networks could enhance NH_4^+ mobilization from deep to surface sediments, stimulating nitrification (Nizzoli et al., 2007). Compared to Site 1, Sites 2 and 3 were characterized by lower denitrification rates, due both to the lower NO_3^- availability and to the limited bioturbation activity. These two sites, however, showed similar values of total denitrification, suggesting no effects of clam biomass on this process, a result that is in agreement with previous studies conducted in the same sites of the Goro Lagoon

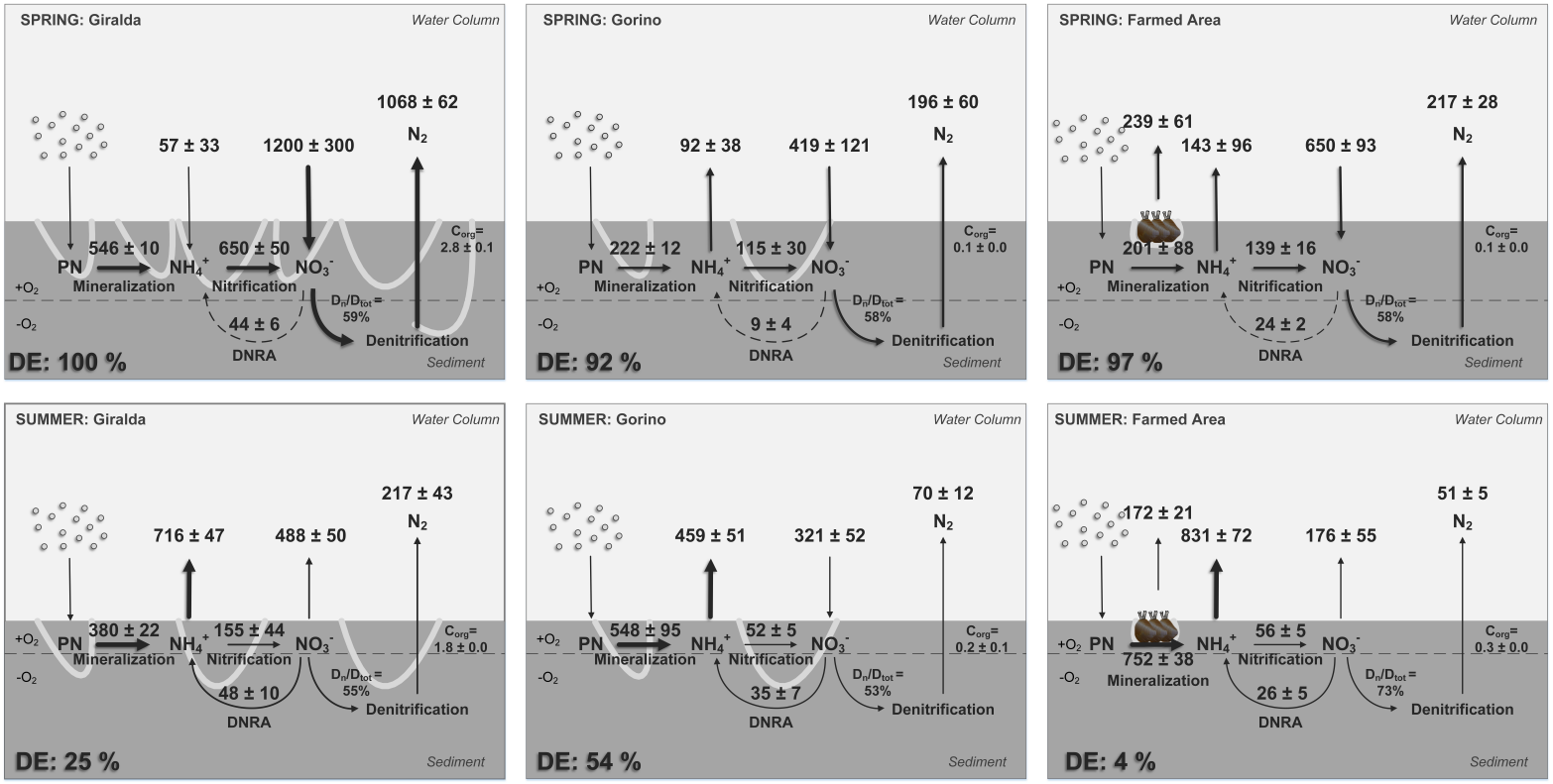

Figure 3.5: Graphic representation of benthic N cycling in spring and summer at the three sampling sites. Fluxes and process rates were derived from direct measurements and calculations. Net O_2 fluxes were converted into theoretical rates of organic N mineralization. The absolute values of O_2 fluxes were assumed to be equivalent to CO_2 fluxes (RQ, Respiratory Quotient, $|O_2|/|CO_2|=1$) (Strickland and Parson, 1972) and were divided by the measured C:N molar ratios of the organic matter in surface sediments. Nitrification rates were estimated, as minimum rates, from the sum of D_n and $DNRA_n$. The contribution of clam respiration and excretion was calculated multiplying biomass-specific excretion rates reported in (Welsh et al., 2015) by the biomass of the clams retrieved in our experiments. Mean rates (averages ± standard errors) are expressed in $\mu mol\,N\,m^{-2}\,h^{-1}$, C_{org} content is expresses as percentage value (averages ± standard errors). Denitrification efficiency (DE) was calculated as the ratio between dinitrogen (N_2) flux and the sum of N_2 and DIN effluxes.

(Murphy et al., 2018). Despite a small amount of NO_3^- being reduced to NH_4^+ via DNRA, denitrification was the main pathway of NO_3^- reduction. At Site 3 the contribution of DNRA to nitrate reduction processes slightly increased compared to the two other sites, probably due to the larger availability of labile organic matter in the form of clam biodeposits (Nizzoli, Bartoli & Viaroli, 2006). However, the increase in NH_4^+ efflux derived from DNRA was negligible if compared to direct clam excretion, which was estimated to contribute from 63 to 154% of total NH_4^+ fluxes. Such percentages were calculated multiplying biomass-specific excretion rates of clams (Murphy et al., 2018; Welsh et al., 2015) by the biomass of the clams retrieved in our experiments. During spring therefore, high freshwater discharge resulted in the dominance of denitrification over recycling via mineralization, clam excretion and DNRA.

After few months of low river discharge, during late summer, the elevated temperatures and the low O_2 concentration led to a shift of N processes from the dominance of removal to recycling (Fig. 3.5). Generally, the reduced state of sediments was evidenced by an increased sediment O_2 uptake and a higher net release of NH_4^+. The latter was due to a combination of factors, including high mineralization rates, the disconnection between N removal (via coupled nitrification–denitrification) and mineralization, and the enhancement of DNRA (Kemp et al., 2005; Roberts et al., 2012). The direct contribution of clam metabolism accounted for 21–42% of the net NH_4^+ fluxes, suggesting the dominance of microbial processes also at Site 3. Denitrification rates dropped compared to spring values and showed a decreasing trend along with the 4-folds drop in NO_3^- concentration from the western corner towards the mouth of the lagoon, mainly driven by D_w. At Site 1 the decrease in the coupled nitrification-denitrification was mainly due to the decline in bioturbators abundance, likely due to high temperatures and low O_2 concentration (Pitacco et al., 2018). At Sites 2 and 3 the simultaneous decrease in denitrification rates and increase in the relative contribution of DNRA may depend on several factors including the increment of salinity (Caffrey et al., 2019; Giblin et al., 2010), the higher ratio of labile organic carbon to NO_3^- electron acceptors (Nizzoli et al., 2010; Tiedje, 1988), and the availability of reductants as sulfides (Brunet & Garcia-Gil, 1996) and Fe^{2+} (Robertson et al., 2016). Despite all these factors would be expected to favor DNRA over denitrification, the contribution of this process to total NO_3^- reduction was lower compared to values previously reported for temperate shallow estuaries, where it can equal or exceed denitrification (An & Gardner, 2002; Gardner et al., 2006; Murphy et al., 2018). As a consequence, denitrification remained the dominant process (Murphy et al., 2018).

The denitrification efficiency (DE) was calculated as the ratio of inorganic nitrogen efflux from sediments as N_2 to the total efflux of DIN + N_2 (Eyre & Ferguson, 2009). Calculated values ranged from 92 to 100% in the spring season, with maximum values displayed at Site 1, and dropped in the summer season, ranging from 4 to 25%, with maximum value at Site 2. (Eyre & Ferguson, 2009) reported the highest DE (about 70%) in sediments with moderate organic carbon enrichment and inorganic carbon fluxes ranging between 500 and 1500 $\mu mol\, m^{-2}\, h^{-1}$. Since in the Goro Lagoon respiration rates were always higher than 1500 $\mu mol\, m^{-2}\, h^{-1}$, much lower DE and elevated N recycling

were expected. However, in spring DE displayed high values, likely sustained by the high rates of D_w. High NO_3^- concentrations in the water column determined high DE, despite the elevated sediment organic content. The latter did not significantly affect the macrofauna community, which is composed by tolerant species supporting elevated nitrification rates (Politi et al., 2019). In summer DE was lower at the three sites, suggesting higher N recycling over denitrification. The increased temperatures, the inhibition of nitrification, the increase in DNRA rates and the lower macrofauna activity were likely the main factors determining this drop in summer. Similar results were found by (Bartoli, Castaldelli, Nizzoli & Viaroli, 2012) in an annual study carried out at Site 1 and 2.

Sediments at the three sites displayed elevated O_2 uptake, in the higher range of those reported for other temperate estuaries (Cabrita & Brotas, 2000; Gardner & McCarthy, 2009; Nizzoli et al., 2007). At Site 1 the high organic load was derived mainly from settled particles of fluvial origin, as demonstrated by the higher C:N ratio and by the lower C and N isotopic values, within the range reported for terrestrial organic matter (about -27‰ and of 3‰ for $\delta^{13}C$ and $\delta^{15}N$, respectively, (Lamb et al., 2006)). However, even during the high discharge period, the C:N ratio of Site 1 surface sediments suggested high organic matter quality, whereas material of terrestrial origins usually displays values significantly above 12 (Yamamuro, 2000). At this site in spring the highest O_2 uptake was associated with dense burrow network of amphipod *C. insidiosum*, where O_2 was likely employed for NH_4^+ oxidation via nitrification (Moraes et al., 2018; Pelegrì & Blackburn, 1994), whereas decreased in summer. Sites 2 and 3 were characterized by C:N ratios close to the Redfield one and by higher $\delta^{13}C$ and $\delta^{15}N$ values, closer to values reported for marine systems, suggesting a progressive increase in the proportion of organic matter from autochthonous origins (Liu, 2006; Yamamuro, 2000). The isotopic values, however, were more depleted compared to marine phytoplankton, particularly relative to $\delta^{13}C$ values, usually ranging from -22 to -19‰ (Lamb et al., 2006), suggesting that sedimentary organic matter still derived from the mixture of terrestrial derived material and marine material and from the accumulation of clam biodeposits ($\delta^{13}C$ value of about -23,2‰ , (Mazzola & Sarà, 2001)). Sediment O_2 uptake in these sites showed a distinct seasonal pattern, with higher rates in summer likely regulated by water temperature (Cabrita & Brotas, 2000; Trimmer et al., 1998; Vidal et al., 1997). At Site 3 the higher benthic respiration measured in summer was not related to clam density, since clam contribution to O_2 demand accounted for 21–42% of the total benthic respiration, whereas in spring it represented a major fraction (62–127%) (clam biomass-specific respiration rates were derived from (Murphy et al., 2018; Welsh et al., 2015)).

Projections in the context of climatic anomalies and hydrological extremes

The drivers of macroalgal blooms in the Goro Lagoon were studied for nearly three decades and were associated to anthropogenic nutrient loads (Viaroli et al., 2018), nutrient recycling by clams (Bartoli et al., 2003; Bartoli et al., 2001; Naldi et al., 2020) and introduction of alien species (Milardi et al., 2020). Results from this experimental activity provide evidence of a new possible driver of algal blooms. Hydrological extremes, which are expected to increase in the future, may reduce the role of the Goro Lagoon as biogeo-

chemical filter, with implications for NH_4^+ availability, in particular during prolonged dry periods and heat waves. Different studies targeting the effect of climate changes on nutrients focused on processes at the watershed scale (e.g., increased or decreased runoff) and the implications on hydrology (e.g., increased erosion, sharp reduction or increase in water residence time) (Howarth et al., 2012; Marshall & Randhir, 2008; Wagena et al., 2018); the present study has analyzed the overlooked effects of two climatic extremes on sedimentary N biogeochemistry (Anderson et al., 2013; Bruesewitz et al., 2013; Howarth et al., 2000).

Climate projections forecast the increment of frequency and severity of heavy rainfalls (Vezzoli et al., 2015). The timing of these events is crucial and may determine different effects on the dynamics of transitional areas. These events may contribute to alleviate hypoxia, for example by increased discharge, lower residence time and interruption of water column stratification (Rabalais et al., 2007). High freshwater discharge may contribute to flush phytoplankton downstream, even out of the estuary, and control algal blooms (Phlips et al., 2020; Scavia et al., 2002) or may enhance sediment resuspension resulting in the release of nutrient, favoring pelagic production, or in the oxidation of reduced pools (Niemistö & Lund-Hanses, 2019; Vidal-Durà et al., 2018). The increase in riverine runoff enhances the amount of N exported from the river watershed to the coastal areas, whereas high solid transport and turbidity limit primary producers assimilative N pathways; as a consequence with microbial denitrification remains the most important N-removing dissimilative process (Anderson et al., 2013). A positive relationship between NO_3^- availability and removal capacity has been found across a range of estuaries (Seitzinger et al., 2006). The consequent decrease in water residence time, however, determines a reduction of denitrification potential.

Different models show that the N fraction that is denitrified may be estimated from the residence time (Dettmann, 2001; Nixon et al., 1996; Seitzinger et al., 2006). These models were usually developed with data at the monthly or annual scales, whereas over short time frames the relation between denitrification efficiency and water residence times is more challenging. The annual average residence time of the Goro Lagoon varies between 1 and 12 days, with minimal values in spring in the western portion and at the lagoon-sea interface ($<$5 days) (Maicu et al., 2021). The calculations presented in this study, based on a simple mass balance, show that in spring, despite high denitrification rates, nearly half of the N load entering the lagoon was removed via denitrification. According to the models proposed by (Nixon et al., 1996; Seitzinger et al., 2006), however, a residence time of 5 days determines the removal of 15% of the total N load and this amount may be even lower considering heavy precipitation and the high runoff detected in spring. Many factors, such as depth, water temperature, salinity, O_2 and NO_3^- concentrations, organic carbon in sediments, bioturbation and presence of primary producers may affect denitrification efficiency and produce significant deviations from expected values (Eyre & Ferguson, 2009). Shallow lagoons with marked zonation as the Goro Lagoon are paradigmatic examples where multiple, co-occurring factors regulate locally and set the upper limits of processes as denitrification and where the same factors may undergo sharp spatial (e.g., among stations) and temporal variations (e.g., among wet and dry

periods).

A further increase in river discharge and, consequently, in nutrient amount, may also determine the saturation of the denitrification capacity of transitional areas. Nitrate removal capacity increases with N load, up to the saturation concentrations and asymptotic rates were reported in different studies at 200 µM (Ogilvie et al., 1997), 400 µM (Trimmer et al., 1998) and 600 µM (Dong et al., 2000). These concentration values are much higher than those reported in this study in spring (56–113 µM). The threshold values, however, may be related to local variations in biological and environmental variables or due to differences in acute or chronic nutrient load. This aspect will be deepen in section 3.2.

Different models reported for the Po River Basin that the most significant effects of climate changes are expected in summer, with a strong increase in very dry and low flow periods, followed by significant water deficit, and a large increase in temperature and heatwaves (Cozzi & Giani, 2011; Vezzoli et al., 2015). Extremes in low summer discharge may stimulate river and estuarine eutrophication and large conversion of inorganic nutrients into phytoplankton and in its transfer to coastal areas (Howarth et al., 2000; Rossetti et al., 2009). Under these circumstances, most N would be delivered to sediment in particulate form, also due to filter-feeders activity. Consequently, labile organic matter inputs may fuel sediment respiration, reducing O_2 concentration in the water column and the heath-dependent water column stratification may determine the onset of bottom water hypoxia. Depletion of electron acceptors such as O_2 and NO_3^- leads to the dominance of sulfate reduction with subsequent sulfide accumulation, determining the suppression of nitrification and denitrification and the further increase in DNRA rates (An & Gardner, 2002; Gardner et al., 2006; Giblin et al., 2010). The sulfide build-up may also derive by the increase in salinity, due to high temperature and low freshwater discharge. Oxygen depletion and sulfides affect also macrofauna diversity and abundance and produce positive feedbacks towards more chemically reduced sediment conditions and towards N-recycling dominance over denitrification (Diaz & Rosenberg, 1995; Magni et al., 2005). This was evidenced in a recent study carried out in the nearby Valli di Comacchio lagoon where it was demonstrated that heatwaves pose serious threats to the resilience capacity of the macrobenthic community, favoring short-lived, opportunistic forms (Pitacco et al., 2018). If elevated residence time and heatwaves promote large NH_4^+ recycling through the described cascade mechanisms, assimilation by primary producers may represent an important temporary retention of nutrients. (Naldi et al., 2020) have demonstrated that in the shallow water of the Goro Lagoon, clams control phytoplankton primary production and displace the pelagic production at the benthic level. Under low discharge and high residence time, such top-down control can be even more efficient, resulting in transparent water, enriched by excreted nutrient, which may favor macroalgal growth, with negative effects on the lagoon functioning and clam farming (Bartoli et al., 2001; Naldi et al., 2020; Viaroli et al., 2003).

3.1.4 Conclusions

In the eutrophic Goro Lagoon, as reported in other estuaries and coastal systems, hydrological extremes result in sharp seasonal transitions among dominant microbial processes driving benthic N cycle. The spring, high discharge period is dominated by denitrification due to high NO_3^-, high bioturbation and likely turbidity-limited primary producers-bacteria competition. However, a further increase in river discharge and N loads may determine the saturation of denitrification capacity, and the excess N may be partly exported to the Adriatic Sea, also due to low water residence time. The summer, low discharge period is dominated by NH_4^+ internal recycling, also sustained by increased DNRA, largely exceeding watershed N inputs. Superimposed to and interacting with the effects of hydrological extremes are local regulations of benthic N processes. At Site 1 denitrification always dominated over DNRA as NO_3^- reduction pathway; this was particularly evident during spring mainly due to higher riverine influence, bioturbation and elevated NO_3^- concentrations. At Site 2 and Site 3, in particular during summer, the higher salinity and microbial respiration likely explained the increase in DNRA contribution to NO_3^- demand and large NH_4^+ fluxes. Such NH_4^+ mobilization may increase the intensity, duration, and extent of algal blooms. Results of this study suggest that both the spring and summer hydrological extremes scenarios reduce the effectiveness of lagoons as benthic filter and increase the amount of N exported to the open sea, either in form of NO_3^- or NH_4^+, with implications for coastal eutrophication.

3.2 The response of denitrification and DNRA to increasing nitrate availability

Extremes weather events are expected to increase in the next decades, both in frequency and intensity, as a result of human-induced climate change (IPCC, 2021; Stott, 2016). Floods associated with intense precipitation generate a large runoff and enhance N losses from intensively cultivated areas (Zheng et al., 2020), which have been demonstrated to largely increase after prolonged dry periods (Ascott et al., 2017; Gómez et al., 2012; Klaus et al., 2020). This results in pulse of dissolved N inputs to coastal areas (Paerl et al., 2020; Viaroli et al., 2018).

Coastal ecosystems through multiple biogeochemical processes play a key role in the removal of N loads before they reach the open sea (Asmala et al., 2017). In these systems, heterotrophic denitrification is considered the most important mechanism leading to permanent N removal, through the reduction of NO_3^- to N_2 (Seitzinger, 1988). Nitrate reduction can also take place via the dissimilatory nitrate reduction to ammonium (DNRA), which conversely determines the retention of bioavailable N (Burgin & Hamilton, 2007). Several factors regulate the partitioning between these competitive processes including salinity, temperature, and availability of NO_3^-, organic carbon and reductants as sulfides or dissolved iron (Fe^{2+}) (Burgin & Hamilton, 2007; Kessler, 2018; Nizzoli et al., 2010).

Potential rates of denitrification and DNRA under increasing concentration of NO_3^-, or increasing concentration of alternative reductants were traditionally analyzed via incubations of water or sediment slurries (Bonaglia et al., 2016; Seitzinger, 1988). The latter have been demonstrated to significantly deviate from *in situ* values, due to the disruption of physical and chemical gradients and to the enhanced microbial access to electron donors and acceptors, by removing limitations due to diffusion (Laverman et al., 2006). Comparatively, little has been done with intact sediment cores, which conversely allow to measure the response of sediments to NO_3^- inputs under much closer *in situ* conditions. If sediment slurries allow accurate measurements of the kinetics of biochemical reactions under optimal conditions for microbes and their enzymes, intact sediment cores allow measurement of the kinetics of the same reactions under diffusion-limited *in situ* conditions, stratification of sediment properties, and in presence of a diverse community including meio and macrofauna (Garcia-Ruiz et al., 1998; Joye et al., 1996).

The general aim of this activity was to analyze the *in situ* response of denitrification and DNRA rates to increasing NO_3^- availability, simulating a pulse NO_3^- addition in intact sediment cores. With this purpose, two sites characterized by different hydrodynamic and salinity conditions, different organic matter quantity and quality, and a different macrofauna community have been selected (Politi et al., 2019; Zilius et al., 2015). It has been hypothesized: (1) a positive response of both processes to increasing NO_3^- availability until a saturation threshold, with denitrification as the dominant process, particularly at higher NO_3^- concentration; (2) a decrease in denitrification to DNRA ratio in summer due to the accumulation of reductants in pore water, especially at the more saline site. Results are discussed with respect to the available information on the water column and sediment properties and macrofauna community, to identify the main

factors regulating the lagoon seasonal NO_3^- buffer capacity.

3.2.1 Material and Methods

Sediments sampling and characterization

Samplings were carried out on March 18th (spring campaign) and August 30th (summer campaign) 2021 at Sites 1 and 4, located in the weastern and in the northern corners of the lagoon, respectively (Fig. 3.1). On both occasions, *in situ* water column temperature, pH, salinity, and O_2 concentration were measured through a multiple probe. At both sites and in both seasons, 18 intact sediment cores (Plexiglass liners, i.d. 4.6 cm, length 20 cm) were collected for the determination of denitrification and DNRA rates and nearly 80 L of water was collected for cores maintenance, pre-incubations, and incubations. The intact cores were immediately submerged in in situ cooled water, transferred to the laboratory within a couple of hours and pre-incubated in the dark at *in situ* temperature, according to standard protocols and as described in section 3.1.1.

At each site, 4 additional sediment cores were collected for the characterization of physical and chemical sediment properties and the determination of pore water NH_4^+, DIP, and total dissolved hydrogen sulfides (TDS = H_2S + HS^- + S_2^-) concentrations. Five layers (0-1, 1-2, 2-3, 3-5, and 5-10 cm) were analyzed to determine the density, porosity, and organic matter content. The upper layer of dry sediment was analyzed for C and N content and their isotopic composition as described in section 3.1.1. The remaining aliquot of wet sediment was squeezed under N_2 atmosphere to extract pore water. A water sample (1 mL) was immediately fixed in 1 mL of zinc acetate solution (20%) to determine the TDS concentration following the methods described in (Cline, 1969). The remaining water was filtered and analyzed for the determination of DIP and NH_4^+ concentrations via standard spectrophotometric techniques as detailed in section 3.1.1 (APHA (American Public Health Association), 1992; Bower & Holm-Hansen, 1980).

Measurement of denitrification and DNRA rates

The day after the sampling, cores were incubated for the quantification of denitrification and DNRA rates under increasing $^{15}NO_3^-$ concentrations with the IPT, as described in the section 3.1.1. After overnight pre-incubation, the water within the tanks was renewed, mixed with the core water phases, and then lowered just below the top of the cores. Increasing amounts of labeled nitrate were added to the sediment water phase from a 20 mM $Na^{15}NO_3^-$ stock solution (Sigma Aldrich, 99%). Each enrichment, to final concentrations of 50, 100, 250, 500, 1000, and 2000 µM, was done in 3 replicates. A water sample (5 mL) was collected from each core before and 5 minutes after the $^{15}NO_3^-$ addition, filtered, and transferred to scintillation vials to determine the ^{15}N-enrichment of the NO_3^- pools. Thereafter, the cores were closed with gas-tight lids and incubated for 2-3 hours (Dalsgaard et al., 2000). At the end of the incubation, the whole sediment column was gently mixed with the water column and homogenized. An aliquot of the slurred sediment was transferred to 12-mL exetainers and fixed with 200 µL of 7 M

$ZnCl_2$. The abundance of $^{29}N_2$ and $^{30}N_2$ was determined via MIMS (Kana et al., 1994). Total denitrification rates (D_{tot}), denitrification of NO_3^- diffusing from the water column (D_w) and the coupled nitrification-denitrification (D_n) were calculated as described in the section 3.1.1.

The homogenized cores were also sampled to determine DNRA rates from the production of $^{15}NH_4^+$. An aliquot (30 mL) of the slurred sediment was transferred to 50-mL falcon tubes, treated and analyzed as described in (Warembourg, 1993). Total DNRA rates were calculated from the production of $^{15}NH_4^+$, assuming that DNRA occurs in the same sediment horizon as denitrification. Total DNRA rates were divided into DNRA of water column NO_3^- ($DNRA_w$) and DNRA coupled to nitrification ($DNRA_n$) as reported in (Risgaard-Petersen & Rysgaard, 1995). The experimental procedure and the calculations are detailed in the section 3.1.1.

At the end of incubations, sediments were sieved (0.5 mm mesh size) to retrieve macrofauna. Organisms were sorted, identified by dichotomous keys to the lowest possible taxonomic level and counted. For each species, the dry weight was determined after drying at 80 °C for 48 h.

Statistical analysis

The responses of total denitrification and DNRA rates to increasing NO_3^- concentrations were fitted to a linear model and a non-linear model representing the Michaelis-Menten curve, developed to described enzyme kinetic, represented below:

$$Y = V_{max} \frac{X}{K_m + X} \tag{3.9}$$

where V_{max} is the maximum denitrification or DNRA rate expressed in µmol N m^{-2} h^{-1}, X is the NO_3^- concentration (environment $^{14}NO_3^-$ + added $^{15}NO_3^-$) expressed in µM, K_m is the Michaelis-Menten constant and represents the NO_3^- concentration at which denitrification or DNRA rates reaches 50% of V_{max} (Murray et al., 1989). Values of V_{max} and K_m were estimated through the non-linear least square function using the R software v. 3.5.1 (R Core Team, 2018). The Akaike Information Criteria (AIC) was calculated to select the best model between the two fitted (Burnham & Anderson, 2002). Statistical significance was set at p level lower than 0.05.

3.2.2 Results and discussion

The Goro Lagoon is characterized by an estuarine circulation regulated by the interaction of tides, freshwater inputs, and winds, which lead to the formation of marked physico-chemical gradients. The two selected sites represent extreme conditions within this system as evidenced by the differences in the water residence time (annual averages 2-3 and 11-12 days for Site 1 and 4, respectively) and salinity values (annual averages 10 and 22 for Site 1 and 4, respectively) (Maicu et al., 2021).

At Site 1, located in the plume area of the Po di Volano River, freshwater input is the main driver of sediment and water column features (Politi et al., 2019). The sediment

C and N isotopic values were within the range reported for riverine systems (Lamb et al., 2006), whereas the C:N ratio indicated high organic matter quality compared to the material of terrestrial origin, suggesting a mixing with internal sources (i.e. macroalgae) (Bianchini et al., 2015). Peak water column nutrient concentrations were recorded in spring, overlapping the maximum river discharge, and decreased in summer (Table 3.3).

In both seasons, NO_3^- reduction at Site 1 was mostly driven by denitrification, that at *in situ* NO_3^- concentrations exceeded DNRA by a factor of nearly 2.5 (Fig. 3.6). The response of denitrification to increased NO_3^- concentrations followed the Michaelis-Menten saturation curve, suggesting that the process is generally limited by the electron acceptor availability. The highest V_{max} and K_m estimate values were recorded in spring and almost halved in summer (Fig. 3.6, Table 3.4). In both seasons, the response of DNRA rates to increased NO_3^- availability did not follow Michaelis-Menten kinetic but was linear, with low slopes, indicating a slight enhance along the concentration gradient. As a result, under the simulated pulse addition of NO_3^-, the denitrification to DNRA ratio increased to 6.5 and 5.9 in spring and summer, respectively. Such increase is in agreement with the hypothesis reported in (Tiedje, 1988), who postulated that high NO_3^- concentration favors denitrification over DNRA.

Seasonal variations in the abundance and activity of denitrifiers occur in most systems, and are mainly related to temperature, redox conditions, NO_3^- and organic carbon availability (Seitzinger et al., 2006). Previous studies report for a range of aquatic ecosystems greatest denitrification rates in summer, due to increased temperature and decreased NO_3^- pathlength to reach the denitrification zone (Pina-Ochoa & M., 2006; Revsbech et al., 2005). The opposite trend recorded at Site 1 is likely related to the high NO_3^- availability and the abundance of bioturbating organisms that characterized this area in spring (Bartoli, Castaldelli, Nizzoli & Viaroli, 2012). In this season the collected cores in fact displayed a thick oxidized layer and hosted a rich macrofauna community, dominated by the amphipod *C. insidiosum* ($1846 \pm 277\,\mathrm{ind.\,m^{-2}}$) and the polychaeta *A. succinea* ($445 \pm 83\,\mathrm{ind.\,m^{-2}}$). As reported in section 3.1 high densities of bioturbating organisms determine the increase in denitrification rates. These organisms explore the upper layer of sediments, hosting the more recent and labile carbon pool, and actively pump O_2 and NO_3^- rich bottom water (Moraes et al., 2018; Zilius et al., 2021). In a study on the effects of *Corophium* sp. on denitrification, it has been demonstrated the greater stimulation of denitrification of water column NO_3^-, exceeding that of coupled nitrification-denitrification and microbial O_2 respiration (Pelegrì & Blackburn, 1994). Authors explained the observed pattern by the differences between the diffusive transport of O_2 and NO_3^- in sediments, that for NO_3^- is usually limited by the presence of an oxic layer, and their comparable advective transport within the water pumped through the burrows. At Site 1, in spring, macrofauna bioturbation supported simultaneously the high D_n rates (averaging 50-65% of denitrification, (Bartoli, Castaldelli, Nizzoli & Viaroli, 2012)) and the sharp increase in D_w along with the NO_3^- concentration series. On the contrary, D_n was independent from the NO_3^- additions, which is an important assumption of the IPT (Robertson et al., 2019). The estimated maximum denitrification rates exceed values recorded in previous studies in several estuarine and marine

Table 3.3: Main sediment and water column characteristics at the two sampling sites in spring and summer. Averages ± standard errors are reported.

Parameter	Season	Site 1	Site 4
		Water column	
T (°C)	*Spring*	13.1	12.6
	Summer	21.7	22.5
Salinity	*Spring*	12.5	27.9
	Summer	6.9	16.0
O_2 (% sat)	*Spring*	85	87
	Summer	65	62
NH_4^+ (µM)	*Spring*	28.5 ± 2.2	10.4 ± 0.3
	Summer	17.3 ± 2.1	16.8 ± 2.4
NO_2^- (µM)	*Spring*	4.1 ± 0.2	1.7 ± 0.1
	Summer	2.3 ± 0.6	3.3 ± 0.9
NO_3^- (µM)	*Spring*	148.1 ± 9.1	74.1 ± 16.3
	Summer	48.2 ± 7.4	34.4 ± 14.1
		Sediments	
Type	*Spring*	Clayish-mud	Detrital-mud
	Summer	Clayish-mud	Detrital-mud
Porosity	*Spring*	0.72 ± 0.04	0.79 ± 0.05
	Summer	0.79 ± 0.07	0.77 ± 0.04
TN (%)	*Spring*	0.17 ± 0.02	0.50 ± 0.10
	Summer	0.24 ± 0.03	0.49 ± 0.10
δ^{15}N (‰)	*Spring*	5.65 ± 0.24	9.57 ± 0.25
	Summer	5.34 ± 0.39	9.45 ± 0.27
C_{org} (%)	*Spring*	1.61 ± 0.34	3.53 ± 0.78
	Summer	2.18 ± 0.22	3.41 ± 0.70
δ^{13}C (‰)	*Spring*	-26.45 ± 0.46	-25.10 ± 0.08
	Summer	-27.12 ± 0.03	-25.29 ± 0.13
C:N (mol:mol)	*Spring*	11.06 ± 0.10	8.15 ± 0.76
	Summer	10.23 ± 0.40	8.12 ± 0.28

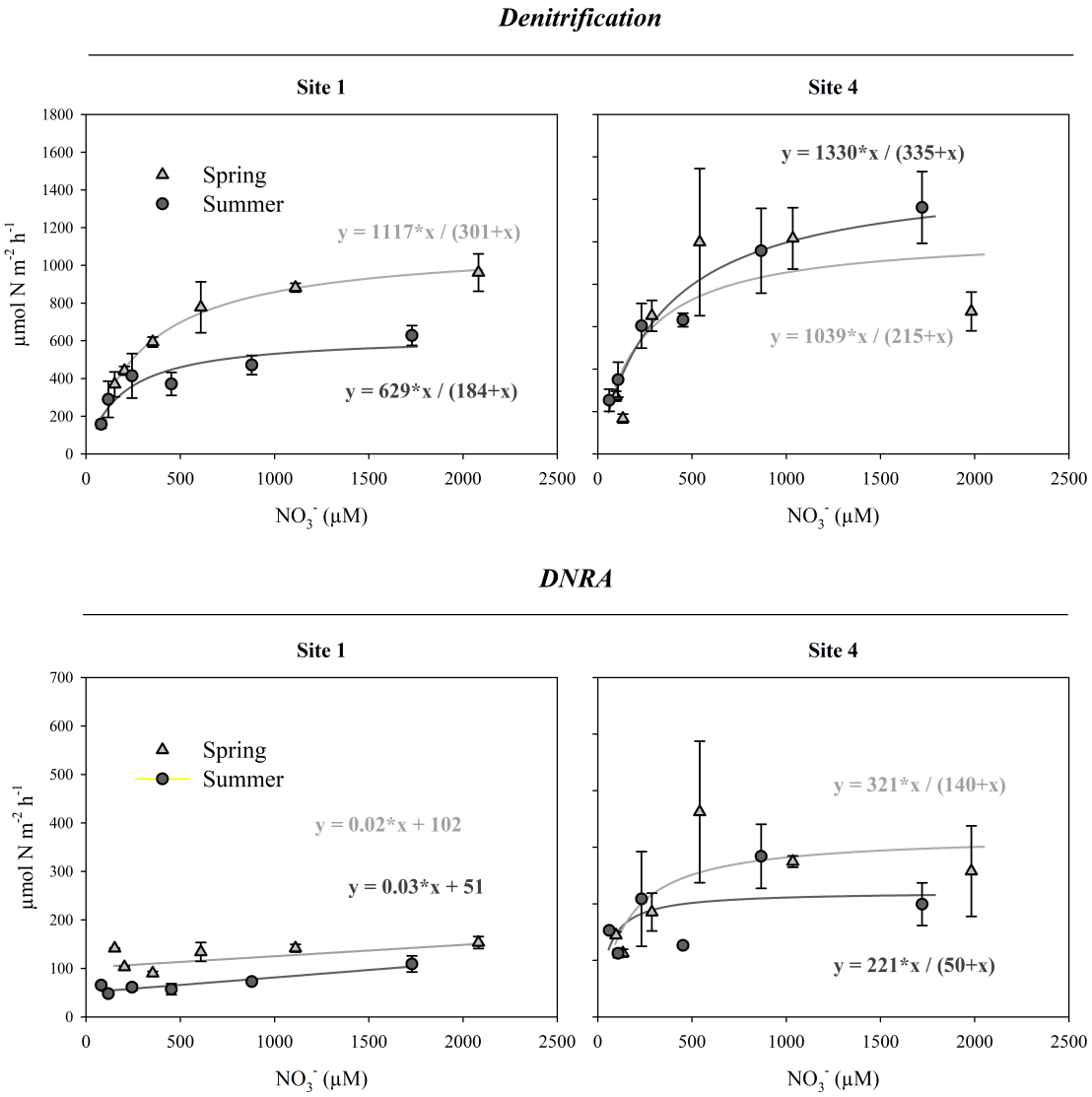

Figure 3.6: Hourly rates of total denitrification and DNRA measured at the two sampling sites in spring (grey triangles) and summer (dark grey circles) as a function of NO_3^- concentration (environment $^{14}NO_3^-$ + added $^{15}NO_3^-$). Average ± standard error are reported. The equations of the best fitted model (linear model, Michaelis Menten model) are reported. Note different scales on the y axis for the two analysed processes.

Table 3.4: Summary of Michaelis-Menten (MM) and linear models (LM) estimated parameters and associated standard errors. Best model was selected through the AIC method. For Michaelis-Menten models (MM) α corresponds to V_{max} (expressed in $\mu mol\,N\,m^{-2}\,h^{-1}$) and β corresponds to K_m (expressed in µM). For linear models (LM) α and β correspond to the slope and the intercept of the identified regression, respectively. For all parameters p-values are reported and significant ones are printed in bold.

Season	Model	α	p	β	p
		Site 1			
Denitrification					
Spring	MM	1116.7 ± 85.1	**<0.001**	300.8 ± 69.8	**<0.001**
Summer	MM	628.6 ± 78.8	**<0.001**	183.8 ± 77.8	**0.03**
DNRA					
Spring	LM	0.02 ± 0.01	**<0.001**	101.7 ± 0.5	**<0.001**
Summer	LM	0.03 ± 0.01	**<0.001**	50.5 ± 0.4	**<0.001**
		Site 2			
Denitrification					
Spring	MM	1038.6 ± 202.8	**<0.001**	214.6 ± 140.2	0.14
Summer	MM	1330.1 ± 179.3	**<0.001**	335.2 ± 126.9	**0.01**
DNRA					
Spring	MM	321.5 ± 59.1	**<0.001**	140.1 ± 99.3	0.17
Summer	MM	221.5 ± 35.6	**<0.001**	49.8 ± 43.3	0.26

environments (from 85 to 750 µmol N m^{-2} h^{-1}), measured both through intact cores and slurry incubations (Joye et al., 1996). In a recent study it has been demonstrated that high densities of bioturbating organisms in nutrient-enriched sediments can determine an increase also in DNRA rates, due to increased NO_3^- supply (Nogaro & Burgin, 2014). Our results support this conclusion, since higher DNRA rates were recorded in spring, at greater macrofauna densities.

Surface and subsurface bioturbation at Site 1 increases the oxidized sediment volume hosting O_2 and NO_3^- and likely solid phase Mn^{4+} and Fe^{3+} pools (Zilius et al., 2015). This is supported by pore water DIP, NH_4^+ and TDS profiles, which displayed low and constant concentrations along the vertical sediment profile (Fig. 3.7). The densities of macrofauna markedly decreased in summer (377 ± 89 ind. m^{-2} and 54 ± 30 ind. m^{-2} for *C. insidiosum* and *A. succinea*, respectively), likely due to temperature increase, higher microbial respiration and lower O_2 availability (Pitacco et al., 2018). This drop determined the decrease in potential denitrification rates, that was coupled to a reduction in K_m, suggesting an increased affinity for NO_3^- by denitrifiers, in response to its lower availability (Silvennoinen et al., 2008). It has been speculated that during summer, the large input of labile organic carbon in this area stimulated the electron transfer to oxidized metal pools, resulting in a moderate build-up of chemically reduced conditions. The latter is supported by the small increase in pore water DIP and TDS, suggesting less Fe^{3+} availability in sediments.The sharp increase of NH_4^+ was interpreted in terms of drop in bioturbation and O_2 availability, limiting nitrification (Fig. 3.7). Bioturbation, the sediment oxygenation and the consequent low availability of reductants in spring and to a lesser extent in summer, together with the low salinity and the low C/NO_3^- ratio, were likely the main reasons that counteracted DNRA at this site (Bonaglia et al., 2016; Kessler, 2018). The high potential for NO_3^- reduction via denitrification is likely due to the environmental stability of this lagoon area, favored by the constant NO_3^- supply from the eutrophic freshwater inlet (Viaroli et al., 2018) and by the transport of iron-rich minerals (Azzoni et al., 2005). Such inputs, together with macrofauna activity, promote relatively small seasonal variations in pore water chemistry, avoiding for example sulfide toxicity (Giordani et al., 1996; Zilius et al., 2015).

Such environmental stability contrasts the condition of Site 4 where a pronounced seasonal shift in the pore water chemistry occurred (Fig. 3.7). In summer, and to a lesser extent during spring, the sediments were covered with fresh macroalgae deposits. Such input turned the dark grey spring sediments into black and sulfidic and affected the abundance and composition of the macrofauna community. In spring, it consisted of chironomids (444 ± 139 ind. m^{-2}), *C. insidiosum* (102 ± 550 ind. m^{-2}) and *A. succinea* (68 ± 47 ind. m^{-2}). These organisms disappeared in summer, except for a few large *A. succinea* individuals. At Site 4, in both seasons, denitrification was the dominant NO_3^- reduction pathway, as found at Site 1. However, under *in situ* NO_3^- levels, denitrification to DNRA ratios were lower at Site 4 than at Site 1 and averaged 1.7, suggesting a relatively higher relevance of DNRA in the more saline and organic impacted site. At Site 4 both denitrification and DNRA followed the Michaelis-Menten kinetic (Fig. 3.6, Table 3.4). Contrary to expectations, in summer potential denitrification rates increased, whereas

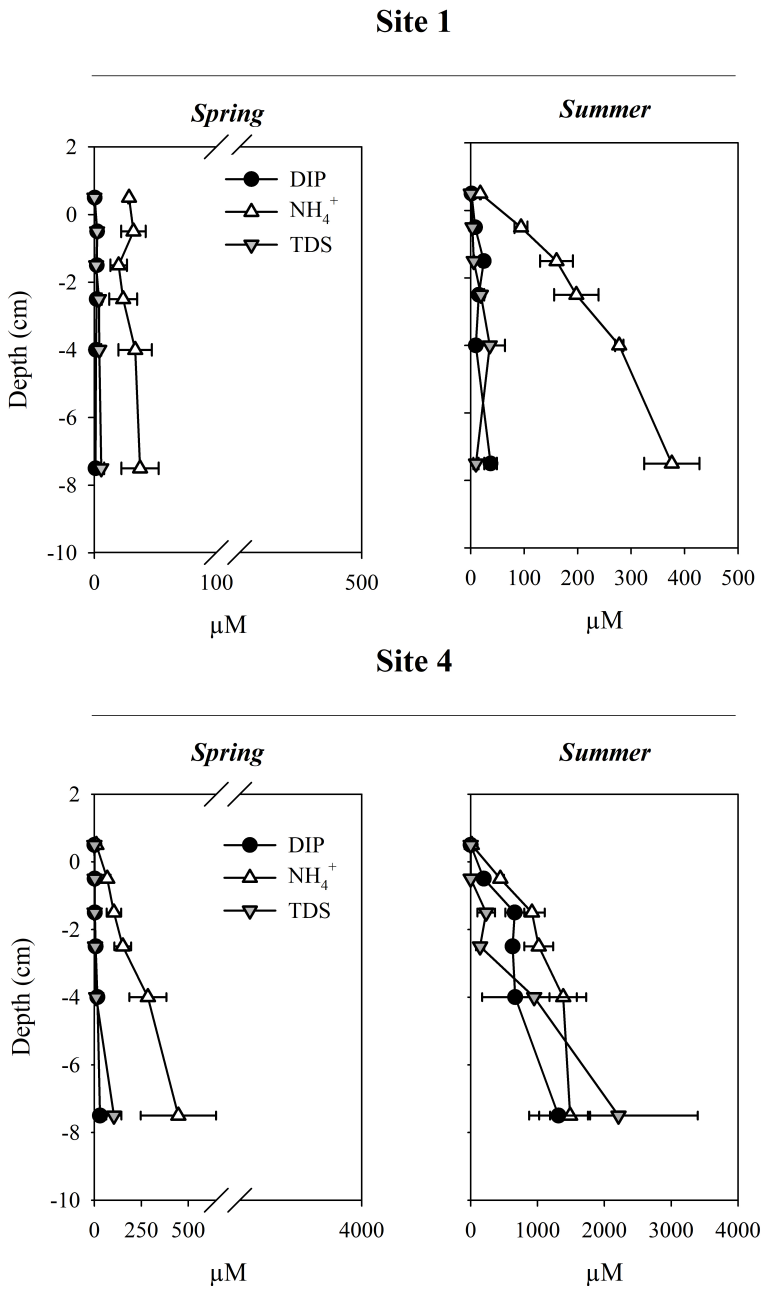

Figure 3.7: Vertical profiles of pore water dissolved inorganic phosphorus (DIP; black circles), ammonium (N-NH_4^+; white triangles) and total dissolved hydrogen sulfides (TDS; grey triangles) concentrations at the two sampling sites measured in spring and summer. Averages ± standard errors are reported. Note different scales on the x axis for the two sites.

DNRA rates decreased. This was surprising, since it is well known that in organic rich, sulfidic sediments DNRA is favored over denitrification (An & Gardner, 2002). Site 4 in summer was in fact characterized by a highly reduced environment that determined a steep increase in NH_4^+, DIP and TDS pore water concentrations (Fig. 3.7). The accumulation of labile organic matter deposits resulted in high mineralization rates, as suggested by the δ^{15}N-enriched values (Table 3.3, (Liu, 2006)), higher than previously reported for the Goro Lagoon (0.9-6.2‰, (Bianchini et al., 2015)). The large demand of electron acceptors and the scarce bioturbation activity likely resulted in quick O_2 and NO_3^- depletion in sediments. Mineralization and coupled nitrification-denitrification were disconnected, leading to large accumulation of NH_4^+ in pore water and its release to the water column (Fig. 3.7, Table 3.3). The black color of the sediment and the high DIP and TDS concentrations in pore water suggest that electron acceptors alternative to O_2 and NO_3^- as Mn^{4+} and Fe^{3+} oxyhydroxides were likely exhausted and that SO_4^{2-} reduction was the main anaerobic mineralization pathway (Canfield, 1994). The reduction of Mn and Fe oxyhydroxides determined the release of the co-precipitated P (Jensen et al., 1995), which accumulated in pore water, with concentrations that increased by a factor of 130 compared to spring Fig. 3.7. At the same time, the occurrence of large rates of dissimilatory microbial sulfate reduction lead to the saturation of the Fe^{2+} buffer, and to the accumulation of TDS in pore water (Giordani et al., 1996; Thamdrup et al., 1994). The TDS concentrations also increased by a factor of 100 from spring to summer (Fig. 3.7).

Free sulfides are generally considered as highly toxic to the denitrifiers community and a factor regulating the denitrification to DNRA ratio (Brunet & Garcia-Gil, 1996). The lack of denitrification inhibition at Site 4 can be explained by the nitrate reduction coupled to anaerobic sulfide oxidation by filamentous sulfur bacteria. The appearance of *Beggiatoa* in summer at this site, after the establishment of anoxic condition it has been reported in (Zilius et al., 2015). This group of bacteria occurs primarily in environments characterized by variable NO_3^- concentration, seasonal anoxia and high sulfide production in sediments (Jørgensen & Nelson, 2004). They colonize the sediment zone where neither O_2 nor TDS occur and migrate up and down through the anoxic but oxidized sediment layer to uptake the required NO_3^-. They catalyze sulfides oxidation both through nitrate reduction to N_2 and to NH_4^+, but the factors affecting their relative ratio are still unknown (Jørgensen & Nelson, 2004; Mußmann et al., 2003). Another possible explanation could derive by the presence of cable bacteria, which couple O_2 or NO_3^- reduction in superficial sediments to sulfides oxidation in deeper anoxic layers. These processes are separated over centimeter-long distances and redox coupling is ensured by long distance electron transport through these multicellular filamentous bacteria acting as conductors (Marzocchi et al., 2014).

At Site 4 the decreased DNRA rates in summer may be explained by a mechanism involving the interaction of DNRA with P, Fe and TDS. Dissolved P in pore water displayed concentrations 10 times higher than those previously recorded at the same site in summer (Zilius et al., 2015). Such high values suggest that accumulated free sulfides mobilized Fe bound phosphate, and precipitated the available iron as FeS, strongly limit-

ing Fe^{2+} bioavailability. The absence of Fe^{2+}, that can act as electron donor for DNRA, can therefore limit nitrate ammonification (Kessler, 2018; Roberts et al., 2014). As hypothesized by (Roberts et al., 2014), Fe^{2+} driven DNRA may play a key role in estuaries as the Goro Lagoon, which accumulates large amount of iron through sedimentation of colloidal material.

3.2.3 Conclusions

Results from this study suggest that pulse NO_3^- addition to the Goro Lagoon stimulate the response of denitrification in both low and high salinity areas and that denitrification capacity largely exceeds reasonable future NO_3^- concentration increase. They also suggest that larger NO_3^- availability in the water column leads to higher denitrification to DNRA ratio in both sites and seasons, even in sulfidic sediments with negligible bioturbation activity. The efficiency of the coastal filter depends on other factors besides the response of denitrifiers, as for example the water residence time in the lagoon which decreases during high discharge events.

An relevant result, which can be worth of future studies, deals with the response of the nitrate-reducer microbial community under prolonged drought periods with low NO_3^- transport. The projection of the identified saturation curves to low NO_3^- concentrations suggests a decrease in denitrification to DNRA ratios. This is expected at sulfidic sites as Site 4 and during summer more than during spring, following the drop in the macrofauna abundance and the exhaustion of inorganic electron acceptors as oxidized metals. Such outcomes are supported by the different K_m values for denitrification (higher than NO_3^- concentration generally measured in the water column) and for DNRA (within the range generally measured). From the perspective of community kinetics of denitrification and DNRA, high NO_3^- pulses result in a stimulation of processes leading to permanent N removal, whereas low NO_3^- inputs might favor DNRA and ammonium recycling, due to higher affinity of ammonifiers to NO_3^-.

3.3 The effects of bioturbation on P retention capacity

The role of bioturbation has been deeply and increasingly investigated in the last decades (Aller, 2014; Kauppi et al., 2018; Kristensen, 2000; Mermillod-Blondin et al., 2004). Benthic macrofunal populations through their feeding, bioturbation, burrow construction and sediment irrigation activities have profound influences on benthic functioning (Welsh, 2003). By enhancing the exchange of solutes between the sediment and overlying water, macrofauna supplies dissolved electron acceptors, alters the spatial and temporal distribution of microbial reactions, and lowers the buildup of potentially inhibitory metabolic products in sediments (Kristensen & Kostka, 2005). A widely recognized role of benthic macrofauna in aquatic ecosystems is the benthic-pelagic coupling, which is facilitated by excretion and bioturbation (Stief, 2013). The overall effect of bioturbating organisms on benthic dynamics can be affected by their different depths distribution (Kristensen & Kostka, 2005). Authors have put different accents on their research, either stressing mechanisms by which invertebrates improve organic matter mineralization or emphasizing macrofauna-associated ecosystem services as the control of eutrophication, by stimulating for example permanent or temporary nutrient removal (Kristensen & Kostka, 2005; Schratzberger & Ingels, 2018). The relationships between macrofauna bioturbation and benthic N cycle have been deeply studied. Studies on N dynamics along such gradients of organic matter and bioturbation have revealed a lower efficiency of denitrification along the organic matter enrichment, in particular in sulphidic sediments where nitrate ammonification can become dominant (An & Gardner, 2002). Little is known about reactive P dynamics along organic matter and bioturbation gradients in sediments, despite the strong dependency of P mobility on redox conditions and despite its relevance on the benthic nutrient stoichiometry as a driver of pelagic primary production.

In this study the effects of bioturbation on reactive P dynamics have been analysed in reconstructed sediments. Dissolved inorganic phosphorus (DIP) net fluxes across the sediment-water interface and pore water chemistry (DIP and metals –Fe^{2+} and Mn^{2+}-concentrations, Eh and pH) have been measured in non-bioturbated sediments (control), and in sediment with bioturbating organisms characterized by a different depth distributions: the surface burrower *Corophium insidiosum*, that colonized the sediment up to 5 cm depth, and the deep burrower *Alitta succinea* that can reach 10-15 cm deep, and in sediments with both macrofauna species. It has been hypothesized that: (1) bioturbated sediments recycle more reactive P than non-bioturbated sediments, due both to macrofauna excretion and advective transport from pore water to the water column due to bioirrigation; (2) bioturbation increases the oxidation status of sediments, and therefore their buffer capacity against massive, oxygen and redox-dependent DIP release under transient anoxia.

3.3.1 Material and methods

Sampling procedure and microcosms set-up

In April 2021, sediment, water and macrofauna were collected from the western portion of the Goro Lagoon (Site 1, Fig. 3.1). The sediments at the sampling site are muddy-clayish and characterized by a density of $1.41 \pm 0.02\,\mathrm{g\,cm^{-3}}$, a porosity of 0.68 ± 0.01 and a percentage of organic matter of 5.90 ± 0.20. As displayed both in section 3.1 and 3.2, in spring, this area is highly bioturbated by surface burrowers, the amphipod *C. insidiosum* and deep burrowers, the polychaete *A. succinea* (Bartoli, Castaldelli, Nizzoli & Viaroli, 2012; Politi et al., 2019). Macrofauna specimens were retrieved by means of plexiglass liners and immediately brought to the laboratory. Here, nearly 15 L of the collected sediment was sieved (500 µm-mesh) to remove large debris and other occasional macrofauna, and gently mixed to a slurry. Once the sediment settled down, 24 bottom capped Plexiglass liners (i.d. 4.6 cm, length 20 cm) were filled with about 10 cm sediment. Thereafter *in situ* water was gently added, after positioning on the sediment surface a floating polystyrene disc to avoid sediment resuspension. At the end of this procedure, 24 identical reconstructed sediment cores were obtained and left for two days to settle in a tank containing *in situ* aerated water. Cores were divided into four experimental treatments each consisting of 6 replicates: control with defaunated sediment (C), sediment with amphipods (*C. insidiosum*) (A), sediment with polychaetes (*A. succinea*) (P) and sediment with both species (AP). Twelve amphipods and four polychaetes were added to sediment cores of treatments A and P, corresponding to $7900\,\mathrm{ind.\,m^{-2}}$ and $2600\,\mathrm{ind.\,m^{-2}}$, respectively, and mimicking *in situ* density (Bartoli, Castaldelli, Nizzoli & Viaroli, 2012). Treatment AP included both species with the same number of organisms of treatments A and P. Macrofauna started digging immediately after addition, and tubes and burrows were visible in all treatments after three days. In all cores a magnetic bar was fixed 6 cm above the sediment interface to stir water, avoiding sediment resuspension. For the acclimatization cores were submerged with the top open in a darkened aerated *in situ* water tank, which was provided with a central magnet rotating at 40 rpm and driving all magnets inside the cores to ensure water exchange with the tank. Water temperature was fixed at $19 \pm 1\,^{\circ}\mathrm{C}$ as *in situ* temperature. Cores were preincubated for 12 days in the darkness to avoid microphytobenthos growth in aerated tanks to allow bacterial communities to grow along sediment horizons and along the new burrow walls built by macrofauna and therefore the chemical gradients to reestablish. Water temperature and salinity were measured continuously by means of a multiple probe to maintain steady state conditions. Animals were fed by adding regularly phytoplankton to the water, which was renewed every two days to maintain *in situ* conditions in term of suspended matter, nutrient concentrations and chemical gradients across the sediment-water interface.

Benthic flux measurements

Benthic fluxes at the sediment-water interface were measured 12, 15, and 19 days after the starting of the preincubation. The short-term batch incubations followed the procedure described in section 3.1.1. At the beginning and at the end of the incubation, water

samples were collected from each core and transferred via over flushing to 12-mL exetainers to measure dissolved O_2 concentration (Winkler, 1988). An aliquot was filtered and transferred into 5-mL glass vial to measure dissolved inorganic phosphorus (DIP) using standard spectrophotometric techniques (Grasshoff et al., 1983). Dissolved solute fluxes were calculated according to the equation 3.1.

Solid-phase and pore water extractions

At the end of incubations, cores were sliced in two layers at 0–3 and 3–6 cm intervals. Briefly, the sediment was extruded and sliced in a N_2 filled glow bag. At each layer, pH and redox potential were measured by means of a pHmeter (Radiometer Copenhagen). Sediment was then homogenized and 1 mL was collected via cut-off syringe and transferred to a pre-weighed 40-mL vial containing 5 mL of 0.5 M HCl to measure solid Fe phase following the method described in (Lovley & Phillips, 1987). Extractable reduced Fe, Fe^{2+}, was analyzed using ferrozine as spectrophotometric reagent (Stookey, 1970). The remaining sediment was transferred to 50-mL plastic tubes, closed under N_2-atmosphere and then centrifuged to extract pore water. The supernatant was filtered, and an aliquot was immediately transferred to 6-mL exetainers added with concentrated HNO_3 (1%) for ferrous iron and manganous manganese analyses via atomic absorption (Varian, Model AA240 Atomic Absorption Spectrometer). Another aliquot of pore water was collected for DIP and TDS spectrophotometric analyses (Cline, 1969; Grasshoff et al., 1983).

Statistical analysis

Two-way repeated measures ANOVA was applied to flux measurements. Factors treatment and time (day) were the fixed parameters, whereas replicates were set as random effects. Two-way analysis of variance was applied to pore water parameters. Factors treatment, layers and their interaction were tested. When ANOVA assumptions were not met, a $\log_{10}$ transformation was applied. All pairwise multiple comparison were performed with Holm-Sidak method. All statistical analyses were performed with R software v. 3.5.1 (R Core Team, 2018). Graphs were made with Sigma Plot 11.0.

3.3.2 Results and discussion

Oxygen and DIP fluxes

Oxygen fluxes significantly differed among treatments ($p = 0.002$) and days ($p < 0.001$, Fig. 3.8a). The stimulation of sediment oxygen demand (SOD) in cores added with amphipods and polychaetes has been reported in different studies and is due to the respiration of the added macrofauna, to the new sediment surface (e.g., burrow walls) where aerobic respiration can occur and to microbially mediated or chemical oxidations (Bartoli et al., 2020; Nizzoli et al., 2007; Pelegri & Blackburn, 1995a). Oxygen (and phosphate) fluxes were higher in all treatments during the first of the three sequential incubations possibly due to larger pools of labile organic matter, that decreased along with core aging

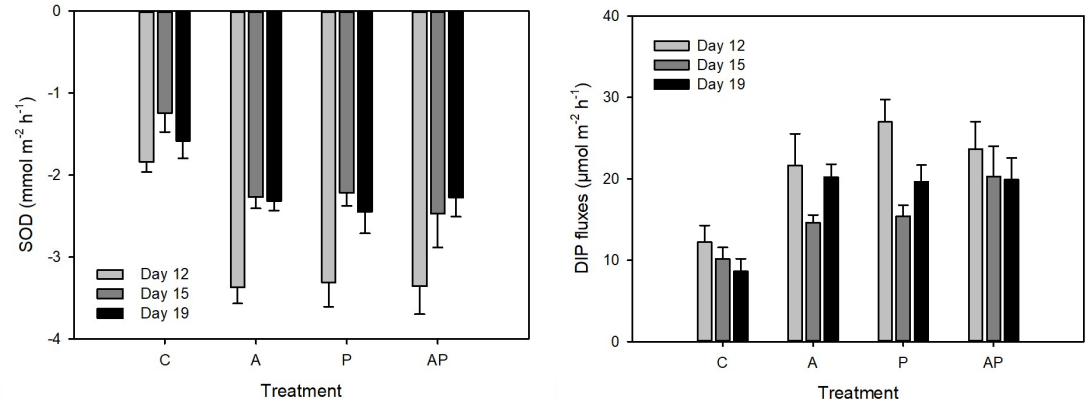

(a) (b)

Figure 3.8: Sediment O_2 demand (a) and DIP fluxes (b) measured during the three dark incubations carried out after 12, 15 and 19 days from cores setup. C = control, A = amphipods, P = polychaetes, AP = amphipods + polychaetes. Averages ± standard errors are reported ($n = 6$).

resulting in lower microbial activity during the second and third incubation. However, the relative difference of fluxes among treatments were consistent in the three incubations (Fig. 3.8a).

Sediment oxygen demand increased by a factor of 1.7 in bioturbated cores ($-2.67 \pm 0.24\,\mathrm{mmol\,m^{-2}\,h^{-1}}$, $n = 18$ as fluxes were not different among bioturbated sediments) compared to control cores ($-1.55 \pm 0.19\,\mathrm{mmol\,m^{-2}\,h^{-1}}$, average±standard error, $n = 6$). (Nizzoli et al., 2007) report a similar stimulation of oxygen consumption in intact sediments collected from the same site, incubated at similar temperatures and added with *A. succinea*. They added variable numbers of the polychaete to intact, already bioturbated sediment, and report respiration rates of control cores (i.e., naturally bioturbated) of $-4.20 \pm 0.20\,\mathrm{mmol\,m^{-2}\,h^{-1}}$. Such value, much higher than those reported in this study, suggests either large losses of labile organic matter during sediment sieving or higher *in situ* densities of macrofauna. Also, (Moraes et al., 2018) measured a higher sediment oxygen demand ($-7.60 \pm 0.96\,\mathrm{mmol\,m^{-2}\,h^{-1}}$) in intact cores from the same site with *C. insidiosum* density much lower than that tested in this study ($4500 \pm 666\,\mathrm{ind.\,m^{-2}}$ versus $7900\,\mathrm{ind.\,m^{-2}}$). This difference supports the evidence that reconstructed cores display lower microbial activity than intact cores, likely to due significant decrease of labile carbon pools, as will be detailed in section 3.4.

DIP fluxes differed among treatments ($p < 0.001$) but not among days. In presence of macrofauna DIP fluxes (15-27 $\mu\mathrm{mol\,m^{-2}\,h^{-1}}$) almost doubled those measured in control cores (8-12 $\mu\mathrm{mol\,m^{-2}\,h^{-1}}$) (Fig. 3.8b). The benthic system was always a net source for DIP, as reported also by (Nizzoli et al., 2007) that found values ranging from 32 to 72 $\mu\mathrm{mol\,m^{-2}\,h^{-1}}$ and by (Moraes et al., 2018) that found values ranging from 13 to 62 $\mu\mathrm{mol\,m^{-2}\,h^{-1}}$.

The absolute values of the molar ratio between SOD and DIP fluxes, calculated for all treatments, is reported in Fig. 3.9. Three identical symbols per treatments indicate the three incubations. The dotted line represents a theoretical reference line for SOD:DIP ratios reflecting the Redfield value of 106, assuming SOD:CO_2=1:1 (Glud, 2008). Such assumption is reasonable as the sampling area receives chlorophyll a rich-waters from the Po di Volano River and is itself a diatom-dominated area of the lagoon, devoid of macroalgae and rooted plants (Viaroli et al., 2006). We therefore hypothesize that organic inputs to sediments at this site are mainly represented by phytoplankton. Two-way ANOVA on the SOD:DIP ratios, with days and treatments as factors, suggest no significant differences and no significant interactions among factors. This means a constant ratio between benthic respiration and phosphate regeneration, regardless the presence or absence of burrowing macrofauna and their functional role (surface versus deep burrowers). This also means that the regeneration of DIP at the study site is mainly driven by oxygen consumption (higher in bioturbated sediments) and it is not influenced by other indirect, bioturbation-related effects (e.g., Fe^{2+} oxidation and restoration of the iron buffer). The latter might have favored DIP retention via iron hydroxide complexes, resulting in much lower DIP fluxes in bioturbated versus non bioturbated sediments. Higher respiration at the bioturbated treatments include the respiration of the macrofauna. Analogously, higher DIP fluxes in bioturbated treatments include DIP excretion by macrofauna. SOD:DIP ratios in bioturbated sediments align with those of control cores, suggesting at this site similar stoichiometry between oxygen consumption and DIP production from microbes, amphipods and polychaetes. The pooled SOD:DIP ratios (all treatments and all sampling days) range 66-718 (min-max), with a median value of 126 (interquartile range 104-176), and suggest either higher C:P of the original organic matter or a slight retention within sediments of DIP, similar in all treatments and close to 15-20% of the total DIP regenerated.

Pore water profiles

The overall effects of treatment, depth and their interaction were significant for the porewater concentrations of DIP, Fe^{2+} and Mn^{2+} (Table A.2). Solute concentrations were higher in the deepest layer in all treatments. DIP and dissolved metals pore water profiles in bare sediment (C) were significantly different compared to other treatments (Fig. 3.10a,b,c). Lower DIP and metals concentrations were observed at both sediment depths in presence of bioturbating fauna when compared to control. Between layers, the highest concentrations of DIP, Fe^{2+} and Mn^{2+} were found in the 3-6 cm layer. However, the presence of the deep burrower *A. succinea* significantly decreased solute concentrations in the pore water, compared to control and to sediments inhabited by amphipods (with DIP as exception). This result suggests that polychaetes either promote reduced solute forms removal because of pore water replenishment or introduce oxidized bottom water deep into the sediment increasing the oxidization of manganous manganese and of ferrous iron and the consequent coprecipitation of phosphorus. Sediment oxidation by macrofauna was visible by eye due to the light brown color of the sediment along burrows.

Pore water pH and redox potential differed between treatments and layers (Table

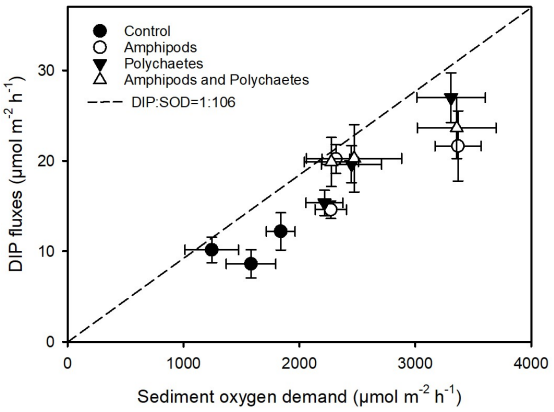

Figure 3.9: Relationship between measured sediment O_2 demand and DIP fluxes. Different symbols indicate different treatments; same symbols are reported for the three incubations. The dotted line represents a theoretical reference line for SOD:DIP ratios reflecting the Redfield value of 106, assuming SOD:CO_2=1:1.

A.2). Values of pH were higher in the deepest layer in all treatments, except in the control (Fig. 3.10d). The more acidic environment might be due to the higher rates of organic matter mineralization in the deep layer compared to the surficial one, producing CO_2 and carbonic acid. Also the concentrations of DIP and reduced Fe and Mn forms were higher in the deeper layer. These results are also sustained by the more negative redox potential measured in the deepest layer, suggesting more reducing conditions in 3-6 cm layer (Fig. 3.10e). Bare sediment displayed the highest (more negative) redox potential compared to bioturbated sediments. Bioturbation resulted in less chemically reduced sediments in both analyzed layers.

Sedimentary Fe pools

Data on the solid phase iron extraction are rather variable, because of sample heterogeneity due to the method applied for the analysis. In the short period of the experiment, this heterogeneity has a higher effect compared to the digenetic processes that naturally occur in sediments. The concentration of the solid phase iron fraction was about 3 orders of magnitude higher than the dissolved fraction in these sediments. Results showed no effect of treatment in Fe_{tot} profiles; however, it differed between the two layers (Table A.2). In the presence of polychaetes the total Fe was lower in the deeper layer compared to the surficial one (Fig. 3.11). The percentage of ferric iron tended to increase in the deepest layer in presence of macrofauna, suggesting that other electron acceptors are used in this portion of sediment inhabited by deep burrowers that can pump deeper oxygenated water. On the contrary, in the control sediment ferric iron tended to be higher in the surficial sediment, suggesting an exhaustion of this electron acceptor in the deeper layers.

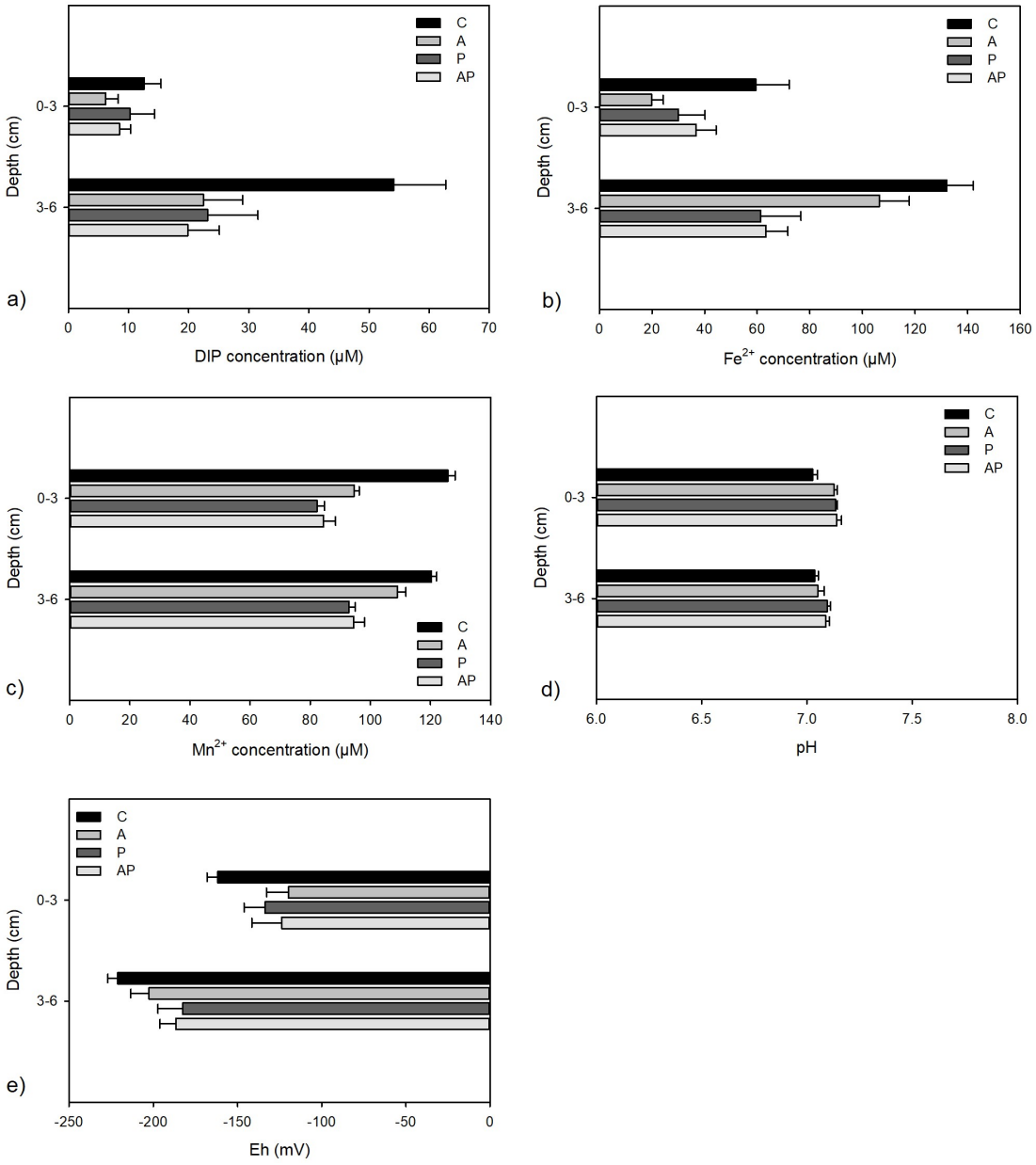

Figure 3.10: Pore water profiles of DIP (a), Fe^{2+} (b), Mn^{2+} (c), pH (d) and redox potential (e) at the end of the experiment (C = control, A = amphipods, P = polychaetes, AP = amphipods + polychaetes). Averages ± standard errors are reported ($n = 6$).

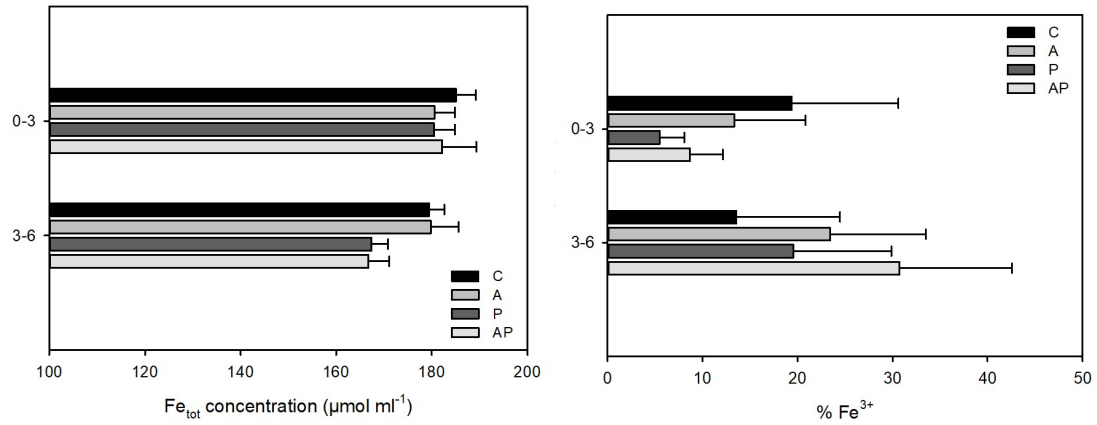

(a) (b)

Figure 3.11: Solid phase profiles of total HCl extractable Fe (a) and the percentage of ferric iron over total Fe (b) at the end of the experiment (C = control, A = amphipods, P = polychaetes, AP = amphipods + polychaetes). Averages ± standard errors are reported ($n = 6$).

3.3.3 Conclusions

The presence of bioturbating organisms seems to have a double effect on P dynamics. DIP effluxes increase in bioturbated compared to bare sediment, although in the latter pore water DIP concentration was the highest. These results suggest that these organisms, the deep burrower *A. succinea* in particular, either via the direct excretion or advective transport due to bioirrigation promotes the efflux of phosphate to the water column. At the same time the lower concentration of DIP and reduced Fe and Mn in pore water in bioturbated compared to bare sediments, indicate low reduction rates and fast DIP, Mn^{2+} and Fe^{2+} removal by sorption or co-precipitation processes (Ferro et al., 2003). Bioturbation increase the oxidation status of sediments, and therefore their buffer capacity against massive, oxygen and redox-dependent DIP release under transient anoxia. Non-bioturbated sediments on the contrary display limited DIP release due to the upper oxidised sediment horizon but accumulate large DIP amounts in the pore water. In this case, transient O_2 shortage may result in the disappearance of such superficial horizon and in dramatic release of large DIP amounts to the water.

3.4 The impacts of bioturbation in intact and reconstructed sediments[2]

Bioturbation by macrofauna is a fascinating topic that has fueled a diversified body of scientific research (Kristensen & Kostka, 2005; Stief, 2013; Welsh, 2003). Macrofauna couple the pelagic and benthic environments in various ways. For instance, feces and pseudofeces deposition by filter feeders, containing viable and active phytoplankton, displaces pelagic primary production at the sediment level (Gergs et al., 2009). Filter feeders activity, such as that of clams, may process the entire water column of shallow water bodies many times per day, assuring water transparency, increased light penetration, and benthic primary production (Swanberg, 1991; Vaughn & Hakenkamp, 2001; Volkenborn et al., 2016). Filter feeders also excrete large amounts of the mineralized phytoplankton biomass back into the water column (Benelli et al., 2017; Nizzoli et al., 2011). Biodeposits can increase the organic content of sediments and stimulate both aerobic and anaerobic metabolic pathways (Murphy & Reidenbach, 2016). Filtration and excretion thus have the potential of maintaining pelagic and benthic primary production elevated. Deposit feeders, such as polychaete worms, explore surficial or deep sediment horizons to extract food and avoid predation. As O_2 penetration in sediments is extremely limited, burrowing macrofauna have evolved different ways to cope with anoxia and potentially toxic concentrations of compounds such as ammonia or sulfide. Burrow architectures may vary among species, but most deposit feeders ventilate their burrows by injecting and circulating oxic bottom water or by extracting pore water from sediments (Benelli et al., 2018; Kristensen & Kostka, 2005). Such a need to get rid of metabolic end-products and to import O_2 for their own respiration produces different biogeochemical side-effects on sediments (Volkenborn et al., 2016). For example, the volume of oxidized sediments in bioturbated areas is much higher than that in their not bioturbated counterparts, which means that the oxidation status of different elements is different depending on the presence of macrofauna. Ecosystem-level implications are multiple as oxidized sediments may retain elements avoiding their release to the water column or favor their permanent loss via coupled oxic–anoxic processes (Hölker et al., 2015; Moraes et al., 2018).

Research activities in the field of bioturbation, with the aim of understanding density-dependent effects of macrofauna on selected processes, have largely adopted experimental approaches based on the addition of a single species to reconstructed sediments (e.g., sieved or freeze-thaw in order to remove other macrofauna species, homogenized and packed back into microcosms) (Bonaglia et al., 2013; De Backer et al., 2011; Nizzoli et al., 2007; Svensson et al., 2001). Results from this kind of studies have allowed to understand how important is macrofauna for a number of biogeochemical processes, including rates of aerobic and anaerobic microbial respiration, nutrient recycling, reworking and mixing of new and old organic matter and oxidation of chemically-reduced metal pools (Kauppi et al., 2018; Pelegrì & Blackburn, 1994; Stocum & Plante, 2006). The level of

[2]Results of this study have been published in: Bartoli, M., Benelli, S., **Magri, M.**, Ribaudo, C., Moraes, P. C., and Castaldelli, G. (2020). Contrasting effects of bioturbation studied in intact and reconstructed estuarine sediments. *Water*, 12(11), 3125.

enhancement or inhibition of specific processes operated by macrofauna and measured with such approaches has been likely used to calibrate models, to upscale processes under varying macrofauna density or to propagate the effects to the water column (Braeckman et al., 2010). However, such approach may lead to a partial understanding of the true effect of macrofauna due to multiple factors. One of them is the absence of other macrofauna groups that may compete with, facilitate or inhibit the target species. Another is the time taken for an organism living in sediment, which is necessary to engineer the environment and, therefore, to change the chemical conditions and the biological communities (e.g., meiofauna and microbes).

In this study, to test the reliability of data collected using this experimental procedure aerobic, anaerobic (denitrification) and total respiration and nutrient fluxes have been measured in intact and reconstructed sediment collected from two areas dominated by filter and deposit feeding organisms. It has been hypothesized that: (1) processes measured under *in situ* conditions, may deeply differ from those measured shortly after sediment manipulation and macrofauna addition; (2) the extent of differences may depend on the macrofauna functional groups.

3.4.1 Material and methods

Sediments sampling

Reconstructed sediments Sediments and water were collected in July at Site 1 and Site 3 (Fig. 3.1). Site 1 was dominated by the polychaete *A. succinea*, whereas Site 3 is located within a licensed area and was dominated by the clam *R. philippinarum*. At each site, nearly 50 L of sediments and 100 L of water were collected. Water and sediments were brought to the laboratory within 2 hours. Here, sediments from the two sites were i) sieved (500 µm) in two tanks containing *in situ* water to remove large macrofauna, ii) homogenized and iii) left to settle during 3 days. The tanks with sieved sediments were maintained in the dark at *in situ* temperature, and the overlying water was kept oxic by air bubbling. Individuals of *A. succinea* and *R. philippinarum* retrieved during the sieving were maintained alive in separate small aquaria with a few cm of sediments and 10 cm of well aerated water phase. After 3 days, 9 cores (Plexiglass liners, i.d. 8.4 cm, length 30 cm) were subsampled from each tank. Water and sediment phases were subsampled by pushing vertically transparent liners in the tanks. Once retrieved, all cores were levelled in order to have a sediment height of 10 cm and a water column of 17 cm. Cores with muddy sediments from Site 1 were treated as follows: 3 cores were used as control, 3 cores were added with 3 individuals of *A. succinea* and 3 cores were added with 6 individuals of *A. succinea*, to reproduce densities (600 and 1200 ind. m^{-2}, respectively) comparable to those measured *in situ*. In a few minutes all added polychaetes burrowed in the sediments. Cores with sandy sediments from Site 3 were treated as follows: 3 cores were used as control, 3 cores were added with 2 clams (*R. philippinarum*) and 3 cores were added with 4 clams, to simulate densities at farmed areas (400 and 800 ind. m^{-2}, respectively). Within 30 minutes from clams addition all organisms burrowed within the sand and only siphons were visible. All 9 + 9 cores were provided with stirring units,

submersed in separate incubation tanks containing aerated and well mixed water from the 2 sites inside a temperature-controlled room and maintained in the dark at *in situ* temperature (25 °C).

Intact sediments After a week, a second sediment and water sampling was carried out. Both at Site 1 and 3, 6 cores (Plexiglass liners, i.d. 8.4 cm, length 30 cm) were randomly collected by hand for flux and denitrification measurements and 5 cores (Plexiglass liners, i.d. 4.6 cm, length 20 cm) were collected for sediment characterization. Besides intact sediments, nearly 80 L of water from each site was collected for preincubation and incubation periods. Water column temperature, O_2, pH and salinity were measured at the two sites by means of a multiple probe. All the material was brought to the laboratory within 2 hours. Here, intact sediment cores from the two sites were submersed into two tanks containing *in situ* aerated and well mixed water inside a temperature controlled room maintained in the dark at *in situ* temperature. Intact cores for flux measurements were provided with a rotating magnet, suspended 6 cm above the sediment-water interface driven by an external motor at 40 rpm.

Dark incubation for benthic flux and denitrification measurements

Five days after macrofauna addition in reconstructed sediments and after an overnight preincubation of the intact sediments, two sequential dark incubations were performed for the measurements of net solute fluxes across the sediment-water interface and of denitrification rates. During the first incubation, measurements of benthic fluxes of dissolved O_2, dissolved inorganic carbon (DIC), N_2 and dissolved inorganic nitrogen (DIN $= NH_4^+ + NO_2^- + NO_3^-$) were performed with a start-end approach as described in section 3.1.1. The incubation lasted between 2 and 3 hours. At time zero water samples ($n = 4$) were collected from each incubation tank. At time final water samples were collected from each core water phase through a valve in the cores lid. Incubation started when gas-tight lids were positioned on the top of each core. Both at the beginning and the end of incubation a 20 mL water sample was disposed in 12-mL exetainers and added with Winkler reagents for O_2 measurements (Winkler, 1988), 20 mL was disposed in 12-mL exetainers for DIC determination, which was measured with 0.1 N HCl titration with an automatic titration unit (ABU91, Radiometer, DK) and a combined pH sensor (Andersen et al., 1986). An aliquot of 20 mL was filtered and transferred to scintillation vials for DIN analysis, that were performed spectrophotometrically as described in section 3.1.1. Fluxes were calculated according to equation 3.1.

After the incubation for flux measurements, lids were removed, the water in each tank was renewed and the cores were submersed. Cores were maintained open, with the stirring on in *in situ* oxygenated and well mixed water in the dark and at the *in situ* temperature. Approximately 5 h later denitrification measurements started. Labelled NO_3^- was added to the water column of each core in order to have a final ^{15}N atom % of 50%, according to the IPT (Nielsen, 1992). Before and after 5 minutes from the addition of the labelled NO_3^- a subsample of the water phase was collected to determine the ^{15}N-enrichment of the NO_3^- pools. The incubation length of the denitrification experiment overlapped that

of flux measurements. At the end of the incubation the cores were opened, slurred and samples were collected for labelled N_2 analyses via MIMS (Kana et al., 1994). Water samples for labelled N_2 analyses were poisoned with $ZnCl_2$ to stop microbial activity. Rates of total denitrification (D_{tot}), denitrification coupled to nitrification (D_n) and water column nitrate-driven denitrification (D_w) were calculated as described in section 3.1.1. Denitrification Efficiency (DE) was calculated as the ratio between denitrification and cumulative flux of N from sediment (N_2 + DIN) and expressed in percentage as described in section 3.1.3 and reported in (Eyre & Ferguson, 2009). At the end of the incubations, the slurry in each core was sieved (0.5 mm) to collect all macrofauna; macrofauna was recognized, and dry weight was quantified after drying the soft tissue at 80 °C to a constant weight.

Statistical analysis

Differences among net solute fluxes or denitrification rates measured in the intact cores of the 2 sites and in the reconstructed cores of C (control), L (low density) and H (high density) treatments were tested via one-way analysis of variance (ANOVA) followed by the post-hoc Holm Sidak test. The dependency of solute fluxes or denitrification rates on macrofauna biomass were tested using linear regression analysis. Normality of residuals was confirmed numerically with a Shapiro-Wilks test.

The comparison of regressions between the biomass and measured process rates or calculated respiratory quotients and denitrification efficiency in intact and reconstructed cores were performed via analysis of covariance (ANCOVA). Statistical significance was set at p level lower than 0.05. All statistical analyses were performed with R software v. 3.5.1 (R Core Team, 2018). Graphs were made with Sigma Plot 11.0.

3.4.2 Results and discussion

General features of the study sites

Site 1 had soft, organic sediments, with lower density and higher porosity, organic matter, C and N content as compared to Site 3 (Table 3.5). The biomass of macrofauna was one order of magnitude higher at Site 3 mostly due to high size of the cultivated *R. philippinarum*. At Site 1 the dominant organism retrieved from sediments was the deep burrower *A. succinea*, with a density of $870 \pm 530\,\mathrm{ind.\,m^{-2}}$. Besides *A. succinea*, the macrofauna community at Site 1 included other small polychaetes and occasional individuals of *C. insidiosum*, *Chironomus salinarius*, *Hydrobia* spp. and *Capitella capitata*, whose pooled biomass was <10% of the total. At Site 3, *R. philippinarum* dominated the macrofauna community, with a density of $630 \pm 490\,\mathrm{ind.\,m^{-2}}$. Besides clams, sediments hosted also a few individuals of *C. insidiosum* and *Echinogammarus* spp., whose pooled biomass was <1% of the total. Site 1 was influenced by the freshwater inputs of the Po di Volano and had lower salinity and higher concentrations of DIN as compared to Site 3, with NO_3^- as dominant chemical species.

Table 3.5: Main sediment and water column characteristics at the two sampling sites. Averages standard errors ($n = 4$) are reported.

Parameter	Site 1	Site 3
	Water column	
T (°C)	25	25
Salinity	5	17
NH_4^+ (µM)	1.8 ± 0.3	14.6 ± 1.7
NO_2^- (µM)	6.6 ± 0.5	1.3 ± 0.4
NO_3^- (µM)	31.7 ± 3.4	3.2 ± 1.1
	Sediments	
Type	Clayish-mud	Sand
Porosity	0.74 ± 0.06	0.47 ± 0.01
TN (%)	0.20 ± 0.01	0.04 ± 0.01
C_{org} (%)	1.79 ± 0.04	0.35 ± 0.02
C:N (mol:mol)	10.44 ± 0.32	10.20 ± 0.53

Benthic respiration, DIN fluxes and rates of denitrification in intact cores

Respiration rates tended to be higher at Site 3, dominated by *R. philippinarum*, however differences were not significant (Fig. 3.12). Similar net O_2 uptake and DIC release at the two sites, despite large difference in organic matter content, were probably the result of much higher contribution of macrofauna metabolic activity at the sandy Site 3, sustained by clams. Both Sites recycled large and not statistically different amounts of NH_4^+. At the muddy, organic rich Site 1 such amounts are likely sustained by high microbial ammonification whereas at Site 3 such amounts are likely excreted by clams (Nizzoli et al., 2007). Net inorganic carbon to NH_4^+ efflux ratios averaged 6.9 ± 0.7 and 13.9 ± 4.7 at Site 1 and 3, respectively, suggesting in general the labile nature of the available organic matter. The low ratio measured at Site 1, very close to that of phytoplankton, may be due to much higher rates of NH_4^+ oxidation within sediments via nitrification (Moraes et al., 2018). This is confirmed by higher net NO_2^- and NO_3^- fluxes, averaging $119 \pm 5\,\mu mol\,N\,m^{-2}\,h^{-1}$ and $122 \pm 15\,\mu mol\,N\,m^{-2}\,h^{-1}$, respectively, and by denitrification rates of NO_3^- produced within sediments, all significantly higher at Site 1. Elevated nitrification rates at Site 1 are supported by the activity of burrowers, increasing O_2 availability within NH_4^+-rich pore waters, as reported in sections 3.1 and 3.2 (Boesch, 2002; Pelegri & Blackburn, 1995b; Svensson et al., 2001). Rates of total denitrification were higher at Site 1 due to higher denitrification coupled to nitrification and to higher denitrification of water column NO_3^- (Table 3.5). Denitrification efficiency was higher by a factor of 3 at Site 1 (15%) than at Site 3, due to similar NH_4^+ regeneration but much higher denitrification. Despite such difference, at both sites the major dissolved inorganic N flux was towards the water column as recycled NH_4^+, whereas the fraction lost to the atmosphere was minor.

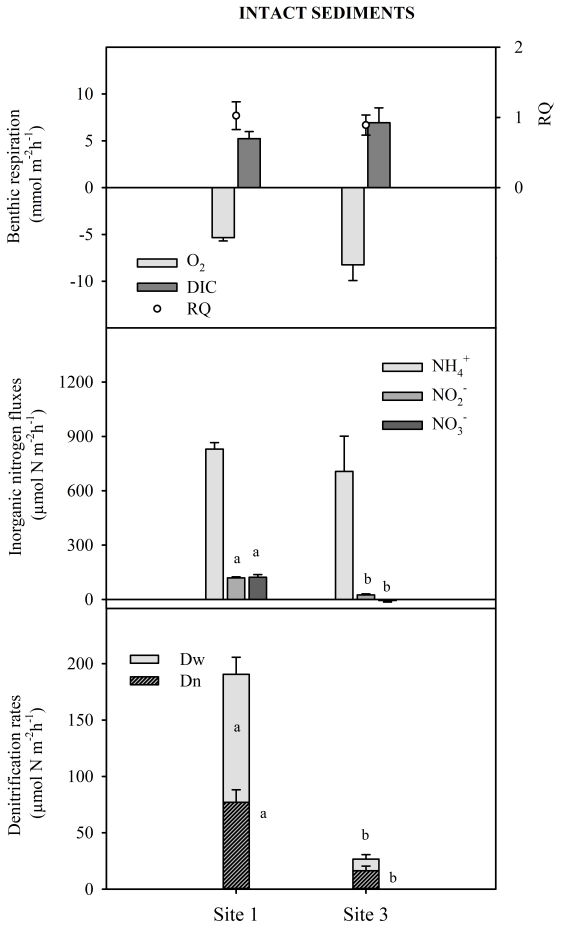

Figure 3.12: Dark fluxes of dissolved O_2 and dissolved inorganic carbon (DIC), dissolved inorganic nitrogen (DIN), and rates of denitrification measured in intact sediment cores at the two sites. In the upper panel, the y-axes on the right reports the respiratory quotient (RQ), calculated as the ratio between DIC and O_2 fluxes (absolute value). Where present, letters above bars indicate statistically significant differences. Averages standard errors ($n = 6$) are reported.

Benthic respiration, DIN fluxes and rates of denitrification in reconstructed cores

Increasing densities of *A. succinea* and *R. philippinarum* in reconstructed sediments significantly stimulated benthic respiration, including the consumption of O_2 and the production of DIC (Fig. 3.13). The degree of stimulation of O_2 and DIC fluxes was different along with the density gradient, resulting in an increase of the respiratory quotient, approaching the unit in the high density treatment. Both macrofauna functional groups largely enhanced NH_4^+ regeneration, whereas their net effects on NO_2^- and NO_3^- fluxes were less marked likely due to simultaneous stimulation of multiple microbial processes (e.g., nitrification and denitrification, Fig. 3.13) (Bartoli et al., 2001). The IPT revealed a significant effect of *A. succinea* on the removal of water column NO_3^- via denitrification (D_w), whereas the same was not apparent with *R. philippinarum* (Nizzoli et al., 2007). Both macrofauna groups did not stimulate denitrification coupled to nitrification (D_n) (Fig. 3.13). In reconstructed cores denitrification efficiency tended to decrease along with increasing macrofauna densities ($p = 0.088$ and $p = 0.152$ for *A. succinea* and *R. philippinarum*, respectively) confirming a major effect of both deposit-feeding and filter-feeding macrofauna biomass on N recycling than on N losses (Stief, 2013). Denitrification efficiencies overlapped values determined in intact cores and averaged 15% (range 11-18%) and 5% (range 2-8%) in the *A. succinea* and *R. philippinarum* treatments, respectively.

These results allow to perform simple linear regressions between measured process rates and macrofauna biomass to calculate the degree of enhancement of a certain process (Table 3.6 and Table 3.7). The biomass of added *A. succinea* ($10 \pm 4\,g_{dw}\,m^{-2}$ and $21 \pm 5\,g_{dw}\,m^{-2}$ for L and H, respectively) was an order of magnitude lower than that of added *R. philippinarum* ($222 \pm 38\,g_{dw}\,m^{-2}$ and $410 \pm 69\,g_{dw}\,m^{-2}$ for L and H, respectively), however the effects produced on benthic biogeochemistry was comparable, except for denitrification rates. Burrowing *A. succinea* contributed less to respiration and excretion than *R. philippinarum*, but produced a much larger effect on microbial activity, that compensated the different biomass. This interpretation is supported by the higher degree of stimulation of D_w by *A. succinea*. Denitrification in fact is not performed by deposit-feeding macrofauna but by the microbes growing along burrows that take advantage from the macrofauna-mediated bioirrigation, transporting NO_3^--rich water within sediments (Benelli et al., 2019; Benelli et al., 2018; Pelegrì & Blackburn, 1994). Burrowing and ventilation activities moreover mobilize pore water solutes as NH_4^+, which is released in large amounts in *A. succinea* L and H treatments. Fluxes measured in sediments with *R. philippinarum* are likely sustained by clams excretion (Murphy et al., 2018; Welsh et al., 2015).

Macrofauna stimulate differentially biogeochemical processes in intact and in reconstructed sediments

Table 3.6 and Table 3.7 report the slopes of linear regressions between measured fluxes or calculated rates and biomass of *A. succinea* and *R. philippinarum* in intact and reconstructed cores, whereas Table 3.8 reports the results of ANCOVA where such regressions

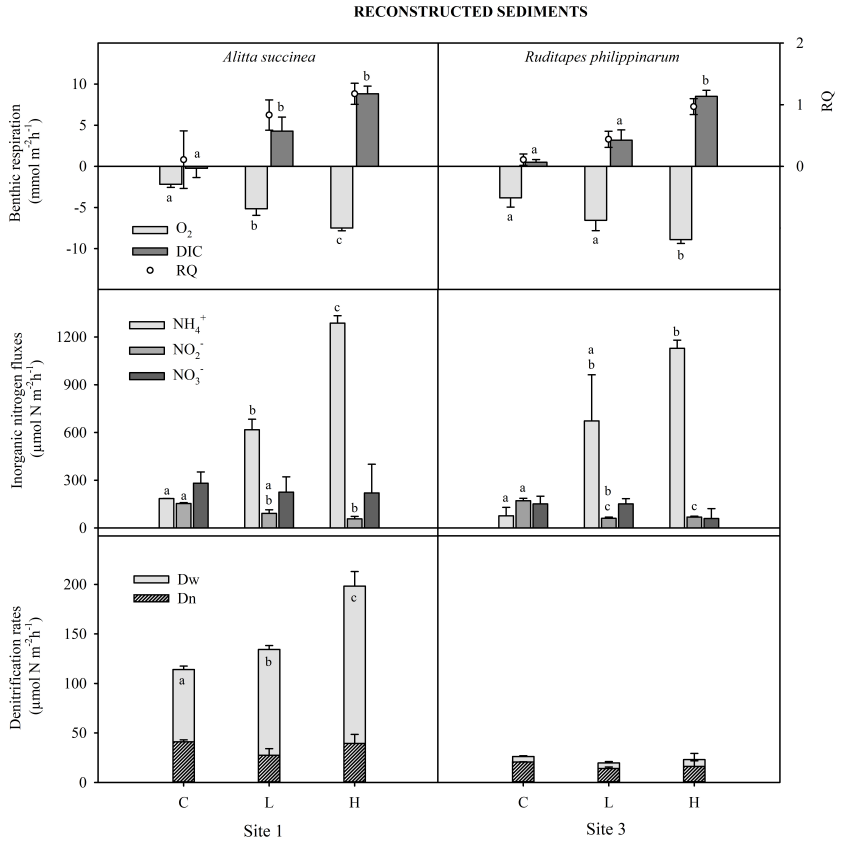

Figure 3.13: Dark fluxes of dissolved O_2 and DIC, DIN, and rates of denitrification measured in reconstructed sediment cores added with *Alitta succinea* (Site 1) and *Ruditapes philippinarum* (Site 3). C indicates the control treatment, L the low density treatment (600 and 400 ind. m^{-2} for polychaetes and clams, respectively), and H the high density treatment (1200 and 800 ind. m^{-2} for polychaetes and clams, respectively). In the upper panels, the y-axes on the right reports the respiratory quotient (RQ), calculated as the ratio between DIC and O_2 fluxes (absolute value). Where present, letters above bars indicate statistically significant differences. Averages ± standard errors ($n = 3$) are reported.

were compared. As a general outcome, the enhancement of specific processes by the two functional groups of macrofauna (e.g., oxygen uptake, NH_4^+ efflux and D_w) suggested much larger effects of the deposit feeder as compared to the filter feeder (Table 3.6 and Table 3.7). For example, the increase of benthic oxygen consumption per gram of dry weight of the burrower varied between 81 and 156 $\mu mol\, g_{dw}^{-1}\, h^{-1}$. This is likely due to the construction and irrigation of subsurface burrow structures, to the increased sediment-water exchange surface and to the stimulation of microbial activity within sediments (Nizzoli et al., 2007).

Interestingly, the stimulatory effects of *A. succinea* on most measured benthic fluxes, with NO_3^- as only exception, were generally different in intact and reconstructed sediments, whereas this was not true for *R. philippinarum* (Table 3.6, Table 3.7, Table 3.8). In reconstructed cores *A. succinea* produced much higher enhancement of O_2 respiration and of water column NO_3^- consumption via denitrification (by a factor of 2) and of NH_4^+ recycling (by a factor 5) as compared to intact sediments. In unmanipulated sediments, *A. succinea* stimulated denitrification of NO_3^- produced via nitrification, which is expected, whereas this was not apparent in reconstructed sediments. In the latter, *A. succinea* stimulated the denitrification of water column NO_3^-, likely due to recently constructed burrows with sharp redox gradients and limited numbers of nitrifying bacteria on their walls.

Besides differences in the degree of stimulation of certain processes, measurements in intact and reconstructed bioturbated sediments led sometimes to contrasting effects of macrofauna. For example, *A. succinea* in intact cores enhanced DIC retention in sediments whereas the same organism in reconstructed cores stimulated DIC release to the water (Table 3.6, Table 3.7, Table 3.8). Opposite effects by burrowing fauna were apparent also for NO_2^- fluxes. Interestingly, the effects of *R. philippinarum* on solute fluxes in intact and reconstructed cores were not statistically different (Table 3.6, Table 3.7, Table 3.8). Clams may drive fluxes mostly through their metabolic activities but produce a limited effect, at least in the short-term, on sedimentary variables and on microbial communities within sediments.

3.4.3 Conclusions

The present study suggests that results of experiments with sediments and macrofauna manipulations need to be carefully considered. The degree of stimulation of commonly measured biogeochemical processes as aerobic, anaerobic (e.g., denitrification) and total respiration or nutrient fluxes by macrofauna can be substantially different when calculated in intact, not manipulated natural sediments and when calculated in reconstructed microcosms. Reasons are probably multiple and include first of all the effect of sediment sieving and packing which deeply alter vertical gradients, organic matter distribution, the sediment redox, the pore water chemistry and likely affect important fractions of reactive components of the organic matter pools. Sieving removes also all the macrofauna in order to highlight the biogeochemical effects of a single species. This helps to shed light on the main mechanisms driving nutrient dynamics, but on the other hand the simplification of the community removes an unaccountable number of ecological interac-

Table 3.6: Slope, intercept, p and r^2 values of linear regressions between solutes fluxes ($\mu mol\, m^{-2}\, h^{-1}$), respiratory quotient, denitrification rates ($\mu mol\, m^{-2}\, h^{-1}$) and efficiency and macrofauna biomass of *Alitta succinea* ($g_{dw}\, m^{-2}$) retrieved in intact and reconstructed cores from the two sites. Significant values are printed in bold.

Parameter	Slope	Intercept	p	r^2
		Intact cores		
O_2	-81.75 ± 25.67	-4031.78 ± 461.74	**0.033**	0.72
DIC	-137.11 ± 75.55	7417.94 ± 1359.12	0.144	0.45
RQ	-0.04 ± 0.02	1.71 ± 0.29	0.055	0.64
NH_4^+	5.90 ± 3.86	736.22 ± 69.37	0.201	0.37
NO_2^-	1.13 ± 0.45	-101.37 ± 8.12	0.067	0.61
NO_3^-	-2.46 ± 1.63	161.53 ± 29.26	0.205	0.36
DIN	4.57 ± 4.49	999.12 ± 80.79	0.367	0.21
D_w	1.28 ± 0.93	93.19 ± 16.65	0.239	0.32
D_n	2.61 ± 0.75	35.31 ± 13.51	**0.025**	0.75
D_{tot}	3.89 ± 0.61	128.50 ± 10.88	**0.003**	0.91
DE	0.21 ± 0.08	11.73 ± 1.52	0.068	0.61
		Reconstructed cores		
O_2	-158.53 ± 13.25	-2283.70 ± 291.41	$<$ **0.001**	0.95
DIC	264.35 ± 45.38	-144.03 ± 997.82	$<$ **0.001**	0.83
RQ	0.04 ± 0.01	-0.09 ± 0.28	**0.015**	0.59
NH_4^+	31.43 ± 2.71	169.36 ± 59.60	$<$ **0.001**	0.95
NO_2^-	-2.66 ± 0.71	145.65 ± 15.53	**0.007**	0.67
NO_3^-	-2.19 ± 4.68	279.11 ± 102.81	0.654	0.03
DIN	26.59 ± 4.77	594.12 ± 104.93	$<$ **0.001**	0.82
D_w	2.48 ± 0.29	71.43 ± 6.30	$<$ **0.001**	0.91
D_n	0.06 ± 0.30	34.99 ± 6.53	0.852	0.01
D_{tot}	2.53 ± 0.33	106.42 ± 7.29	$<$ **0.001**	0.89
DE	-0.11 ± 0.05	15.20 ± 1.09	0.054	0.43

Table 3.7: Slope, intercept, p and r^2 values of linear regressions between solutes fluxes ($\mu mol\, m^{-2}\, h^{-1}$), respiratory quotient, denitrification rates ($\mu mol\, m^{-2}\, h^{-1}$) and efficiency and macrofauna biomass of *Ruditapes philippinarum* ($g_{dw}\, m^{-2}$) retrieved in intact and reconstructed cores from the two sites. Significant values are printed in bold.

Parameter	Slope	Intercept	p	r^2
		Intact cores		
O_2	-12.80 ± 2.94	-5417.04 ± 1016.76	**0.012**	0.83
DIC	12.57 ± 2.26	4150.56 ± 781.78	**0.005**	0.89
RQ	-0.0001 ± 0.0006	0.918 ± 0.207	0.850	0.01
NH_4^+	0.87 ± 0.69	514.09 ± 239.52	0.276	0.28
NO_2^-	-0.03 ± 0.02	30.42 ± 7.14	0.286	0.27
NO_3^-	-0.05 ± 0.02	5.76 ± 8.53	0.103	0.53
DIN	0.79 ± 0.68	550.26 ± 234.96	0.307	0.26
D_w	0.004 ± 0.005	9.33 ± 1.75	0.432	0.16
D_n	-0.007 ± 0.017	17.90 ± 5.91	0.705	0.04
D_{tot}	-0.003 ± 0.016	27.22 ± 5.67	0.885	0.01
DE	-0.005 ± 0.006	6.21 ± 2.08	0.436	0.16
		Reconstructed cores		
O_2	-6.98 ± 2.27	-4149.12 ± 969.48	**0.018**	0.57
DIC	12.09 ± 1.75	112.07 ± 748.16	$<$ **0.001**	0.87
RQ	0.001 ± 0.001	0.067 ± 0.082	$<$ **0.001**	0.88
NH_4^+	1.47 ± 0.40	145.15 ± 169.82	**0.008**	0.66
NO_2^-	-0.15 ± 0.05	149.04 ± 19.52	**0.014**	0.60
NO_3^-	-0.09 ± 0.11	148.70 ± 46.32	0.458	0.08
DIN	1.24 ± 0.40	442.88 ± 168.65	**0.017**	0.58
D_w	0.001 ± 0.001	5.66 ± 0.59	0.434	0.09
D_n	-0.009 ± 0.007	19.98 ± 2.86	0.213	0.21
D_{tot}	-0.008 ± 0.008	25.64 ± 3.27	0.329	0.14
DE	-0.007 ± 0.003	6.29 ± 1.20	**0.042**	0.47

Table 3.8: Results of the ANCOVA between the slopes of fluxes or calculated respiratory quotients and denitrification efficiency and macrofauna biomass in intact and reconstructed sediments from the two sites. While for *Ruditapes philippinarum* most comparisons are not significant, for *Alitta succinea* the two conditions lead to rather different slopes.

Parameter	F	p
Alitta succinea		
O_2	6.559	**0.027**
DIC	16.723	**0.002**
RQ	10.439	**0.008**
NH_4^+	20.424	**0.001**
NO_2^-	7.909	**0.017**
NO_3^-	0.001	0.976
DIN	5.550	**0.038**
D_w	2.149	0.171
D_n	11.740	**0.006**
D_{tot}	3.409	0.092
DE	9.041	**0.012**
Ruditapes philippinarum		
O_2	2.486	0.143
DIC	0.029	0.869
RQ	7.809	**0.017**
NH_4^+	0.662	0.433
NO_2^-	4.115	0.067
NO_3^-	0.057	0.816
DIN	0.371	0.555
D_w	0.586	0.459
D_n	0.121	0.735
D_{tot}	0.118	0.737
DE	0.089	0.771

tions that shape the true functioning of the benthic ecosystems. Results obtained from manipulated sediments are real, as they are measured, but are likely never found *in situ*, due to oversimplification of the experimental approach, including the removal of chemical gradients and multiple ecological interactions. One of the main aim of this thesis is to collect results from experimental data that will be used to construct nutrient models at whole system level. By using the degree of process stimulation calculated in this study and couple them with data on macrofauna abundance at the lagoon scale the obtained results may be quite far from the reality. A major fraction of the effects of macrofauna on sediments are indirect, and associated to the way they affect microbial communities and metabolic activities and with them chemical microgradients within sediment, that are flux drivers. Measurements in manipulative experiments should also consider these aspects, and consider or quantify how long it takes for macrofauna to produce a steady state in terms of microbial communities, activities and chemical gradients in manipulated sediments. The latter require long conditioning time before measurements and the preincubation period is probably closer to weeks than days.

3.5 Main findings and general remarks

The Goro Lagoon is a vulnerable environment highly impacted by multiple anthropogenic pressures, first of all, the large nutrient load delivered from one of the most exploited areas in Europe (the Po River Basin) and the molluscs farming activity (Viaroli et al., 2006). Since the 1990s, different management measures have been adopted at the watershed level to decrease the external nutrient load and within the lagoon to limit the internal regeneration, through the increase of water circulation and the sand-capping of organic-enriched sediments. These actions have led to the decrease in the frequency and intensity of macroalgal blooms, mainly in the last decade. Results from the experiments carried out in this study demonstrated how ongoing global changes may overwhelm the applied measurements, by affecting the functioning of this area, which proved to be especially vulnerable during dry periods.

The benthic compartment, indeed, in the spring season, during a high precipitation and discharge event and even with a simulated NO_3^- pulse addition, displayed a high buffer capacity against N pollution. Removal out-competed recycling processes in all the analysed sites and the denitrification capacity largely exceeded the reasonable future increase in NO_3^- concentration. The high removal capacity of the lagoon is strictly related to the presence of bioturbating organisms. Even if composed by a low biodiverse community, macrofauna largely enhances the N removal rates and increases the P retention potential capacity. The limiting element to the filter action of the lagoon could derive from the decrease in water residence time. The time it takes for any water parcel to travel through the transitional areas is considered one of the main factors regulating the processing of nutrients and organic matter (Nixon et al., 1996). Generally, a short residence time determines lower sedimentation rates restricting the role and the efficiency of the benthic compartment (Seitzinger et al., 2006).

Prolonged dry periods characterized by high temperature and low river discharge led to the increase in sediment N regeneration, largely exceeding external nutrient inputs and removal rates. This was due to a combination of factors, including high mineralization rates, the disconnection between N removal and mineralization, mostly due to the decline in bioturbators abundance, and the decrease in denitrification to DNRA ratio, due to the higher affinity of ammonifiers to nitrate. The extent of the seasonal shift in dominant processes varied among the analysed sites due to the heterogeneous hydrology and sediment composition, and it was more evident in stagnant areas prone to sulfides accumulation or in areas largely affected by the presence of cultivated clams. Benthic regeneration plays a key role in this shallow transitional area and may contrast the effects of environmental policies aimed at reducing external loads. Prolonged dry period may result in anoxia events, further decreasing the functioning of the benthic filter, with respect to both N and P. Studies in the Goro Lagoon have focused mainly on N, since this element has been identified as the main driver of macroalgal blooms. The seasonal transition from high to prolonged low discharge period may influence also the P dynamics, due to redox-dependent P release mechanisms and, as demonstrated in this study, to the bioturbation decrease. The unbalance in nutrient stoichiometry may deeply affect the

lagoon functioning, with a series of cascading events that start from the variation in the composition of primary producers' community (Paerl et al., 2016). Future investigation would benefit from the simultaneous analysis of N and P dynamics, both under *in situ* and simulated extreme conditions.

The data deriving from experimental activities reported in this thesis will be systematized, implemented, and combined with hydrological data with the aim to compile the N and P flow networks at the whole lagoon scale. This approach has been adopted in the Curonian Lagoon, and results are presented in the next chapter. Here, a large-scale investigation on the stoichiometry of benthic regeneration under oxic and anoxic conditions has been carried out. The obtained data, together with information on pelagic and benthic biological diversity and processes collected mostly in the last decade, have been used to construct seasonal models of N and P that have been analysed via the Ecological Network Analysis.

Chapter 4

Curonian Lagoon

The Curonian Lagoon (Lithuania-Russia Federation) is located in the south-eastern part of the Baltic Sea; with a total surface of 1584 km^2 it is the largest European lagoon. This estuary is shallow (average depth 3.8 m) and non-tidal and is connected to the Baltic Sea by a narrow, 11 km long strait (0.4-1.1 km wide, 8-15 m depth) located in the northern corner (Fig. 4.1). The water temperature ranges from 1 °C to 29 °C and the lagoon is covered by ice on average for 110 days per year, except for the strait, which is always ice-free (S. Li, 2006). A pronounced shortening of the ice season duration in the lagoon has been observed at a rate of 1.6–2.3 days per year during the period 2002–2017 (Idzelyte et al., 2019). The main freshwater input is represented by the Nemunas River which accounts for ∼95% of total discharge; it enters the central part of the lagoon and creates a unidirectional northward water flow to the strait (Ferrarin et al., 2008). The river is characterized by a seasonally variable discharge (200-2200 $m^3\,s^{-1}$), peaking during snowmelt in March and April and dropping to minimum values in August and September (Vybernaite-Lubiene et al., 2018). The river discharge and the limited water exchange with the Baltic Sea determine the freshwater character of the lagoon, with the presence of low salinity waters (generally 1-2, up to 7) limited to the northern area (Zemlys et al., 2013). The Nemunas inflow divides the lagoon into two subareas: a northern transitional area and a southern confined area (Fig. 4.1). The transitional area ($\sim$ 404 m^2) is shallow (mean depth 1.75 m), is influenced by intrusions of brackish waters and river discharge, which determine the relatively low residence time (ranging from 50 to 100 days), and the dominance of coarse and sandy sediments. The confined area ($\sim$ 1180 km^2) is characterized by a higher depth (mean 3.5 m) and a higher residence time (ranging from 100 to 250 days) than the transitional area and by organic-rich fine muddy deposits. Here, the water circulation is regulated mainly by wind, whose direction determine water exchanges with the transitional area (Ferrarin et al., 2008; Umgiesser et al., 2016).

The seasonal phytoplankton succession exhibits a pattern typical of eutrophic or hypertrophic systems. Diatoms dominate the spring bloom in April and May, with a monthly average Chl-*a* concentration of $47 \pm 14\,\mu g\,L^{-1}$. After a short clear-water phase, usually in June, the biomass of N-fixing and other groups of filamentous cyanobacteria

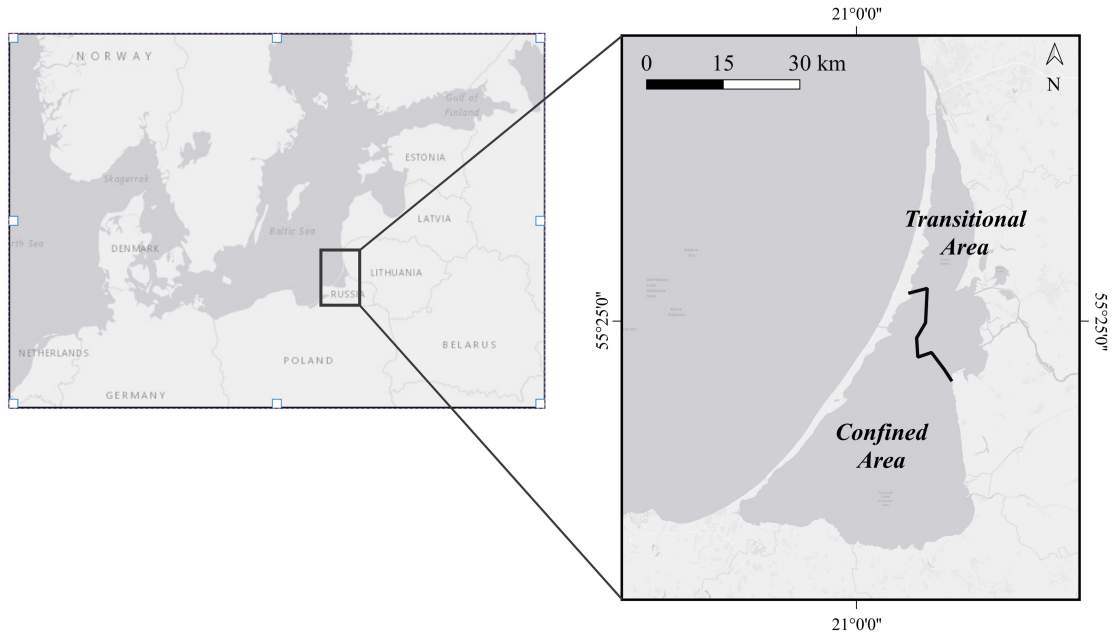

Figure 4.1: Map of the Curonian Lagoon and subdivision between the northern transitional area and the southern confined area.

increases, peaking in August and September, with a monthly average Chl-*a* concentration of $96 \pm 56\,\mu g\,L^{-1}$. During extreme blooms events Chl-*a* can exceed $400\,\mu g\,L^{-1}$ (Bartoli et al., 2018; Bresciani et al., 2014; Pilkaityte, 2007a; Vaičiūtė et al., 2021).

The interplay among hydrologic factors, favorable nutrient stoichiometry, and top-down and bottom-up mechanisms mediated by organisms was identified as the main driver of this phenomenon (Bartoli et al., 2018). Retrospective analysis via satellite remote sensing revealed the temporal variability and the patchiness distribution of blooms and suggested that they occur mainly under high summer temperatures and low wind (Bresciani et al., 2014; Vaičiūtė et al., 2015). These factors promote the establishment of stagnant conditions and offer a competitive advantage to positive buoyant cyanobacteria as *Aphanizomenon flos-aquae*, mostly in the south-southwestern and in the central areas of the lagoon (Bresciani et al., 2014; Bresciani et al., 2012; Vaičiūtė et al., 2021). N-fixing cyanobacteria dominate in areas characterized by a severe N deficiency due to their ability to use atmospheric and relatively inert molecular N_2. For this reason, their abundance in the water column is likely controlled by the availability of inorganic P (Dolman et al., 2012; Paerl et al., 2011). Monthly analysis of riverine loads, revealed a pronounced transition in nutrient stoichiometry from early spring to summer, driven by variations in freshwater discharge. The monthly discharge generally peaks in the spring season and is characterized by a large N excess and P limitation compared to the theoretical Redfield ratio (DIN:DIP=16, (Redfield, 1958)). The summer season is characterized by minimum values of freshwater discharge and by a sharp reduction in N loads, whereas P conversely displays lower variations due to constant inputs from sewage

treatments plants, resulting in a lower stoichiometric N:P ratio (Vybernaite-Lubiene et al., 2017; Vybernaite-Lubiene et al., 2018). Studies on sedimentary processes carried out in different areas of the lagoon revealed strong seasonal transitions also in N and P benthic dynamics, affecting the ratios between removal and recycling processes. In spring, N removal processes dominate, mostly via sediment burial and denitrification (Zilius et al., 2018). Conversely, the summer season is characterized by the increase in cyanobacteria mediate N_2-fixation, in mineralization rates, and by the decrease in coupled nitrification-denitrification, enhancing the availability of reactive N (Zilius, Bartoli, Daunys et al., 2012; Zilius et al., 2014; Zilius et al., 2021). Summer cyanobacteria blooms and associated high respiration rates induce transient hypoxia phenomena and determine the increase in redox-dependent P release mechanisms (Petkuviene et al., 2016; Zilius et al., 2015).

Recurring bloom events affect the structure and the composition of the entire trophic food web. In spring the zooplankton community is dominated by predatory cyclopoids (*Cyclops strenuus*), while large herbivorous such as *Daphnia longispina* appear at the beginning of summer. Like most eutrophic water bodies, at the appearance of cyanobacteria colonies, a shift towards the dominance of small-bodied species such as *Chydorus sphaericus* occurs (Gasiunaite & Razinkovas-Baziukas, 2004; Gasiūnaitė et al., 2012). Recurring phytoplankton blooms increase the water turbidity especially along the western and southern shores, resulting in an unfavourable light climate for macrophytes, which in most of the lagoon are restricted up to 500 m wide belt to the littoral area (Zaromskis, 2002). Macrophytes stands are characterized by a diverse macrofauna community as compared to most of the lagoon sediments, which host few species due to high organic matter content and low oxygen concentrations (Daunys, 2001). Among them, oligochaetes and chironomids dominate in muddy sediments, whereas coarser sediments host also freshwater mussels, including both native unionids and the invasive *Dreissena polymorpha* (Bubinas & Vaitonis, 2005; Zettler & Daunys, 2007). Due to high turbidity, frequent hypoxic/anoxic crises, and large sedimentation rates, benthivorous species dominated the fish community (Repečka, 2003, 2009). The Curonian Lagoon hosts a large and diverse waterbird community that undergoes wide seasonal number fluctuations. The great cormorant (*Phalacrocorax carbo sinensis*) represents the most abundant breeding species and during the summer season forms large colonies along the Curonian Spit, the narrow sand dune that divides the lagoon from the sea (Morkune et al., 2020; Švažas et al., 2011).

Benthic and pelagic consumers have been demonstrated to affect primary producers' activity both through top-down (i.e., grazing) and bottom-up (i.e., nutrient regeneration) mechanisms. The summer season is characterized by a sharp decrease in primary producers consumption, due to the prevalence of large filamentous colonies and toxic forms of cyanobacteria, inhibiting zooplankton and macrofauna grazing, which in turn switch to alternative food sources given a competitive advantage to the same cyanobacteria (Grinienė et al., 2016; Semenova & Aleksandrov, 2009). On the opposite side, consumer mediated nutrient recycling by different groups of organisms, particularly large colonies of piscivorous birds and invasive dreissenids, have been demonstrated to contribute to the unbalance in the nutrient stoichiometry of this system, increasing the relative amount of

reactive P compared to N (Benelli et al., 2019; Morkune et al., 2020; Petkuviene et al., 2019).

After the entrance of Lithuania into the European Union and the adoption of the Baltic Sea Action Plan (BSAP) by HELCOM contracting parties, different policies have been implemented to control cyanobacteria blooms and reduce the Nemunas River nutrient load to the Baltic Sea (BSAP, 2007). As happened in other European watersheds, these policies resulted in a substantial reduction of P, but did not affect the N loads, mostly constituted by NO_3^- deriving from diffuse sources (Vybernaite-Lubiene et al., 2018). Despite the relative reduction of reactive P compared to N, a recent study underlined a consistent tendency towards longer and later-lasting cyanobacteria bloom events, mostly in the last 10 years (Vaičiūtė et al., 2021).

Benthic regeneration may play a key role and contribute to extend cyanobacteria blooms over a long time span. The increase in organic inputs to sediments during these events has been demonstrated to turn bottom water hypoxic and favor the release of reactive P, creating a positive feedback that fuels cyanobacteria production (Petkuviene et al., 2016; Zilius et al., 2014). This mechanism is only described in a few areas of the lagoon. A spatially extended survey is needed to verify whether summer P recycling, exceeds external inputs and can support algal blooms. Section 4.1 reports the results of experimental activities carried out in 19 stations of the Curonian Lagoon, during which benthic respiration, inorganic nutrient, and reduced metal (Mn^{2+} and Fe^{2+}) fluxes were measured under oxic and anoxic conditions. The main aim of this study was to analyse how the stoichiometry of benthic nutrient regeneration was affected by O_2 shortage events. It has been hypothesized a relative increase in P regeneration compared to N and Si, with rates exceeding external input and partly explaining the longer persistence of blooms. These data, together with the available information on benthic and water column processes, the composition and the activity of autotrophic and heterotrophic organisms derived from experimental activities realized in the last 20 years in the Curonian Lagoon, have been collected to construct models depicting N and P circulation both in the transitional and the confined area (section 4.2). Due to the complex nature of factors underlying the development of blooms, spring and summer models have been constructed with the main aim to identify the factors that seasonally affect the N and P dynamics at the whole system scale, favouring the shift from diatoms to cyanobacteria.

4.1 The effect of anoxia on the stoichiometry of nutrient recycling[3]

Human activities have altered the global biogeochemical cycles of the main nutrients (N, Si and P), with detrimental consequences for the functioning of aquatic environments (Bernot & Dodds, 2005; Han & Allan, 2012; Mulholland et al., 2008; Paerl, 2009). Recent investigations indicate that unbalanced and fluctuating nutrient stoichiometry may cause food web destabilization and determine seasonal shift in phytoplankton composition and dominance of the main algal groups (Glibert, 2012). There was traditionally more focus on loads and stoichiometry of diffuse and point external nutrient inputs (e.g., from watersheds), whereas the stoichiometry of internal recycling (e.g., from sediments) and its regulation by environmental factors (e.g. sediment composition, oxygen levels) is comparatively less studied (Conley et al., 1988; Vybernaite-Lubiene et al., 2018). The total and relative amount of nutrients recycled from sediments are of special interest during summer, when they may exceed external inputs and sustain algal blooms (Ding et al., 2018; Zilius et al., 2014). An interesting question is to analyze how the stoichiometry of benthic nutrients regeneration might be affected by variable O_2 levels in bottom water (Abril et al., 1999; Neubacher et al., 2011; Siipola et al., 2016; Viktorsson et al., 2013).

In this study, aerobic benthic respiration, inorganic nutrient and reduced metal (Mn^{2+} and Fe^{2+}) fluxes have been analysed under oxic and anoxic conditions in 19 stations of the Curonian Lagoon. The aims of this study were to analyze the effects of transient anoxia on benthic fluxes of the macronutrients N, Si and P and on their stoichiometry at the whole estuarine scale, with a special focus on the mechanisms buffering P mobility. It was hypothesized that: (1) high labile organic input and high water temperatures, leading to O_2 shortage in sediments and exhaustion of the oxidized forms of Mn and Fe, may lead to P regeneration in excess over N and Si; (2) under low external nutrient input, which characterizes the summer and late summer periods, anoxic P regeneration may exceed external P loading and explain the long-term persistence of cyanobacteria blooms.

4.1.1 Material and methods

Sediments sampling and benthic flux measurements

Samplings were carried out between 20th July and 10th August 2018. The intact sediment cores were collected manually, by diving, at 19 stations within the Lithuanian sector of the Curonian Lagoon (Fig. 4.2). At each sampling site, 4 cores (Plexiglass liners, i.d. 8.4 cm, length 30 cm) were collected for dark measurements of benthic fluxes, whereas 3 cores (Plexiglass liners, i.d. 4.6 cm, length 20 cm) were collected for sediment characterization. Immediately after collection, the cores were submerged with the top open in tanks containing *in situ* aerated and cooled water and transferred to the laboratory within a

[3]Results of this study have been published in: Bartoli, M., Benelli, S., Lauro, M., **Magri, M.**, Vybernaite-Lubiene, I., and Petkuviene, J. (2021). Variable oxygen levels lead to variable stoichiometry of benthic nutrient fluxes in a hypertrophic estuary. *Estuaries and Coasts*, 44(3), 689-703.

Figure 4.2: Location of the 19 stations within the Lithuanian sector of the Curonian Lagoon. The dashed black line represents the confine between the Lithuanian and Russian sector.

few hours. Here, the tanks were placed in a temperature-controlled room maintained at 24 °C, close to *in situ* conditions, for overnight sediment stabilization. Water in the tanks was gently mixed by aquarium pumps and constantly aerated. Each core was provided with a stirring unit driven by an external motor as described in section 3.1.1.

The morning after the sampling, sediment–water fluxes of O_2, NH_4^+, SiO_2, PO_4^{3-}, Fe^{2+} and Mn^{2+} were measured via dark incubations. Samples were immediately collected the water phase of each core (t_0) and then each core was sealed with a floating lid. Another sample (t_1) was collected after 1-2 hours of incubation from each core water column through a valve in the lid (oxic, OX). The dark incubation was prolonged and additional water samples (t_2 and t_3) were collected in order to measure a second flux under anoxic conditions (anoxic, AN). Anoxic conditions were set at O_2 values in the cores water column below 50 µM. Oxygen concentration in the cores water phase was inspected with a microsensor inserted through the lids. The total incubation time varied between 15 and 24 hours; differences between sites depended upon different respiration rates.

Samples collected from the cores water column (20 mL) were replaced with water from the tank. Each water sample underwent the same processing: an aliquot of 10 mL was filtered and transferred to a 10-mL plastic vial in order to analyze NH_4^+, SiO_2 and PO_4^{3-}. Dissolved reactive P was immediately measured, whereas samples for NH_4^+ and SiO_2 analyses were frozen (−20 °C) and analyzed within a week from the experiment as described in section 3.1.1. Another aliquot of 10 mL was transferred to a 12-mL exetainer for Fe^{2+} and Mn^{2+} analyses. The latter was acidified with 100 µL of concentrated HNO_3 and analysed as described in section 3.3.1. Dissolved O_2 was monitored with an microelectrode (OX-50, Unisense A/S, DK) directly through a sampling port on the lid. Oxygen, nutrient and metal fluxes were calculated according to the equation 3.1.

To provide context for the flux measurements, internal loads recycled from sediments under oxic and anoxic conditions were compared with external loads from the Nemunas River measured during summer (July and August monitoring data for the 2012-2016 period reported in (Vybernaite-Lubiene et al., 2018)).

Sediment and pore water caracterization

The 3 additional sediment cores were extruded and sliced in five layers: 0-1, 1-2, 2-3, 3-5 and 5-10 cm for physical and chemical sediment characterization. Each slice was immediately homogenized and 5 g of fresh sediment was collected and treated as described in section 3.1.1 for density, water content, porosity and organic matter analyses.

Statistical analysis

Comparison of oxic and anoxic fluxes of Mn^{2+}, Fe^{2+}, NH_4^+, PO_4^{3-} and SiO_2 were made with a paired t-test unless normality assumptions were not met. In this case, we used the non-parametric Wilcoxon Signed Rank test for dependent samples. Spearman's correlation tests were used to determine whether fluxes and sediment properties were correlated. All statistical analyses were performed with R software v. 3.5.1 (R Core Team, 2018). Graphs were made with Sigma Plot 11.0.

4.1.2 Results

Sedimentary Features

The 19 stations were scattered along heterogeneous sedimentary environments of the study area in terms of grain size and organic matter content (Table 4.1). Stations 1, 2, 13 and 14, aligned along the western lagoon border, had a prevalence of clay with median particle size around 30 µm and porosity ≥0.90. These sites displayed fluffy, organic (up to 23%) and chemically-reduced black sediments with little evidence of bioturbation. Stations located in central and eastern areas, influenced by the solid transport of the Nemunas River, were generally sandier, with lower organic matter content and porosity (∼ 1% and ≤0.4, respectively) and with burrow structures. Sediments within the area always affected by the Nemunas River plume (stations 4, 5, 6 and 12) were covered by a thick layer of *D. polymorpha* shells. The spatial distribution of clayish and sandy sites approximately reflected the lagoon zonation described by (Ferrarin et al., 2008), based on water residence time. More organic, clayish areas overlapped areas with longer water residence time.

Organic matter content was negatively correlated with median particle size and with sediment density (Table A.3). Clay-rich sediments had organic matter content higher than 15% whereas in sandy sediments organic matter content was less than 2%. Sediment density was positively correlated with median particle size: finest grained sediments had a density close to water value, which increased logarithmically reaching a plateau around $1.8\,\mathrm{g\,cm^{-3}}$ for sediments with median particle size >200 µm (Table 4.1 and Table A.3).

Benthic Fluxes of O_2, Mn^{2+} and Fe^{2+}

In July the high water temperature (24 ℃ in the incubation room, up to 26 ℃ *in situ*) resulted in elevated benthic respiration, averaging $-3265 \pm 227\,\mu\mathrm{mol\,m^{-2}\,h^{-1}}$, with a maximum of $-5662 \pm 380\,\mu\mathrm{mol\,m^{-2}\,h^{-1}}$ measured at the station 9 and a minimum of $-1905 \pm 238\,\mu\mathrm{mol\,m^{-2}\,h^{-1}}$ measured at the station 6 (Fig. 4.3a). In the 19 analyzed stations the benthic O_2 demand was not correlated with the measured sedimentary features (Table A.3).

Manganous manganese fluxes averaged $54 \pm 16\,\mu\mathrm{mol\,m^{-2}\,h^{-1}}$ under oxic conditions and increased by a factor of ∼ 3 ($186 \pm 23\,\mu\mathrm{mol\,m^{-2}\,h^{-1}}$) under anoxic conditions (Fig. 4.3b and Fig. 4.4). Oxic Mn^{2+} fluxes included some negative (down to $-66 \pm 8\,\mu\mathrm{mol\,m^{-2}\,h^{-1}}$, station 4) and many largely positive values (up to $206 \pm 10\,\mu\mathrm{mol\,m^{-2}\,h^{-1}}$, station 13); they were also not correlated with sediment properties. Under anoxic conditions Mn^{2+} fluxes became all positive, from a minimum of $37 \pm 7\,\mu\mathrm{mol\,m^{-2}\,h^{-1}}$ to a maximum of $393 \pm 95\,\mu\mathrm{mol\,m^{-2}\,h^{-1}}$, measured at the stations 14 and 3, respectively. Oxygen shortage resulted in generally increasing Mn^{2+} efflux, with the fine-grained stations 2, 13 and 14 as only exceptions: here Mn^{2+} fluxes decreased or were comparable in the two conditions. Oxic Mn^{2+} fluxes were positively correlated with O_2 fluxes, whereas anoxic Mn^{2+} fluxes were positively correlated with the median particle size (Table A.3).

During oxic incubations Fe^{2+} fluxes ranged from $-32 \pm 8\,\mu\mathrm{mol\,m^{-2}\,h^{-1}}$ (station 5) to $58 \pm 7\,\mu\mathrm{mol\,m^{-2}\,h^{-1}}$ (station 13) and averaged $9 \pm 5\,\mu\mathrm{mol\,m^{-2}\,h^{-1}}$. Anoxia increased

Table 4.1: Sediment features measured at the 19 stations within the Lithuanian sector of the Curonian Lagoon. The first 10 cm of sediment were pooled in order to produce a mean value for each station. Averages ± standard errors are reported in the table ($n = 3$).

Stn	**Density**	**Porosity**	**Organic Matter**	**Sandy**	**Clay**	**Silt**	**Median Particle Size**
	$g\,cm^{-3}$	$mm\,mm^{-1}$	%	%	%	%	µm
1	1.12 ± 0.02	0.90 ± 0.01	16.1 ± 1.1	23.4 ± 2.0	71.8 ± 2.1	4.7 ± 0.4	36.0 ± 2.2
2	1.09 ± 0.01	0.91 ± 0.01	18.2 ± 0.9	24.0 ± 1.2	72.0 ± 1.3	4.0 ± 0.1	37.6 ± 1.1
3	1.78 ± 0.02	0.33 ± 0.01	0.3 ± 0.1	97.2 ± 0.7	2.3 ± 0.6	0.5 ± 0.1	239.4 ± 1.8
4	1.81 ± 0.02	0.37 ± 0.01	1.2 ± 0.1	91.2 ± 0.7	7.6 ± 0.5	1.3 ± 0.1	310.9 ± 2.5
5	1.29 ± 0.04	0.84 ± 0.02	7.2 ± 0.1	34.8 ± 1.4	61.2 ± 1.5	4.0 ± 0.2	45.2 ± 1.7
6	1.82 ± 0.02	0.37 ± 0.01	1.4 ± 0.2	90.8 ± 2.4	7.7 ± 1.0	1.5 ± 0.1	252.5 ± 7.2
7	1.72 ± 0.06	0.51 ± 0.05	1.5 ± 0.2	58.8 ± 6.6	38.3 ± 3.8	2.9 ± 0.2	81.1 ± 8.2
8	1.75 ± 0.02	0.34 ± 0.01	0.6 ± 0.1	95.6 ± 0.7	3.6 ± 0.6	0.9 ± 0.1	242.8 ± 1.4
9	1.57 ± 0.10	0.61 ± 0.08	2.3 ± 0.6	73.8 ± 7.4	23.7 ± 5.8	2.4 ± 0.4	159.7 ± 27.6
10	1.76 ± 0.01	0.42 ± 0.02	1.0 ± 0.1	89.5 ± 2.8	9.0 ± 1.1	1.5 ± 0.1	187.6 ± 6.4
11	1.81 ± 0.02	0.37 ± 0.01	0.5 ± 0.1	96.9 ± 1.1	2.4 ± 0.2	0.7 ± 0.1	226.2 ± 2.0
12	1.79 ± 0.01	0.37 ± 0.01	0.7 ± 0.1	95.6 ± 2.4	3.6 ± 0.6	0.9 ± 0.1	214.1 ± 4.8
13	1.09 ± 0.01	0.92 ± 0.01	22.8 ± 1.8	14.8 ± 0.7	80.0 ± 0.7	5.2 ± 0.1	29.6 ± 0.9
14	1.10 ± 0.01	0.93 ± 0.01	22.3 ± 1.1	19.8 ± 0.9	76.0 ± 1.2	4.2 ± 0.1	34.4 ± 0.8
15	1.76 ± 0.01	0.40 ± 0.02	0.7 ± 0.1	93.1 ± 1.7	5.7 ± 0.2	1.2 ± 0.1	209.8 ± 1.7
16	1.86 ± 0.13	0.61 ± 0.13	1.3 ± 0.2	85.2 ± 4.4	12.8 ± 2.7	1.9 ± 0.3	158.2 ± 10.3
17	1.77 ± 0.01	0.43 ± 0.02	0.9 ± 0.1	91.3 ± 1.8	7.3 ± 0.3	1.4 ± 0.1	179.8 ± 3.0
18	1.62 ± 0.10	0.36 ± 0.03	0.7 ± 0.1	93.7 ± 1.4	5.4 ± 0.4	0.9 ± 0.1	246.9 ± 2.5
19	1.78 ± 0.02	0.41 ± 0.02	0.7 ± 0.1	90.0 ± 1.4	9.0 ± 1.1	1.0 ± 0.1	292.1 ± 5.2

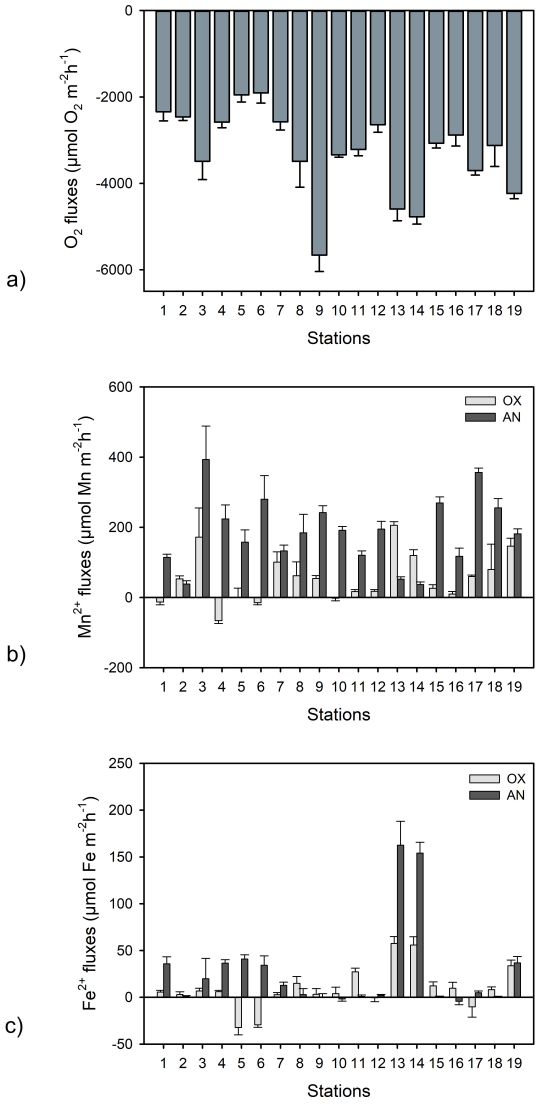

Figure 4.3: Dark O_2 fluxes (a) measured across the sediment–water interface at the 19 sampling stations in the Curonian Lagoon under oxic conditions. Dark Mn^{2+} (b) and Fe^{2+} (c) fluxes measured in the same stations under oxic (*light grey bars*) and anoxic (*dark grey bars*) conditions. Averages ± standard errors are reported ($n = 4$)

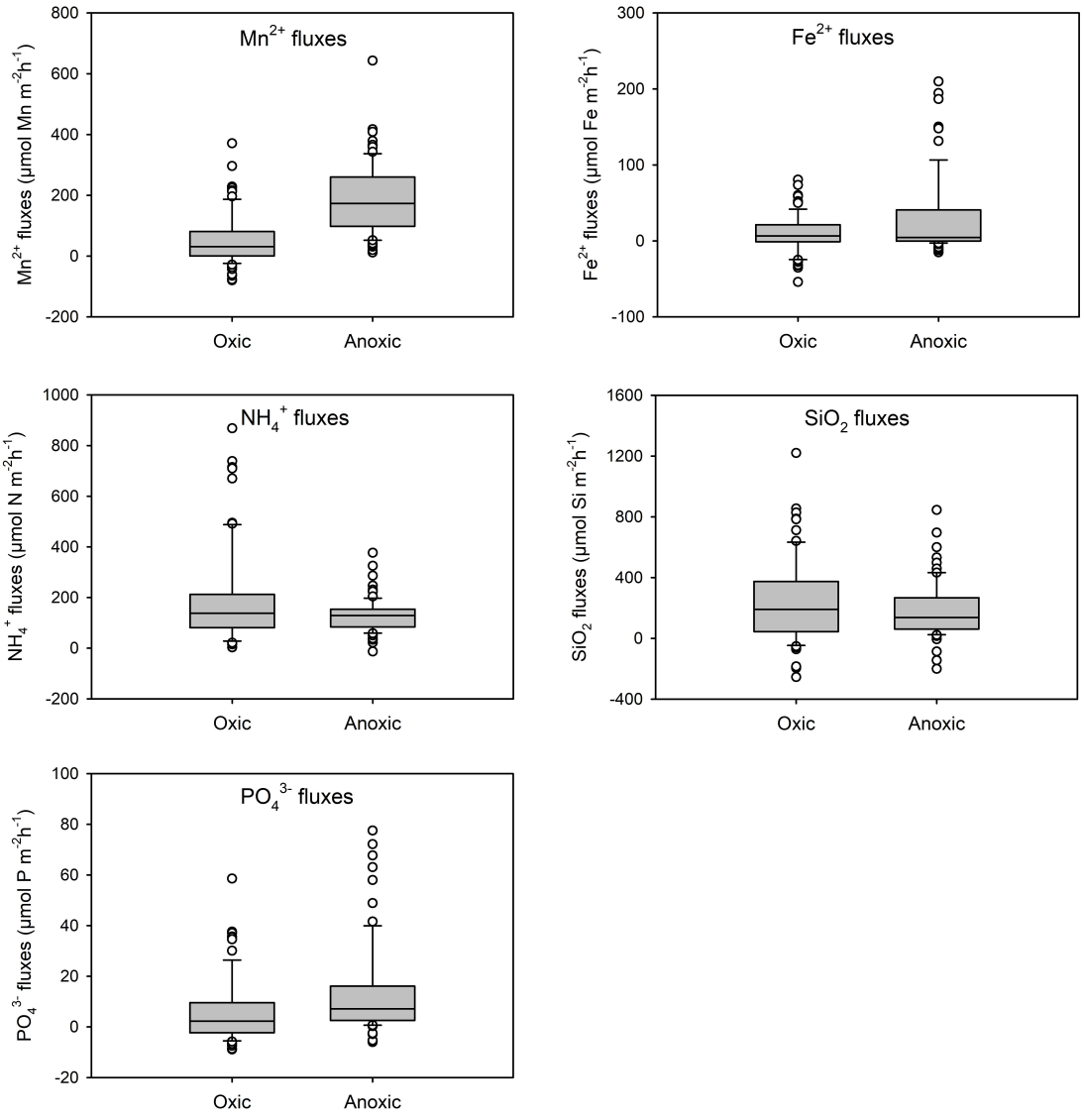

Figure 4.4: Boxplot of Mn^{2+}, Fe^{2+}, NH_4^+, SiO_2 and PO_4^{3-} fluxes measured under oxic and anoxic conditions. *Boxes* cover the 25 and 75% percentiles ($n = 76$) and bars show the 10 and 90% percentiles. *Dots* represent the outlier fluxes

the efflux of ferrous iron from the sediment in 12 out of 19 sites, with stations 8, 9, 10, 11, 15, 16 and 18 as exceptions (Fig. 4.3c and Fig. 4.4). Under anoxic conditions Fe^{2+} net fluxes increased by a factor of $\sim$ 3 and averaged $28 \pm 11\,\mu mol\,m^{-2}\,h^{-1}$. Minimum and maximum values were $-4 \pm 4\,\mu mol\,m^{-2}\,h^{-1}$ and $165 \pm 26\,\mu mol\,m^{-2}\,h^{-1}$, measured at the transitional, well flushed station 16 and at the confined station 13, respectively. Oxic Fe^{2+} fluxes were positively correlated with O_2 fluxes and with oxic Mn^{2+} production (Table A.3).

Benthic Fluxes of NH_4^+, SiO_2 and PO_4^{3-}

All investigated sediments were net NH_4^+ sources to the water column, but rates were highly variable among stations (Fig. 4.4 and Fig. 4.5a). Under oxic conditions NH_4^+ fluxes averaged $190 \pm 41\,\mu mol\,m^{-2}\,h^{-1}$, with minimum and maximum values of $20 \pm 13\,\mu mol\,m^{-2}\,h^{-1}$ and $741 \pm 44\,\mu mol\,m^{-2}\,h^{-1}$ measured at the station 5 and station 13, respectively. In 11 out of 19 stations, NH_4^+ fluxes tended to decrease under anoxic conditions, although they remained always positive, resulting in an average flux of $129 \pm 13\,\mu mol\,m^{-2}\,h^{-1}$. Oxic NH_4^+ fluxes were positively correlated with O_2 fluxes and with oxic Fe^{2+} and Mn^{2+} production (Table A.3).

Under oxic conditions the vast majority of the lagoon sediments regenerated large SiO_2 amounts, averaging $242 \pm 55\,\mu mol\,m^{-2}\,h^{-1}$ However, fluxes were highly variable and ranged between $-179 \pm 38\,\mu mol\,m^{-2}\,h^{-1}$ (station 11) and $751 \pm 159\,\mu mol\,m^{-2}\,h^{-1}$ (station 14) (Fig. 4.4 and Fig. 4.5b). Anoxic SiO_2 fluxes averaged $177 \pm 30\,\mu mol\,m^{-2}\,h^{-1}$ and in 12 out of 19 analyzed stations SiO_2 fluxes tended to decrease. The range of anoxic SiO_2 fluxes varied between a minimum of $-22.3 \pm 7.9\,\mu mol\,m^{-2}\,h^{-1}$ (station 13) and a maximum of $464 \pm 46\,\mu mol\,m^{-2}\,h^{-1}$ (station 7). Oxic SiO_2 fluxes were positively correlated with OM content (Table A.3).

Dissolved inorganic phosphorus fluxes under oxic conditions varied between a minimum of $-7 \pm 1\,\mu mol\,m^{-2}\,h^{-1}$ at the station 5 and a maximum of $39 \pm 7\,\mu mol\,m^{-2}\,h^{-1}$ at the station 19 and averaged $6 \pm 3\,\mu mol\,m^{-2}\,h^{-1}$ (Fig. 4.4 and Fig. 4.5c). Anoxic incubations resulted in increased PO_4^{3-} fluxes in the majority of sampling sites. Rates varied from $-0.8 \pm 0.2\,\mu mol\,m^{-2}\,h^{-1}$ (station 11) to $59 \pm 8\,\mu mol\,m^{-2}\,h^{-1}$ (station 14) and averaged $14 \pm 4\,\mu mol\,m^{-2}\,h^{-1}$. Exceptions were stations 9, 10, 16 and 19, aligned along the central-eastern lagoon sector that showed lower fluxes in the anoxic incubation compared to the fluxes measured under oxic condition. Oxic PO_4^{3-} fluxes were positively correlated with O_2 fluxes and with the oxic fluxes of Mn^{2+}, Fe^{2+}, NH_4^+ and SiO_2 (Table A.3). Anoxic PO_4^{3-} fluxes were positively correlated with OM content and with anoxic Fe^{2+} fluxes (Table A.3).

Internal versus External Loads and Stoichiometry

Internal recycling of NH_4^+ and PO_4^{3-} under aerobic conditions exceeded external loads by a factor of $\sim$ 66 and $\sim$ 2, respectively, whereas SiO_2 loads recycled from the sediments and transported by the Nemunas River were comparable (Table 4.2). Under oxic conditions, summer benthic nutrient regeneration recycled similar amounts of N

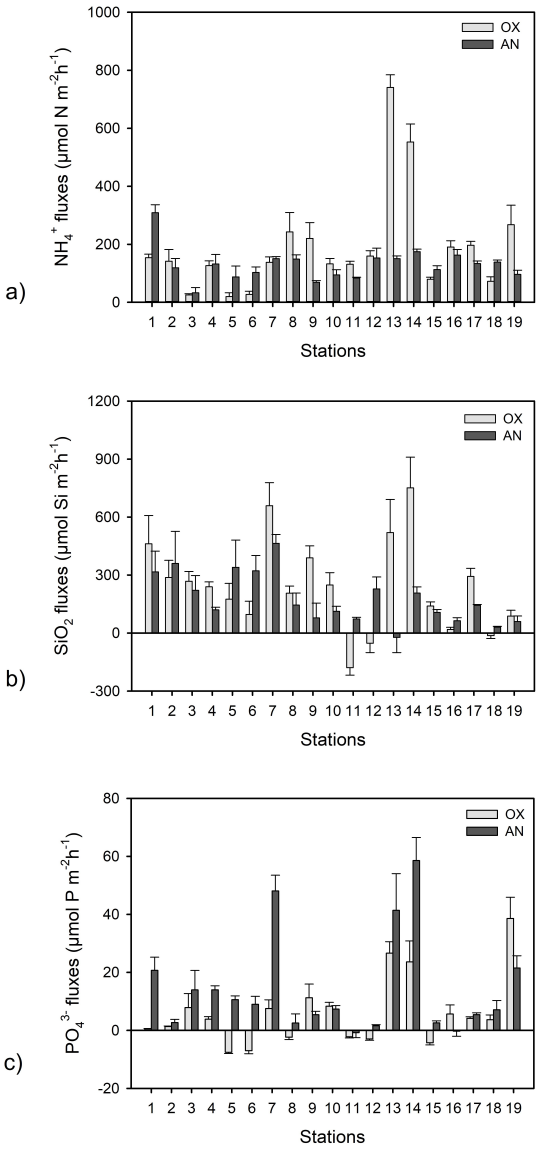

Figure 4.5: Dark NH_4^+ (a), SiO_2 (b) and PO_4^{3-} (c) fluxes measured across the sediment–water interface at 19 sampling stations in the Curonian Lagoon under oxic (*light grey bars*) and anoxic (*dark grey bars*) conditions. Averages ± standard errors are reported ($n = 4$)

Table 4.2: External inorganic nutrient loads from the Nemunas River, the main freshwater input to the Curonian Lagoon, and from the lagoon sediments under oxic and anoxic conditions. The reported external loads are averages ± standard errors from the period July-August of 2012-2016 (Vybernaite-Lubiene et al., 2018). Oxic and anoxic sedimentary fluxes are averages ± standard errors of 19 stations from the present study (July-August 2018).

	NH_4^+	SiO_2	PO_4^{3-}	NH_4^+/PO_4^{3-}	SiO_2/PO_4^{3-}
	$\mu mol\,m^{-2}\,h^{-1}$	$\mu mol\,m^{-2}\,h^{-1}$	$\mu mol\,m^{-2}\,h^{-1}$	mol : mol	mol : mol
Nemunas River external load	2.9 ± 1.8	216.2 ± 55.4	3.0 ± 2.1	1.0 ± 1.3	72.9 ± 69.5
Sediment fluxes (oxic)	190.5 ± 22.5	241.8 ± 28.5	6.2 ± 2.7	31.0 ± 17.5	39.3 ± 22.2
Sediment fluxes (anoxic)	129.1 ± 15.2	177.4 ± 20.9	14.3 ± 3.9	9.0 ± 3.5	12.4 ± 4.9

and Si, largely exceeding P sedimentary fluxes and resulting in unbalanced, P-limited stoichiometry of benthic regeneration (*sensu* (Redfield, 1958)). Results from the anoxic incubations suggest that hyperblooms and O_2 shortage in the study area may result in a 25-30% decrease of inorganic N and Si recycling from sediments and in a 130% increase of inorganic P benthic regeneration. Anoxia would increase the role of sediments as P sources as compared to external loads (4.7 times larger) and would significantly decrease the stoichiometry of benthic NH_4^+:PO_4^{3-} and SiO_2:PO_4^{3-} fluxes (Table 4.2). Under oxic conditions, heterotrophic sedimentary processes would therefore alleviate the inorganic N limitation of external nutrient loads whereas O_2 shortage would enhance N (and Si) limitation for phytoplankton growth -or enhance P availability- (Table 4.2).

4.1.3 Discussion

Aerobic respiration rates and PO_4^{3-}, Mn^{2+} and Fe^{2+} fluxes under oxic and anoxic conditions

Oxygen demand measured in the sediments of the Curonian Lagoon was comparable or higher than rates reported in the summer period by (Zilius et al., 2015; Zilius et al., 2014). The measured benthic respiration in 6 out of 19 stations may turn the bottom water hypoxic ($<$50 $\mu mol\,L^{-1}$) in less than 10 hours and that in 9 out of the remaining 13 stations hypoxia is reached between 10 and 20 hours of dark incubation. Such results emphasize the elevated O_2 consumption of the Curonian Lagoon sediments and suggest that the forecasted increase of water temperature and stratification would augment the occurrence of benthic hypoxia (Störmer, 2011). Benthic O_2 demand was measured along a wide range of sediment typologies, both in terms of organic matter content (from $<$1 to 23%) and median particle size (from nearly 30 to 300 µm). However, these features were poor predictors of benthic respiration, suggesting the relevance of the organic matter quality more than its quantity as driver of benthic respiration (De Vicente et al., 2010;

Pusceddu et al., 2009; Relexans et al., 1992). Unexpected lower respiration rates in organic-rich, muddy sites than in organic-poor, sandy areas might be also due to different levels of macrofauna bioturbation, higher in sandy sediments. Macrofauna activity may play an important role in benthic metabolism and respiration by macrofauna can exceed microbial O_2 consumption (Glud, 2008; Webb & Eyre, 2004). In different sites of the Curonian Lagoon, for example in areas with high density of *D. polymorpha* or chironomid larvae, macrofauna O_2 consumption is demonstrated to drive aerobic respiration (Benelli et al., 2018; Zaiko et al., 2010).

Short-term O_2 depletion produced element- and site-specific effects on PO_4^{3-}, Mn^{2+} and Fe^{2+}. A few studies have simultaneously analyzed the dynamics of these solutes in intact sediment cores and under changing O_2 levels (Conley et al., 1988; Ghaisas et al., 2019; Zilius et al., 2015). In a slurry experiment, where alternating aerobic and anaerobic conditions were reproduced, it has been demonstrated how Mn, Fe, P and N biogeochemical transformations are coupled and vary depending on the initial sedimentary pools of the oxidized metals (Anschutz et al., 2019). The spatial analysis of oxic and anoxic fluxes reveals the presence of hot-spots of PO_4^{3-} release and Fe^{2+} production aligned along the western border of the lagoon, coinciding with zones characterized by clayish, organic-rich sediments and longer water residence time (Ferrarin et al., 2008) (Fig. 4.6). Such zones are scattered in a background of sandy sediments subjected to the influence of the Nemunas plume and river-mediated hydrodynamic effects. In these riverine influenced areas, the increase in Mn^{2+} fluxes during anoxia is clear, whereas differences in PO_4^{3-} and Fe^{2+} production are much less evident (Fig. 4.4 and Fig. 4.6). The zonation where Mn^{2+} and Fe^{2+} effluxes change along with decreasing O_2 levels overlaps the maps reporting water residence time and sediment transport due to freshwater circulation (Ferrarin et al., 2008; Umgiesser et al., 2016) (Fig. 4.6). This evidence, together with the positive correlation between the median particle size and anoxic Mn^{2+} effluxes, suggest elevated concentrations of microbially reducible Mn^{4+} in the terrigenous material exported from the Nemunas basin (Kruopiene, 2007).

At the scale of the Lithuanian sector of the Curonian Lagoon (nearly $500\,km^2$), O_2 shortage tripled average Mn^{2+} fluxes. Manganese reduction and its quantitative importance for organic carbon mineralization is reported in a few studies as compared to other anaerobic mineralization processes as denitrification, iron or sulphate reduction or methanogenesis (Canfield et al., 2005). Denitrification has been and is still extensively studied as it is one of the few and most important processes permanently removing reactive N from aquatic ecosystems and therefore contrasting eutrophication phenomena (Seitzinger, 1990). However, during summer, denitrification in estuarine areas drops due to low nitrate concentrations in the water and to low rates of nitrification in poorly oxygenated sediments (Rysgaard et al., 1995). As a consequence, in this period the share of CO_2 production supported by denitrification is scarce (Canfield et al., 2005). Iron and sulphate reduction have been extensively studied in coastal lagoons and estuarine areas due to the abundance of Fe in sediments, of dissolved sulphate in marine waters and to the Fe-S-P loop that may regulate the mobility of reactive P (Azzoni et al., 2005; Giordani et al., 1996). Anoxic Fe^{2+} fluxes suggest that iron reduction is likely to be an

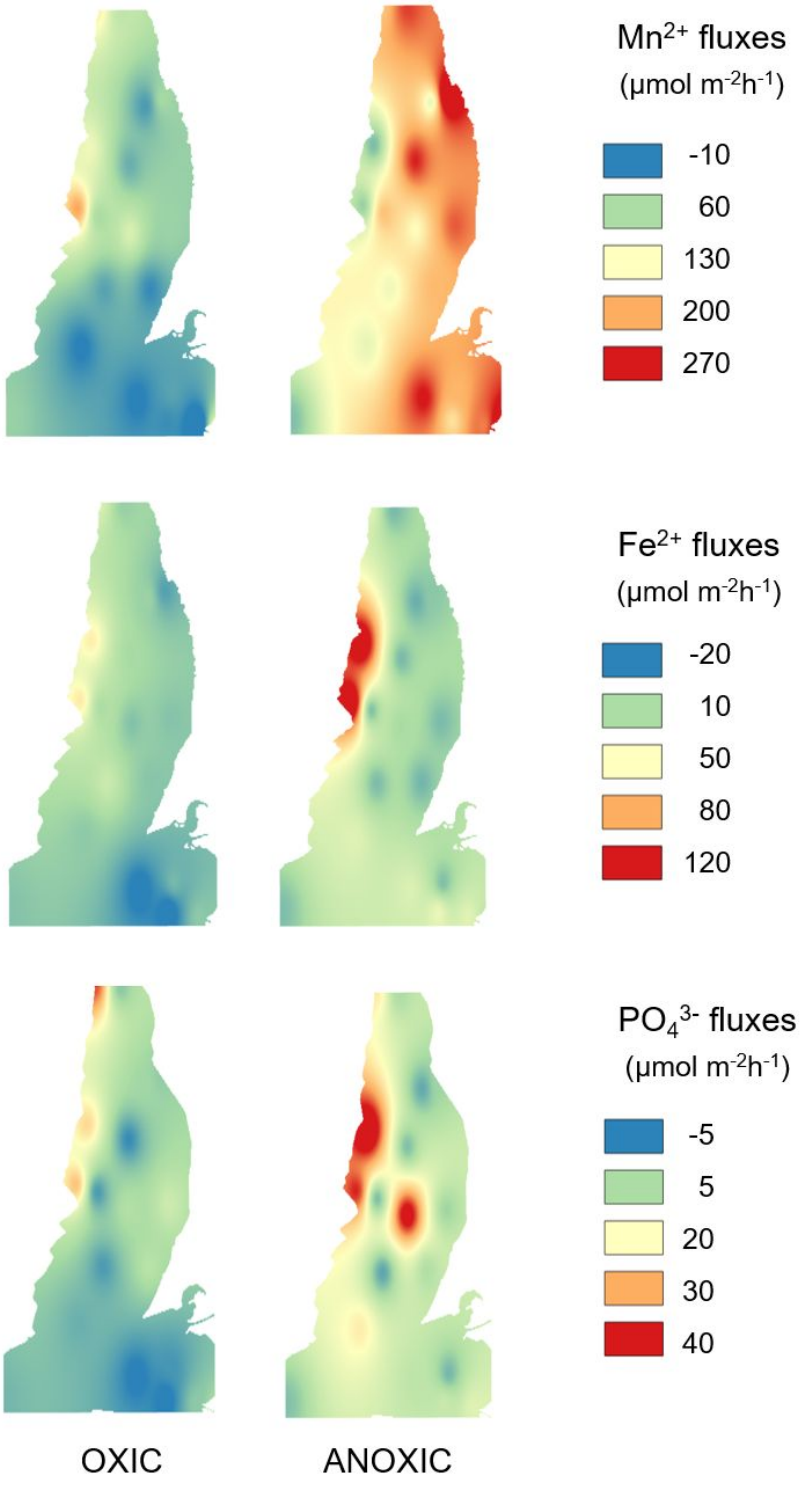

Figure 4.6: Spatial distribution patterns of Mn^{2+}, Fe^{2+} and PO_4^{3-} fluxes interpolated from oxic and anoxic dark incubations at the 19 sampling stations in the Curonian Lagoon

important anaerobic process in the Curonian Lagoon, while low sulphate concentrations in freshwater and the limited marine intrusion in the lagoon suggest a minor importance of sulphate reduction rates in this freshwater estuary, as reported by (Pimenov et al., 2013). Methanogenesis has an important role in freshwater sediments and may be responsible for a major portion of organic matter mineralization; high rates were measured in the Curonian Lagoon silty sediments during summer (Pimenov et al., 2013; Ulyanova et al., 2014).

Results from the present study suggest that under oxic and anoxic conditions manganese reduction is likely responsible for an important fraction of anaerobic CO_2 production, as demonstrated elsewhere (Canfield et al., 1993). Manganese fluxes reported in this study are in a range of those reported for shallow coastal regions, mostly oxic, by (Aller, 1994; Friedl et al., 1998; Pakhomova et al., 2007; Warnken et al., 2001). Large pools of microbially-reducible Mn^{4+} can represent natural geochemical buffers against P release, as Mn^{4+} reduction occurs at higher redox potentials than iron reduction. The present work lacks the quantification of the Mn-P and Fe-P pools in surface sediments; measured fluxes suggest positive correlation between PO_4^{3-} release and Fe^{2+} effluxes under anoxic conditions. The mechanisms underlying P release from the Curonian Lagoon sediments were analyzed in detail in two stations (Petkuviene et al., 2016; Zilius et al., 2015; Zilius, 2016; Zilius et al., 2014). Manipulative experimental studies, simulating the deposition of cyanobacteria cells, resulted in an increase of dissimilative nitrate reduction over denitrification and in a large CH_4 production from sediments, but in a limited release of reactive P (Zilius, 2016). Seasonal measurements of reactive P fluxes in a sandy and in a muddy area revealed large summer PO_4^{3-} release at the muddy site, coinciding with the occurrence of cyanobacterial blooms, and the onset of hypoxia and anoxia in the water column (Petkuviene et al., 2016; Zilius et al., 2014). These events were concurrent with specific climatic conditions as multiple consecutive days with stable weather, no wind and high air and water temperatures. Benthic PO_4^{3-} release occurred when the oxidized pools of metals within sediments were exhausted. Despite short-term, this event produced a significant effect on the lagoon P budget, and resulted in a large export of P (Petkuviene et al., 2016).

Ammonium and reactive silica regeneration under oxic and anoxic conditions

The Curonian Lagoon sediments were large sources of NH_4^+ and SiO_2 to the water column, with small differences under aerobic and anaerobic conditions. Oxygen to NH_4^+ and O_2 to SiO_2 flux ratios, that are proxies of CO_2:NH_4^+ and CO_2:SiO_2 ratios, had as median values 20.4 and 10.7, respectively, either suggesting incomplete mineralization of the sedimentary organic N pool, large production of dissolved organic N or dissolution of lithogenic Si on the surface sediments (Conley et al., 1988; Zilius, 2016).

Since 2009, O_2 penetration depth, total and diffusive benthic O_2 demand, pore water nutrient concentrations and their fluxes were measured or calculated at 2-3 sites representative of dominant sedimentary environments in the Curonian Lagoon, including littoral, pelagic, transitional and confined zones (Petkuviene et al., 2016; Zilius, Bartoli, Daunys et al., 2012; Zilius et al., 2015; Zilius et al., 2014). The Curonian Lagoon

has turbid waters, and most of sediment surface is not illuminated and heterotrophic. Benthic photosynthesis is confined in shallow areas representing a minor fraction (5%) of the total; here benthic algae may retain nutrients and prevent their regeneration to the water column (Benelli et al., 2018; Zilius, Bartoli, Daunys et al., 2012). Spring and summer phytoplankton blooms and the large flux of organic particles to the bottom resulted in limited O_2 penetration in sediments (<1 mm) (Zilius, Bartoli, Daunys et al., 2012; Zilius, 2016). This may explain the general absence of a significant effect of anoxia on NH_4^+ fluxes. Anoxia might be expected to enhance NH_4^+ effluxes due to inhibition of nitrification, however our dataset suggests a generalized decrease of NH_4^+ fluxes. We explain this result in terms of limited nitrification even under oxic conditions and as a consequence of anoxia on macrofauna metabolic activity and bioturbation. Oxygen data suggest that macrofauna may play in some areas an important effect on benthic biogeochemistry and the shortage of O_2 may impact its activity depressing burrowing, ventilation and excretion rates, resulting in lower NH_4^+ production (Bartoli et al., 2009). Anoxia tended also to decrease the large SiO_2 regeneration, suggesting the redox-independence of Si sedimentary pools in the Curonian Lagoon. To the best of our knowledge there are a few studies analyzing the effects of O_2 levels on silica, whose mobility seems mostly driven by dissolution (Conley et al., 1988; Dixit & Van Cappellen, 2002; Yamada & D'Elia, 1984).

Internal versus external nutrient inputs

During the summer period, under aerobic and anaerobic conditions, sedimentary processes recycle to the water column much higher amounts of inorganic N and P compared to those delivered by the Nemunas River. Calculations reported in Table 4.2 suggest that under aerobic conditions benthic fluxes contrast the strong N limitation of external loads, recirculating NH_4^+ in the water mass. They also suggest that if hyperblooms, calm weather and heat waves determine O_2 shortage in bottom water, anaerobic sediment metabolism and large PO_4^{3-} release may turn the water mass N (and Si) limited for phytoplankton growth (Conley et al., 1988). This mechanism, which is supported by a robust dataset, would favor the growth of cyanobacteria, which sometimes extends to September and October (Gasiūnaitė et al., 2006).

4.1.4 Conclusions

This study analysed benthic nutrient regeneration in late July, a critical period for the Curonian Lagoon. Results indicate that heterogeneous sedimentary environments, under oxic conditions, release large amounts of NH_4^+, SiO_2 and PO_4^{3-}. Transient anoxia further stimulates PO_4^{3-} regeneration, whereas it does not affect or slightly decreases dissolved inorganic N and Si effluxes, altering the stoichiometry of benthic regeneration at the lagoon scale. Experimental conditions simulated in this experiment can be realistic at the study site, due to demonstrated water stratification during blooms under calm weather conditions, resulting in decreased O_2 concentration in bottom water (Zilius et al., 2014). For this reason, a further reduction of P inputs from the watershed may not decrease the

frequency of late-summer cyanobacterial blooms in the short term, but in the mid-term, could lead to the increase in water transparency and benthic primary production, favoring the sediment oxidation and the P retention, with a negative feedback for blooms. This study underlines the importance of including the stoichiometry of benthic regeneration as complementary approach to the multi element analysis of external inputs. During low discharge periods, heterotrophic sedimentary processes may not only support most of the pelagic primary production but they also have the potential to affect algal community composition, by changing the relative nutrient availability.

4.2 Temporal and spatial differences in N and P dynamics revealed via Ecological Network Analysis

The combined action of anthropogenic pressures and climate change has demonstrated, multiple effects on nutrients processing in transitional ecosystems, the overall estuarine functioning and the provision of services.

Experimental activities aimed at analysing N and P dynamics usually are focused on single processes and lack the possibility of estuarine biogeochemistry holistic assessments, due to the complexity of mechanisms and their multiple interactions and feedbacks. The evaluation of whole estuarine biogeochemical functioning, the estuarine filter or source role, and the metabolic shifts along environmental gradients and pressures can be only tackled with the application of integrative modelling tools (Christian et al., 2012; Wulff et al., 2012). One such modelling technique is the Ecological Network Analysis (ENA) a suite of algorithms developed to holistically analyse the ecosystem's structure and functioning (Kay et al., 1989; Szyrmer & Ulanowicz, 1987; Ulanowicz, 2004).

Despite most networks have been based on C as currency (Ulanowicz, 2012), several studies demonstrated the potential of targeting N transfers to investigate biogeochemical features of ecosystems (Baird et al., 1995; Christian et al., 1996; Finn & Leschine, 1980). These networks provided insights about dominant processes in different seasons (Christian & Thomas, 2003), the role of multiple interactions among bacteria, macrofauna, and primary producers (Hines et al., 2012; Magri et al., 2018) and on nitrogen budget through direct and indirect exchange paths (Small et al., 2014).

In this study, N and P spring and summer networks were compiled both for the transitional and the confined area of the Curonian Lagoon. The main objectives of this study were to analyse, via the use of the ENA, the main factors that seasonally affect N and P dynamics, to get insight into their different behaviour, and to understand how the identified differences can favour the shift from diatoms to cyanobacteria dominance. It has been hypothesized that (1) the hydrology-driven zonation and the seasonality differentially affect N and P estuarine recycling rates, which increase from the northern transitional to the southern confined area, from the spring to the summer season, and from N to P; (2) the nutrient transfer through the food web crashes at low trophic levels mostly due to the inefficient use of the high primary production; (3) biological control on cyanobacteria blooms from higher trophic levels increase from the spring to the summer seasons, and mostly affect P than N dynamics.

4.2.1 Material and methods

Database and network construction

N and P seasonal networks were constructed for both the transitional and the confined areas for a total of 8 models (*NTSP* - N network-Transitional area-SPring season; *NCSP* - N network-Confined area-SPring season; *PTSP* - P network-Transitional area-SPring season; *PCSP* - P network-Confined area-SPring season; *NTSU* - N network-Transitional area-SUmmer season; *NCSU* - N network-Confined area-SUmmer season; *PTSU* - P

network-Transitional area-SUmmer season; *PCSU*, P network-Confined area-SUmmer season). The spring networks were compiled exploiting data collected in March, April, and May, whereas data collected in July, August, and September were used to build the summer networks. June was excluded because it is characterized by variable conditions among different years, intermediate between the spring and the summer season, and because it is the month when the clear-water phase generally occurs (Pilkaityte, 2007b). When available, data from 2015 have been used, since it was a year characterized by a large data availability, and by a strong summer decrease of the Nemunas River discharge and an intense cyanobacteria bloom in the estuary, which determined spring and summer extreme conditions. Most of the information to construct network models was derived from data obtained from the literature on the Curonian Lagoon as well as from unpublished information provided by experts working at the Marine Research Institute of the Klaipeda University, Lithuania.

Each network consisted of 22 living and 8 non-living compartments. The large data availability allowed to represent non-living compartments with a high level of resolution, separating particulate from dissolved, and inorganic from organic compounds, both in the water column and within the sediments. Regarding the primary producers' community, phytoplankton was given prominence and was divided into 5 dominant groups. Heterotrophic organisms were aggregated according with their prevalent diet. For each compartment the standing stocks were quantified as µmol N/P m^{-2}, whereas inter-compartmental flows, input from, and output to the outside environment were expressed as µmol N/P m^{-2} h^{-1}. Since the communities of the two subareas do not overlap exactly, to maintain the same model configuration, a minimum value for standing stock ($1*10^{-5}$ µmol N/P m^{-2}), input and output ($1*10^{-5}$ µmol N/P m^{-2} h^{-1}) was assumed for those species that were not in common. Such an approach does not affect the outcomes of the analysis (Baird et al., 1998). All the eight final models had the same structure and the same level of aggregation to allow seasonal and spatial comparisons. The nutrient budget was constructed for each heterotrophic compartment according to the steady state equation:

$$C_{N/P} = P_{N/P} + F_{N/P} + U_{N/P} \tag{4.1}$$

in which the total nutrient consumption (C) equals the sum of the secondary production (P), the particulate egestion (F) and the excretion (U). Compared to networks constructed using C or energy as currency, nutrient networks do not include the term representing dissipation or respiration flows. Using the generalized equation each compartment resulted in steady-state conditions, where the sum of the inputs equalled the sum of the outputs.

Non-living compartments

Standing stocks Eight non-living compartments, representing particulate and dissolved nutrient compounds, have been identified. They include dissolved organic N/P in the water column and in the pore water ("DON/P_w", "DON/P_{pw}", respectively), dissolved

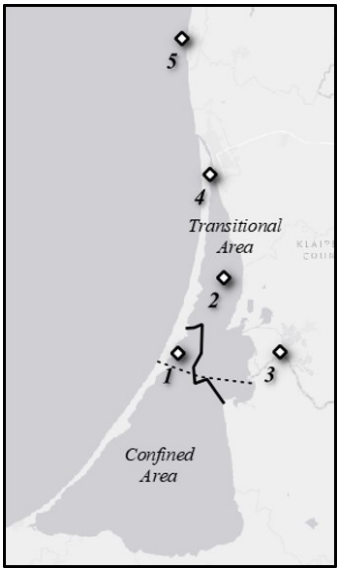

Figure 4.7: Map of the Curonian Lagoon. The subdivision between the northern transitional area and the southern confined area and between the Lithuanian and the Russian sector are indicated by the solid and dashed black line, respectively. The sampling sites reported in (Zilius et al., 2018) are indicated by the white diamonds.

inorganic N/P in the water column and in the pore water ("DIN/P_w", "DIN/P_{pw}", respectively), particulate organic N/P in the water column and in the sediments ("PON/P_w" "PON/P_s", respectively) and particulate inorganic N/P in the water column and in the sediments ("PIN/P_w", "PIN/P_s", respectively). Information concerning concentration values in both subareas and seasons were derived from experimental activities performed in April and August 2015. Samplings were carried out at two sites: the first was dominated by silty sediments and was considered as representative of the confined area (Site 1, 55° 35′ 43″ N 21° 46′ 26″ E, Fig. 4.7), the second was dominated by sandy substrate and considered as representative of the transitional area (Site 2, 55° 41′ 80″ N 21° 43′ 23″ E, Fig. 4.7). Data related to N compounds were reported in (Zilius et al., 2018), whereas data on P have not been published. Concentration values (µmol N/P L^{-1}) were converted to the proper units for standing stocks, by multiplying the same values by the volume of the water column (L m^{-2}), considering an average depth of 1.75 m and 3.5 m for the transitional and the confined area, respectively. Nutrient concentrations in the Curonian Lagoon have been seasonally monitored since 2010 and the reliability of data was verified by comparisons with published information (Bartoli et al., 2021; Petkuviene et al., 2016; Zilius et al., 2015; Zilius et al., 2014).

Inter-compartmental fluxes Seasonal data of nutrient inter-compartmental fluxes were derived from experimental activities carried out in April and August 2015 at Sites 1 and 2 ((Zilius et al., 2018) and unpublished data). Water column production, respiration and N_2-fixation, as well as N and P exchanges at the sediment-water interface were

measured to completely characterize internal processes.

Production and respiration in the water column were measured using the light-dark bottle technique to derive rates of assimilatory and dissimilatory nutrient fluxes. In the transitional area, given the shallow depth of the analysed site ($\sim$ 1 m), measurements were carried out only at the water surface, whereas in the confined area measurements were carried out at three different depths (0-1 m, 1-2.5 m, and 2.5-3.5 m). Volumetric rates were converted to areal rates using the average depth and the proportional contribution of each layer as detailed in (Zilius et al., 2018). Mineralization rates (conversion from particulate to dissolved organic and inorganic nutrients) were estimated by multiplying oxygen fluxes measured under dark conditions (respiration rates) by site-specific stoichiometric ratios for seston reported in (Broman et al., 2021; Zilius et al., 2021). N_2-fixation rates in the water column were determined at the same sites and the same depths, but only in the summer season, because spring rates have been assumed to be negligible (Zilius et al., 2018) and identified ranges were compared with measurements reported in (Broman et al., 2021; Zilius et al., 2021).

Nutrient fluxes at the sediment-water interface were derived from intact core incubations carried out in the same data under dark and light conditions ((Zilius et al., 2018) and unpublished data). DOP, DIP, DIN ($NH_4^+ + NO_2^- + NO_3^-$), and N_2 fluxes have been quantified. Summer fluxes were integrated with data derived from the experimental activities reported in section 4.1, by averaging values collected in sites representative for the transitional and the confined area. Mineralization rates within the sediment were derived from O_2 measurements as reported for the water column, using C:N and C:P ratios for the sediment organic matter reported in (Bartoli et al., 2021; Petkuviene et al., 2016; Zilius et al., 2014). Molecular N fluxes were used to derive the N_2-fixation and denitrification rates. Nitrification rates in sediments have not been directly measured in the Curonian Lagoon, but this process has been assumed to be negligible, mainly in the summer season, due to the limited oxygen penetration depth within the sediments (generally $<$0.5 mm, (Zilius, Bartoli, Daunys et al., 2012)). Daily fluxes were derived considering the average number of dark and light hours corresponding to the date when processes were measured. The obtained data were then compared to results from different studies carried out in sites representative for both the transitional and the confined areas (Bartoli et al., 2021; Broman et al., 2021; Petkuviene et al., 2016; Zilius, Bartoli, Daunys et al., 2012; Zilius, Daunys, Petkuviene et al., 2012; Zilius et al., 2015; Zilius et al., 2014; Zilius et al., 2021).

Input from/Output to the outside environment The transitional area receives external inputs from the Nemunas River, from two minor tributaries (Minija and Danes rivers), from the confined area and from the Baltic Sea, whereas it exports nutrients both to the sea and to the confined area. The confined area receives external inputs from the Deima River and from the transitional area and it exports nutrient to the transitional area. To quantify the riverine inputs to the two subareas, data on nutrient concentration at sites located at the closing sections of the Nemunas (Site 3, Fig. 4.7), Minija and Danes rivers, were derived from monthly measurements performed in 2015

(data reported in (Vybernaite-Lubiene et al., 2018)). The main tributary to the confined area, the Deima River, flows into the Russian area and there are no available data on nutrient concentrations. For this reason, average values of tributaries to the transitional area have been applied (Vybernaite-Lubiene et al., 2017; Vybernaite-Lubiene et al., 2018). For all the tributaries data of the hourly water river discharges related to 2015 were provided by the Lithuanian Hydrometeorological Service and averaged to obtain seasonal values. The hourly riverine nutrient load was obtained by multiplying the concentration values of the different N and P compounds ($\mu mol\,N/P\,L^{-1}$) by the mean river discharge ($L\,h^{-1}$) for the different seasons. The obtained loads ($\mu mol\,N/P\,h^{-1}$) were then divided by the surfaces of the transitional and the confined areas to obtain hourly loads per square meter.

To estimate the nutrient input from and output to the Baltic Sea water samples were collected at a station located in the coastal area of the Baltic Sea, close to the city of Palanga (Site 5, 55° 92′ 07″ N 21° 04′ 43″ E, Fig. 4.7) and in the Klaipeda Strait (Site 4, 55° 66′ 27″ N 21° 13′ 75″ E, Fig. 4.7), respectively. Samplings were performed monthly in 2015 and averaged to obtain seasonal values ((Zilius et al., 2018) and unpublished data). Water exchanges between the lagoon and the Baltic Sea as well as between the transitional and the confined area were derived by the results of a one-year simulation (2015) of the finite element model SHYFEM previously calibrated for the Curonian Lagoon (Ferrarin et al., 2008; Umgiesser et al., 2016; Zemlys et al., 2013). Results from the model simulations returned hourly outcoming or incoming volume of water ($L\,h^{-1}$), which have been averaged to obtain seasonal data. These data were then multiplied by seasonal dissolved and particulate N and P concentrations measured at Sites 4 and 5 to calculate the nutrient exchanges between the lagoon and the sea and at sites representative of the transitional and the confined area (Sites 1 and 2) to calculate exchanges between the areas. The obtained loads ($\mu mol\,N/P\,h^{-1}$) were then divided by the surfaces of the transitional and the confined areas to obtain hourly loads per square meter.

Primary producers

Standing stocks The phytoplankton community was divided into 5 different compartments ("Non N-fixing Cyanobacteria"; "N-fixing Cyanobacteria"; "Diatomophyceae"; "Chlorophyceae"; "Phyto-all others"). Values of Chl-*a* concentration referred to 2015 were derived from sampling activities carried out monthly at Site 1 and 2 (unpublished data). The reliability of these data was attested by comparisons with literature data, mainly large spatial and temporal analysis via remote sensing application to the Curonian Lagoon (Bresciani et al., 2014; Bresciani et al., 2012; Vaičiūtė et al., 2015; Vaičiūtė et al., 2021). Data of Chl-*a* concentration ($\mu g\,L^{-1}$) have been converted in C concentration by using a C:Chl-*a* ratio spanning from 34 to 99, and specific for each phytoplankton group (Sathyendranath et al., 2009) and in N and P concentration by using specific C:N:P ratios derived from the literature (Klausmeier et al., 2008; Klausmeier et al., 2004). The obtained concentration values ($\mu mol\,N/P\,L^{-1}$) were multiplied by the water column volume of the photic zone ($L\,m^{-2}$) and converted into areal values. The photic zone volume in

the transitional area represents 95% and 75% of the entire water column volume in the spring and the summer season, respectively, whereas in the confined area it represents 53% and 13% of the entire volume in the spring and the summer season, respectively (Petkuviene et al., 2016; Zilius et al., 2014).

Primary producers were then represented by microphytobenthos ("MPB") and another compartment including both macroalgae and macrophytes ("Malgae-Mphytes"). Microphytobenthos pools were calculated starting from data on sediment Chl-*a* concentration ($\mu g\, m^{-2}$) obtained from the experimental activities carried out seasonally at Sites 1 and 2 in 2015 (unpublished data). Microphytobenthos distribution has been assumed to be limited to the 0-1 cm depth. Chlorophyll concentration has been converted in C concentration by using a C:Chl-*a* =40 (Jones, 1979) and in N and P concentration by using a C:N:P=158:18:1 (Kahlert, 1998). The main species included in "Malgae-Mphytes" compartment are *Chara aspera*, *Chara contraria*, *Potamogeton perfoliatus*, *Potamogeton rutilus*, *Stuckenia pectinata*, *Myriophyllum spicatum*, *Nitellopsis obtusa*, and *Cladophora glomerata*. Data on biomass were derived from samplings carried out in July 2020 in different stations located in the littoral area of the Curonian Lagoon (unpublished data). Average values were calculated, and distribution was considered uniform for areas characterized by depth $<2\,m$, which represents about 30% of the total surface of the transitional area and less than 5% of the total surface of the confined area. Biomass values ($g_{dw}\, m^{-2}$) were converted in N and P concentration using species-specific nutrient percentage content derived from the literature (%N ranging from 0.5 to 3.3, %P ranging from 0.1 to 0.4) (Demars & Edwards, 2007, 2008; Duarte, 1992; Rojo et al., 2020).

Inter-compartmental fluxes Data on phytoplankton net and gross primary production were derived from the experimental activities carried out via the light-dark bottle techniques at Sites 1 and 2 in 2015. As reported for water column respiration and mineralization, the measured volumetric rates were converted to areal rates using the average depth and the proportional contribution of each layer (Zilius et al., 2018). Nutrient assimilation rates were calculated by multiplying net primary production rates by C:N:P ratios derived from the literature and specific for each phytoplankton group (Klausmeier et al., 2008; Klausmeier et al., 2004). Exudates production (fluxes directed from phytoplankton to dissolved organic N/P) was assumed 12% of the total organic C production, as reported for the Curonian Lagoon in (Krevs et al., 2007). Phytoplankton sedimentation rates were derived from results of experimental activities carried out in the spring and the summer season in the Curonian Lagoon (Bukaveckas et al., 2019). Phytoplankton mortality (fluxes directed from phytoplankton to particulate organic N/P) were derived from mass balance procedures. Data on microphytobenthos net and gross primary production were derived from results of intact core incubations carried out under light and dark conditions at Sites 1 and 2 in 2015 and then compared with literature data (Bartoli et al., 2021; Benelli et al., 2018). As reported for phytoplankton production N and P uptake was calculated starting from net primary production by using a C:N:P=158:18:1 (Kahlert, 1998). Data on macroalgae and macrophytes production were calculated by using specific biomass-production rates derived from experimental activities carried out

in the Curonian Lagoon (Politi et al., 2021) and in similar environments (Kotta et al., 2021; Nõges et al., 2010; Torn et al., 2006).

Input from/Output to the outside environment Data of Chl-*a* concentration of the five phytoplankton groups at the closing section of the Nemunas River (Site 3) were derived from seasonal samplings carried out in 2015 (unpublished data) and used to calculate riverine phytoplankton inputs. These concentration values were used also to calculate inputs from the minor tributaries since specific data were not available. Chlorophyll concentrations were also seasonally monitored at Sites 1 and 2 and Sites 4 and 5, and these data were used to determine phytoplankton exchanges between the two subareas and between the lagoon and the sea. Chlorophyll values were converted in N and P concentration as described in section 4.2.1 and then combined with hydrological data to calculate all the inputs from and the outputs to the outside environment as described for non-living compartments in section 4.2.1.

Zooplankton

Standing stocks and fluxes The zooplankton community was divided in three different compartments, according to the prevalent diet ("zooplankton-Herbivorous"; "zooplankton-Omnivorous"; "zooplankton-Predators"). The main species included in the herbivorous compartment are *Daphnia longispina*, *Diaphanosoma brachiorum*, *Eudiaptomus graciloides*, *Bosmina* sp., *Chidorus sphaericus*; the main species included in the omnivorous compartment is *Mesocyclops leuckarti*; the main species included in the predators compartment are *Cyclops strenuus* and *Leptodora Kindtii* (Gasiunaite & Razinkovas-Baziukas, 2004; Gasiūnaitė et al., 2006; Lesutienė et al., 2012).

Values of biomass per liter ($\mu g\, C\, L^{-1}$) for each group were derived from samplings carried out in spring and summer 2015 at Sites 1 and 2 (unpublished data) and the reliability of data was assessed by comparison with published information (Dmitrieva & Semenova, 2012; Gasiūnaitė et al., 2012; Lesutienė et al., 2012; Semenova, 2011). Data were converted in N and P values using stoichiometric ratios specific for copepods, cladoceran and rotifers derived from literature (Ventura, 2006). The distribution of the zooplankton was not considered uniform along the whole water column, but the vertical migration depth of zooplankton was calculated considering the thickness of the photic zone according to the model reported in (Dodson, 1990).

Data on feeding intake and N and P excretion and egestion rates were calculated according to the model developed by (Ejsmont-Karabin, 1984). Zooplankton taxa feed upon phytoplankton, particulate organic N or P and in some cases prey upon other zooplankton compartments. Since we did not know the relative species composition of each group to characterize the diet, we could not apply criteria based on food size selection. The overall intake of each group was apportioned among various donor (prey) compartments in proportion to their standing stocks.

Input from/Output to the outside environment Data of zooplankton biomass per liter at the closing section of the Nemunas River (Site 3) were derived from seasonal samplings carried out in 2015 (unpublished data) and used to calculate riverine inputs. These values were used also to calculate inputs from the minor tributaries since specific data were not available. Zooplankton biomass were seasonally monitored in 2015 at Sites 1 and 2, at Site 4, and at a station located in the coastal area of the Baltic Sea (55° 75′ 40″ N 20° 81′ 25″ E). These data were used to determine zooplankton exchanges between the two subareas and between the lagoon and the sea. Values were converted in N and P concentration as described for standing stocks calcultions and then combined with hydrological data to calculate all the inputs from and the outputs to the outside environment as described for non-living compartments.

Macrofauna

The macrofauna has been divided in five different compartments, representing the dominant categories within the Curonian Lagoon (Bubinas & Vaitonis, 2005; Daunys, 2001). The complete inventory of the species present is reported in (Zettler & Daunys, 2007). Two compartments represent the dominant filter feeding species, the first include the invasive *Dreissena polymorpha* (Macrofauna-Dreissena) and the second (Macrofauna-Unio/Anodonta) include the native unionids (mostly *Unio tumidus*) and anodonta (mostly *Anodonta anatina*). Two compartments, Macrofauna-Oligochaeta and Macrofauna-Chironomidae, include mainly deposit feeder organisms and are the most widespread groups in the Curonian Lagoon. The last group (Macrofauna-all others) include mainly amphipods inhabiting the littoral area. Biomass values of the first four groups (Macrofauna-Dreissena, Macrofauna-Unio/Anodonta, Macrofauna-Oligochaeta and Macrofauna-Chironomidae) were derived from unpublished data collected in May from 2015 to 2018 in different stations representative of both the transitional and the confined subareas. The macrofauna distribution within the lagoon is very patchy and collected data were therefore characterized by a high variability. For this reason, to obtain the most representative average values and ranges, we decided to consider measurements derived from all years and not just from 2015. Biomass values of the last compartment (Macrofauna-all others) were obtained from published information derived from experimental activities carried out in different areas of the Curonian Lagoon (Arbačiauskas et al., 2013; Berezina et al., 2017).

The biomass values of macrofauna ($g_{ww}\,m^{-2}$) were converted in dry weight values assuming a dry mass/wet mass percentage ratio ranging from 8.50 to 14.00%, specific for the different groups (Ricciardi & Bourget, 1998), and then converted in N and P using nutrient percentage content (%N ranging from 8.57 to 12.57, %P ranging from 0.82 to 1.25) derived from (Allgeier et al., 2020; Andrieux et al., 2020).

Intake rates were calculated according to (Cammen, 1980), whereas N and P excretion and egestion rates were calculated according to (Vanni & McIntyre, 2016). Secondary production was derived from mass balancing procedure and compared with literature data (Asmus & Helgoland, 1982; Warwick et al., 1979). Filter feeding organisms consume mainly zooplankton, phytoplankton and water column particulate organic N and P, whereas deposit feeding organisms consume mainly sedimentary particulate organic N

or P within the sediment and microphytobenthos. The overall intake of each group was apportioned among various donor (prey) compartments in proportion to their standing stocks.

Fishes

Almost 60 fish species were identified in the Curonian Lagoon and the complete inventory is reported in (Repečka, 2003). The community was divided in three different compartments ("Fish-Predators"; "Fish-Benthivorous"; "Fish-Planktivorous"). The benthivorous fishes represent the dominant group, mainly composed by Roach (*Rutilus rutilus*), Bream (*Abramis brama*), Silver bream (*Blicca bjoerkna*), Vimba (*Vimba vimba*) and Ruffe (*Gymnocephalus cernuus*), whereas predators are mainly represented by Perch (*Perca fluviatilis*) and Pikeperch (*Sander lucioperca*). There are few species of strictly planktivorous, and this group is mainly composed by juveniles. There is limited information about the fish stocks in the Curonian Lagoon. Areal biomass values ($g_{ww}\,m^{-2}$) for the Lithuanian and the Russian area are reported only for the dominant species, whereas the remaining species are pooled together (Repečka, 2008, 2009; Žydelis & Kontautas, 2008). The biomass values were converted in dry weight values considering the dry mass to be 23.50% of the wet mass. The dry biomass was then converted in N and P pools assuming nutrient percentage content vales (%N ranging from 9.00 to 13.00, %P ranging from 2.30 to 7.50) derived from the literature (Allgeier et al., 2020; Andrieux et al., 2020; Czamanski et al., 2011; Pilati & Vanni, 2007; Tanner et al., 2000).

Nitrogen and P excretion and egestion rates were calculated according to (Vanni & McIntyre, 2016), whereas food intake rates were calculated according to (Palomares & Pauly, 1998; Pauly, 1989). Secondary production was derived from mass balance procedures and compared with literature data (Schindler & Eby, 1997; Vanni et al., 2013). Diet information of the dominant species was derived from studies carried out in the Curonian Lagoon (Bubinas & Ložys, 2000; Rakauskas, 2020; Rakauskas et al., 2013) and in similar environments (Costa et al., 1992; Fieszl et al., 2011; Gallagher & Dick, 2015; Jacobson et al., 2019; Kallio-Nyberg et al., 2007; F. L. Kelly & King, 2001; Krpo-Ćetković et al., 2010; Malbrouck et al., 2006; Pyrzanowski et al., 2019; Skóra et al., 2018; Syväranta et al., 2009). Starting from the diet composition, the amount of each prey was converted in the amount of consumed C and then N and P using the appropriate elemental ratios (Allgeier et al., 2020; Andrieux et al., 2020). Data on catches of the main species both in the Lithuanian and in the Russian Area were derived from an official report from the Fisheries Department of the Ministry of Agriculture containing information from 1950 to 2010.

Birds

About 35 bird species were identified in the Curonian Lagoon and the complete inventory is reported in (Morkune et al., 2020). The community was divided in four different compartments, according to the prevalent diet ("Bird-Piscivorous"; "Bird-Omnivorous"; "Bird-Herbivorous"; "Bird-Benthivorous"). Data used for model construction derived from

visual bird surveys performed monthly from March to November 2018 in the Lithuanian part of the Curonian Lagoon (Morkune et al., 2020). Data on the Russian area are not available and individual densities calculated for the Lithuanian area have been used. Birds abundance values (ind. m^{-2}) were converted in biomass values ($g_{ww}\, m^{-2}$) using average body masses values for each identified species as reported in (Dunning, 2008). These values were converted in dry weight values ($g_{dw}\, m^{-2}$) assuming a dry mass/wet mass percentage ratio of 34.98% and then in N and P pools assuming nutrient percentage content (%N ranging from 5.71 to 14.57, %P ranging from 1.00 to 7.50) derived from (Allgeier et al., 2020; Andrieux et al., 2020).

Excretion and egestion rates were calculated by using species-specific rates derived from literature studies carried out in environments similar to the Curonian Lagoon (Adhurya et al., 2020; Goc et al., 2005; Gwiazda et al., 2010; Hahn et al., 2007; Hatano et al., 2013; Marion et al., 1994; Somura et al., 2015). Food intake was calculated for each species according to the model proposed by (Nagy, 2001). Diet information, when available, was derived from the literature on the Curonian Lagoon (Putys & Zarankaite, 2010; Rakauskas et al., 2013; Švažas et al., 2011; Žydelis & Kontautas, 2008), otherwise from studies carried out in similar environments (Beintema, 1997; Gilbert & Servello, 2005; Koli & Soikkeli, 1974; Kubetzki & Garthe, 2003; Lemmetyinen, 1973; Nilsson, 2005; Stempniewicz et al., 2012; Švažas et al., 1994; van der Winden & Nesterenko, 2003). Starting from the diet composition, the amount of each prey was converted in the amount of consumed C and then N and P using the appropriate elemental ratios (Allgeier et al., 2020; Andrieux et al., 2020).

Because of the large and complex databases, the data used for network analysis are reported in Supplementary Material. Table A.4 and Table A.5 contain the complete list of N and P pools, respectively. Table A.6 and Table A.7 contain the complete list of fluxes of N and P, respectively, including the inputs from (indicate as fluxes from donor compartment number 0) and the outputs to (indicate as fluxes to receiving compartment number 0) the external environment, and internal exchanges of each compartment and for each analysed model.

Ecological Network Analysis

The ENA is a suite of different analyses based mostly on matrix algebra described in detail in (Kay et al., 1989; Ulanowicz, 2004). The structure of each network is represented by a matrix of exchanges, where energy or matter flows from row compartments to column compartments. Three column vectors representing imports, exports, and standing stocks for each compartment complete the input data that were fed to the package *enaR* developed for the network analysis in the R environment (Borrett & Lau, 2014; R Core Team, 2018). To balance each compartment as required by the steady state assumption, adjustments were made to the flows within the identified variation ranges to reach at least 15% unbalanced in respect to each compartment throughflow (Scharler & Borrett, 2021). The overall balancing of the network was done by using the algorithm developed by (Allesina & Bondavalli, 2003).

The ecosystem size and activity were estimated by the total system throughflow

(TST), which represents the total amount of medium flowing through the network and is computed as the sum of all flows (inputs, outputs and inter-compartmental flows) (Finn, 1976; Kay et al., 1989). Higher TST values indicate a bigger or more active system. The TST can be partitioned into acyclic and cycled flow. In networks, a cycle represents a series of transfers among compartments, which begins and ends in the same compartment without crossing it twice. The biogeochemical cycles analysis allows to assess the structure and the magnitude of cycles within the system and to quantify the total amount of material that flows through cycles of various lengths. The Finn cycling index (FCI) is calculated from the ratio between the cycled flow and the TST (Baird & Ulanowicz, 1989; Finn, 1980). This index quantifies how much material is reused within the systems and it is an indicator of their retention capacity (Baird et al., 2011; de la Vega, Schückel et al., 2018). Another indicator related to the development degree of the system is the Average Path Length (APL), which represents the average number of compartments that a unit of matter imported from the outside crosses before leaving the system (Finn, 1976). The APL is defined as (TST - Z)/Z, where Z represents the sum of all exogenous inputs (Kay et al., 1989). Higher values are indicative of a more developed and connected system, characterized by longer pathways.

The Output Environ Analysis allows calculating the proportion of any internal exchanges ascribed to a unitary input of matter/energy (Fath & Patten, 1999; Patten et al., 1976). Each import is considered separately, and the results are additive. If applied to nutrient networks it can be used to track the fate of a unit of the imported nutrient, as it passes through the system until it leaves. Results indicate how often imported nutrients pass through each pathway or process. These frequencies are often portrayed as percentages and values greater than 100 reflect rapid recycling within the system. In this study, we focused on the fate of a unit of dissolved inorganic N or P (DIN/P) imported into the system to quantify the frequency with which it was taken up by phytoplankton before being exported and to determine in which forms it leave the systems (Christian & Thomas, 2003; Small et al., 2014).

The Total Dependency Analysis allows assessing the dependency of any compartment on any other compartment activity, through direct and indirect pathways. The algorithm constituting the total dependency analysis produces a matrix in which the coefficients express the fraction of each compartment's throughflow that previously resided in another compartment (Kay et al., 1989; Szyrmer & Ulanowicz, 1987). This analysis can be used to depict the extended diet (or the main sources of uptake) of a species or compartment, not considering only direct relationships but also indirect ones. The diagonal elements of the dependency matrix are interpreted as the fractions of throughput that compartments recycle back to themselves and values higher than 100 suggest high recycling activity. In this study, we focused on the dependency of dominant groups of phytoplankton.

The Lindeman trophic analysis allows collapsing a complex ramified network into a linear sequence of transfers from one trophic level to the next, known as the Lindeman Spine (Ulanowicz & Kemp, 1979). The Lindeman Spine informs about how much matter or energy each level receives from the preceding one and from the outside environment, as well as the fraction that is lost from each level through export or recycled back to

the detritus pool. This analysis allows calculating the efficiency of nutrient transfer from each level to the next, whereas the overall systems trophic efficiency was calculated as the geometric mean of trophic efficiency of single transfers (Baird et al., 2011). In carbon or energy networks the first trophic level is represented both by autotrophs organisms and detritus pool, whereas in nutrient networks the first level is represented by dissolved and particulate pools of N or P, with primary producers shifted to the second level since they consume dissolved N and P.

Uncertainty analysis

Most of the data used for the networks construction are derived from experimental activities and carry a given amount of uncertainty, which differed for each parameter used. These uncertainties determine the existence of a set of plausible networks for each tested model. To assess the robustness of ENA results, we performed an uncertainty analysis according to (Hines et al., 2018), which allows to quantify how the combined error in all parameters propagates through the model calculations. This analysis is based on Monte Carlo simulation and produces ranges of variability of ENA outputs, starting from variations in model inputs (Hines et al., 2018; Scharler & Borrett, 2021). 1000 model parametrizations for each of the eight tested models have been created with a linear inverse modelling approach using the limSolve package for R and tested using the enaUncertainty function from *enaR* package (Borrett & Lau, 2014; Borrett et al., 2018; Hines et al., 2018). Each of the plausible models was constrained to be in steady-state conditions and every parameter used was sampled considering a uniform distribution of the uncertainty ranges assigned to each network flow. This allowed calculating the 95% confidence intervals for each output. The differences between indices were considered to be significant if the 95% confidence intervals did not overlap (de la Vega, Horn et al., 2018; de la Vega, Schückel et al., 2018).

4.2.2 Results

Flow Analysis

The TST values, calculated from N and P networks, revealed striking temporal, spatial, and nutrient-specific differences (Fig. 4.8a and Fig. 4.8b). TST is indicative of the total system activity, including both imports from the outside and internal processing rates. Values ranged from 4000 to 10000 µmol m^{-2} h^{-1} and from 200 to 600 µmol m^{-2} h^{-1} for N and P networks, respectively, and differed by a factor of nearly 20 between the two nutrients. In spring, TST was significantly higher in the transitional area compared to the confined area for N networks, whereas values derived from P networks were not significantly different between areas. Both N and P summer networks showed higher TST compared to the spring ones and significantly higher in the confined than in the transitional area.

The percentage of TST involved in recycling, quantified by FCI, generally increased from the transitional to the confined area, from the spring to the summer season, and

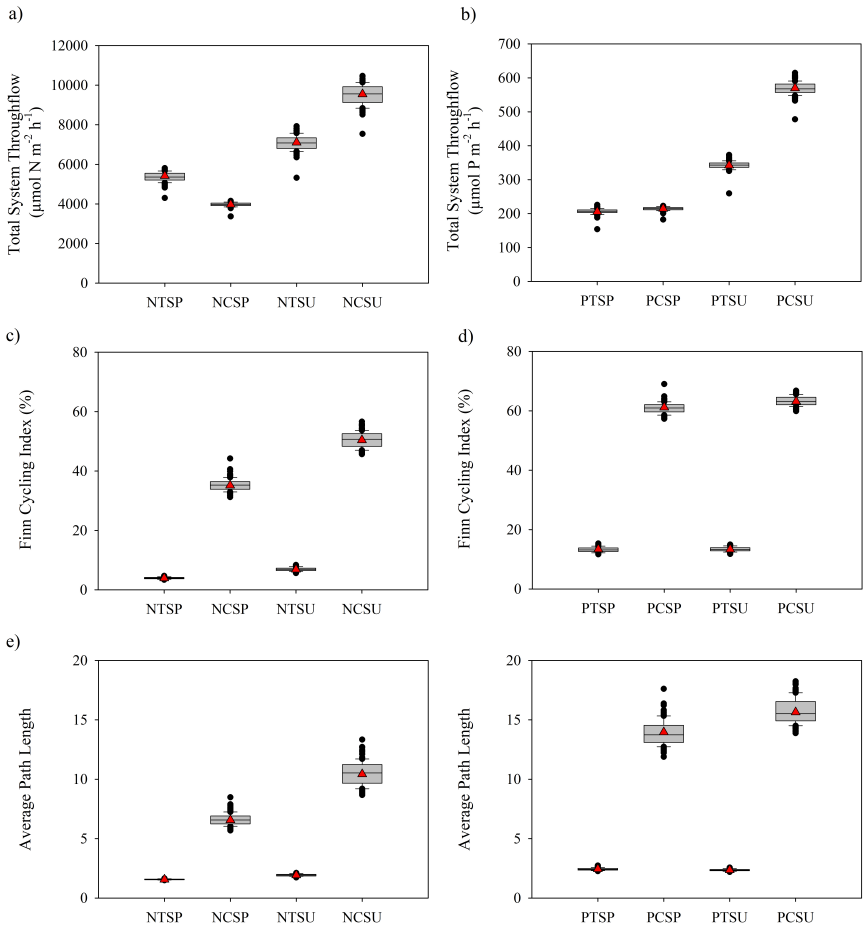

Figure 4.8: Total system throughflow (TST), Finn Cycling Index (FCI), and Average Path Length (APL) calculated from N (plots a, c, e, respectively) and P (plots b, d, f, respectively) networks. Graphs display both values derived from initial networks (*red triangles*) and 95% confidence intervals derived from the application of the uncertainty analyses (*grey boxes*). Abbreviations indicate: *NTSP* (N network-Transitional area-SPring season), *NCSP* (N network-Confined area-SPring season), *NTSU* (N network-Transitional area-SUmmer season), *NCSU* (N network-Confined area-SUmmer season), *PTSP* (P network-Transitional area-SPring season), *PCSP* (P network-Confined area-SPring season), *PTSU* (P network-Transitional area-SUmmer season), *PCSU* (P network-Confined area-SUmmer season).

from N to P (Fig. 4.8c and Fig. 4.8d). In both seasons, the transitional area recycled less than 10% of N and slightly more (13%) P; this indicates that almost 90% of the imported nutrients were exported to the outside without being involved in cycling. Seasonal FCI values for the confined area ranged from 35% to 50% for N, and from 61% to 63% for P in spring and summer, respectively. The APL followed the same trend of FCI and was linearly correlated with it (Fig. 4.8e and Fig. 4.8f, data on linear correlations not shown). APL values revealed that within the transitional area most of N and P cycled over short path lengths, involving no more than 3 compartments, whereas within the confined area, nutrients were transferred over longer loops, with values ranging from 6 to 15, with this latter that characterized the P network in the summer season. The distribution of the plausible results, derived from the application of the uncertainty analysis, allowed us to observe for both FCI and APL indices significant differences between areas and between N and P networks, whereas differences between seasons were significant only for N networks (Fig. 4.8c-f).

Lindeman Spine

To understand the distribution of the total flow through the trophic food web, the N and P networks have been reshaped into the Lindeman Spine, consisting of a discrete trophic levels chain (Fig. 4.9 and Fig. 4.10). In all these chains, the first trophic level represents non-living compartments (dissolved and particulate nutrients forms), the second level includes all primary producers (different phytoplankton groups, microphytobenthos, and the compartment grouping macroalgae and macrophytes). The community of heterotrophs was apportioned to the higher trophic levels according to their dietary composition. The imports and exports from and to the outside system and the amount of nutrients returned to the detrital pool are also shown. From the trophic analyses, up to nine integer trophic levels have been identified, but after the sixth level, only negligible amounts of nutrients were transferred. Within the transitional area most of the nutrient inflow to the first level was sustained by external inputs (2806 and 2113 $\mu mol\,N\,m^{-2}\,h^{-1}$, and 43 and 47 $\mu mol\,P\,m^{-2}\,h^{-1}$, in spring and summer respectively), representing 82% and 71% of the total N input to the first level in spring and summer, respectively (3431 and 2975 $\mu mol\,N\,m^{-2}\,h^{-1}$ in spring and summer respectively), and about 50% of total P in both seasons (85 and 104 $\mu mol\,P\,m^{-2}\,h^{-1}$ in spring and summer respectively), whereas the remaining portion was sustained by internal recycling. In both seasons the amount of N exported from the lagoon ecosystem (2907 and 2248 $\mu mol\,N\,m^{-2}\,h^{-1}$ in spring and summer, respectively) was higher than the imported amount, indicating that this area of the lagoon acted as a net source of particulate or dissolved N, whereas P inputs almost equalled the outputs (49 $\mu mol\,P\,m^{-2}\,h^{-1}$ in both seasons).

In the confined area the amount of nutrients imported from the main tributary and the transitional area (484 and 536 $\mu mol\,N\,m^{-2}\,h^{-1}$ and 7 and 12 $\mu mol\,P\,m^{-2}\,h^{-1}$ in spring and summer, respectively) represented a minor portion of the total input to the first level (1338 and 2857 $\mu mol\,N\,m^{-2}\,h^{-1}$ and 65 and 165 $\mu mol\,P\,m^{-2}\,h^{-1}$ in spring and summer, respectively), ranging from 19% to 36% and from 7% to 11% for N and P, respectively, with higher values displayed in the spring season. For both N and P

Figure 4.9: The Lindeman Spines of N and P networks in the spring season. All values are indicated in $\mu mol\,N/P\,m^{-2}\,h^{-1}$. The roman numbers inside the boxes indicate the identified discrete trophic levels. Blue arrows indicate nutrients transfer through trophic levels, red diagonal arrows on the top of the boxes indicate inputs from the outside, green grounding symbols on the bottom indicate output to the outside, whereas dashed blue arrows indicate the amount of nutrients returned to the detrital pool. Percentage values within the boxes indicate the fraction of the input to the same trophic level that is transferred to the next one. Abbreviations indicate: *NTSP* (N network-Transitional area-SPring season), *NCSP* (N network-Confined area-SPring season), *PTSP* (P network-Transitional area-SPring season), *PCSP* (P network-Confined area-SPring season).

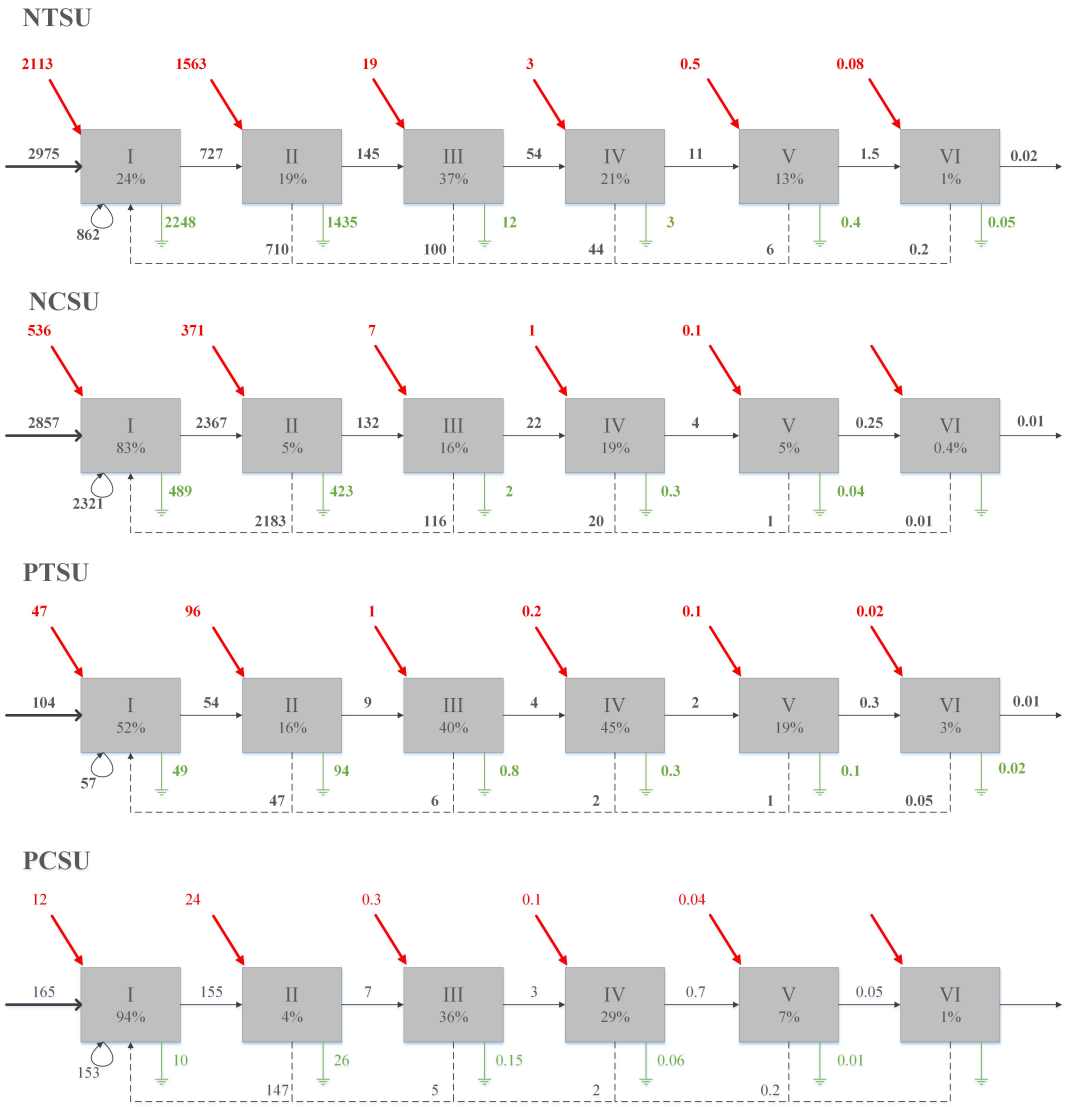

Figure 4.10: The Lindeman Spines of N and P networks in the summer season. All values are indicated in μmol N/P m^{-2} h^{-1}. The roman numbers inside the boxes indicate the identified discrete trophic levels. Blue arrows indicate nutrients transfer through trophic levels, red diagonal arrows on the top of the boxes indicate inputs from the outside, green grounding symbols on the bottom indicate output to the outside, whereas dashed blue arrows indicate the amount of nutrients returned to the detrital pool. Percentage values within the boxes indicate the fraction of the input to the same trophic level that is transferred to the next one. Abbreviations indicate: *NTSU* (N network-Transitional area-SUmmer season), *NCSU* (N network-Confined area-SUmmer season), *PTSU* (P network-Transitional area-SUmmer season), *PCSU* (P network-Confined area-SUmmer season).

networks, the available nutrients were transferred to primary producers (transfers from the first to the second level) with higher efficiency in the confined area (ranging from 63% to 94%) compared to the transitional one (ranging from 15% to 52%). The amount of nutrient imported from the outside to the transitional area directly to the second level, like phytoplankton, increased in summer (from 658 $\mu mol\,N\,m^{-2}\,h^{-1}$ in spring to 1563 $\mu mol\,N\,m^{-2}\,h^{-1}$ in summer and from 40 $\mu mol\,P\,m^{-2}\,h^{-1}$ in spring to 96 $\mu mol\,P\,m^{-2}\,h^{-1}$ in summer) whereas for the confined area this amount represented a small portion of the total input to the second trophic level. The grazing efficiency (transfers from the second to the third level) within the transitional area for both N and P ranged from 16% to 19%, with minimal seasonal differences. Within the confined area these values decreased compared to the transitional area, and for both nutrients halved from the spring to the summer season (from 10% to 5% for N and from 8% to 4% for P, respectively). The remaining portion was either exported to the outside or returned to the first level, the latter representing the dominant process within the confined area, with amounts increasing from spring to summer. For higher trophic levels, P was more effectively transported to and used by consumers compared to N. The systems trophic efficiency ranged from 12% to 18% for N and from 20% to 22% for P.

Output Environ Analysis

In this study, Output Environ Analysis has been applied to assess the fate of imported nutrients as they leave the analysed systems. In particular, we focused on dissolved inorganic nutrients because they are the most significant and readily available sources of N and P for phytoplankton. Dissolved inorganic nitrogen (DIN), comprising NH_4^+, NO_2^- and NO_3^-, is supposed to leave the system in dissolved or particulate inorganic or organic forms, to be permanently stored within the sediment, or to be converted to molecular N_2 gas via denitrification, mostly within the sediment (this process is here represented as output from DIN_{pw} compartment). Fig. 4.11a shows the probability that a unit of imported DIN is exported by one of the designated processes. It shows that in spring more than 80% of DIN imported into the transitional area left the system in the same form as it enters, whereas about 5% was permanently removed via sediment storage or denitrification, and the remaining portion was exported to the outside as phytoplankton. In the same season, in the confined area, the proportion of N exported in particulate forms, both as PON_w and phytoplankton, or as DON_w increased, together with the contribution of permanent removal processes as sediment storage (PN_s, 17%) and denitrification (DIN_{pw}, 10%). In summer, in both areas, the amount of N exported as particulate organic N increased, peaking at 83% in the confined area, whereas the remaining portion was mostly represented by DON_w. In the transitional area DIN_w still contributed to 35% of exports. In summer the contribution of permanent removal processes decreased, representing less than 3% in both areas.

In spring dissolved inorganic phosphorous (DIP_w) was exported from the transitional area mainly as phytoplankton (36%) and water column DIP_w (27%), whereas about 26% was stored within sediments (PN_s, Fig. 4.11b). In the same area, the amount exported as DIP_w decreased in summer, and the amount stored within the sediment was

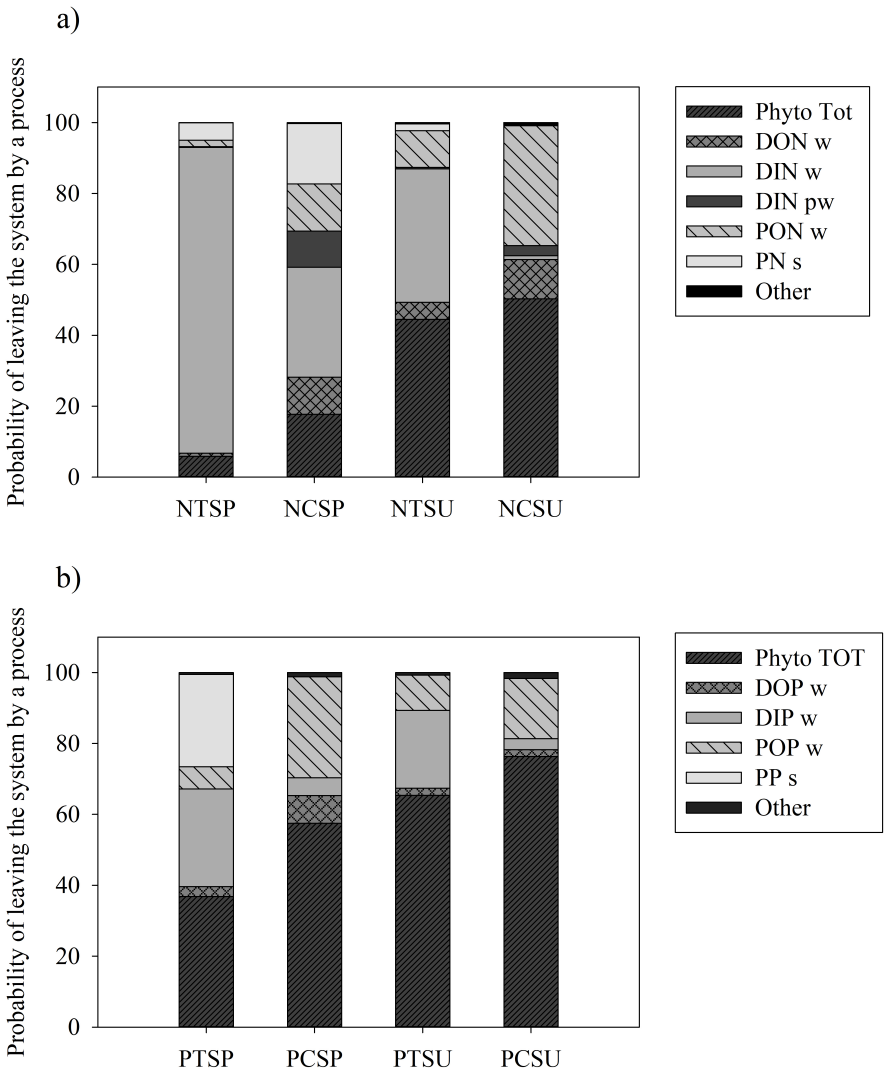

Figure 4.11: Probability by which a unit of imported DIN_w (a) and DIP_w (b) will be exported from the transitional or the confined area as one of the indicated forms. Abbreviations indicate: *NTSP* (N network-Transitional area-SPring season), *NCSP* (N network-Confined area-SPring season), *NTSU* (N network-Transitional area-SUmmer season), *NCSU* (N network-Confined area-SUmmer season), *PTSP* (P network-Transitional area-SPring season), *PCSP* (P network-Confined area-SPring season), *PTSU* (P network-Transitional area-SUmmer season), *PCSU* (P network-Confined area-SUmmer season).

negligible, whereas the amount exported as particulate organic forms augmented. In the confined area, in both seasons, most of the imported DIP_w was exported as POP_w or phytoplankton, representing about 85% and 93% of total exports in spring and summer, respectively.

Output Environ Analysis allowed also to calculate how many times a unit of DIN_w or DIP_w loaded into the networks was incorporated into the phytoplankton compartments before being exported to the outside (Fig. 4.12a and Fig. 4.12b). Phytoplankton uptake of a unit of imported N was less than 1 for the transitional area, both in spring and summer. Values increased for the confined area, to 1.25 and 2.96 in spring and summer respectively, partly sustained by the uptake of DON_w deriving from recycling processes. The frequency of uptake increased for P in both areas, but values within the transitional area remained below 1, whereas within the confined area they exceeded 4 both in spring and summer.

Total Dependency Matrices

Recycling can occur both among non-living compartments within the water column or at the sediment-water interface or can be mediated by living compartments. The contribution of different compartments to overall system recycling and primary producers' activity was assessed via the Total Dependency Matrices (Fig. 4.13 and Fig. 4.14). These matrices provide insights on how dependent each compartment is on all other compartments. Dependency is measured as the percentage of the throughflow of a compartment that once resided in every other compartment. Both direct and indirect interactions contribute to each compartment's dependency and so they are all quantitatively estimated. We focused on the dependency of the dominant phytoplankton groups, diatoms in spring and cyanobacteria in summer. Since the only direct inputs to phytoplankton are DIN/P_w and DON/P_w, any positive values related to the other compartments indicated a consumer-mediated recycling activity with a positive indirect effect on phytoplankton. In the transitional area both in spring and summer less than 20% of the primary producers activity was sustained by DIN_w and DON_w, which only in the summer season were related to mineralization processes within the water column (dependency on PON_w) and within the sediments (dependency on PON_s, DOP_{pw} and DIP_{pw}) (Fig. 4.13a and Fig. 4.13b). Both in spring and summer, the sum of all dependency values was less than 100, indicating a missing amount of nutrients to sustain primary producers activity. Since the dependency matrix is computed starting from the matrix of direct flows (Ulanowicz, 2004), external inputs are not accounted for, and this fraction constitutes the missing portion. Within the confined area, both in spring and summer the dependency of phytoplankton activity on DON_w and DIN_w ranged from 68 to 81%. In spring these compartments were mostly sustained by PON_w (55%) and to a lesser extent by PON_s and DON_{pw} (20%). The contribution of sediment mineralization processes increased in the summer season, with dependency values reaching about 30% on PON_s, DON_{pw}, and DIN_{pw}. The diagonal elements of each dependency matrix return the amount by which each compartment is dependent upon its own activity via cycling pathways. In spring, the dependency of diatoms on pooled phytoplankton compartments almost equalled values of

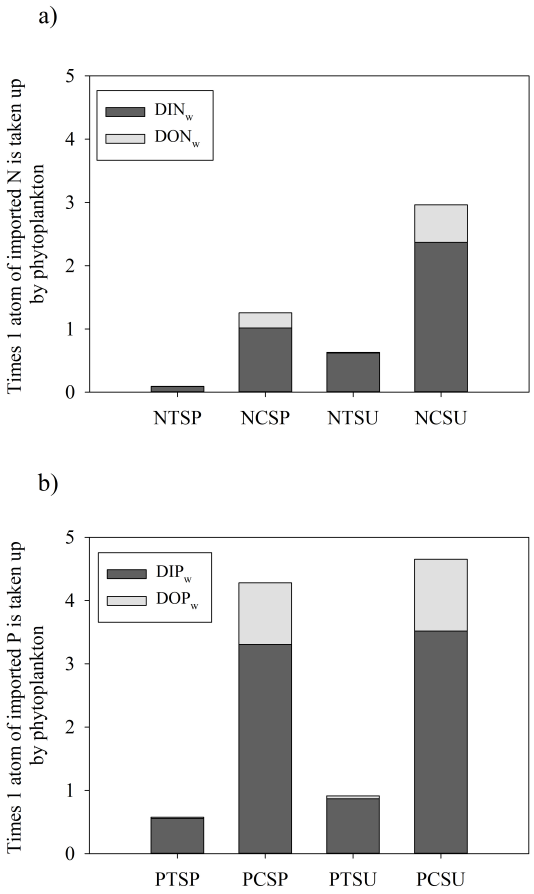

Figure 4.12: Frequency of use by phytoplankton of a unit of DIN_w (a) or DIP_w (b) imported to the transitional or the confined area, before being exported to the outside. Abbreviations indicate: *NTSP* (N network-Transitional area-SPring season), *NCSP* (N network-Confined area-SPring season), *NTSU* (N network-Transitional area-SUmmer season), *NCSU* (N network-Confined area-SUmmer season), *PTSP* (P network-Transitional area-SPring season), *PCSP* (P network-Confined area-SPring season), *PTSU* (P network-Transitional area-SUmmer season), *PCSU* (P network-Confined area-SUmmer season).

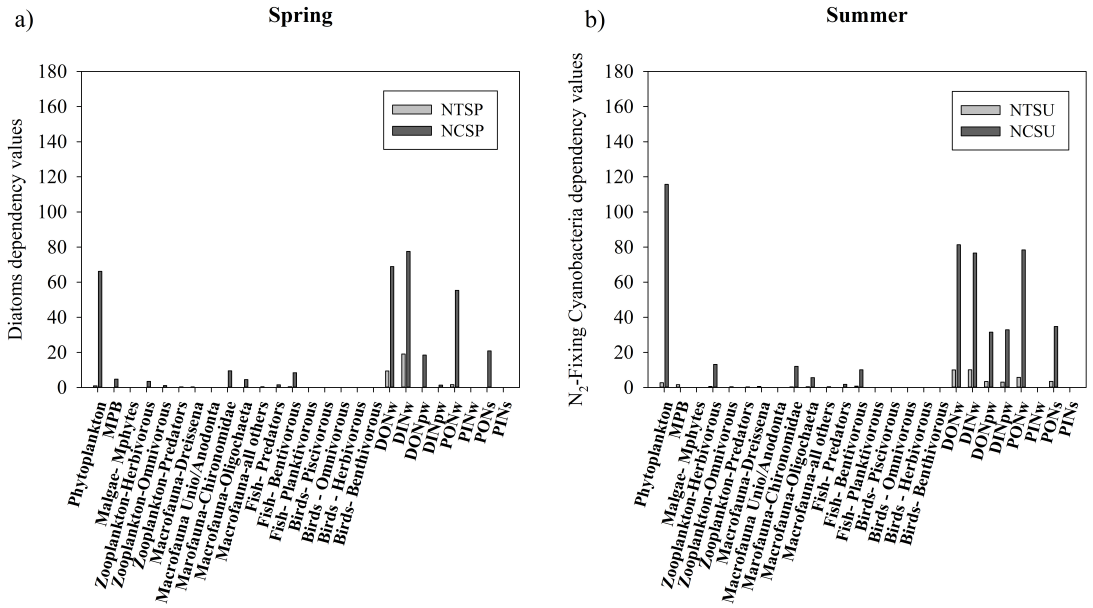

Figure 4.13: Dependency values (%) of diatoms in spring (a) and N-fixing cyanobacteria in summer (b) derived from N networks. Abbreviations indicate: *NTSP* (N network-Transitional area-SPring season), *NCSP* (N network-Confined area-SPring season), *NTSU* (N network-Transitional area-SUmmer season), *NCSU* (N network-Confined area-SUmmer season).

dissolved N. In summer the dependency of N-fixing cyanobacteria on phytoplankton compartments reached 115%, suggesting high recycling activity. Higher values of dependency on phytoplankton compared to PON_w suggested that these compartments contributed to recycling non only through water column loop among phytoplankton - PON_w - DON_w - DIN_w, but also through secondary pathways as exudates production, settlement of organic matter that partly sustain sediment mineralization, or feeding higher trophic levels.

Dependency matrices derived from P networks on the transitional area displayed similar trends both in spring and summer (Fig. 4.14a and Fig. 4.14b). In both seasons, as for N, less than 20% of phytoplanktonic production was sustained by DOP_w and DIP_w. Most of the water column dissolved P derived from POP_w, but the relative contribution of sediment processes slightly increased from spring to summer. Within the confined area, more than 80% of phytoplankton production was sustained by the water column loop among POP_w, DOP_w, and DIP_w. The contribution of sediment mineralization processes (POP_s - DOP_{pw} - DIP_{pw}) was about 35% in both seasons. Dependency values related to pooled phytoplankton compartments increased from spring (140%) to summer (160%). Compared to N networks the dependency values on living compartments increased, particularly those on herbivorous zooplankton, chironomids, oligochaetes, predators and benthivorous fishes. These dependency values ranged from

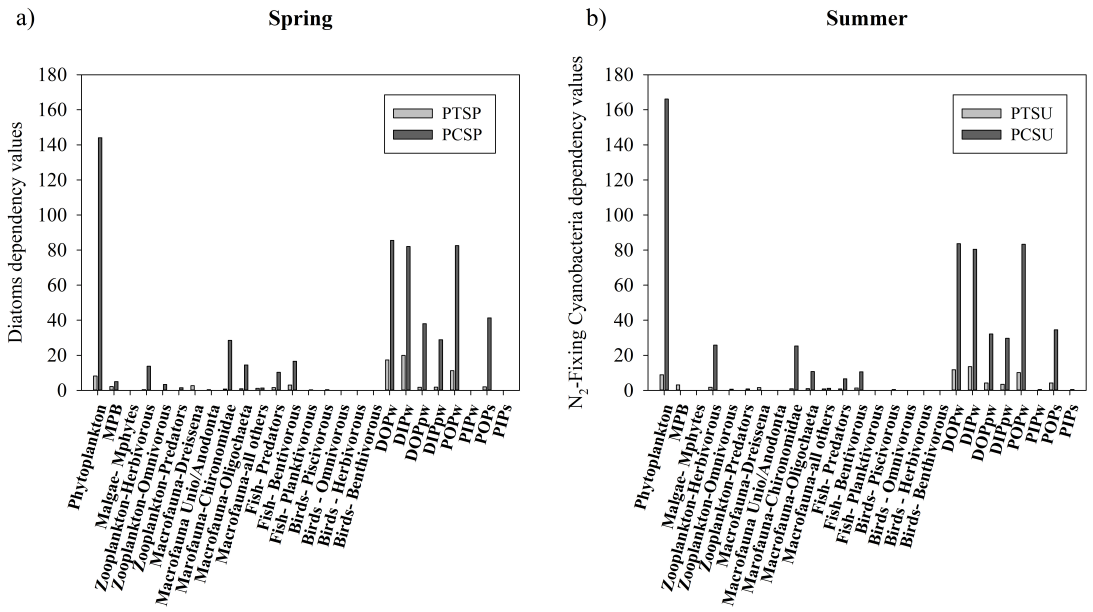

Figure 4.14: Dependency values (%) of diatoms in spring (a) and N-fixing cyanobacteria in summer (b) derived from P networks. Abbreviations indicate: *PTSP* (P network-Transitional area-SPring season), *PCSP* (P network-Confined area-SPring season), *PTSU* (P network-Transitional area-SUmmer season), *PCSU* (P network-Confined area-SUmmer season).

10% to 28% in spring, with the highest value on chironomids, and from 10% to 25% in summer, with the highest value on herbivorous zooplankton.

4.2.3 Discussion

The Curonian Lagoon, a single estuary integrating two contrasting subareas

This study organizes, models, and extends the outcomes of a large body of experimental research carried out in the Curonian Lagoon over the last 30 years. Differently from previous investigations, targeting single compartments, organism or processes within the lagoon, it aims at providing a holistic analysis of N and P seasonal dynamics. Results of ENA suggest striking differences between the two nutrient pathways in the transitional and confined areas. In the transitional area the high riverine water and nutrient inputs, particularly during spring, result in limited retention and cycling through the food webs and in large export. This lagoon area displays a riverine-like behaviour with passive drift of not-assimilated and not-transformed nutrients, and their transfer to the sea. Conversely, the confinement of the southern lagoon area likely played a major role in unbalancing the equilibrium between internal recycling and external loading. The former set of processes largely exceeded the importance of the latter, in particular during summer and more for P than for N. These differences between the northern and southern lagoon subareas align with what characterized other costal lagoons and estuaries with heterogeneous hydrology and water residence time (Gameiro et al., 2004; Pérez-Ruzafa et al., 2005; Roselli et al., 2013). Many coastal lagoons have confined, stagnant zones that are prone to anoxia and dystrophy; however, the surface of such confined zones represents a minor fraction of the total. This makes a large difference with the Curonian Lagoon, where the confined area represents roughly 60% of the total lagoon surface (Umgiesser et al., 2016). Higher recycling in confined areas depend on concurrent processes including higher primary production, consumers-mediated recycling overcoming nutrient limitation, higher sedimentation fuelling microbial activities and redox-dependent nutrient release mechanisms (Benelli et al., 2019; Petkuviene et al., 2019; Zilius et al., 2018; Zilius et al., 2014). In the confined area, extremely high rates of primary production saturate the grazing capacity of higher trophic levels resulting in inefficient use of phytoplankton-associated N and P, as described in (Grinienė et al., 2016; Semenova & Aleksandrov, 2009; Tomczak et al., 2009).

Estuarine hydrology differently drives seasonal N and P dynamics

The application of the ENA to two separate subareas of the Curonian Lagoon, characterized by different hydrodynamics, follows the experimental or theoretical outputs of several papers (Ferrarin et al., 2008; Remeikaitė-Nikienė et al., 2017; Vybernaitė-Lubienė et al., 2022; Zilius et al., 2018; Zilius et al., 2014). As demonstrated in previous studies, in the Curonian Lagoon hydrology affects both the amount of nutrients delivered to the two areas and their processing time (i.e., the main paths nutrients follow across food webs and how fast they are recycled).

The nutrient load to the transitional area and to the entire lagoon is mainly delivered by the Nemunas River and, as the freshwater discharge, is characterized by a high seasonal variability, peaking in spring and with minimum values in summer (Vybernaite-Lubiene et al., 2017; Vybernaite-Lubiene et al., 2018). The transitional area represents the main nutrient source to the confined area, exceeding Deima River inputs, but it transfers only a minor portion of the total received load (Vybernaitė-Lubienė et al., 2022). The input of nutrients normalized by the total surfaces of the two subareas, revealed that the transitional area receives N and P loads from 6 to 10 times higher compared to the confined areas, with the highest differences recorded in the spring season. Variations in river discharge and in prevailing winds contribute to the high spatial and temporal variability in the lagoon water residence time, with minimum values recorded close to the Nemunas Delta (<20 days), and higher values in the south-western area (>200 days) (Ferrarin et al., 2008; Umgiesser et al., 2016). The nutrient turnover time, calculated as the ratio between standing stock of DIN/P_w and outputs (Small et al., 2014) confirmed this large difference increasing on average from about 3 to 50 days from the transitional to the confined area. These results partly explain the large differences in FCI and APL values recorded for the two subareas.

Hydrology alone cannot explain the Curonian Lagoon functioning as this factor has significant interactions with the seasonality, attributable to increasing water temperatures and biological activity, as suggested by the TST. Despite the decrease in external inputs, total fluxes increase from spring to summer both for N and P. The seasonal increase in N fluxes was lower in the transitional lagoon area (23%) as compared to the confined one (140%) as it was partially balanced by the concurrent seasonal decrease in N inputs from the Nemunas River (Vybernaite-Lubiene et al., 2018). The seasonal increase in P fluxes, by 75 and 187% in the transitional and confined area, respectively, was comparatively higher than that of N. Such differences between the elements and between the lagoon subareas are due to a number of element–specific features of N and P including their different origin (i.e. mostly allochthonous for N, largely internal for P) and their pathways (i.e. the presence of a dissipative process as denitrification, connecting the water compartment to the atmosphere for N and the absence of a similar process for P). Clarifying how the interaction between seasonality and hydrology differentially affects N and P cycling, as highlighted by ENA, may help understanding the mechanisms driving the functioning of the Curonian and other lagoons, where cyanobacteria hyperblooms occur. Details on the different behaviour of N and P will be discussed in the following paragraphs.

N and P biogeochemical cycles in the transitional area

The high N load, and the faster water turnover likely determine a passive drift of DIN to the sea across the transitional area, mostly in the spring season. Assimilatory uptake by primary producers, denitrification and sediment storage together accounted for only a small portion of DIN exports and were scarcely noticeable compared to the total import. In a variety of transitional ecosystems, N removal have been demonstrated to be strictly related both to water residence time and loading (Nixon et al., 1996; Seitzinger

et al., 2006). The longer the water residence time, the more times N can be repeatedly cycled for example through uptake by phytoplankton and deposition of organic matter to sediments and therefore coupled nitrification/denitrification or buried into the sediments (Dettmann, 2001; Nixon et al., 1996; Seitzinger et al., 2006). As demonstrated by results from the Output Environ Analysis, this does not happen within the transitional area, where the number of times a unit of imported DIN is taken up by phytoplankton is much less than 1 and most of the imported DIN left the system without being processed, especially in spring. A positive relationship between N loading and N removal rates has been demonstrated in a range of transitional ecosystems (Seitzinger, 1988; Seitzinger et al., 2006). However, different studies reported increasing rates until reaching a asymptotic threshold, due to saturation of the microbial enzymatic activity (Dong et al., 2000; Joye et al., 1996; Ogilvie et al., 1997). These threshold values largely differed among analysed systems and depend upon the biological and environmental variables as described in section 3.2 or to differences in acute or chronic nutrient load. In the transitional area, characterized by sandy and flushed sediments with low organic matter content, it is likely that the low potential denitrification is overcome by large pulse of NO_3^- (Bartoli et al., 2021).

A significant amount of the export of DIP occurred via sediment storage. Most of this output derived from a flux added during mass balancing procedures. The microphytobenthos compartment was characterized by an excess of nutrients that derived from high measured uptake rates. To ensure steady state conditions, this excess nutrient has been transferred to particulate organic pool within the sediment and subsequently indicated as an export to the outside. These values can be revisited as a microphytobenthos biomass increase and represent a nutrient temporary storage. The same surplus for the microphytobenthos compartment was reported for N, but it was less evident as compared to the total pool of N. Microphytobenthos has been demonstrated to represent an important driver of benthic fluxes in the transitional area, due to the shallow water column and the high light availability, mostly in the spring season (Bartoli et al., 2021; Benelli et al., 2018; Zilius, Bartoli, Daunys et al., 2012). Experimental activities carried out in the sediments of this area demonstrated how the activity of microphytobenthos inhibits denitrification and contributes or stimulates N-fixation processes, further increasing the external N input despite the high availability, likely due to the low NH_4^+/NO_3^- ratio (Bartoli et al., 2021; Benelli et al., 2018; Zilius et al., 2018). Besides microphytobenthos activity, in estuarine and shallow ecosystems, P dynamics are strictly related to manganese (Mn) and iron (Fe) compounds. Oxidized Fe and Mn bind and co-precipitate DIP in solid phase (Canfield, 1994). Some of these compounds are redox sensitive and O_2 shortage conditions induce metals reduction and the consequent release of reactive P (Viktorsson et al., 2013). As demostrated in section 4.1 the terrigenous material transported by the Nemunas River is characterized by elevated concentrations of microbially reducible Mn^{4+} and Fe^{3+}, which represent a natural geochemical buffer against P release in the transitional area, even under anoxic conditions. It is therefore likely that in the river plume area, part of reactive P released by mineralization processes could be trapped within sediments, which due to the high hydrodynamics and the combined

action of microphytobenthos and bioturbating fauna, preserve oxidized Mn and Fe pools (Zilius et al., 2015).

N and P biogeochemical cycles in the confined area

Within the confined area the longer residence time provides conditions to increase the amount and relevance of internal processes, resulting in a more diverse picture of exports. Both water column primary production and remineralization rates intensified compared to the northern area (Zilius et al., 2018; Zilius et al., 2014), resulting in increased export of dissolved and particulate organic N forms. Nitrogen assimilation by primary producers, the subsequent deposition of phytodetritus and the sediment storage represent an important mechanism for the permanent N removal in the southern area (Zilius et al., 2018). Sediment storage in this case was not related to microphytobenthos activity, which was limited by low light penetration in deeper and turbid water (Bartoli et al., 2021; Zilius et al., 2018). Net retention was likely due to decoupled rates of organic matter sedimentation and degradation and to large benthic nitrate consumption sustaining microbial respiration and growth (Lin & Stewart, 1997; Luque-Almagro et al., 2011). Muddy sediments in the confined area displayed higher denitrification rates as compared to the transitional area, especially during spring, sustained by large availability of both high quality organic matter from phytoplankton and water column nitrate (Bartoli et al., 2021; Zilius et al., 2018).

Unlike N, which is partly removed by benthic processes or stored within sediment, assimilative uptake by phytoplankton represented in spring the main process driving DIP export. These outcomes confirmed the results of a recent work by (Vybernaitė-Lubienė et al., 2022), where authors via the application of the LOICZ budgeting approach demonstrated that the confined area of the Curonian Lagoon on an annual base acted as a net DIP sink and a TP source. Muddy sediments display ten times higher P concentration compared to sandy ones and most of the pools that bind P are reactive and more sensitive to bottom water chemical changes (Petkuviene et al., 2016). However, experimental studies demonstrated that both in spring and summer, sediments mostly prevent inorganic P regeneration (Petkuviene et al., 2016; Zilius et al., 2015). As demonstrated in section 4.1 the largest DIP effluxes were measured in summer, coinciding with extreme redox conditions occuring during bloom and post bloom events and leading to the exhaustion of oxidized Mn pool. These events are particularly significant since the specific conditions that favour PO_4^{3-} release produced smaller effects on benthic N cycling, either limiting the already low rates of nitrification or the ammonium efflux, mostly due to the inhibition of macrofauna metabolic activity. Since these large DIP effluxes were reported occasionally, they are not included in this study, which is based on average seasonal rates and adopted a conservative approach, with the exclusion of outlier values. However, their relevance is potentially high, since they could contribute to further unbalance the N:P recycling ratio depicted by results of the ENA. Furthermore, they might trigger the water column blooms-collapse-blooms sequences, in specific areas identified as hotspots, sustaining and prolonging this phenomenon over time (Vaičiūtė et al., 2021).

In the summer season, in the confined area, as in the transitional one, a major fraction

of imported N and P was exported in particulate organic form, most as living phytoplankton, and cyanobacteria in particular (Vybernaite-Lubiene et al., 2017; Zilius et al., 2018; Zilius et al., 2014). As demonstrated by (Bukaveckas et al., 2019) in a set of experimental activities carried out in the Curonian Lagoon, when the macroscopic colonies of *Aphanizomenon flos-aquae* dominated primary producers' community, the proportion of settleable Chl-*a* significantly decreased, due to the positive buoyancy capacity of these organisms. These negligible settling rates further favours the exports of algal biomass and phytodetritus, resulting in lower retention through sedimentation and burial, or benthic removal processes (Vybernaite-Lubiene et al., 2017; Zilius et al., 2014).

Pelagic nutrient turnover sustains high primary production, which undergoes limited transfer along the food web

Pelagic production in shallow ecosystems is generally sustained by sediment mineralization processes (Fisher et al., 1982; Tobias et al., 2003). In this study, results of the dependency matrices conversely demonstrated that nutrients demand of phytoplankton was mainly sustained by high water column turnover rates via coupled organic matter oxidation and assimilation. Previous studies carried out in different areas of the Curonian Lagoon and based on experimental measurements and mass balance approaches, have already demonstrated that sediment regeneration and cyanobacteria mediated N-fixation accounted for a minor portion of phytoplankton requirements (Broman et al., 2021; Zilius et al., 2018; Zilius et al., 2014). Water column regeneration has been reported to exceed both tributaries input and sediment regeneration in different shallow lakes or coastal ecosystems, and it has been identified as a direct consequence of eutrophication, resulting in a shift from benthic to pelagic processes (J. Li & Reardon, 2017; Mccarthy et al., 2013; Mccarthy et al., 2016).

Despite water column coupled primary production and decomposition processes seems to drive nutrient dynamics within the Curonian Lagoon, results derived from the Lindeman Spine analysis indicated that the nutrient transfer through the trophic food web displayed a low efficiency. (Tomczak et al., 2009) analysed averaged annual carbon flows in five south-eastern Baltic coastal ecosystems, including the Curonian Lagoon, using ECOPATH models (Christensen et al., 2005). Results showed that the largest portion of the total primary production was not transferred to higher trophic levels, but instead channelled into the detritus pool. The turbid Curonian Lagoon, specifically, displayed the highest primary production but the lowest trophic transfer efficiency (7%) among studied systems. Authors attributed these results to the dominance of filamentous and inedible cyanobacteria, which are not efficiently grazed by the planktivorous communities (Heymans et al., 2014; Karpowicz et al., 2020). In this study, the lowest nutrient transfer efficiency across the food web was indeed recorded in summer within the confined area, where non-fixing and N-fixing cyanobacteria, together constituted more than 80% of total phytoplankton. Higher transfer efficiency values recorded within the transitional area can be explained by the prevalence of filter-feeding bivalves (e.g. *Dreissena polymorpha* and native unionids) compared to mainly deposit-feeding oligochaeta and chironomidae which dominate the macrofauna community in the confined area (Zettler & Daunys,

2007). Previous studies demonstrated how the shift from diatoms to cyanobacteria is followed by a decline in grazing efficiency, from 34% to 8% of net primary production in the transitional area and from 60% to 4% in the confined area (Bartoli et al., 2018; Semenova & Aleksandrov, 2009). Due to the lack of data, microzooplankton (size category 20-200 µm) was not included in this study, despite it has been demonstrated to significantly contribute to total grazing and be partly responsible for biomass accumulation control (Grinienė et al., 2016). Microzooplankton activity was here included as part of the microbial loop among phytoplankton and non-living compartments and its exclusion could have determined an underestimation of values and explain differences among literature values and consumption rates estimated in this study. Stable isotopes analyses and studies based on the accumulation of cyanotoxins, showed how cyanobacteria support secondary production in the Curonian Lagoon, contributing up to 80% of fast-growing primary consumers production (e.g. planktonic crustacea and chironomids), and to a much smaller extent also higher trophic levels (e.g. *Leptodora kindtii* and benthivorous fishes) (Bukaveckas et al., 2017; Lesutiene et al., 2014). The magnitude and duration of the cyanobacteria blooms likely preclude avoidance by grazing and filtering organisms, which however have limited control on primary production. Low transfer efficiency at higher trophic level can be partly related to the dominance of benthivorous fishes over planktivorous, which diet was partly sustained by deposit-feeding macrofauna (Bubinas & Ložys, 2000).

Low nutrient transfer efficiency in the pelagic compartment translates in the transitional area into large export of energy and matter to the sea, limiting the filter and reactor service that characterize estuaries. In the confined area this translated into excess organic matter and nutrient inputs to the benthic compartment, producing a cascade of negative consequences on oxygen availability, macrofauna abundance and diversity, capacity of microbial consortia to process organic inputs and exhaustion of geochemical buffers, affecting system resilience to stress. Inefficient pelagic nutrient transfer across the network makes therefore also benthic processes inefficient and not linear, producing positive feedbacks on the pelagic compartment.

Cyanobacteria and consumers induce higher P recycling

A few studies simultaneously described C, N, and P dynamics in aquatic ecosystems using network analysis (Baird et al., 2008, 2011; Scharler et al., 2015; Scharler & Ayers, 2019; Ulanowicz & Baird, 1999). All of them reported high recycling rates (as FCI) for N and P compared to C, and generally higher rates for P compared to N. (Baird et al., 2008), in a study carried out in the Sylt-Rømø Bight ecosystem, attributed these differences to the N dissipation processes (mostly N_2 and N_2O via denitrification), which do not have an equivalent in P transformations. This hypothesis was confirmed in a subsequent study, where the authors analysed some sub-systems of the same marine basin not taking into account denitrification, and found a variable ratio between N and P recycling rates (Baird et al., 2011). This could partly justify our results. If FCI normalized by P are compared, $N{:}P_{FCI}$ in both area increase from spring to summer, according to decreased denitrification rates, reaching a maximum values of 0.8:1 for

the confined area. (Scharler et al., 2015) associated the same trend to stoichiometric variations along the food web. Heterotrophic organisms incorporated proportionally more N and P than C, and more N or P depending on their limiting resources. They found high recycling rates for the nutrient that showed the higher trophic transfer efficiency and was considered the limiting resource (Vanni, 2002). In the Curonian Lagoon higher recycling rates were associated to heterotrophic organisms (e.g., herbivorous zooplankton, chironomids, benthivorous fishes) for P networks, which also displayed higher trophic transfer efficiency. The consumer-mediated nutrient recycling is of primary importance to supply primary producers nutrient requirements in nutrient poor systems such as the mangrove island analyzed by (Scharler et al., 2015). In the present study these values were not very significant if compared to external inputs or water column regeneration rates but contributed to explain differences between N and P dynamics.

The Curonian Lagoon hosts a high diversity and number of waterbirds. The Great cormorant is the most abundant breeding species and in the summer season till late autumn constitute large aggregations (Morkune et al., 2020; Putys & Zarankaite, 2010; Švažas et al., 2011). Recent studies demonstrated how faeces of waterbirds and particularly piscivorous birds excretion may significantly contribute to P balance and stimulate algal blooms within the Curonian Lagoon (Morkune et al., 2020; Petkuviene et al., 2019). The release of reactive P mediated by these organisms has been calculated to range from 1 to 12% of the total load delivered by the Nemunas river, peaking in summer at minimum riverine water discharge. Results from ENA contrast these experimental outputs as they suggest that bird excretion has a minor importance as P source for phytoplankton. Data used in this manuscript miss the real consistency of bird populations in the Russian area, that was estimated according to Lithuanian records. As discussed for sediment regeneration, large colonies of piscivorous birds have probably a local impact, that may determine confined blooms rapidly expanding to large surfaces via already described mechanisms (Bresciani et al., 2014; Vaičiūtė et al., 2021). Benthivorous fishes, which dominate in the Curonian Lagoon due to specific conditions of this estuary (turbidity, frequent hypoxic/anoxic crises, large sedimentation rates), have a large potential to support nutrient recycling, and in particular DIP via sediment resuspension (Breukelaar et al., 1994; Tarvainen et al., 2005). There were not available studies on the role of fishes in nutrient recycling in the Curonian Lagoon and, as described for sediments, we adopted a conservative approach, excluding mechanisms that could be of local relevance. Furthermore, as for birds, knowledge on the consistency of fish communities in Lithuanian as well as in Russian water is limited. More research should address these biological compartments in terms of inventory and functional roles.

4.2.4 Conclusions

This is one of the first study that simultaneously analyses the N and P dynamics via the ENA. The developed models combine characteristics that are typical of networks constructed to analyse both nutrient cycling and trophic dynamics (Borrett et al., 2016). They are characterized by a high-resolution degree for non-living compartments, which is typical of biogeochemical networks, and allowed to analyse N and P pattern circulations

at low trophic levels, which constitute the bulk of the system. At the same time the models present a high degree of detail in the representation of the trophic food web, which allowed to analyse the nutrient transfer efficiency and clarify the contribution of single compartments to the overall recycling activity.

Results underlined large differences in N and P dynamics in the two analyzed subareas of the Curonian Lagoon, partly driven by different hydrology. The northern transitional area, regardless the analysed season, receives from the outside a large amount of nutrient, mostly in dissolved forms from the Nemunas River in spring and in particulate forms from the southern confined area in summer. The elevated flushing prevents internal processes to represent important fractions of inputs. The southern area has completely different dynamics as smaller nutrient inputs are coupled with longer water residence time, promoting recycling and reuse of both N and P but also N loss (via denitrification) and P regeneration (favoured by oxygen shortage) across the two investigated seasons. Despite the high primary production rates, ENA results indicate a low nutrient transfer efficiency to the higher levels in the food web. The low trophic transfer efficiency, mostly in the confined area, translated into excess organic matter to the benthic compartment, that contribute to the increase in prominence of internal recycling processes. This infers that phytoplankton itself maintain blooming, particularly during summer, through the microbial loop linking assimilation and recycling processes.

The results of this study allow to depict the whole N and P circulation within the two subareas of the lagoon. The identified spatial and temporal differences contribute to deep our understanding of mechanisms promoting cyanobacteria blooms. Further efforts seek to increase the model resolution and include local events that may trigger the blooms-collapse-blooms mechanisms identified as the main driver of this phenomenon.

4.3 Main findings and general remarks

The Curonian Lagoon ecosystem provides many provisioning, environmental and cultural services, but its functioning, as several coastal and open marine areas in the Baltic Sea region, is deeply affected by cyanobacteria blooms (Stal et al., 2003; Vahtera et al., 2007). Experimental activities carried out in the last 20 years have shed light on multiple mechanisms which promote these events, but they lack the overall assessments of estuarine biogeochemistry. In this study, the large-scale investigation on the stoichiometry of benthic regeneration, coupled to the holistic evaluation of the N and P biogeochemistry contributed to fill this gap. Results revealed pronounced differences in the functioning of the flushed and the stagnant area of the lagoon, which are amplified in the summer season, affecting P more than N dynamics.

Hydrology is one of the main factors driving, both directly and indirectly, the nutrient circulation, by affecting the external loads, the water renewal time, and the sediment composition. The transitional area receives a high nutrient load, but the elevated flushing and the resulting low residence time make internal recycling processes scarcely relevant from a biogeochemical perspective. The sandy, organic-poor and highly oxidized sediments display an elevated buffer capacity, retaining nutrient both via temporary and permanent storage processes. Conversely, results from both the experimental and modelling activities emphasized the vulnerable nature of the confined area. Here, the water stagnation promotes high rates of internal recycling, largely exceeding external inputs, mainly in the summer season. Muddy and organic-rich sediments displayed a limited buffer capacity against nutrients release, mainly of P, contributing to the imbalance in the stoichiometry of the internal processes of the overall system, revealed via the ENA. These conditions favour the establishment and the persistence of cyanobacteria blooms. The high primary production rates coupled to the low trophic transfer efficiency, determine the accumulation of large amount of organic matter, establishing a water column loop between mineralization and uptake, that fuel primary producers' activity and is typical of turbid and eutrophic system. High mineralization rates may lead to anoxia with a consequent increase in redox dependent P release mechanisms. Results of nutrient regeneration derived from simulated oxygen shortage events were not included in the model construction, since they represent extreme conditions, but may further imbalance the overall regeneration of P compared to N, with positive feedback for cyanobacteria.

Since the confined area covers more than half of the entire surface, this cascade of negative effects affects the resilience of the whole lagoon. According to different climatic scenarios, it is likely that the Nemunas River flow will experience a hydrologic shift towards higher winter discharge and lower summer-early fall discharge (Cerkasova & Umgiesser, 2021). This shift will further increase the large seasonal differences in water residence time, lowering already low values in winter and increasing already high values in summer (Umgiesser et al., 2016). This trend, together with the forecasted summer increase in the frequency and intensity of heatwaves may further promote the extension of the stagnant sector in the dry period, increasing the proportion of the lagoon prone to high P regeneration, cyanobacteria blooms and anoxia events. This large potential

for internal recycling, will likely offset the effectiveness of any management measures implemented in the next few decades aimed at reducing external loads, especially since they would potentially affect more N than P, for which significant reductions have already been achieved (Vybernaite-Lubiene et al., 2018).

Chapter 5

Conclusions and future insights

This study investigated the factors regulating the coastal filter function of transitional ecosystems in the Goro and Curonian lagoons, two eutrophic European systems characterized by different climates (boreal and mediterranean) and salinity (oligohaline and mesohaline). Both lagoons are located downstream of heavily exploited watersheds and are impacted by wide and intense micro and macroalgal blooms, mainly driven by excess N and P for the Goro and the Curonian Lagoon, respectively. Results from this thesis suggest that ongoing global changes may further influence the functioning of these areas, already affected by decades of organic enrichment due to eutrophication.

Experimental and modelling approaches have been combined to deepen the N and P dynamics at different spatial scales, also due to large differences in data availability. The Goro Lagoon was intensively studied in the 90's of the last century whereas limited experimental data were available for the last two decades. The Curonian Lagoon has been intensively studied, particularly in the last 20 years, but for this system a holistic evaluation of the N and P biogeochemistry was missing. In both systems, the experimental activities aimed at investigating variations in the nutrient retention capacity under different scenarios, particularly during climatic extremes, anoxia events, and in presence of different bioturbating organisms. Activities have been characterized by an increasing degree of complexity. Incubations of reconstructed sediments under controlled conditions have been carried out to shed light on the scarcely known interactions between bioturbating organisms, and P and metals dynamics. In this work, it has been demonstrated how results from incubations of manipulated sediments significantly differed from those derived from intact sediments, but they help to reduce the complexity of the benthic system and disentangle the role of the single components. The N dynamics within the Goro Lagoon have been deeply investigated in the last decades, but in this study, they have been analysed with respect to new environmental pressures. The effects of present and simulated, future extreme events have been characterized in different areas and the extent of removal and recycling processes has been interpreted with respect to their hydrological, biological, and sedimentary issues. Finally, a large-scale investigation on benthic regeneration has been carried out in a variety of sedimentary environments of the Curonian Lagoon and the N and P dynamics have been simultaneously analysed under *in*

situ conditions and a simulated oxygen shortage event. These detailed measurements of benthic processes carried out at the microscale have been implemented with a large body of available information on water column nutrient and biological dynamics to depict the N and P circulation at the whole lagoon scale.

All the obtained results underline the high vulnerability of the analysed systems, mostly in summer and under heat waves and dry periods, as detailed in sections 3.5 and 4.3. These events may reverse the filter action of the lagoons due to large increase of internal recycling and export processes. These shallow estuaries that have retained and accumulated nutrients for long period have the potential to mobilize from sediments large amounts of N and P and may generate in the future or already generate positive feedback on the activity of primary producers.

In both systems, hydrology is one of the main factors driving, both directly and indirectly, the nutrient circulation, by affecting the external loads, the water renewal time, the sediment composition, and the organic matter accumulation. High hydrodynamics areas are characterized by organic poor and oxidized sediments inhabited by bioturbating macrofauna, which plays a key role in benthic biogeochemistry, increasing the nutrient retention or removal capacity. The effectiveness of the filter action is strongly limited by the low water residence time and these areas, especially under high discharge events, are characterized by the passive drift of a large amount of nutrients, moving the problem of fertilization to the coastal zone. Conversely, stagnant areas are characterized by muddy, organic-rich, and chemically reduced sediments, where the high turbidity, the low oxygen concentration, and the accumulation of toxic compounds limit the presence of a biodiverse benthic community. Here, recycling processes overcome removal and external inputs.

This contrast is more evident in the Curonian Lagoon compared to Goro Lagoon. The latter, due to its small dimension, and the relative wider sea mouth and larger river discharge and tidal amplitude is characterized by a smaller morphological and hydrological variability, with annual average residence time ranging from 1 to 12 days (Maicu et al., 2021). The Curonian Lagoon is characterized by residence time 10 times higher, up to 100 and 250 days for the transitional and the confined area, respectively (Umgiesser et al., 2016). In this condition, the relevance of internal dynamics largely increases, particularly in large muddy and stagnant areas, where the macrofauna is absent or dominated by oligohcaeta and chironomidae.

The large benthic regeneration contrasts the effectiveness of environmental policies aimed at reducing the external loads. These measures, that have been implemented starting from 30 years ago, have been more effective in regulating point sources compared to diffuse one, and in both the analysed systems have determined a significant reduction of P load, whereas N ones have either stayed the same or even increased (Viaroli et al., 2018; Vybernaite-Lubiene et al., 2017). Future measurements may therefore affect more N than P and their relative stoichiometry, with unpredictable consequences on the community of primary producers of the Goro Lagoon and further worsening the functioning of the Curonian Lagoon.

The reduction of internal recycling is a difficult target especially in the short term and largely depends on the relative size of stagnant and confined areas. Most of the

measures aimed at reducing internal nutrient regeneration acted on the increase in water circulation, by dredging of internal canals or enlarging the connections between the lagoons and the open sea, or on the decrease in sediment organic content, via sand-capping techniques. In the Goro Lagoon, after a particularly severe anoxic crisis in August 1992, a new connection with the Adriatic Sea was realized via cutting the Scanno di Goro, a sand-bar between the lagoon and the open sea. Hydrodynamic models have later demonstrated how the new channel increased the water circulation, particularly in the eastern area (Marinov et al., 2006). The continuous erosion of the spit between the two channels led to its submersion and the actual configuration of the lagoon mouth. At the same time, the sedimentation of terrigenous material delivered from the Po di Goro led to a gradual decrease in the width of the new eastern channel. Continuous activities of dredging are necessary for the maintenance of this opening, and they are coupled to measures that provided the deposition of the dredged sands on organic-enriched sediments (Corbau et al., 2016). The latter has an immediate negative effect on the resident macrofauna, but recolonization is evident after a few days from the interventions. The applied measurements have reduced the number of episodes of water anoxia and harmful algal blooms in the last few years (Corbau et al., 2016). However, a recent study demonstrated that further dredging measurements may not significantly affect the water circulation within the lagoon (Maicu et al., 2021). These measures had significant effects on the small Goro Lagoon, but they are less viable or may be less effective in the Curonian Lagoon, where the confined and vulnerable area covers about 60% of the 1584 km^2 total surface. Sand-capping techniques have proved to be effective when performed under controlled conditions (Svenja Oncken et al., 2022), but they can be applied on small surfaces. These applications could benefit from the identification of particularly sensitive areas, considered hotspots of algal blooms (Vaičiūtė et al., 2021). Hydrological models demonstrated how the opening or the enlargements of the inlets may decrease the water stagnation in large enclosed systems (Szydłowski et al., 2019), but they may negatively affect the sediment transport and the lagoon biology, due to variations in salinity, temperature, connectivity, and current intensity, even with moderate actions (García-Oliva et al., 2018).

The restoration of the ecological functionality of coastal lagoons may depend on the combinations of measurements carried out at the watershed scale and within the lagoons. The decrease in external load does not affect the frequency and intensity of blooms in the short-term, due to the large accumulation of nutrients in soils and sediments, but in the long-term may determine the increase of the water transparency and benthic primary production, favouring the sediment oxidation and the nutrient retention. The effectiveness of measurements carried out within the lagoon systems is site-specific and depends on their previous environmental, geomorphological, and ecological characteristics. These measurements need to be carefully considered and their effects evaluated at the whole system scale (García-Oliva et al., 2019).

Coastal lagoons are highly dynamic and productive environments, subjected to multiple environmental and anthropic pressures. The effectiveness of their "coastal filter" function is actually threatened by the interplay between eutrophication and climate

change. This study, through the investigation on the effects of emerging environmental pressures and the simultaneous analysis of N and P dynamics, even at the whole lagoon scale, contributes to increasing the knowledge on the biogeochemistry of these systems and on the main factors affecting their nutrient removal and retention capacity.

Chapter 6

Summary in Lithuanian

6.1 Įvadas

6.1.1 Temos aktualumas

Priekrantės lagūnos – tai seklios, dinamiškos sistemos, įsiterpusios tarp sausumos ir jūrų bei vandenynų ekosistemų. Lagūnoms būdinga didelė buveinių įvairovė ir aktyvūs biogeocheminiai procesai, todėl šios ekosistemos yra svarbios tiek gamtine, tiek ir ekonomine prasme (Newton ir kt., 2014). Dėl aktyvių biogeocheminių procesų lagūnos veikia kaip filtras, kuris upių atneštą organinę medžiagą ir maistmedžiages transformuoja, nusodina ant nuosėdų paviršiaus ar dujų pavidalu negrįžtamai pašalina iš sistemos (Asmala ir kt., 2017; Carstensen ir kt., 2020). Šis lagūnų vaidmuo itin svarbus mažinant maistmedžiagių prietaką į jūras ir vandenynus.

Pastaraisiais dešimtmečiais priekrantės lagūnų funkcionavimas priklauso nuo eutrofikacijos, klimato kaitos ir jų sąveikos (Lloret et al., 2008). Nors eutrofikacija gali būti ir natūraliai vykstantis procesas, tačiau paskutiniais dešimtmečiais priekrantės lagūnose ją spartina suintensyvėjusi žmogaus ūkinė veikla: kalnakasyba, intensyvus trąšų naudojimas ir iškastinio kuro deginimas. Dėl šių veiklų azoto (N) ir fosforo (P) kiekis priekrantės ekosistemose padvigubėjo (Nixon, 1995). Maistmedžiagių perteklius išbalansavo pusiausvyrą tarp organinės medžiagos produkcijos ir jos metabolizmo ir sukėlė deguonies stygių, pakeitė adsorbciją ir nusėdimą bei oksidacijos-redukcijos procesus, paskatino skaidymo produktų kaupimąsi, padidino bestuburių, žuvų ar makrofitų mirtingumą. Dėl šių priežasčių mažėja bioįvairovė, prarandamos ekosisteminės paslaugos, keičiasi ekologinė maistmedžiagių stechiometrija (Cloern, 2001). Siekiant švelninti šias pasekmes Europos upių baseinuose imtasi įgyvendinti aplinkosaugos priemones, kontroliuojančias maistmedžiagių prietaką iš žemės ūkio naudmenų ir nuotekų valymo įrenginių. Visgi taikomų priemonių efektyvumą gali mažinti sukauptas didelis maistmedžiagių kiekis dirvožemyje ir pačių lagūnų ekosistemose (Bouraoui ir Grizzetti, 2011; Viaroli ir kt., 2018).

Priekrantės lagūnos yra gana jautrios klimato kaitos poveikiui (Anthony ir kt., 2009). Tai ypač akivaizdu šiaurinėse platumose, kurių ekosistemas reikšmingai veikia besikeičianti ledo dangos periodo trukmė, atlydžių dinamika, kritulių kiekis ir intensyvumas, tem-

peratūros režimas (Trenberth, 2005). Manoma, kad su klimato kaita sietini ir ekstremalūs įvykiai, kurių dažnumas ir intensyvumas turėtų padidėti, taigi, dažnės liūčių, netikėtų potvynių, o sausuoju metų laikotarpiu sumažės upių prietaka (Lehner ir kt., 2006). Tikėtina, kad dėl klimato kaitos keisis ir maistmedžiagių dinamika bei lagūnų ekosistemų funkcionavimas; šie pokyčiai gali turėti įtakos ištirpusių ir dalelinių maistmedžiagių koncentracijai, jų ekologinei stechiometrijai ir transformacijos procesams dugno nuosėdose (Statham, 2012). Iš dugno nuosėdų atsipalaiduojančios maistmedžiagės ateityje gali sumenkinti gamtosaugos priemonių, skirtų mažinti taršą maistmedžiagėmis iš upės baseino, efektyvumą. Dėl vidinės apkrovos maistmedžiagėmis gali suintensyvėti dumblių žydėjimai, išsibalansuoti ekosistemos funkcionavimas ar sunykti bioįvairovė (Duarte ir kt., 2009).

Sąveikos tarp klimato kaitos ir eutrofikacijos poveikis lagūnų ekosistemoms yra įvairus, daugialypis ir sunkiai nuspėjamas. Eksperimentiniai tyrimai suteikia galimybę fundamentaliai suprasti biogeocheminius procesus, kurie reguliuoja maistmedžiagių sulaikymą ir transformacijas lagūnose, ar aplinkos veiksnius, turinčius įtakos biogeocheminių procesų intensyvumui. Visgi tokia metodologija stokoja holistinio vertinimo, kuris leistų suprasti visos ekosistemos vaidmenį sulaikant ar transformuojant maistmedžiages. Todėl vertinant lagūnų ekosistemų funkcionavimą būtų pravartu taikyti integruotus modeliavimo įrankius (Wulff ir kt., 2012). Vienas iš tokių įrankių galėtų būti Ekologinė tinklo analizė (ETA), susidedanti iš algoritmų, aprašančių ekosistemos struktūrą ir sąveiką tarp skirtingų jos komponentų (Kay ir kt., 1989; Szyrmer ir Ulanowicz, 1987; Ulanowicz, 2004, 1986). Tokie tinkliniai modeliai geba aprašyti visus galimus medžiagų srautus tarp biotinių ir abiotinių ekosistemos komponentų, lemiančių medžiagų pernašą dėl mitybos, detrito susidarymo ir biogeocheminių virsmų (Fath ir kt., 2007). Viena iš pagrindinių problemų taikant ETA yra duomenų prieinamumas ir jų kokybė (Scharler ir Borrett, 2021). Siekiant panaudoti ETA būtina gerai suplanuoti eksperimentus ir stebėjimus. Šio darbo tikslas buvo įgyvendintas atlikus eksperimentinius tyrimus dviejose estuarinėse sistemose: Sacca di Goro lagūnoje ir Kuršių mariose. Gauti rezultatai leis toliau vystyti ETA Sacca di Goro lagūnai. Tuo tarpu Kuršių mariose naudojant jau esamus eksperimentinius ir monitoringo duomenis buvo atlikta ETA analizė N ir P ciklui.

6.1.2 Tyrimo tikslas ir pagrindiniai uždaviniai

Pagrindinis darbo tikslas – įvertinti azoto ir fosforo kaitą Sacca di Goro lagūnoje ir Kuršių mariose lauko ir skaitmeniniais eksperimentais, siekiant suprasti kaip lagūnų filtro vaidmuo priklauso nuo eutrofikacijos, klimato kaitos ir jų sąveikos.

Eksperimentinių ir skaitmeninių tyrimų uždaviniai:

1. įvertinti ekstremalių hidrologinių įvykių – liūčių ir aukštos temperatūros – poveikį lagūnos filtro vaidmeniui sulaikant N;

2. nustatyti ribines disimiliacinės nitratų redukcijos procesų prisotinimo vertes ir identifikuoti veiksnius, reguliuojančius balansą tarp skirtingų redukcijos procesų;

3. ištirti dugno nuosėdose besirausiančių makroorganizmų įtaką reaktyvaus neorganinio P sulaikymui;

4. nustatyti eksperimentinių duomenų patikimumą vykdant nesuardytos struktūros dugno nuosėdų kolonėlių ir rekonstruotų nuosėdų mikrokosmų eksperimentus;

5. įvertinti anoksijos poveikį maistmedžiagių virsmams nuosėdose ir jų apykaitos įtaką ekologinei stechiometrijai;

6. nustatyti aplinkos veiksnių įtaką N ir P virsmams ir jų pernašai skirtinguose ekosistemos komponentuose, lemiančiuose melsvabakterių žydėjimą.

6.1.3 Darbo naujumas

Šis tyrimas pateikia kokybiškai naują informaciją apie mechanizmus, kurie reguliuoja eutrofikacijos fenomeną stipriai paveiktose estuarinėse sistemose. Nepaisant to, kad Sacca di Goro lagūna buvo aktyviai tyrinėjama praeito amžiaus devintame dešimtmetyje, iki šiol trūksta tyrimų, kurie parodytų kaip pasikeitė ši estuarinė ekosistema po moliuskų akvakultūros įrengimo. Tai tapo ypač aktualu besikeičiančio klimato kontekste, nes trūksta žinių apie biogeocheminius maistmedžiagių virsmus, galinčius turėti įtakos tolimesniam moliuskų akvakultūros plėtojimui. Eksperimentų metu gauti rezultatai užpildė šias žinių spragas ir suteikė galimybę ateityje plėtoti ETA analizę N ciklui (Christian 1996), identifikuojant svarbiausius jo virsmus ir palyginant ekosistemos funkcijas praeityje ir šiuo metu. Pastaraisiais metais vis dažniau pasikartojančių klimato anomalijų poveikis maistmedžiagių virsmams ir sulaikymui dugno nuosėdose buvo ištirtas in situ ir eksperimentais taikant skirtingus scenarijus. Kuršių marios pastarąjį dešimtmetį yra ypač aktyviai tyrinėjamos, visgi stokojama holistinio supratimo apie N ir P ciklus šioje estuarinėje ekosistemoje. Integruoti eksperimentinių tyrimų ir ETA analizės rezultatai užpildo šią spragą ir paaiškina, kaip maistmedžiagių srautai gali reguliuoti melsvabakterių žydėjimą vandens storymėje.

6.1.4 Rezultatų mokslinė ir praktinė reikšmė

Pastaraisiais metais taikytos gamtosaugos priemonės, skirtos eutrofikacijos proceso pasekmėms mažinti, apsiribojo pavienėmis veiklomis, vykdytomis upės baseine ir žemupyje esančiose lagūnose. Upės baseinuose buvo siekiama mažinti maistmedžiagių srautus iš žemėnaudos ir žmogaus gyvenamosios aplinkos. Nepaisant ženklaus progreso mažinant taršą P junginiais, to nepavyko pasiekti su N (Bouraoui ir Grizzetti, 2011). Tuo tarpu lagūnose eutrofikacijos problema buvo sprendžiama gerinant vandens cirkuliaciją, pagilinus ar praplatinus kanalus su jūra ir, pastaruoju metu, dugno nuosėdų paviršių padengiant aktyviu dumblu sumaišytu su smėliu (García-Oliva ir kt., 2018; Svenja Oncken ir kt., 2022).

Tyrimo metu gauti rezultatai suteikia informacijos, kiek svarbūs yra dugno nuosėdose vykstantys maistmedžiagių virsmai lagūnų ekosistemoms, parodo, kaip juos gali veikti eutrofikacija ir klimato kaita (Sacca di Goro lagūna) arba šių faktorių sąveikos, lemiančios

hidrologiją ir vandens apykaitos laiką sistemoje (Kuršių marios). Šiame darbe fundamentaliai analizuojami aplinkos veiksnių – liūčių, sausros, deguonies trūkumo ar sumažėjusios bioįvairovės – įtaka ekosistemos funkcionavimui. Holistinis ir integruotas maistmedžiagių srautų vertinimas seklių lagūnų ekosistemoje naudojant ETA tik patvirtino šio metodo privalumą atvaizduojant svarbiausius N ir P virsmus cikluose. Gauti rezultatai glaudžiai siejasi su maistmedžiagių sulaikymo ir pašalinimo iš ekosistemos mechanizmais, kurių supratimas yra svarbus kuriant ir taikant efektyvias gamtosaugos ir eutrofikacijos mažinimo priemones.

6.1.5 Mokslinių rezultatų pristatymas

Disertacijos rengimo metu gauti rezultatai buvo pristatyti šiose konferencijose:

1. XVI Ekologijos ir vandens mokslų doktorantų ir jaunųjų tyrėjų susitikimas, Ostana, Italija, 2019 m. balandis.
2. Mokslinė praktinė konferencija "Jūros ir krantų tyrimai–2019", Klaipėda, Lietuva, 2019 m. gegužė.
3. XXIV Italijos okeonologijos ir limnologijos asociacijos kongresas, Bolonija, Italija, 2019 m. birželis.
4. XXIX Italijos ekologijos bendrijos kongresas (S.It.E), Ferara, Italija, 2019 m. spalis.
5. XVII Ekologijos ir vandens mokslų doktorantų ir jaunųjų tyrėjų susitikimas, Neapolis, Italija (nuotolinė konferencija), 2021 m. balandis.
6. ECSA 58 – „EMECS 13 Estuaries and coastal seas in the Anthropocene" Hull, Jungtinės karalystės (nuotolinė konferencija), 2021 m. rugsėjo mėn.

Disertacijos tema parengtos publikacijos:

1. **Magri, M.**, Benelli, S., Bonaglia, S., Zilius, M., Castaldelli, G., and Bartoli, M. (2020). The effects of hydrological extremes on denitrification, dissimilatory nitrate reduction to ammonium (DNRA) and mineralization in a coastal lagoon. *Science of The Total Environment*, 740, 140169.
2. Bartoli, M., Benelli, S., **Magri, M.**, Ribaudo, C., Moraes, P. C., and Castaldelli, G. (2020). Contrasting effects of bioturbation studied in intact and reconstructed estuarine sediments. *Water*, 12(11), 3125.
3. Bartoli, M., Benelli, S., Lauro, M., **Magri, M.**, Vybernaite-Lubiene, I., and Petkuviene, J. (2021). Variable oxygen levels lead to variable stoichiometry of benthic nutrient fluxes in a hypertrophic estuary. *Estuaries and Coasts*, 44(3), 689-703.
4. Vybernaite-Lubiene, I., Zilius, M., Bartoli, M., Petkuviene, J., Zemlys, P., **Magri, M.**, Giordani G. (2022). Biogeochemical budgets of nutrients and metabolism in the Curonian Lagoon (South East Baltic Sea): spatial and temporal variations. *Water*, 14,124.

5. **Magri, M.**, Benelli, S., Castaldelli, G., and Bartoli, M. (2022). The seasonal response of *in situ* denitrification and DNRA rates to increasing nitrate availability. *Estuarine, Coastal and Shelf Science*. (Simply modification asked after the first round of review)

6. **Magri, M.**, Bartoli, M., Bondavalli, C., Benelli, S., Zilius, M., Petkuviene, J., Vyberaite-Lubiene, I., Vaiciute, D., Griniene, E., Zemlys, P., Morkune, R., Daunys, D., Solovjova, S., Bucas, M., Baziukas-Razinkovas, A., and Bodini, A. (2022). Temporal and spatial differences of N and P biogeochemistry and estuarine functioning revealed via Ecological Network Analysis. (In Preparation)

7. Benelli, S., Janas, U., **Magri, M.**, and Bartoli, M. (2022). Burrowing macrofauna promotes reactive phosphorus recycling in an oxidised sedimentary environment. (In Preparation)

6.1.6 Disertacijos struktūra

Disertaciją sudaro penki skyriai: Įvadas (1 skyrius), Literatūros apžvalga (2 skyrius), Rezultatai ir diskusija (3 ir 4 skyriai, kuriuose pateikiami rezultatai iš vykdytų eksperimentinių tyrimų Kuršių mariose ir Sacca di Goro lagūnoje) ir Išvados (5 skyrius). Taip pat pateiktas Priedas, kuriame yra papildoma informacija, neįtraukta į pagrindinius skyrius. Disertacijos apimtis – 205 puslapiai; tyrimo medžiaga ir rezultatai pateikiami 29 paveiksluose, 11 lentelių pagrindiniuose skyriuose ir 7 lentelėse prieduose.

6.1.7 Padėka

Norėčiau padėkoti mano vadovams Prof. Marco Bartoli, Prof. Antonio Bodini ir Prof. Artūrui Razinkovui-Baziukui už pagalbą ruošiant šį darbą. Taip pat dėkoju Prof. Pierluigi Viaroli ir dr. Jūratei Lesutienei už pagalbą siekiant dvigubo diplomo. Taip pat esu dėkinga mano kolegoms Parmoje ir Klaipėdoje, kurie dalijosi savo duomenimis ir įžvalgomis. Esu dėkinga savo mylimai šeimai ir draugui, kurių paramą jaučiau visą laiką ruošdama šį darbą.

6.2 Tyrimų medžiaga ir metodai

6.2.1 Tyrimų rajonas

Šis darbas buvo atliktas dviejose eutrofikuotose lagūnose: Sacca di Goro (Italija) ir Kuršių mariose (Lietuvos Respublika–Rusijos Federacija). Sacca di Goro yra sekli Šiaurės Adrijos (Italija) lagūna, kurioje yra išvystyta moliuskų akvakultūra. Kartu su Po upės nuotekomis, kuriose yra gausų azoto junginių, tai sukelia makrofitų žydėjimus, stebimus nuo 1980-jų metų (Viaroli et al., 2006). Kuršių marios yra didžiausia Europos lagūna, esanti pietrytinėje Baltijos jūros dalyje (Lietuvos Respublika–Rusijos Federacija), kuriai būdingi pasikartojantys melsvadumblių žydėjimai (Bartoli ir kt., 2018).

Abiem lagūnoms būdingi pasikartojantys masiniai dumblių žydėjimai, hipoksijos ir anoksijos atvejai šiltuoju laikotarpiu, kuriuos lydi ekosistemos distrofija, turinti įtakos vietinei ekonomikai (Bartoli ir kt., 2018; Viaroli ir kt., 2006). Kaip ir daugelį Europos lagūnų, šias dvi sistemas tiesiogiai ir netiesiogiai veikia klimato kaita, jose didėja tiek vidutinė, tiek ir maksimali vandens temperatūra (Coppola ir Giorgi, 2010; Dailidienė ir kt., 2011), mažėja upių debitas ir vandens lygis, dėl kritulių pokyčių kinta hidrologinis upių sezoniškumas (Cozzi ir Giani, 2011) ir trumpėja padengimo sniego ir ledo danga periodas (Dailidienė ir Davulienė, 2008; Idzelytė ir kt., 2019).

6.2.2 Eksperimentiniai metodai

Šio darbo tikslai [1–5] buvo įgyvendinti atliekant eksperimentus, kurių metu buvo matuojami bentoso procesai, inkubuojant nepažeistas arba rekonstruotas dugno nuosėdų kolonėles. Kolonėlėse pagal 3.1 lygtį buvo matuojami O_2, N_2, DIN, DIP, Fe^{2+} ir Mn^{2+} srautai tarp dugno nuosėdų ir vandens storymės. Įgyvendinant 5 tikslą inkubacijos buvo tęsiamos tol, kol buvo pasiektos anoksinės sąlygos. Denitrifikacijos ir DNRA greičiai buvo nustatyti taikant izotopų poravimo metodus (Nielsen, 1992). Taip pat buvo atlikta nuosėdų analizė.

Dispersine analize (ANOVA) įvertinti veiksniai, paaiškinantys skirtumus tarp išmatuotų procesų. Dispersijos normalumas ir homogeniškumas buvo patikrinti atitinkamai Shapiro-Wilk testu ir Levene medianos testu. Daugkartinis porinis vidurkių palyginimas buvo atliktas naudojant Tukey testą visiems reikšmingiems veiksniams.

6.2.3 Modeliavimo metodai

N ir P srautų tinklai buvo sudaryti atskirai pavasario ir vasaros sezonams dviem atskiroms Kuršių marių dalims – tranzitinei ir stagnacinei; iš viso sudaryti 8 modeliai, kurie buvo analizuojami ENA (6 tikslas). Buvo apskaičiuoti indeksai, susiję su visos sistemos apykaita ir trofinio perdavimo efektyvumu (Ulanowicz, 2004). Kiekvienas modelis buvo parametrizuojamas 1000 kartų, kuriant ENA išdavų neapibrėžtumo diapazonus, kurie leido įvertinti rezultatų patikimumą (Hines ir kt., 2018).

6.3 Rezultatai

3.1 skyriaus rezultatai rodo, kad Goro lagūnoje, esant dideliam upės nuotėkiui, dominavo denitrifikacija, o vasarą suintensyvėjo išorės prietaką padvigubinę transformacijos procesai. 3.2 skyriaus (2 tikslas) rezultatai parodė, kaip NO3 prietaka paskatino denitrifikacijos atsaką, kuris pasiekė prisotinimo slenkstį esant didelei koncentracijai (400-700 µM). 3.3 skyriaus (3 tikslas) rezultatai parodė, kad bioturbuojantys organizmai skatina P atpalaidavimą iš dugno nuosėdų, bet tuo pačiu didina oksiduotų nuosėdų sluoksnio gylį ir potencialų fosforo surišimą dugno nuosėdose. 3.4 skyriaus (4 tikslas) rezultatai atskleidė, kad srautai, išmatuoti nepažeistose ir modifikuotose nuosėdose, ryškiai skiriasi. 4.1 skyriaus (5 tikslas) rezultatai atskleidė Kuršių marių bentoso regeneracijos stechiometrijos skirtumus oksinėse ir anoksinėse sąlygose; pastarosiose P srautas padvigubėjo.

Matematinio modeliavimo rezultatai (4.2 skyrius, 6 tikslas) atskleidė ryškius tranzitinės ir stagnacinės zonos apykaitos skirtumus, stagnacinėje zonoje transformacijos procesai, ypač P junginių vasarą, yra gerokai intensyvesni.

6.4 Diskusija

Goro lagūnoje atliktų eksperimentų rezultatai parodė, kaip globalūs pokyčiai gali paveikti šios sausais laikotarpiais ypač pažeidžiamos lagūnos funkcionavimą. Pavasarį, kuomet yra gausu kritulių ir didelis nuotėkis bei papildomai imituojama nitratų prietaka, bentoso sistemai būdinga didelė buferinė talpa N taršai. Šalinimas viršijo transformacijos procesus visose analizuojamose vietose, o denitrifikacijos pajėgumas gerokai viršijo galimą nitratų koncentracijos padidėjimą. Didelis šios lagūnos biogenų šalinimo pajėgumas yra susijęs su bioturbuojančiais organizmais. Net ir stokodama biologinės įvairovės, makrofaunos bendrija labai padidina N pašalinimo greitį ir P sulaikymo potencialą. Dėl užsitęsusių sausų periodų, susijusių su aukšta temperatūra ir mažu upių nuotėkiu, padidėjo N regeneracija nuosėdose, gerokai viršijanti išorinės maistinių medžiagų prietakos ir jų pašalinimo greitį. Tai lėmė daugybė veiksnių, įskaitant didelį mineralizacijos greitį, atotrūkį tarp N šalinimo ir mineralizacijos, susiformavusį dėl sumažėjusios bioturbatorių gausos, bei denitrifikacijos ir DNRA santykio sumažėjimo dėl didesnio amonifikatorių ryšio su nitratų koncentracija. Dominuojančių procesų sezoninio poslinkio mastas įvairiose analizuojamose vietose skyrėsi dėl nevienalyčių hidrologinių sąlygų ir nuosėdų sudėties; šie poslinkiai buvo ryškesni stagacinėse zonose, kuriose gali kauptis sulfidai, arba ten, kur auginami moliuskai.

Tiek eksperimentiniai, tiek matematinio modeliavimo rezultatai Kuršių mariose atskleidė ženklius tranzitinės ir stagnacinės zonų funkcionavimo skirtumus, kurie yra ypač ryškūs vasarą ir turi didesnį poveikį P junginių dinamikai. Į tranzitinę zoną priteka dideli maistmedžiagių kiekiai, bet dėl aktyvios hidrodinamikos sutrumpėjęs vandens atsinaujinimo laikas sumažina vidinių transformacijos procesų reikšmę. Smėlėtoms, mažai organinės medžiagos turinčioms ir labai oksiduotoms nuosėdoms būdingos stiprios buferinės savybės, jos geba tiek laikinai sulaikyti maistines medžiagas, tiek surišti ir palaidoti jas visam laikui. Eksperimentai ir modeliavimas parodė stagnacinės Kuršių marių zonos pažeidžiamumą. Čia vandens sąstingis skatina maistmedžiagių transformacijos procesus, gerokai viršijančius išorinę prietaką, ypač vasaros sezono metu. Dumblėtų ir daug organinių medžiagų turinčių nuosėdų buferinės savybės, apsaugančios nuo maistinių medžiagų (ypač P) išsiskyrimo, yra menkos; tai prisideda prie visos sistemos biogeocheminių procesų stechiometrijos disbalanso, atskleisto ENA. Šios sąlygos yra palankios melsvadumblių žydėjimui susiformuoti ir palaikyti.

6.5 Išvados

Visi tyrimų metu gauti rezultatai byloja apie didelį analizuojamų sistemų pažeidžiamumą, ypač vasarą, karščio bangų ir sausrų laikotarpiais. Šie veiksniai gali didinti biogeninių

medžiagų transformacijos ir eksporto procesų intensyvumą bei pakeisti lagūnų kaip biogeocheminio filtro funkciją. Seklios lagūnos, ilgą laiką kaupusios maistines medžiagas, gali tapti jų šaltiniu, iš nuosėdų mobilizuoti didelius kiekius N ir P ir skatinti įvairaus tipo žydėjimus. Abiejose sistemose hidrologiniai veiksniai yra svarbiausi maistinių medžiagų dinamikos reguliavimui, jie veikia prietaką, vandens atsinaujinimo laiką ir nuosėdų sudėtį. Hidrodinamiškai aktyvioms zonoms yra būdingos oksiduotos nuosėdos, kuriose gausu bioturbuojančių makrofaunos organizmų, padidinančių maistinių medžiagų sulaikymo ir pašalinimo potencialą. Tuo tarpu staganacinėse zonose nuosėdos yra dumblingos ir chemiškai redukuotos, žema deguonies koncentracija ir toksiškų junginių kaupimasis riboja bentoso makrobestuburių bendrijos veiklą. Čia transformacijos procesai viršija šalinimą ir išorės prietaką. Reikšminga biogeninių medžiagų regeneracija iš dugno nuosėdų sausringų periodų metu gali sumenkinti išorinės biogenų prietakos mažinimo veiksmingumą. Šių sistemų ekologinio funkcionalumo atkūrimui reikalingos ne tik priemonės, skirtos biogenų prietakos iš baseino mažinimui, bet ir žinios apie procesus, padedančius sumažinti vidinę N ir P junginių regeneraciją.

Appendix A

Supplementary Material

Table A.1: Results of the two-way ANOVA to test the effects of seasons and sites on inorganic N (NH_4^+, NO_2^-, NO_3^-, N_2) and O_2 fluxes, and D_{tot}, D_w, D_n and $DNRA_{tot}$ rates. *df* indicate the degree of freedom, SS the sum of squares, MS the mean of squares, F is the F-statistics, and p is p-value. Significant values are printed in bold. NH_4^+, NO_2^- and N_2 fluxes were $\log x^2$ transformed.

Source of variation	*df*	SS	MS	F	p
		NH_4^+			
Season	1	13307287.2	6653644.5	112.6	$<$ **0.001**
Site	2	1538002.3	769001.7	13.0	$<$ **0.001**
Season:Site	2	227558.7	113779.8	1.9	0.161
Residuals	34	2009428.7	59101.2		
Total	39	17082275.4	7595525.2		
		NO_2^-			
Season	1	292.4	146.2	173.0	$<$ **0.001**
Site	2	22.6	11.3	13.4	$<$ **0.001**
Season:Site	2	1.9	0.9	1.1	0.337
Residuals	34	27.9	0.8		
Total	39	344.8	159.3		
		NO_3^-			
Season	1	7071820.8	7071820.8	56.9	$<$ **0.001**
Site	2	269774.4	134887.2	1.0	0.349
Season:Site	2	3627505.5	1813752.7	14.6	$<$ **0.001**
Residuals	34	4220475.0	124131.6		
Total	39	15355293.3	393725.4		
		N_2			
Season	1	758.8	379.4	874.0	$<$ **0.001**
Site	2	5.5	2.8	6.3	**0.004**

Season:Site	2	4.3	2.2	4.9	**0.013**
Residuals	34	14.8	0.4		
Total	39	783.4	384.8		
			O_2		
Season	1	1047.4	523.7	174.1	$<$ **0.001**
Site	2	74.8	37.4	12.4	$<$ **0.001**
Season:Site	2	92.6	46.3	15.4	$<$ **0.001**
Residuals	34	102.3	3.0		
Total	39	1317.1	610.4		
			D_{tot}		
Season	1	888.1	444.0	3286.2	$<$ **0.001**
Site	2	16.6	8.3	61.3	$<$ **0.001**
Season:Site	2	0.6	0.3	2.1	0.137
Residuals	38	5.1	0.1		
Total	43	910.4	452.7		
			D_w		
Season	1	586.9	293.4	1233.8	$<$ **0.001**
Site	2	18.7	9.4	39.4	$<$ **0.001**
Season:Site	2	1.3	0.6	2.7	0.081
Residuals	38	9.0	0.2		
Total	43	615.9	303.6		
			D_n		
Season	1	715.1	357.6	2300.4	$<$ **0.001**
Site	2	14.9	7.4	47.9	$<$ **0.001**
Season:Site	2	0.7	0.4	2.3	0.108
Residuals	38	5.9	0.2		
Total	43	736.6	365.6		
			$DNRA_{tot}$		
Season	1	349.0	174.5	752.3	$<$ **0.001**
Site	2	3.8	1.9	8.1	**0.001**
Season:Site	2	3.6	1.8	7.7	**0.002**
Residuals	38	8.6	0.2		
Total	43	365.0	178.4		

Table A.2: Results of two-way analysis of variance of the parameters measured in the pore water at the end of the experiment. Significant values are marked in bold.

Source of Variation	*df*	SS	MS	F	*p*	Post hoc multiple comparison
			DIP			
Treatment	3	3055.1	1018.4	5.492	**0.003**	C vs AP, C vs A, C vs P
Layer	1	5041.3	5041.3	27.186	< **0.001**	A, C
Interaction	3	1799.2	599.7	3.234	**0.032**	C 3-6 vs AP 3-6, C 3-6 vs A 3-6, C 3-6 vs P 3-6
Residual	40	7417.6	185.4			
Total	47	17313.2	368.4			
			Fe^{2+}			
Treatment	3	18409.9	6136.6	9.329	< **0.001**	C vs P, C vs AP, C vs A
Layer	1	35337.6	35337.6	53.721	< **0.001**	A, P, C
Interaction	3	8032.4	2677.5	4.070	**0.013**	C 3-6 vs P 3-6, C 3-6 vs AP 3-6, A 3-6 vs P 3-6, A 3-6 vs AP 3-6
Residual	40	26311.8	657.8			
Total	47	88091.6	1874.3			
			Mn^{2+}			
Treatment	3	9575.7	3191.9	73.128	< **0.001**	C vs P, C vs AP, C vs A, A vs P, A vs AP
Layer	1	656.0	656.0	15.028	< **0.001**	A, P, AP
Interaction	3	699.2	233.1	5.339	**0.003**	C 0-3 vs P 0-3, C 0-3 vs AP 0-3, C 0-3 vs A 0-3, A 0-3 vs P 0-3, A 0-3 vs AP 0-3; C 3-6 vs P 3-6, C 3-6 vs AP 3-6, A 3-6 vs P 3-6, A 3-6 vs AP 3-6, C 3-6 vs A 3-6
Residual	40	1745.9	43.6			
Total	47	12676.7	269.7			

			pH			
Treatment	3	0.058	0.019	8.013	$<$ **0.001**	P vs C, AP vs C, A vs C
Layer	1	0.020	0.020	8.145	**0.007**	A
Interaction	3	0.012	0.004	1.703	0.182	A 0-3 vs C 0-3, P 0-3 vs C 0-3, A 0-3 vs C 0-3
Residual	40	0.096	0.003			
Total	47	0.185	0.004			
			Eh			
Treatment	3	10222.2	3407.4	3.965	**0.014**	AP vs C, P vs C
Layer	1	48387.0	48387.0	56.309	$<$ **0.001**	A, P, AP, C
Interaction	3	1782.2	594.1	0.691	0.563	
Residual	40	34372.3				
Total	47	94763.7				
			Fe_{tot}			
Treatment	3	467.4	155.8	2.587	0.068	
Layer	1	637.4	637.4	10.583	**0.002**	P, AP
Interaction	3	271.1	90.4	1.500	0.231	
Residual	36	2168.1	60.2			
Total	43	3437.3	79.9			
			Fe^{3+}			
Treatment	3	0.0845	0.0282	0.105	0.957	
Layer	1	0.813	0.813	3.035	0.090	
Interaction	3	1.076	0.359	1.339	0.278	
Residual	35	9.381	0.268			
Total	42	11.377	0.271			

Table A.3: Results of the Spearman correlation between sedimentary features (OM=organic matter; MPS = median particle size) and oxic and anoxic fluxes. Oxygen data were multiplied by -1 in order to have positive fluxes. Sigificant values are printed in bold. a indicates significant values at $p<0.001$, b indicates significant values at $p<0.01$, c indicates significant values at $p<0.05$.

	OM	Density	MPS	O_2	Mn^{2+} OX	Mn^{2+} AN	Fe^{2+} OX	Fe^{2+} AN	NH_4^+ OX	NH_4^+ AN	SiO_2 OX	SiO_2 AN	PO_4^{3-} OX	PO_4^{3-} AN
OM	1													
Density	**-0.63^b**	1												
MPS	**-0.75^a**	**0.70^a**	1											
O_2	-0.12	-0.17	-0.04	1										
Mn^{2+} OX	-0.05	-0.39	-0.16	**0.67^b**	1									
Mn^{2+} AN	**-0.61^b**	**0.46^c**	**0.66^b**	0.03	-0.07	1								
Fe^{2+} OX	-0.11	-0.09	0.01	**0.60^b**	**0.48^c**	-0.36	1							
Fe^{2+} AN	-0.40	-0.29	-0.16	0.04	0.23	-0.25	0.11	1						
NH_4^+ OX	0.31	-0.28	-0.36	**0.65^b**	**0.45^c**	**-0.47^c**	**0.47^c**	0.18	1					
NH_4^+ AN	0.35	-0.23	-0.41	-0.10	0.05	**-0.49^c**	0.19	0.15	**0.49^c**	1				
SiO_2 OX	**0.66^b**	**-0.67^b**	**-0.64^b**	0.25	0.32	-0.29	-0.01	0.41	0.37	0.24	1			
SiO_2 AN	0.23	-0.16	-0.22	**-0.62^b**	-0.25	-0.06	**-0.67^b**	0.22	-0.33	0.06	0.31	1		
PO_4^{3-} OX	0.24	-0.20	-0.20	**0.71^a**	**0.59^b**	-0.21	**0.46^c**	0.17	**0.58^b**	0.04	**0.48^c**	**-0.44^c**	1	
PO_4^{3-} AN	**0.51^c**	-0.42	-0.24	0.08	0.32	-0.21	0.11	**0.76^a**	0.12	0.17	**0.65^b**	0.17	**0.50^c**	1

Table A.4: List of the N pools of all the analysed compartments, both for the transitional and the confined area, in spring and summer. Averages and standard deviations are reported, all values are indicated in µmol N m^{-2}.

		N							
		SPRING				SUMMER			
		Transitional		*Confined*		*Transitional*		*Confined*	
n	**name**	**mean**	**std dev**	**mean**	**std dev**	**mean**	**std dev**	**mean**	**std dev**
1	Non N-fixing Cyanobacteria	1.14E+04	2.28E+03	1.72E+04	3.44E+03	4.15E+04	8.30E+03	1.30E+04	2.60E+03
2	N-fixing Cyanobacteria	6.65E+02	1.33E+02	9.23E+02	1.85E+02	6.44E+04	1.29E+04	5.90E+04	1.18E+04
3	Diatomophyceae	2.41E+04	4.83E+03	4.13E+04	8.26E+03	1.22E+04	2.43E+03	5.26E+03	1.05E+03
4	Chlorophyceae	1.10E+04	2.20E+03	1.35E+04	2.70E+03	8.44E+03	1.69E+03	3.58E+03	7.16E+02
5	Phyto-all others	1.04E+03	2.09E+02	3.34E+03	6.68E+02	2.41E+03	4.82E+02	9.91E+02	1.98E+02
6	Microphytobenthos	8.27E+04	3.43E+03	3.75E+04	6.16E+03	3.27E+04	2.40E+03	2.50E+04	1.31E+03
7	Mphytes-Malgae	3.11E+02	1.40E+02	3.79E+01	1.71E+01	3.11E+02	1.40E+02	3.79E+01	1.71E+01
8	Zooplankton herbivorous	2.42E+02	1.05E+02	8.70E+02	4.31E+02	8.65E+02	4.82E+02	2.02E+03	6.05E+02
9	Zooplankton omnivorous	2.73E+02	1.33E+00	4.84E+02	1.62E+02	2.02E+02	6.05E+01	1.87E+02	5.60E+01
10	Zooplankton predators	1.00E-05	1.00E-05	9.44E+01	3.73E+01	5.62E+02	1.68E+02	7.53E+01	2.26E+01
11	Macrofauna-Dreissena	3.22E+03	2.00E+03	7.98E+00	7.98E+00	3.22E+03	2.00E+03	7.98E+00	7.98E+00
12	Macrofauna-Unio/Anodonta	1.02E+03	1.02E+03	1.00E-05	1.00E-05	1.02E+03	1.02E+03	1.00E-05	1.00E-05
13	Macrofauna-Chironomidae	1.11E+03	8.44E+02	6.21E+03	5.28E+03	1.11E+03	8.44E+02	6.21E+03	5.28E+03
14	Macrofauna-Oligochaeta	2.11E+03	1.08E+03	3.96E+03	1.41E+03	2.11E+03	1.08E+03	3.96E+03	1.41E+03
15	Macrofauna-all others	1.46E+03	8.37E+02	8.59E+02	4.94E+02	1.46E+03	8.37E+02	8.59E+02	4.94E+02
16	Fish-Predators	7.81E+03	1.42E+03	7.81E+03	1.42E+03	7.81E+03	1.42E+03	7.81E+03	1.42E+03
17	Fish-Benthivorous	3.35E+04	6.08E+03	3.35E+04	6.08E+03	3.35E+04	6.08E+03	3.35E+04	6.08E+03
18	Fish-Planktivorous	3.89E+02	7.07E+01	3.89E+02	7.07E+01	3.89E+02	7.07E+01	3.89E+02	7.07E+01
19	Birds-Piscivorous	1.15E+02	6.99E+01	3.94E+01	2.39E+01	2.47E+02	1.62E+02	8.45E+01	5.54E+01
20	Birds-Omnivorous	2.86E+01	1.80E+01	9.78E+00	6.17E+00	3.54E+01	2.28E+01	1.21E+01	7.82E+00
21	Birds-Herbivorous	1.58E+02	1.01E+02	5.40E+01	3.45E+01	1.24E+02	8.02E+01	4.25E+01	2.74E+01
22	Birds-Benthivorous	1.97E+01	1.38E+01	6.75E+00	4.71E+00	2.16E+00	1.60E+00	7.39E-01	5.48E-01
23	DON/Pw	4.19E+04	2.51E+03	1.14E+05	7.80E+03	7.60E+04	1.01E+04	1.78E+05	4.43E+03
24	DIN/Pw	9.01E+04	1.27E+03	1.68E+05	9.30E+03	5.45E+03	1.75E+03	1.07E+04	3.70E+03
25	DON/Ppw	1.00E-05	1.00E-05	1.00E-05	1.00E-05	1.00E-05	1.00E-05	1.00E-05	1.00E-05
26	DIN/Ppw	1.72E+03	5.15E+02	3.26E+04	9.78E+03	5.13E+03	1.54E+03	4.64E+04	1.39E+04
27	PON/Pw	6.03E+04	2.93E+03	1.41E+05	5.32E+03	1.69E+05	2.91E+04	5.33E+05	1.01E+05
28	PIN/Pw	1.00E-05	1.00E-05	1.00E-05	1.00E-05	1.00E-05	1.00E-05	1.00E-05	1.00E-05
29	PON/PS	6.59E+06	1.98E+06	2.20E+07	6.59E+06	7.14E+06	2.14E+06	1.43E+07	4.29E+06
30	PIN/PS	1.00E-05	1.00E-05	1.00E-05	1.00E-05	1.00E-05	1.00E-05	1.00E-05	1.00E-05

Table A.5: List of the P pools of all the analysed compartments, both for the transitional and the confined area, in spring and summer. Averages and standard deviations are reported, all values are indicated in µmol P m^{-2}.

		P							
		SPRING				SUMMER			
		Transitional		*Confined*		*Transitional*		*Confined*	
n	**name**	**mean**	**std dev**	**mean**	**std dev**	**mean**	**std dev**	**mean**	**std dev**
1	Non N-fixing Cyanobacteria	7.11E+02	1.42E+02	1.08E+03	2.15E+02	2.59E+03	5.19E+02	8.13E+02	1.63E+02
2	N-fixing Cyanobacteria	4.16E+01	8.31E+00	5.77E+01	1.15E+01	4.03E+03	8.05E+02	3.69E+03	7.38E+02
3	Diatomophyceae	1.51E+03	3.02E+02	2.58E+03	5.16E+02	7.59E+02	1.52E+02	3.29E+02	6.58E+01
4	Chlorophyceae	6.89E+02	1.38E+02	8.44E+02	1.69E+02	5.28E+02	1.06E+02	2.24E+02	4.48E+01
5	Phyto-all others	6.52E+01	1.30E+01	2.09E+02	4.18E+01	1.51E+02	3.01E+01	6.19E+01	1.24E+01
6	Microphytobenthos	4.60E+03	1.90E+02	2.08E+03	3.42E+02	1.82E+03	1.34E+02	1.39E+03	7.26E+01
7	Mphytes-Malgae	1.51E+01	4.50E+00	1.84E+00	5.49E-01	1.51E+01	4.50E+00	1.84E+00	5.49E-01
8	Zooplankton herbivorous	1.25E+01	7.01E+00	4.50E+01	2.88E+01	5.60E+01	3.22E+01	1.30E+02	3.91E+01
9	Zooplankton omnivorous	1.24E+01	6.04E-02	2.20E+01	7.38E+00	9.17E+00	2.75E+00	8.48E+00	2.54E+00
10	Zooplankton predators	1.00E-05	1.00E-05	5.20E+00	2.05E+00	2.55E+01	7.66E+00	3.42E+00	1.03E+00
11	Macrofauna-Dreissena	1.14E+02	8.80E+01	2.83E-01	2.83E-01	1.14E+02	8.80E+01	2.83E-01	2.83E-01
12	Macrofauna-Unio/Anodonta	3.63E+01	3.63E+01	1.00E-05	1.00E-05	3.63E+01	3.63E+01	1.00E-05	1.00E-05
13	Macrofauna-Chironomidae	3.95E+01	3.37E+01	2.20E+02	2.00E+02	3.95E+01	3.37E+01	2.20E+02	2.00E+02
14	Macrofauna-Oligochaeta	7.47E+01	5.25E+01	1.40E+02	8.54E+01	7.47E+01	5.25E+01	1.40E+02	8.54E+01
15	Macrofauna-all others	5.17E+01	3.83E+01	3.05E+01	2.26E+01	5.17E+01	3.83E+01	3.05E+01	2.26E+01
16	Fish-Predators	1.57E+03	8.34E+02	1.57E+03	8.34E+02	1.57E+03	8.34E+02	1.57E+03	8.34E+02
17	Fish-Benthivorous	6.74E+03	3.57E+03	6.74E+03	3.57E+03	6.74E+03	3.57E+03	6.74E+03	3.57E+03
18	Fish-Planktivorous	7.82E+01	4.15E+01	7.82E+01	4.15E+01	7.82E+01	4.15E+01	7.82E+01	4.15E+01
19	Birds-Piscivorous	1.10E+01	7.46E+00	3.78E+00	2.55E+00	2.37E+01	1.69E+01	8.10E+00	5.79E+00
20	Birds-Omnivorous	2.74E+00	1.90E+00	9.38E-01	6.52E-01	3.39E+00	2.40E+00	1.16E+00	8.21E-01
21	Birds-Herbivorous	1.51E+01	1.06E+01	5.18E+00	3.63E+00	1.19E+01	8.42E+00	4.07E+00	2.88E+00
22	Birds-Benthivorous	1.89E+00	1.42E+00	6.47E-01	4.86E-01	2.07E-01	1.63E-01	7.08E-02	5.57E-02
23	DON/Pw	3.22E+02	2.58E+02	1.34E+03	1.20E+03	4.56E+02	2.46E+02	1.06E+03	4.33E+02
24	DIN/Pw	2.87E+02	1.08E+02	5.88E+02	2.27E+02	5.08E+02	1.22E+02	1.27E+03	5.81E+02
25	DON/Ppw	3.62E+01	9.98E+00	1.17E+02	3.05E+01	4.32E+01	1.89E+01	1.22E+03	3.13E+02
26	DIN/Ppw	7.31E+01	9.80E+00	1.87E+02	4.19E+01	5.27E+01	3.33E+00	1.46E+03	4.42E+02
27	PON/Pw	1.40E+03	1.60E+02	4.95E+03	2.82E+02	2.85E+03	2.38E+02	9.15E+03	9.55E+02
28	PIN/Pw	7.04E+02	1.60E+02	2.39E+03	2.82E+02	1.01E+03	2.38E+02	5.07E+03	9.55E+02
29	PON/PS	3.43E+04	1.52E+04	1.18E+06	3.77E+05	3.58E+04	9.06E+03	1.12E+06	2.35E+04
30	PIN/PS	2.51E+05	1.67E+05	2.53E+05	1.87E+04	2.90E+05	1.74E+04	3.22E+05	7.73E+03

Table A.6: List of the N fluxes both for the transitional and the confined area, in spring and summer. The first and the second columns indicate the numbers of the donor and the receiving compartments as listed in Table A.4. The number 0 refers to the outside environment. Averages and standard deviations are reported, all values are indicated in $\mu mol\,N\,m^{-2}\,h^{-1}$.

		N							
		SPRING				SUMMER			
		Transitional		*Confined*		*Transitional*		*Confined*	
From	**To**	**mean**	**std dev**	**mean**	**std dev**	**mean**	**std dev**	**mean**	**std dev**
0	1	1.35E+02	2.70E+01	2.04E+01	4.08E+00	2.97E+02	5.94E+01	8.46E+01	1.69E+01
0	2	7.16E+00	1.43E+00	1.19E+00	2.38E-01	1.24E+03	2.48E+02	1.31E+02	2.62E+01
0	3	4.18E+02	8.36E+01	4.51E+01	9.01E+00	1.28E+02	2.56E+01	2.49E+01	4.99E+00
0	4	1.14E+02	2.29E+01	1.98E+01	3.97E+00	1.17E+02	2.33E+01	1.78E+01	3.56E+00
0	5	3.59E+01	7.19E+00	2.08E+00	4.17E-01	2.46E+01	4.93E+00	4.95E+00	9.91E-01
0	8	3.45E+00	2.29E+00	3.52E-01	2.45E-01	2.95E+01	2.95E+01	1.48E+00	1.21E+00
0	9	2.31E+00	9.52E-01	4.63E-01	9.07E-02	3.83E+00	3.79E+00	3.52E-01	3.52E-01
0	10	8.16E-01	2.79E-01	2.67E-03	2.66E-03	1.76E+00	1.16E+00	8.95E-01	8.95E-01
0	19	5.49E-01	7.41E-02	1.88E-01	2.54E-02	1.31E+00	4.70E-02	4.47E-01	1.61E-02
0	20	1.66E-01	2.70E-02	5.68E-02	9.24E-03	9.42E-02	3.79E-03	3.23E-02	1.30E-03
0	21	3.97E-02	0.00E+00	1.36E-02	0.00E+00	5.53E-03	0.00E+00	1.89E-03	0.00E+00
0	23	6.79E+02	1.55E+02	8.02E+01	3.96E+01	6.42E+02	1.80E+02	1.13E+02	6.08E+01
0	24	1.48E+03	3.09E+02	1.91E+02	9.73E+01	5.49E+01	1.81E+01	8.94E+00	7.12E+00
0	26	1.24E+02	2.08E+01	1.00E-05	1.00E-05	1.00E-05	1.00E-05	1.00E-05	1.00E-05
0	27	6.07E+02	1.61E+02	1.07E+02	5.16E+01	1.46E+03	7.68E+02	2.46E+02	1.43E+02
0	28	1.00E-05	1.00E-06	1.00E-05	1.00E-06	1.00E-05	1.00E-06	1.00E-05	1.00E-06
1	0	9.91E+01	1.98E+01	3.30E+01	6.60E+00	4.32E+02	8.64E+01	8.54E+01	1.71E+01
2	0	1.24E+01	2.47E+00	1.77E+00	3.54E-01	5.55E+02	1.11E+02	3.87E+02	7.74E+01
3	0	2.78E+02	5.56E+01	7.92E+01	1.58E+01	1.11E+02	2.22E+01	3.45E+01	6.91E+00
4	0	1.01E+02	2.02E+01	2.59E+01	5.18E+00	9.92E+01	1.98E+01	2.35E+01	4.70E+00
5	0	1.43E+01	2.86E+00	6.40E+00	1.28E+00	2.35E+01	4.70E+00	6.50E+00	1.30E+00
8	0	6.27E+00	1.03E+00	1.15E+00	7.82E-01	1.24E+01	3.58E+00	9.22E+00	9.22E+00
9	0	3.35E+00	3.86E-01	7.50E-01	3.26E-01	2.86E+00	1.35E+00	8.68E-01	8.68E-01
10	0	1.00E-05	1.00E-06	1.46E-01	7.23E-02	5.02E+00	3.40E+00	3.20E-01	3.20E-01
19	0	1.80E-01	1.44E-01	6.15E-02	4.91E-02	4.58E-01	3.83E-01	1.57E-01	1.31E-01
20	0	3.29E-02	2.31E-02	1.13E-02	7.92E-03	1.91E-02	1.41E-02	6.54E-03	4.83E-03
21	0	2.32E-02	1.86E-02	7.93E-03	6.38E-03	3.35E-03	2.73E-03	1.15E-03	9.35E-04
23	0	5.87E+02	1.77E+02	1.13E+02	3.93E+01	6.48E+02	2.28E+02	1.51E+02	5.17E+01
24	0	1.25E+03	4.26E+02	1.82E+02	7.48E+01	1.74E+02	1.26E+02	8.82E+00	4.98E+00
26	0	1.50E+01	4.50E+00	6.00E+01	1.50E+01	1.03E+01	1.03E+01	4.00E+01	2.00E+01
27	0	6.60E+02	2.27E+02	1.36E+02	4.66E+01	1.27E+03	5.17E+02	4.44E+02	2.61E+02
28	0	1.00E-05	1.00E-06	1.00E-05	1.00E-06	1.00E-05	1.00E-06	1.00E-05	1.00E-06
29	0	2.00E+02	1.00E+00	1.00E-05	1.00E-06	1.00E-05	1.00E-06	1.00E-05	1.00E-06
30	0	1.00E+02	1.00E+00	1.00E+02	1.00E+00	5.00E+01	1.00E+00	1.00E-05	1.00E-06
23	1	8.61E+00	1.23E+00	2.49E+01	2.26E+00	3.75E+01	8.03E+00	8.25E+01	2.20E+01
24	1	2.01E+01	2.87E+00	5.80E+01	5.28E+00	8.75E+01	1.87E+01	1.92E+02	5.13E+01
23	2	5.03E-01	7.19E-02	1.33E+00	1.21E-01	5.82E+01	1.25E+01	3.74E+02	9.97E+01
24	2	1.17E+00	1.68E-01	3.11E+00	2.83E-01	1.36E+02	2.91E+01	8.72E+02	2.33E+02
23	3	4.36E+01	6.22E+00	1.42E+02	1.29E+01	2.62E+01	5.61E+00	7.95E+01	2.12E+01
24	3	1.02E+02	1.45E+01	3.32E+02	3.02E+01	6.11E+01	1.31E+01	1.86E+02	4.95E+01
23	4	7.84E+00	1.12E+00	1.83E+01	1.67E+00	7.16E+00	1.53E+00	2.13E+01	5.69E+00
24	4	1.83E+01	2.61E+00	4.28E+01	3.89E+00	1.67E+01	3.58E+00	4.97E+01	1.33E+01
23	5	1.11E+00	1.59E-01	6.81E+00	6.19E-01	3.07E+00	6.57E-01	8.85E+00	2.36E+00
24	5	2.60E+00	3.71E-01	1.59E+01	1.44E+00	7.16E+00	1.53E+00	2.06E+01	5.51E+00
23	6	3.67E+01	1.56E+01	9.06E+00	2.26E+00	4.53E+01	9.06E+00	1.00E-05	1.00E-06
24	6	3.93E+01	3.37E+00	9.06E+00	2.26E+00	4.53E+01	9.06E+00	1.00E-05	1.00E-06
25	6	3.67E+01	1.56E+01	9.06E+00	2.26E+00	4.53E+01	9.06E+00	1.00E-05	1.00E-06
26	6	1.51E+02	1.22E+00	9.06E+00	2.26E+00	4.53E+01	9.06E+00	1.00E-05	1.00E-06
23	7	9.77E-01	9.77E-01	1.27E-01	1.27E-01	9.77E-01	9.77E-01	1.27E-01	1.27E-01
24	7	9.77E-01	9.77E-01	1.27E-01	1.27E-01	9.77E-01	9.77E-01	1.27E-01	1.27E-01
1	8	5.66E-01	4.36E-01	1.48E+00	1.29E+00	8.63E+00	5.03E+00	3.93E+00	1.97E+00
2	8	3.31E-02	2.55E-02	7.92E-02	6.89E-02	1.34E+01	7.80E+00	1.78E+01	8.91E+00
3	8	2.79E+00	2.15E+00	8.45E+00	7.36E+00	6.03E+00	3.51E+00	3.79E+00	1.90E+00
4	8	5.15E-01	3.97E-01	1.09E+00	9.48E-01	1.65E+00	9.60E-01	1.02E+00	5.08E-01
5	8	7.32E-02	5.63E-02	4.04E-01	3.52E-01	7.06E-01	4.11E-01	4.22E-01	2.11E-01
27	8	3.22E+00	2.47E+00	1.52E+01	1.33E+01	3.09E+01	1.80E+01	1.25E+02	6.24E+01
1	9	3.07E-01	1.50E-03	3.90E-01	1.31E-01	5.70E-01	2.85E-01	1.02E-01	5.11E-02
2	9	1.79E-02	8.74E-05	2.09E-02	7.01E-03	8.85E-01	4.42E-01	4.63E-01	2.32E-01
3	9	1.55E+00	7.57E-03	2.23E+00	7.48E-01	3.98E-01	1.99E-01	9.85E-02	4.93E-02
4	9	2.79E-01	1.36E-03	2.88E-01	9.64E-02	1.09E-01	5.45E-02	2.64E-02	1.32E-02
5	9	3.96E-02	1.93E-04	1.07E-01	3.58E-02	4.67E-02	2.33E-02	1.10E-02	5.48E-03
8	9	9.58E-03	4.67E-05	2.90E-02	9.73E-03	1.97E-02	9.83E-03	2.74E-02	1.37E-02
9	9	1.07E-02	5.23E-05	1.55E-02	5.20E-03	3.83E-03	1.91E-03	1.97E-03	9.84E-04
27	9	1.74E+00	8.49E-03	4.12E+00	1.38E+00	2.08E+00	1.04E+00	3.30E+00	1.65E+00
8	10	1.00E-05	1.00E-06	1.81E+00	7.94E-01	8.27E+00	4.14E+00	2.91E+00	1.45E+00
9	10	1.00E-05	1.00E-06	1.05E+00	4.59E-01	1.79E+00	8.95E-01	2.28E-01	1.14E-01
10	10	1.00E-05	1.00E-06	2.19E-01	9.65E-02	4.98E+00	2.49E+00	9.22E-02	4.61E-02
1	11	3.70E+00	1.82E+00	3.77E-03	3.76E-03	6.63E+00	3.27E+00	1.77E-03	1.77E-03

2	11	2.16E-01	1.07E-01	2.02E-04	1.99E-04	1.03E+01	5.07E+00	8.02E-03	8.02E-03
3	11	1.87E+01	9.22E+00	2.16E-02	2.16E-02	4.63E+00	2.28E+00	1.71E-03	1.70E-03
4	11	3.37E+00	1.66E+00	2.78E-03	2.77E-03	1.27E+00	6.24E-01	4.58E-04	4.55E-04
5	11	4.78E-01	2.36E-01	1.03E-03	1.03E-03	5.43E-01	2.67E-01	1.90E-04	1.87E-04
8	11	7.48E-02	3.68E-02	1.81E-04	1.78E-04	1.72E-02	8.47E-03	3.23E-05	2.96E-05
27	11	2.10E+01	1.03E+01	3.97E-02	3.97E-02	2.42E+01	1.19E+01	5.70E-02	5.70E-02
1	12	4.90E-01	4.90E-01	2.67E-06	2.67E-07	8.77E-01	8.77E-01	2.67E-06	2.67E-07
2	12	2.86E-02	2.86E-02	2.67E-06	2.67E-07	1.36E+00	1.36E+00	2.67E-06	2.67E-07
3	12	2.48E+00	2.48E+00	2.67E-06	2.67E-07	6.12E-01	6.12E-01	2.67E-06	2.67E-07
4	12	4.46E-01	4.46E-01	2.67E-06	2.67E-07	1.68E-01	1.68E-01	2.67E-06	2.67E-07
5	12	6.33E-02	6.33E-02	2.67E-06	2.67E-07	7.18E-02	7.18E-02	2.67E-06	2.67E-07
27	12	2.78E+00	2.78E+00	2.67E-06	2.67E-07	3.20E+00	3.20E+00	2.67E-06	2.67E-07
1	13	1.20E+00	8.13E-01	2.76E+00	2.21E+00	2.16E+00	1.46E+00	1.30E+00	1.03E+00
2	13	7.04E-02	4.75E-02	1.48E-01	1.18E-01	3.35E+00	2.26E+00	5.87E+00	4.69E+00
3	13	6.09E+00	4.11E+00	1.58E+01	1.26E+01	1.51E+00	1.02E+00	1.25E+00	9.98E-01
4	13	1.10E+00	7.40E-01	2.04E+00	1.63E+00	4.12E-01	2.78E-01	3.35E-01	2.68E-01
5	13	1.56E-01	1.05E-01	7.56E-01	6.04E-01	1.76E-01	1.19E-01	1.39E-01	1.11E-01
6	13	1.12E+00	7.54E-01	9.06E-02	7.24E-02	4.73E-01	3.19E-01	7.80E-02	6.23E-02
27	13	6.84E+00	4.62E+00	2.91E+01	2.33E+01	7.86E+00	5.31E+00	4.18E+01	3.34E+01
29	13	1.43E+01	9.68E+00	5.06E+01	4.04E+01	1.50E+01	1.01E+01	5.06E+01	4.04E+01
6	14	3.22E+00	1.12E+00	8.80E-02	1.22E-02	1.36E+00	4.73E-01	7.58E-02	1.05E-02
29	14	4.13E+01	1.43E+01	4.91E+01	6.81E+00	4.32E+01	1.50E+01	4.91E+01	6.81E+00
1	15	2.02E+00	9.52E-01	1.54E-01	7.29E-02	3.59E+00	1.70E+00	7.21E-02	3.41E-02
2	15	1.18E-01	5.57E-02	8.27E-03	3.91E-03	5.58E+00	2.64E+00	3.27E-01	1.54E-01
3	15	1.02E+01	4.82E+00	8.83E-01	4.17E-01	2.51E+00	1.19E+00	6.95E-02	3.29E-02
4	15	1.83E+00	8.67E-01	1.14E-01	5.37E-02	6.87E-01	3.24E-01	1.86E-02	8.81E-03
5	15	2.60E-01	1.23E-01	4.22E-02	1.99E-02	2.94E-01	1.39E-01	7.74E-03	3.66E-03
8	15	6.29E-02	2.97E-02	1.15E-02	5.42E-03	1.24E-01	5.86E-02	1.93E-02	9.12E-03
9	15	7.05E-02	3.33E-02	6.14E-03	2.90E-03	2.41E-02	1.14E-02	1.39E-03	6.56E-04
10	15	1.60E-06	1.60E-07	1.31E-03	6.21E-04	6.72E-02	3.17E-02	5.61E-04	2.65E-04
27	15	1.14E+01	5.40E+00	1.62E+00	7.68E-01	1.31E+01	6.20E+00	2.33E+00	1.10E+00
11	16	7.17E-01	5.70E-01	9.39E-04	7.46E-04	1.01E+00	8.03E-01	1.65E-03	1.31E-03
12	16	1.35E-01	1.08E-01	1.00E-06	1.00E-07	1.91E-01	1.52E-01	1.00E-06	1.00E-07
13	16	7.62E-02	6.05E-02	7.26E-01	5.77E-01	1.07E-01	8.53E-02	1.28E+00	1.02E+00
14	16	8.92E-02	7.09E-02	3.41E-01	2.71E-01	1.26E-01	9.99E-02	6.01E-01	4.77E-01
15	16	8.64E-02	6.86E-02	3.65E-02	2.90E-02	1.22E-01	9.67E-02	6.44E-02	5.11E-02
16	16	2.34E+00	1.86E+00	2.34E+00	1.86E+00	3.30E+00	2.62E+00	4.13E+00	3.27E+00
17	16	1.00E+01	7.96E+00	1.00E+01	7.96E+00	1.41E+01	1.12E+01	1.77E+01	1.40E+01
18	16	1.17E-01	9.25E-02	1.17E-01	9.25E-02	1.64E-01	1.30E-01	2.05E-01	1.63E-01
1	17	2.55E-01	2.07E-01	2.34E-01	1.90E-01	7.30E-01	5.93E-01	4.68E-01	3.81E-01
2	17	1.49E-02	1.21E-02	1.26E-02	1.02E-02	1.13E+00	9.21E-01	2.12E+00	1.73E+00
3	17	1.29E+00	1.05E+00	1.34E+00	1.09E+00	5.10E-01	4.14E-01	4.52E-01	3.67E-01
4	17	2.32E-01	1.88E-01	1.73E-01	1.40E-01	1.39E-01	1.13E-01	1.21E-01	9.84E-02
5	17	3.29E-02	2.68E-02	6.41E-02	5.21E-02	5.97E-02	4.85E-02	5.03E-02	4.08E-02
7	17	3.66E-01	3.00E-01	3.66E-01	3.00E-01	5.16E-01	4.23E-01	6.46E-01	5.29E-01
8	17	8.57E-01	6.99E-01	1.08E+00	8.82E-01	1.45E+00	1.18E+00	2.85E+00	2.32E+00
9	17	9.35E-01	7.63E-01	5.85E-01	4.77E-01	2.85E-01	2.32E-01	2.22E-01	1.81E-01
10	17	1.00E-05	1.00E-06	1.25E-01	1.02E-01	7.92E-01	6.46E-01	8.96E-02	7.31E-02
11	17	3.46E+01	2.75E+01	4.53E-02	3.60E-02	4.94E+01	3.93E+01	8.09E-02	6.43E-02
12	17	6.53E+00	5.20E+00	1.00E-06	1.00E-07	9.34E+00	7.43E+00	1.00E-06	1.00E-07
13	17	3.68E+00	2.92E+00	3.50E+01	2.79E+01	5.25E+00	4.18E+00	6.25E+01	4.97E+01
14	17	4.30E+00	3.42E+00	1.64E+01	1.31E+01	6.15E+00	4.89E+00	2.94E+01	2.34E+01
15	17	4.16E+00	3.31E+00	1.76E+00	1.40E+00	5.95E+00	4.73E+00	3.15E+00	2.50E+00
16	17	1.47E-01	1.18E-01	1.47E-01	1.18E-01	1.65E-02	1.30E-02	2.06E-02	1.63E-02
17	17	6.32E-01	5.05E-01	6.32E-01	5.05E-01	7.05E-02	5.59E-02	8.82E-02	6.98E-02
18	17	7.34E-03	5.86E-03	7.34E-03	5.86E-03	8.19E-04	6.49E-04	1.02E-03	8.11E-04
27	17	7.32E-01	5.76E-01	7.32E-01	5.76E-01	1.29E+00	1.01E+00	1.29E+00	1.01E+00
1	18	4.58E-03	3.66E-03	4.21E-03	3.37E-03	1.31E-02	1.05E-02	8.42E-03	6.73E-03
2	18	2.68E-04	2.14E-04	2.26E-04	1.81E-04	2.04E-02	1.63E-02	3.82E-02	3.05E-02
3	18	2.32E-02	1.85E-02	2.41E-02	1.93E-02	9.16E-03	7.32E-03	8.12E-03	6.49E-03
4	18	4.17E-03	3.33E-03	3.11E-03	2.48E-03	2.51E-03	2.00E-03	2.18E-03	1.74E-03
5	18	5.92E-04	4.73E-04	1.15E-03	9.21E-04	1.07E-03	8.59E-04	9.03E-04	7.22E-04
7	18	2.13E-02	1.77E-02	2.13E-02	1.77E-02	3.00E-02	2.50E-02	3.76E-02	3.12E-02
8	18	3.43E-01	2.71E-01	4.33E-01	3.43E-01	5.80E-01	4.59E-01	1.14E+00	9.02E-01
9	18	3.75E-01	2.96E-01	2.34E-01	1.85E-01	1.14E-01	9.02E-02	8.89E-02	7.03E-02
10	18	1.00E-05	1.00E-06	5.01E-02	3.96E-02	3.17E-01	2.51E-01	3.59E-02	2.84E-02
11	18	5.21E-02	4.12E-02	6.82E-05	5.40E-05	7.34E-02	5.81E-02	1.20E-04	9.51E-05
12	18	9.84E-03	7.79E-03	1.00E-06	1.00E-07	1.39E-02	1.10E-02	1.00E-06	1.00E-07
13	18	5.54E-03	4.38E-03	5.27E-02	4.17E-02	7.80E-03	6.18E-03	9.29E-02	7.36E-02
14	18	6.48E-03	5.13E-03	2.48E-02	1.96E-02	9.14E-03	7.23E-03	4.36E-02	3.45E-02
15	18	6.27E-03	4.97E-03	2.65E-03	2.10E-03	8.84E-03	7.00E-03	4.68E-03	3.70E-03
27	18	1.91E-03	1.42E-03	1.91E-03	1.42E-03	3.36E-03	2.50E-03	3.36E-03	2.50E-03
16	19	1.03E-01	4.67E-02	3.52E-02	1.60E-02	1.92E-01	1.02E-01	6.58E-02	3.48E-02
17	19	4.40E-01	2.00E-01	1.51E-01	6.86E-02	8.23E-01	4.35E-01	2.82E-01	1.49E-01
18	19	5.11E-03	2.33E-03	1.75E-03	7.97E-04	9.56E-03	5.06E-03	3.27E-03	1.73E-03
7	20	2.27E-03	1.55E-03	7.76E-04	5.32E-04	1.21E-02	7.09E-03	4.15E-03	2.43E-03
8	20	6.17E-04	3.49E-04	2.67E-04	1.51E-04	4.93E-04	3.33E-04	2.65E-04	1.79E-04
9	20	6.74E-04	3.81E-04	1.44E-04	8.16E-05	9.68E-05	6.54E-05	2.07E-05	1.40E-05
10	20	1.00E-05	1.00E-06	3.08E-05	1.74E-05	2.69E-04	1.82E-04	8.34E-06	5.64E-06
11	20	7.96E-02	3.44E-02	3.57E-05	1.54E-05	1.06E-01	5.08E-02	4.75E-05	2.28E-05
12	20	1.50E-02	6.49E-03	1.00E-06	1.00E-07	2.00E-02	9.60E-03	1.00E-06	1.00E-07
13	20	8.45E-03	3.65E-03	2.76E-02	1.19E-02	1.13E-02	5.40E-03	3.67E-02	1.76E-02
14	20	9.90E-03	4.28E-03	1.30E-02	5.59E-03	1.32E-02	6.32E-03	1.73E-02	8.27E-03

15	20	9.58E-03	4.14E-03	1.39E-03	6.00E-04	1.28E-02	6.12E-03	1.85E-03	8.86E-04
16	20	4.02E-03	1.92E-03	1.38E-03	6.59E-04	3.07E-03	1.41E-03	1.05E-03	4.83E-04
17	20	1.72E-02	8.25E-03	5.90E-03	2.82E-03	1.32E-02	6.05E-03	4.50E-03	2.07E-03
18	20	2.00E-04	9.58E-05	6.85E-05	3.28E-05	1.53E-04	7.02E-05	5.23E-05	2.40E-05
7	21	1.70E-01	9.92E-02	5.82E-02	3.40E-02	1.59E-01	9.70E-02	5.45E-02	3.32E-02
11	22	1.77E-01	1.06E-01	7.93E-05	4.75E-05	2.11E-02	1.38E-02	9.46E-06	6.18E-06
12	22	3.34E-02	2.00E-02	1.00E-06	1.00E-07	3.99E-03	2.61E-03	1.00E-06	1.00E-07
13	22	1.88E-02	1.13E-02	6.13E-02	3.67E-02	2.24E-03	1.47E-03	7.32E-03	4.78E-03
14	22	2.20E-02	1.32E-02	2.88E-02	1.72E-02	2.63E-03	1.72E-03	3.44E-03	2.25E-03
15	22	2.13E-02	1.28E-02	3.09E-03	1.85E-03	2.54E-03	1.66E-03	3.68E-04	2.41E-04
16	22	6.25E-03	3.52E-03	2.14E-03	1.20E-03	1.31E-04	9.04E-05	4.49E-05	3.10E-05
17	22	2.68E-02	1.51E-02	9.17E-03	5.16E-03	5.62E-04	3.87E-04	1.92E-04	1.33E-04
18	22	3.11E-04	1.75E-04	1.07E-04	5.99E-05	6.53E-06	4.50E-06	2.24E-06	1.54E-06
1	23	3.45E+00	4.92E-01	9.95E+00	9.04E-01	1.50E+01	3.21E+00	3.30E+01	8.80E+00
2	23	2.01E-01	2.88E-02	5.34E-01	4.85E-02	2.33E+01	4.99E+00	1.50E+02	3.99E+01
3	23	1.74E+01	2.49E+00	5.69E+01	5.18E+00	1.05E+01	2.24E+00	3.18E+01	8.48E+00
4	23	3.13E+00	4.48E-01	7.34E+00	6.67E-01	2.86E+00	6.14E-01	8.53E+00	2.27E+00
5	23	4.45E-01	6.36E-02	2.72E+00	2.47E-01	1.23E+00	2.63E-01	3.54E+00	9.44E-01
6	23	1.55E+01	3.75E+00	2.17E+00	5.43E-01	1.09E+01	2.17E+00	1.00E-05	1.00E-06
7	23	1.00E-04	1.00E-05	1.00E-05	1.00E-06	1.00E-05	1.00E-06	1.00E-05	1.00E-06
8	23	1.28E+00	9.89E-01	4.77E+00	4.15E+00	1.09E+01	6.37E+00	2.71E+01	1.36E+01
9	23	7.06E-01	3.44E-03	1.29E+00	4.31E-01	7.34E-01	3.67E-01	7.20E-01	3.60E-01
10	23	1.00E-05	1.00E-06	5.48E-01	2.41E-01	2.69E+00	1.34E+00	5.76E-01	2.88E-01
11	23	2.51E+00	1.43E+00	6.22E-03	6.22E-03	4.43E+00	2.52E+00	8.77E-03	8.77E-03
12	23	2.38E-01	2.38E-01	3.33E-07	3.33E-08	4.19E-01	4.19E-01	2.67E-07	2.67E-08
15	23	1.48E+00	6.96E-01	2.75E-01	1.30E-01	2.60E+00	1.23E+00	3.88E-01	1.83E-01
16	23	2.72E+00	2.16E+00	2.72E+00	2.16E+00	3.83E+00	3.04E+00	4.79E+00	3.80E+00
17	23	1.22E+01	9.76E+00	1.22E+01	9.76E+00	1.73E+01	1.38E+01	2.16E+01	1.72E+01
18	23	1.88E-01	1.49E-01	1.88E-01	1.49E-01	2.65E-01	2.10E-01	3.32E-01	2.63E-01
19	23	1.82E-02	1.46E-02	6.22E-03	5.00E-03	3.60E-02	3.02E-02	1.23E-02	1.03E-02
20	23	3.22E-03	2.25E-03	1.10E-03	7.69E-04	5.50E-03	3.68E-03	1.88E-03	1.26E-03
21	23	9.05E-03	6.54E-03	3.10E-03	2.24E-03	8.76E-03	6.55E-03	3.00E-03	2.24E-03
22	23	8.87E-03	6.93E-03	3.04E-03	2.37E-03	1.02E-03	8.41E-04	3.50E-04	2.88E-04
25	23	1.00E-04	1.00E-05	1.40E+02	1.87E+01	4.82E+01	2.08E+01	1.00E-05	1.00E-06
27	23	1.37E+02	1.96E+01	4.89E+02	5.87E+01	2.80E+02	7.63E+01	1.24E+03	1.41E+02
8	24	1.28E+00	9.89E-01	4.77E+00	4.15E+00	1.09E+01	6.37E+00	2.71E+01	1.36E+01
9	24	7.06E-01	3.44E-03	1.29E+00	4.31E-01	7.34E-01	3.67E-01	7.20E-01	3.60E-01
10	24	1.00E-05	1.00E-06	5.48E-01	2.41E-01	2.69E+00	1.34E+00	5.76E-01	2.88E-01
11	24	2.51E+00	1.43E+00	6.22E-03	6.22E-03	4.43E+00	2.52E+00	8.77E-03	8.77E-03
12	24	2.38E-01	2.38E-01	3.33E-07	3.33E-08	4.19E-01	4.19E-01	2.67E-07	2.67E-08
15	24	1.48E+00	6.96E-01	2.75E-01	1.30E-01	2.60E+00	1.23E+00	3.88E-01	1.83E-01
16	24	2.72E+00	2.16E+00	2.72E+00	2.16E+00	3.83E+00	3.04E+00	4.79E+00	3.80E+00
17	24	1.22E+01	9.76E+00	1.22E+01	9.76E+00	1.73E+01	1.38E+01	2.16E+01	1.72E+01
18	24	1.88E-01	1.49E-01	1.88E-01	1.49E-01	2.65E-01	2.10E-01	3.32E-01	2.63E-01
19	24	1.41E-01	1.13E-01	4.82E-02	3.87E-02	2.79E-01	2.34E-01	9.56E-02	8.00E-02
20	24	2.50E-02	1.74E-02	8.54E-03	5.96E-03	4.27E-02	2.85E-02	1.46E-02	9.77E-03
21	24	7.01E-02	5.07E-02	2.40E-02	1.73E-02	6.79E-02	5.07E-02	2.33E-02	1.74E-02
22	24	6.87E-02	5.37E-02	2.35E-02	1.84E-02	7.92E-03	6.52E-03	2.71E-03	2.23E-03
23	24	1.37E+02	1.96E+01	4.89E+02	5.87E+01	2.80E+02	7.63E+01	9.44E+02	1.41E+02
26	24	1.00E-04	1.00E-05	1.00E-05	1.00E-06	1.42E+02	9.66E+01	3.65E+02	2.51E+02
28	24	1.00E-04	1.00E-05	1.00E-05	1.00E-06	1.00E-05	1.00E-06	1.00E-05	1.00E-06
6	25	1.55E+01	3.75E+00	2.17E+00	5.43E-01	1.09E+01	2.17E+00	1.00E-05	1.00E-06
13	25	2.07E+00	1.50E+00	1.16E+01	9.60E+00	3.66E+00	2.65E+00	1.63E+01	1.35E+01
14	25	2.70E+00	1.20E+00	5.07E+00	1.37E+00	4.75E+00	2.12E+00	7.15E+00	1.93E+00
23	25	3.67E+01	1.56E+01	1.00E-05	1.00E-06	1.00E-05	1.00E-06	1.31E+00	1.31E+00
29	25	6.64E+01	1.62E+01	1.47E+02	1.97E+01	3.33E+02	5.30E+01	3.75E+02	9.87E+01
13	26	2.07E+00	1.50E+00	1.16E+01	9.60E+00	3.66E+00	2.65E+00	1.63E+01	1.35E+01
14	26	2.70E+00	1.20E+00	5.07E+00	1.37E+00	4.75E+00	2.12E+00	7.15E+00	1.93E+00
24	26	3.93E+01	3.37E+00	1.63E+02	1.90E+01	1.00E-05	1.00E-06	1.00E-05	1.00E-06
25	26	6.64E+01	1.62E+01	7.35E+00	9.85E-01	2.40E+02	2.31E+01	3.75E+02	9.87E+01
1	27	2.24E+01	3.20E+00	6.47E+01	5.88E+00	9.75E+01	2.09E+01	2.17E+02	5.79E+01
2	27	1.31E+00	1.87E-01	3.47E+00	3.15E-01	1.51E+02	3.24E+01	9.85E+02	2.63E+02
3	27	1.13E+02	1.62E+01	3.70E+02	3.36E+01	6.80E+01	1.46E+01	2.09E+02	5.58E+01
4	27	2.04E+01	2.91E+00	4.77E+01	4.34E+00	1.86E+01	3.99E+00	5.61E+01	1.50E+01
5	27	2.89E+00	4.13E-01	1.77E+01	1.61E+00	7.98E+00	1.71E+00	2.33E+01	6.21E+00
7	27	1.00E-04	1.00E-05	1.00E-05	1.00E-06	1.00E-05	1.00E-06	1.00E-05	1.00E-06
8	27	2.70E+00	2.08E+00	1.00E+01	8.73E+00	2.30E+01	1.34E+01	5.70E+01	2.85E+01
9	27	1.48E+00	7.24E-03	2.70E+00	9.04E-01	1.54E+00	7.71E-01	1.51E+00	7.56E-01
10	27	1.00E-04	1.00E-05	1.15E+00	5.06E-01	5.64E+00	2.82E+00	1.21E+00	6.05E-01
16	27	2.72E+00	2.16E+00	2.72E+00	2.16E+00	3.83E+00	3.04E+00	4.79E+00	3.80E+00
17	27	2.45E+01	1.95E+01	2.45E+01	1.95E+01	3.45E+01	2.75E+01	4.32E+01	3.44E+01
18	27	3.77E-01	2.98E-01	3.77E-01	2.98E-01	5.31E-01	4.21E-01	6.64E-01	5.26E-01
19	27	2.27E-02	1.82E-02	7.78E-03	6.25E-03	4.50E-02	3.77E-02	1.54E-02	1.29E-02
20	27	4.02E-03	2.81E-03	1.38E-03	9.61E-04	6.88E-03	4.60E-03	2.36E-03	1.58E-03
21	27	1.13E-02	8.17E-03	3.87E-03	2.80E-03	1.10E-02	8.18E-03	3.75E-03	2.80E-03
22	27	1.11E-02	8.66E-03	3.80E-03	2.96E-03	1.28E-03	1.05E-03	4.38E-04	3.60E-04
29	27	1.00E-04	1.00E-05	1.00E-05	1.00E-06	1.00E-05	1.00E-06	1.00E-05	1.00E-06
24	28	1.00E-04	1.00E-05	1.00E-05	1.00E-06	1.00E-05	1.00E-06	1.00E-05	1.00E-06
30	28	1.00E-04	1.00E-05	1.00E-05	1.00E-06	1.00E-05	1.00E-06	1.00E-05	1.00E-06
1	29	3.96E+00	1.31E+00	5.36E+00	1.78E+00	1.40E+00	4.67E-01	1.27E+00	4.23E-01
2	29	2.31E-01	7.63E-02	2.87E-01	9.53E-02	2.18E+00	7.25E-01	5.75E+00	1.92E+00
3	29	2.00E+01	6.60E+00	3.07E+01	1.02E+01	9.79E-01	3.26E-01	1.22E+00	4.08E-01
4	29	3.60E+00	1.19E+00	3.95E+00	1.31E+00	2.68E-01	8.93E-02	3.28E-01	1.09E-01

5	29	5.11E-01	1.69E-01	1.47E+00	4.86E-01	1.15E-01	3.82E-02	1.36E-01	4.54E-02
7	29	1.84E+02	2.51E+01	2.54E+01	6.34E+00	1.27E+02	2.54E+01	1.00E-05	1.00E-06
11	29	5.03E+00	2.86E+00	1.24E-02	1.24E-02	8.86E+00	5.04E+00	1.75E-02	1.75E-02
12	29	4.76E-01	4.76E-01	3.33E-07	3.33E-08	8.38E-01	8.38E-01	2.67E-07	2.67E-08
13	29	4.15E+00	3.01E+00	2.31E+01	1.92E+01	7.31E+00	5.30E+00	3.26E+01	2.71E+01
14	29	5.39E+00	2.41E+00	1.01E+01	2.73E+00	9.50E+00	4.24E+00	1.43E+01	3.85E+00
15	29	2.95E+00	1.39E+00	5.50E-01	2.59E-01	5.20E+00	2.45E+00	7.75E-01	3.65E-01
19	29	3.29E-01	1.50E-01	1.13E-01	5.12E-02	6.15E-01	3.25E-01	2.10E-01	1.11E-01
20	29	8.85E-02	3.93E-02	3.49E-02	2.04E-02	1.16E-01	5.61E-02	3.27E-02	1.99E-02
21	29	1.02E-01	5.95E-02	3.49E-02	2.04E-02	9.56E-02	5.82E-02	3.27E-02	1.99E-02
22	29	1.84E-01	1.09E-01	6.28E-02	3.74E-02	1.99E-02	1.30E-02	6.82E-03	4.46E-03
27	29	7.01E+01	2.29E+01	8.19E+01	2.70E+01	1.97E+02	6.44E+01	3.09E+02	1.02E+02
26	30	1.00E+02	1.00E+00	1.00E+02	1.00E+00	5.00E+01	1.00E+00	1.00E-05	1.00E-06
28	30	1.00E-04	1.00E-05	1.00E-05	1.00E-06	1.00E-05	1.00E-06	1.00E-05	1.00E-06

Table A.7: List of the P fluxes both for the transitional and the confined area, in spring and summer. The first and the second columns indicate the numbers of the donor and the receiving compartments as listed in Table A.5. The number 0 refers to the outside environment. Averages and standard deviations are reported, all values are indicated in $\mu mol\,P\,m^{-2}\,h^{-1}$.

		P							
		SPRING				SUMMER			
		Transitional		*Confined*		*Transitional*		*Confined*	
From	**To**	**mean**	**std dev**	**mean**	**std dev**	**mean**	**std dev**	**mean**	**std dev**
0	1	8.44E+00	1.69E+00	1.27E+00	2.55E-01	1.86E+01	3.71E+00	5.29E+00	1.06E+00
0	2	4.48E-01	8.95E-02	7.43E-02	1.49E-02	7.74E+01	1.55E+01	8.20E+00	1.64E+00
0	3	2.61E+01	5.22E+00	2.82E+00	5.63E-01	7.99E+00	1.60E+00	1.56E+00	3.12E-01
0	4	7.15E+00	1.43E+00	1.24E+00	2.48E-01	7.30E+00	1.46E+00	1.11E+00	2.22E-01
0	5	2.25E+00	4.49E-01	1.30E-01	2.61E-02	1.54E+00	3.08E-01	3.10E-01	6.19E-02
0	8	2.29E-01	1.52E-01	2.34E-02	1.63E-02	1.96E+00	1.96E+00	9.85E-02	8.02E-02
0	9	1.05E-01	4.33E-02	2.10E-02	4.12E-03	1.74E-01	1.72E-01	1.60E-02	1.60E-02
0	10	4.49E-02	1.54E-02	1.47E-04	1.37E-04	9.71E-02	6.36E-02	4.93E-02	4.92E-02
0	19	1.10E-01	9.22E-03	3.78E-02	3.16E-03	2.63E-01	4.87E-03	9.01E-02	1.67E-03
0	20	1.35E-02	1.26E-03	4.61E-03	4.31E-04	7.00E-03	1.77E-04	2.40E-03	6.06E-05
0	21	1.97E-03	0.00E+00	6.73E-04	0.00E+00	2.74E-04	0.00E+00	9.38E-05	0.00E+00
0	23	6.42E+00	5.36E+00	5.69E-01	5.69E-01	3.61E+00	2.29E+00	7.13E-01	7.13E-01
0	24	5.75E+00	1.81E+00	5.25E-01	4.81E-01	7.49E+00	3.21E+00	7.81E-01	6.36E-01
0	26	1.00E-05	1.00E-05	1.00E-05	1.00E-05	1.00E-05	1.00E-05	1.00E-05	1.00E-05
0	27	2.23E+01	8.20E+00	2.44E+00	1.73E+00	2.88E+01	1.27E+01	4.38E+00	2.90E+00
0	28	1.32E+01	4.79E+00	1.24E+00	1.00E+00	1.65E+01	8.01E+00	1.56E+00	1.26E+00
1	0	6.19E+00	1.24E+00	2.06E+00	4.12E-01	2.70E+01	5.40E+00	5.34E+00	1.07E+00
2	0	7.72E-01	1.54E-01	1.11E-01	2.21E-02	3.47E+01	6.93E+00	2.42E+01	4.84E+00
3	0	1.74E+01	3.47E+00	4.95E+00	9.90E-01	6.93E+00	1.39E+00	2.16E+00	4.32E-01
4	0	6.32E+00	1.26E+00	1.62E+00	3.24E-01	6.20E+00	1.24E+00	1.47E+00	2.94E-01
5	0	8.93E-01	1.79E-01	4.00E-01	8.01E-02	1.47E+00	2.94E-01	4.06E-01	8.13E-02
8	0	4.16E-01	6.83E-02	7.62E-02	5.21E-02	8.22E-01	2.38E-01	6.12E-01	6.12E-01
9	0	1.52E-01	1.76E-02	3.41E-02	1.48E-02	1.30E-01	6.12E-02	3.95E-02	3.95E-02
10	0	1.00E-05	1.00E-06	8.05E-03	3.98E-03	2.77E-01	1.87E-01	1.76E-02	1.76E-02
19	0	9.14E-02	6.23E-02	3.13E-02	2.13E-02	2.31E-01	1.70E-01	7.90E-02	5.82E-02
20	0	9.55E-03	7.26E-03	3.27E-03	2.49E-03	5.55E-03	4.38E-03	1.90E-03	1.50E-03
21	0	2.17E-03	1.61E-03	7.42E-04	5.52E-04	3.13E-04	2.37E-04	1.07E-04	8.11E-05
23	0	5.75E+00	3.87E+00	1.36E+00	1.36E+00	3.40E+00	2.51E+00	9.04E-01	7.58E-01
24	0	4.01E+00	1.97E+00	5.97E-01	4.93E-01	4.44E+00	2.26E+00	1.08E+00	9.61E-01
26	0	1.00E-05	1.00E-06	1.00E-05	1.00E-06	1.00E-05	1.00E-06	1.00E-05	1.00E-06
27	0	1.36E+01	6.73E+00	5.03E+00	2.49E+00	2.35E+01	1.11E+01	7.81E+00	4.18E+00
28	0	8.81E+00	4.30E+00	2.42E+00	1.35E+00	9.20E+00	4.79E+00	4.33E+00	2.68E+00
29	0	1.00E+01	1.00E+00	1.00E-05	1.00E-06	1.00E-05	1.00E-06	1.00E-05	1.00E-06
30	0	1.00E+00	1.00E-01	1.50E+00	1.00E-02	1.00E-05	1.00E-06	1.00E-05	1.00E-06
23	1	5.38E-01	7.69E-02	1.55E+00	1.41E-01	2.34E+00	5.02E-01	5.15E+00	1.37E+00
24	1	1.26E+00	1.79E-01	3.63E+00	3.30E-01	5.47E+00	1.17E+00	1.20E+01	3.21E+00
23	2	3.15E-02	4.49E-03	8.34E-02	7.58E-03	3.64E+00	7.79E-01	2.34E+01	6.23E+00
24	2	7.34E-02	1.05E-02	1.95E-01	1.77E-02	8.49E+00	1.82E+00	5.45E+01	1.45E+01
23	3	2.72E+00	3.89E-01	8.90E+00	8.09E-01	1.64E+00	3.50E-01	4.97E+00	1.33E+00
24	3	6.35E+00	9.08E-01	2.08E+01	1.89E+00	3.82E+00	8.18E-01	1.16E+01	3.09E+00
23	4	4.90E-01	7.00E-02	1.15E+00	1.04E-01	4.48E-01	9.59E-02	1.33E+00	3.55E-01
24	4	1.14E+00	1.63E-01	2.67E+00	2.43E-01	1.04E+00	2.24E-01	3.11E+00	8.29E-01
23	5	6.96E-02	9.94E-03	4.25E-01	3.87E-02	1.92E-01	4.11E-02	5.53E-01	1.47E-01
24	5	1.62E-01	2.32E-02	9.92E-01	9.02E-02	4.47E-01	9.59E-02	1.29E+00	3.44E-01
23	6	4.05E+00	9.76E-01	1.09E+00	2.72E-01	2.83E+00	5.66E-01	1.00E-05	1.00E-06
24	6	4.05E+00	9.76E-01	1.09E+00	2.72E-01	2.83E+00	5.66E-01	1.00E-05	1.00E-06
25	6	4.05E+00	9.76E-01	1.09E+00	2.72E-01	2.83E+00	5.66E-01	1.00E-05	1.00E-06
26	6	4.05E+00	9.76E-01	1.09E+00	2.72E-01	2.83E+00	5.66E-01	1.00E-05	1.00E-06
23	7	4.75E-02	4.75E-02	6.17E-03	6.16E-03	4.75E-02	4.75E-02	6.17E-03	6.16E-03
24	7	4.75E-02	4.75E-02	6.17E-03	6.16E-03	4.75E-02	4.75E-02	6.17E-03	6.16E-03
1	8	4.02E-02	3.10E-02	1.05E-01	9.14E-02	6.16E-01	3.57E-01	2.81E-01	1.40E-01
2	8	2.35E-03	1.81E-03	5.63E-03	4.90E-03	9.56E-01	5.55E-01	1.27E+00	6.36E-01
3	8	1.98E-01	1.53E-01	6.01E-01	5.23E-01	4.30E-01	2.50E-01	2.71E-01	1.35E-01
4	8	3.66E-02	2.82E-02	7.74E-02	6.74E-02	1.18E-01	6.83E-02	7.26E-02	3.63E-02
5	8	5.20E-03	4.01E-03	2.87E-02	2.50E-02	5.04E-02	2.93E-02	3.01E-02	1.51E-02
27	8	2.28E-01	1.76E-01	1.08E+00	9.43E-01	2.20E+00	1.28E+00	8.92E+00	4.46E+00
1	9	1.45E-02	7.06E-05	1.84E-02	6.17E-03	2.69E-02	1.35E-02	4.82E-03	2.41E-03
2	9	8.46E-04	4.13E-06	9.88E-04	3.31E-04	4.18E-02	2.09E-02	2.19E-02	1.09E-02
3	9	7.33E-02	3.57E-04	1.05E-01	3.53E-02	1.88E-02	9.39E-03	4.65E-03	2.33E-03
4	9	1.32E-02	6.42E-05	1.36E-02	4.55E-03	5.14E-03	2.57E-03	1.25E-03	6.23E-04
5	9	1.87E-03	9.12E-06	5.04E-03	1.69E-03	2.20E-03	1.10E-03	5.17E-04	2.59E-04
8	9	4.52E-04	2.20E-06	1.37E-03	4.59E-04	9.28E-04	4.64E-04	1.29E-03	6.46E-04
9	9	5.07E-04	2.47E-06	7.33E-04	2.45E-04	1.81E-04	9.04E-05	9.29E-05	4.65E-05
27	9	8.22E-02	4.01E-04	1.94E-01	6.51E-02	9.82E-02	4.91E-02	1.56E-01	7.79E-02
8	10	1.00E-05	1.00E-06	1.18E-01	5.49E-02	4.61E-01	2.31E-01	1.89E-01	9.44E-02
9	10	1.00E-05	1.00E-06	6.81E-02	3.17E-02	9.99E-02	4.99E-02	1.48E-02	7.42E-03
10	10	1.00E-05	1.00E-06	1.43E-02	6.66E-03	2.78E-01	1.39E-01	5.99E-03	3.00E-03
1	11	3.27E-01	1.61E-01	1.74E-04	1.72E-04	5.85E-01	2.88E-01	8.20E-05	7.93E-05

2	11	1.91E-02	9.40E-03	9.36E-06	6.69E-06	9.08E-01	4.47E-01	3.72E-04	3.69E-04
3	11	1.65E+00	8.14E-01	9.99E-04	9.96E-04	4.09E-01	2.01E-01	7.90E-05	7.64E-05
4	11	2.97E-01	1.46E-01	1.29E-04	1.26E-04	1.12E-01	5.51E-02	2.12E-05	1.85E-05
5	11	4.22E-02	2.08E-02	4.77E-05	4.51E-05	4.79E-02	2.36E-02	8.79E-06	6.13E-06
8	11	6.60E-03	3.25E-03	8.36E-06	5.69E-06	1.52E-03	7.47E-04	1.50E-06	1.47E-06
27	11	1.85E+00	9.13E-01	1.84E-03	1.84E-03	2.13E+00	1.05E+00	2.64E-03	2.64E-03
1	12	4.32E-02	4.32E-02	2.67E-06	2.67E-07	7.73E-02	7.73E-02	2.67E-06	2.67E-07
2	12	2.53E-03	2.52E-03	2.67E-06	2.67E-07	1.20E-01	1.20E-01	2.67E-06	2.67E-07
3	12	2.19E-01	2.19E-01	2.67E-06	2.67E-07	5.40E-02	5.40E-02	2.67E-06	2.67E-07
4	12	3.93E-02	3.93E-02	2.67E-06	2.67E-07	1.48E-02	1.48E-02	2.67E-06	2.67E-07
5	12	5.58E-03	5.58E-03	2.67E-06	2.67E-07	6.33E-03	6.33E-03	2.67E-06	2.67E-07
27	12	2.45E-01	2.45E-01	2.67E-06	2.67E-07	2.82E-01	2.82E-01	2.67E-06	2.67E-07
1	13	1.06E-01	7.17E-02	1.28E-01	1.02E-01	1.90E-01	1.28E-01	6.00E-02	4.79E-02
2	13	6.21E-03	4.19E-03	6.86E-03	5.48E-03	2.95E-01	1.99E-01	2.72E-01	2.17E-01
3	13	5.37E-01	3.63E-01	7.32E-01	5.85E-01	1.33E-01	8.96E-02	5.78E-02	4.62E-02
4	13	9.66E-02	6.53E-02	9.43E-02	7.54E-02	3.63E-02	2.45E-02	1.55E-02	1.24E-02
5	13	1.37E-02	9.27E-03	3.50E-02	2.80E-02	1.56E-02	1.05E-02	6.44E-03	5.14E-03
6	13	9.85E-02	6.65E-02	4.19E-03	3.35E-03	4.17E-02	2.82E-02	3.61E-03	2.89E-03
27	13	6.03E-01	4.07E-01	1.35E+00	1.08E+00	6.93E-01	4.68E-01	1.93E+00	1.55E+00
29	13	1.26E+00	8.54E-01	2.34E+00	1.87E+00	1.32E+00	8.92E-01	2.34E+00	1.87E+00
6	14	2.84E-01	9.85E-02	4.08E-03	5.65E-04	1.20E-01	4.17E-02	3.51E-03	4.87E-04
29	14	3.64E+00	1.27E+00	2.28E+00	3.15E-01	3.81E+00	1.32E+00	2.28E+00	3.15E-01
1	15	1.78E-01	8.40E-02	7.14E-03	3.37E-03	3.17E-01	1.50E-01	3.34E-03	1.58E-03
2	15	1.04E-02	4.91E-03	3.83E-04	1.81E-04	4.92E-01	2.32E-01	1.51E-02	7.16E-03
3	15	8.99E-01	4.25E-01	4.09E-02	1.93E-02	2.21E-01	1.05E-01	3.22E-03	1.52E-03
4	15	1.62E-01	7.64E-02	5.27E-03	2.49E-03	6.06E-02	2.86E-02	8.64E-04	4.08E-04
5	15	2.30E-02	1.09E-02	1.95E-03	9.23E-04	2.59E-02	1.23E-02	3.58E-04	1.69E-04
8	15	5.55E-03	2.62E-03	5.32E-04	2.51E-04	1.09E-02	5.16E-03	8.95E-04	4.23E-04
9	15	6.22E-03	2.94E-03	2.84E-04	1.34E-04	2.13E-03	1.01E-03	6.44E-05	3.04E-05
10	15	1.60E-06	1.60E-07	6.09E-05	2.88E-05	5.93E-03	2.80E-03	2.60E-05	1.23E-05
27	15	1.01E+00	4.76E-01	7.53E-02	3.56E-02	1.16E+00	5.47E-01	1.08E-01	5.10E-02
11	16	2.55E-02	2.23E-02	3.33E-05	2.91E-05	3.59E-02	3.14E-02	5.87E-05	5.14E-05
12	16	4.81E-03	4.21E-03	1.00E-06	1.00E-07	6.78E-03	5.93E-03	1.00E-06	1.00E-07
13	16	2.70E-03	2.37E-03	2.58E-02	2.25E-02	3.81E-03	3.33E-03	4.54E-02	3.97E-02
14	16	3.17E-03	2.77E-03	1.21E-02	1.06E-02	4.46E-03	3.90E-03	2.13E-02	1.86E-02
15	16	3.06E-03	2.68E-03	1.30E-03	1.13E-03	4.32E-03	3.78E-03	2.29E-03	2.00E-03
16	16	4.72E-01	4.16E-01	4.72E-01	4.16E-01	6.65E-01	5.86E-01	8.31E-01	7.32E-01
17	16	2.02E+00	1.78E+00	2.02E+00	1.78E+00	2.85E+00	2.51E+00	3.56E+00	3.14E+00
18	16	2.35E-02	2.07E-02	2.35E-02	2.07E-02	3.31E-02	2.92E-02	4.14E-02	3.65E-02
1	17	2.69E-02	2.25E-02	2.48E-02	2.06E-02	7.71E-02	6.43E-02	4.95E-02	4.13E-02
2	17	1.57E-03	1.31E-03	1.33E-03	1.11E-03	1.20E-01	9.98E-02	2.24E-01	1.87E-01
3	17	1.36E-01	1.14E-01	1.42E-01	1.18E-01	5.38E-02	4.49E-02	4.77E-02	3.98E-02
4	17	2.45E-02	2.04E-02	1.83E-02	1.52E-02	1.47E-02	1.23E-02	1.28E-02	1.07E-02
5	17	3.48E-03	2.90E-03	6.77E-03	5.65E-03	6.31E-03	5.26E-03	5.31E-03	4.43E-03
7	17	1.83E-02	1.47E-02	1.83E-02	1.47E-02	2.57E-02	2.07E-02	3.22E-02	2.58E-02
8	17	1.18E-01	9.53E-02	1.49E-01	1.20E-01	2.00E-01	1.61E-01	3.93E-01	3.17E-01
9	17	1.29E-01	1.04E-01	8.08E-02	6.51E-02	3.93E-02	3.17E-02	3.07E-02	2.47E-02
10	17	1.00E-05	1.00E-06	1.73E-02	1.39E-02	1.09E-01	8.82E-02	1.24E-02	9.97E-03
11	17	1.27E+00	1.11E+00	1.66E-03	1.45E-03	1.81E+00	1.58E+00	2.97E-03	2.59E-03
12	17	2.40E-01	2.09E-01	1.00E-06	1.00E-07	3.43E-01	2.99E-01	1.00E-06	1.00E-07
13	17	1.35E-01	1.18E-01	1.28E+00	1.12E+00	1.93E-01	1.68E-01	2.29E+00	2.00E+00
14	17	1.58E-01	1.38E-01	6.03E-01	5.27E-01	2.26E-01	1.97E-01	1.08E+00	9.40E-01
15	17	1.53E-01	1.33E-01	6.47E-02	5.64E-02	2.18E-01	1.90E-01	1.15E-01	1.01E-01
16	17	7.17E-03	6.30E-03	7.17E-03	6.30E-03	3.31E-03	2.92E-03	4.14E-03	3.65E-03
17	17	3.07E-02	2.70E-02	3.07E-02	2.70E-02	1.42E-02	1.25E-02	1.78E-02	1.56E-02
18	17	3.57E-04	3.14E-04	3.57E-04	3.14E-04	1.65E-04	1.45E-04	2.06E-04	1.82E-04
27	17	6.45E-02	5.08E-02	6.45E-02	5.08E-02	9.09E-02	7.15E-02	1.14E-01	8.94E-02
1	18	4.84E-04	3.98E-04	4.45E-04	3.66E-04	1.39E-03	1.14E-03	8.90E-04	7.32E-04
2	18	2.83E-05	2.33E-05	2.39E-05	1.96E-05	2.15E-03	1.77E-03	4.03E-03	3.32E-03
3	18	2.45E-03	2.01E-03	2.55E-03	2.09E-03	9.68E-04	7.96E-04	8.58E-04	7.05E-04
4	18	4.41E-04	3.62E-04	3.28E-04	2.70E-04	2.65E-04	2.18E-04	2.30E-04	1.89E-04
5	18	6.26E-05	5.15E-05	1.22E-04	1.00E-04	1.13E-04	9.33E-05	9.54E-05	7.85E-05
7	18	1.06E-03	8.57E-04	1.06E-03	8.57E-04	1.49E-03	1.21E-03	1.86E-03	1.51E-03
8	18	1.66E-02	1.43E-02	2.10E-02	1.81E-02	2.81E-02	2.42E-02	5.51E-02	4.76E-02
9	18	1.81E-02	1.56E-02	1.13E-02	9.78E-03	5.51E-03	4.76E-03	4.30E-03	3.71E-03
10	18	1.00E-05	1.00E-06	2.42E-03	2.09E-03	1.53E-02	1.32E-02	1.74E-03	1.50E-03
11	18	1.85E-03	1.61E-03	2.42E-06	2.11E-06	2.61E-03	2.28E-03	4.27E-06	3.72E-06
12	18	3.49E-04	3.05E-04	1.00E-06	1.00E-07	4.92E-04	4.30E-04	1.00E-06	1.00E-07
13	18	1.96E-04	1.72E-04	1.87E-03	1.63E-03	2.77E-04	2.42E-04	3.30E-03	2.88E-03
14	18	2.30E-04	2.01E-04	8.79E-04	7.67E-04	3.24E-04	2.83E-04	1.55E-03	1.35E-03
15	18	2.23E-04	1.94E-04	9.42E-05	8.23E-05	3.14E-04	2.74E-04	1.66E-04	1.45E-04
27	18	1.68E-04	1.25E-04	1.68E-04	1.25E-04	2.37E-04	1.76E-04	2.96E-04	2.20E-04
16	19	2.07E-02	1.42E-02	7.08E-03	4.87E-03	3.87E-02	2.82E-02	1.32E-02	9.66E-03
17	19	8.86E-02	6.09E-02	3.03E-02	2.09E-02	1.66E-01	1.21E-01	5.67E-02	4.14E-02
18	19	1.03E-03	7.08E-04	3.52E-04	2.42E-04	1.93E-03	1.40E-03	6.59E-04	4.81E-04
7	20	1.11E-04	6.83E-05	3.79E-05	2.34E-05	5.92E-04	2.93E-04	2.03E-04	1.00E-04
8	20	3.24E-05	2.23E-05	1.40E-05	9.64E-06	2.59E-05	1.99E-05	1.39E-05	1.07E-05
9	20	3.54E-05	2.43E-05	7.57E-06	5.22E-06	5.08E-06	3.90E-06	1.08E-06	8.33E-07
10	20	1.00E-05	1.00E-06	1.62E-06	1.11E-06	1.41E-05	1.09E-05	4.38E-07	3.36E-07
11	20	2.82E-03	1.85E-03	1.27E-06	8.28E-07	3.76E-03	2.57E-03	1.69E-06	1.15E-06
12	20	5.34E-04	3.49E-04	1.00E-06	1.00E-07	7.11E-04	4.85E-04	1.00E-06	1.00E-07
13	20	3.00E-04	1.96E-04	9.79E-04	6.40E-04	4.00E-04	2.73E-04	1.30E-03	8.90E-04
14	20	3.51E-04	2.30E-04	4.60E-04	3.01E-04	4.68E-04	3.20E-04	6.12E-04	4.18E-04

15	20	3.40E-04	2.22E-04	4.93E-05	3.22E-05	4.53E-04	3.09E-04	6.56E-05	4.48E-05
16	20	8.09E-04	5.67E-04	2.77E-04	1.94E-04	6.18E-04	4.26E-04	2.12E-04	1.46E-04
17	20	3.47E-03	2.43E-03	1.19E-03	8.32E-04	2.65E-03	1.83E-03	9.07E-04	6.26E-04
18	20	4.03E-05	2.82E-05	1.38E-05	9.67E-06	3.08E-05	2.12E-05	1.05E-05	7.27E-06
7	21	8.41E-03	4.49E-03	2.88E-03	1.54E-03	7.89E-03	4.42E-03	2.70E-03	1.51E-03
11	22	6.28E-03	4.74E-03	2.82E-06	2.13E-06	7.49E-04	5.91E-04	3.36E-07	2.65E-07
12	22	1.19E-03	8.97E-04	1.00E-06	1.00E-07	1.42E-04	1.12E-04	1.00E-06	1.00E-07
13	22	6.68E-04	5.04E-04	2.18E-03	1.64E-03	7.96E-05	6.28E-05	2.60E-04	2.05E-04
14	22	7.82E-04	5.90E-04	1.02E-03	7.72E-04	9.32E-05	7.36E-05	1.22E-04	9.62E-05
15	22	7.57E-04	5.71E-04	1.10E-04	8.28E-05	9.03E-05	7.12E-05	1.31E-05	1.03E-05
16	22	1.26E-03	9.43E-04	4.31E-04	3.23E-04	2.64E-05	2.17E-05	9.04E-06	7.43E-06
17	22	5.39E-03	4.04E-03	1.85E-03	1.38E-03	1.13E-04	9.30E-05	3.87E-05	3.18E-05
18	22	6.27E-05	4.69E-05	2.15E-05	1.61E-05	1.31E-06	1.08E-06	4.50E-07	3.70E-07
1	23	2.15E-01	3.08E-02	6.22E-01	5.65E-02	9.37E-01	2.01E-01	2.06E+00	5.50E-01
2	23	1.26E-02	1.80E-03	3.34E-02	3.03E-03	1.45E+00	3.12E-01	9.35E+00	2.49E+00
3	23	1.09E+00	1.56E-01	3.56E+00	3.24E-01	6.54E-01	1.40E-01	1.99E+00	5.30E-01
4	23	1.96E-01	2.80E-02	4.59E-01	4.17E-02	1.79E-01	3.84E-02	5.33E-01	1.42E-01
5	23	2.78E-02	3.97E-03	1.70E-01	1.55E-02	7.67E-02	1.64E-02	2.21E-01	5.90E-02
6	23	9.71E-01	2.34E-01	1.36E-01	3.40E-02	6.79E-01	1.36E-01	1.00E-05	1.00E-06
7	23	1.00E-04	1.00E-05	1.00E-05	1.00E-06	1.00E-05	1.00E-06	1.00E-05	1.00E-06
8	23	1.53E-01	1.18E-01	5.69E-01	4.95E-01	1.31E+00	7.59E-01	3.24E+00	1.62E+00
9	23	5.59E-02	2.72E-04	1.02E-01	3.40E-02	5.80E-02	2.90E-02	5.69E-02	2.85E-02
10	23	1.00E-04	1.00E-05	5.98E-02	2.79E-02	2.51E-01	1.25E-01	6.27E-02	3.14E-02
11	23	3.02E-01	1.76E-01	5.98E-04	5.95E-04	4.72E-01	2.75E-01	9.35E-04	9.32E-04
12	23	1.82E-02	1.82E-02	2.67E-07	2.67E-08	2.84E-02	2.84E-02	2.67E-07	2.67E-08
15	23	1.96E-01	9.19E-02	2.92E-02	1.37E-02	3.06E-01	1.44E-01	4.56E-02	2.14E-02
16	23	1.00E-05	0.00E+00	1.00E-05	0.00E+00	1.00E-05	0.00E+00	1.00E-05	0.00E+00
17	23	1.00E-05	0.00E+00	1.00E-05	0.00E+00	1.00E-05	0.00E+00	1.00E-05	0.00E+00
18	23	1.00E-05	0.00E+00	1.00E-05	0.00E+00	1.00E-05	0.00E+00	1.00E-05	0.00E+00
19	23	1.00E-05	0.00E+00	1.00E-05	0.00E+00	1.00E-05	0.00E+00	1.00E-05	0.00E+00
20	23	1.00E-05	0.00E+00	1.00E-05	0.00E+00	1.00E-05	0.00E+00	1.00E-05	0.00E+00
21	23	1.00E-05	0.00E+00	1.00E-05	0.00E+00	1.00E-05	0.00E+00	1.00E-05	0.00E+00
22	23	1.00E-05	0.00E+00	1.00E-05	0.00E+00	1.00E-05	0.00E+00	1.00E-05	0.00E+00
25	23	1.96E-01	1.00E-05	3.53E+00	1.79E+00	3.52E+00	3.52E+00	4.66E+00	4.66E+00
27	23	1.00E-04	1.22E+00	3.06E+01	3.67E+00	1.75E+01	4.77E+00	7.78E+01	8.80E+00
8	24	1.53E-01	1.18E-01	5.69E-01	4.95E-01	1.31E+00	7.59E-01	3.24E+00	1.62E+00
9	24	5.59E-02	2.72E-04	1.02E-01	3.40E-02	5.80E-02	2.90E-02	5.69E-02	2.85E-02
10	24	1.00E-04	1.00E-05	5.98E-02	2.79E-02	2.51E-01	1.25E-01	6.27E-02	3.14E-02
11	24	3.02E-01	1.76E-01	5.98E-04	5.95E-04	4.72E-01	2.75E-01	9.35E-04	9.32E-04
12	24	1.82E-02	1.82E-02	2.67E-07	2.67E-08	2.84E-02	2.84E-02	2.67E-07	2.67E-08
15	24	1.96E-01	9.19E-02	2.92E-02	1.37E-02	3.06E-01	1.44E-01	4.56E-02	2.14E-02
16	24	7.16E-01	6.30E-01	7.16E-01	6.30E-01	1.01E+00	8.89E-01	1.26E+00	1.11E+00
17	24	9.98E-01	8.20E-01	9.98E-01	8.20E-01	1.25E+00	1.01E+00	1.56E+00	1.27E+00
18	24	1.78E-02	1.49E-02	1.78E-02	1.49E-02	2.23E-02	1.83E-02	2.79E-02	2.29E-02
19	24	4.99E-02	3.43E-02	1.71E-02	1.17E-02	9.79E-02	7.21E-02	3.35E-02	2.47E-02
20	24	4.34E-03	3.27E-03	1.49E-03	1.12E-03	5.42E-03	4.15E-03	1.86E-03	1.42E-03
21	24	4.64E-03	2.97E-03	1.59E-03	1.02E-03	4.47E-03	3.00E-03	1.53E-03	1.03E-03
22	24	3.05E-03	2.58E-03	1.04E-03	8.85E-04	3.54E-04	3.10E-04	1.21E-04	1.06E-04
23	24	8.56E+00	1.22E+00	2.56E+01	3.67E+00	1.75E+01	4.77E+00	6.22E+01	7.04E+00
26	24	1.08E+00	1.08E+00	3.26E+00	3.26E+00	4.31E+00	4.31E+00	1.30E+01	1.30E+01
28	24	1.00E-04	1.00E-05	1.00E-05	1.00E-06	1.00E-05	1.00E-06	1.00E-05	1.00E-06
6	25	9.71E-01	2.34E-01	1.36E-01	3.40E-02	6.79E-01	1.36E-01	1.00E-05	1.00E-06
13	25	3.45E-01	2.53E-01	1.54E+00	1.29E+00	5.40E-01	3.96E-01	2.41E+00	2.01E+00
14	25	3.90E-01	1.81E-01	5.87E-01	1.71E-01	6.10E-01	2.83E-01	9.18E-01	2.68E-01
23	25	1.00E-04	1.00E-05	1.00E-05	1.00E-06	1.00E-05	1.00E-06	1.00E-05	1.00E-06
29	25	4.15E+00	1.02E+00	9.18E+00	1.23E+00	2.08E+01	3.31E+00	2.34E+01	6.17E+00
13	26	3.45E-01	2.53E-01	1.54E+00	1.29E+00	5.40E-01	3.96E-01	2.41E+00	2.01E+00
14	26	3.90E-01	1.81E-01	5.87E-01	1.71E-01	6.10E-01	2.83E-01	9.18E-01	2.68E-01
24	26	1.00E-04	1.00E-05	1.00E-05	1.00E-06	1.00E-05	1.00E-06	1.00E-05	1.00E-06
25	26	4.15E+00	1.02E+00	5.69E+00	7.63E-01	1.45E+01	1.12E+00	2.34E+01	6.17E+00
1	27	1.40E+00	2.00E-01	4.04E+00	3.67E-01	6.17E+00	1.32E+00	1.36E+01	3.62E+00
2	27	8.18E-02	1.17E-02	2.17E-01	1.97E-02	9.58E+00	2.05E+00	6.15E+01	1.64E+01
3	27	7.08E+00	1.01E+00	2.31E+01	2.10E+00	4.31E+00	9.23E-01	1.31E+01	3.49E+00
4	27	1.27E+00	1.82E-01	2.98E+00	2.71E-01	1.18E+00	2.53E-01	3.51E+00	9.36E-01
5	27	1.81E-01	2.58E-02	1.11E+00	1.01E-01	5.05E-01	1.08E-01	1.46E+00	3.88E-01
7	27	1.00E-04	1.00E-05	1.00E-05	1.00E-06	1.00E-05	1.00E-06	1.00E-05	1.00E-06
8	27	1.18E-01	9.06E-02	4.37E-01	3.81E-01	1.01E+00	5.84E-01	2.49E+00	1.25E+00
9	27	4.30E-02	2.09E-04	7.82E-02	2.62E-02	4.47E-02	2.23E-02	4.38E-02	2.19E-02
10	27	1.00E-04	1.00E-05	4.60E-02	2.15E-02	1.93E-01	9.65E-02	4.82E-02	2.41E-02
16	27	7.16E-01	6.30E-01	7.16E-01	6.30E-01	1.01E+00	8.89E-01	1.26E+00	1.11E+00
17	27	1.82E-01	1.57E-01	1.82E-01	1.57E-01	2.57E-01	2.21E-01	3.21E-01	2.77E-01
18	27	3.18E-03	2.73E-03	3.18E-03	2.73E-03	4.48E-03	3.85E-03	5.60E-03	4.81E-03
19	27	4.25E-02	2.92E-02	1.46E-02	9.99E-03	8.34E-02	6.15E-02	2.86E-02	2.10E-02
20	27	3.70E-03	2.78E-03	1.27E-03	9.53E-04	4.62E-03	3.53E-03	1.58E-03	1.21E-03
21	27	3.95E-03	2.53E-03	1.35E-03	8.67E-04	3.81E-03	2.56E-03	1.30E-03	8.76E-04
22	27	2.59E-03	2.20E-03	8.88E-04	7.54E-04	3.01E-04	2.64E-04	1.03E-04	9.05E-05
29	27	1.00E-04	1.00E-05	1.00E-05	1.00E-06	1.00E-05	1.00E-06	1.00E-05	1.00E-06
24	28	1.00E-04	1.00E-05	1.00E-05	1.00E-06	1.00E-05	1.00E-06	1.00E-05	1.00E-06
30	28	1.00E-04	1.00E-05	1.00E-05	1.00E-06	1.00E-05	1.00E-06	1.00E-05	1.00E-06
1	29	2.47E-01	8.16E-02	3.35E-01	1.11E-01	8.77E-02	2.92E-02	7.93E-02	2.64E-02
2	29	1.44E-02	4.77E-03	1.80E-02	5.96E-03	1.36E-01	4.53E-02	3.60E-01	1.20E-01
3	29	1.25E+00	4.13E-01	1.92E+00	6.36E-01	6.12E-02	2.04E-02	7.65E-02	2.55E-02
4	29	2.25E-01	7.42E-02	2.47E-01	8.19E-02	1.68E-02	5.58E-03	2.05E-02	6.83E-03

5	29	3.19E-02	1.05E-02	9.16E-02	3.04E-02	7.18E-03	2.39E-03	8.51E-03	2.83E-03
7	29	1.13E+01	2.73E+00	3.04E+00	7.61E-01	7.92E+00	1.58E+00	1.00E-05	1.00E-06
11	29	6.04E-01	3.52E-01	1.20E-03	1.19E-03	9.44E-01	5.50E-01	1.87E-03	1.87E-03
12	29	3.63E-02	3.63E-02	2.67E-07	2.67E-08	5.68E-02	5.68E-02	2.67E-07	2.67E-08
13	29	6.91E-01	5.06E-01	3.08E+00	2.57E+00	1.08E+00	7.91E-01	4.82E+00	4.02E+00
14	29	7.81E-01	3.62E-01	1.17E+00	3.43E-01	1.22E+00	5.65E-01	1.84E+00	5.35E-01
15	29	3.91E-01	1.84E-01	5.83E-02	2.74E-02	6.12E-01	2.87E-01	9.12E-02	4.28E-02
19	29	6.62E-02	4.55E-02	2.27E-02	1.56E-02	1.24E-01	9.03E-02	4.24E-02	3.09E-02
20	29	5.31E-03	3.59E-03	1.73E-03	9.22E-04	5.84E-03	3.93E-03	1.62E-03	9.09E-04
21	29	5.05E-03	2.69E-03	1.73E-03	9.22E-04	4.73E-03	2.65E-03	1.62E-03	9.09E-04
22	29	9.83E-03	7.40E-03	3.37E-03	2.53E-03	7.77E-04	6.16E-04	2.67E-04	2.11E-04
27	29	1.63E+00	5.32E-01	2.87E+00	9.47E-01	3.32E+00	1.08E+00	5.31E+00	1.75E+00
26	30	1.00E-04	1.00E-05	1.00E-05	1.00E-06	1.00E-06	1.00E-07	1.00E-05	1.00E-06
28	30	8.19E-01	2.67E-01	1.38E+00	4.56E-01	1.17E+00	3.82E-01	2.94E+00	9.71E-01

Bibliography

Abril, G., Etcheber, H., Le Hir, P., Bassoullet, P., Boutier, B. & Frankignoulle, M. (1999). Oxic/anoxic oscillations and organic carbon mineralization in an estuarine maximum turbidity zone (The Gironde, France). *Limnology and Oceanography*, *44*(5), 1304–1315. https://doi.org/10.4319/lo.1999.44.5.1304

Adhurya, S., Das, S. & Ray, S. (2020). Guanotrophication by waterbirds in freshwater lakes: a review on ecosystem perspective. *Springer Proceedings in Mathematics and Statistics*, *302*, 253–269. https://doi.org/10.1007/978-981-15-0422-8_22

Aller, R. C. (2014). Sedimentary diagenesis, depositional environments, and benthic fluxes. In M. J. Mottl & H. Elderfield (Eds.), *Treatise on geochemistry, vol. 8: The oceans and marine geochemistry* (2nd, pp. 293–334). Elsevier.

Aller, R. C. (1994). Bioturbation and remineralization of sedimentary organic matter: effects of redox oscillation. *Chemical Geology*, *114*, 331–345. https://doi.org/https://doi.org/10.1016/0009-2541(94)90062-0

Allesina, S. & Bondavalli, C. (2003). Steady state of ecosystem flow networks: a comparison between balancing procedures. *Ecological Modelling*, *165*(2-3), 221–229. https://doi.org/10.1016/S0304-3800(03)00075-9

Allgeier, J. E., Wenger, S. & Layman, C. A. (2020). Taxonomic identity best explains variation in body nutrient stoichiometry in a diverse marine animal community. *Scientific Reports*, *10*, 13718. https://doi.org/10.1038/s41598-020-67881-y

Alvisi, A., Edelvais, S. & Marzocchi, D. (1991). *Indagine quali-quantitativa delle acque superficiali del bacino Burana-Volano*. Dimensione Ambiente, Provincia di Ferrara, Ferrara, Italy.

An, S. & Gardner, W. S. (2002). Dissimilatory nitrate reduction to ammonium (DNRA) as a nitrogen link, versus denitrification as a sink in a shallow estuary (Laguna Madre/Baffin Bay, Texas). *Marine Ecology Progress Series*, *237*, 41–50. https://doi.org/10.3354/meps237041

Andersen, L. G., Hall, P. O., Iverfeldt, A., Rutgers van der Loejf, M. M., Sundby, B. & Westerlund, S. F. (1986). Benthic respiration measured by total carbonate production. *Limnology and Oceanography*, *31*(2), 319–329. https://doi.org/10.4319/lo.1986.31.2.0319

Anderson, I., Brush, M., Piehler, M., Currin, C., Stanhope, J., Smyth, A., Maxey, J. & Whitehead, M. (2013). Impacts of climate-related drivers on the benthic nutrient

filter in a shallow photic estuary. *Estuaries and Coasts*, *37*(1), 46–52. https://doi.org/10.1007/s12237-013-9665-5

Andrieux, B., Signor, J., Guillou, V., Danger, M. & Jabot, F. (2020). Body stoichiometry of heterotrophs: assessing drivers of interspecific variations in elemental composition. *Global Ecology and Biogeography*, *30*(4), 883–895.

Anschutz, P., Bouchet, S., Abril, G., Bridou, R., Tessier, E. & Amouroux, D. (2019). In vitro simulation of oscillatory redox conditions in intertidal sediments: N, Mn, Fe, and P coupling. *Continental Shelf Research*, *177*, 33–41. https://doi.org/10.1016/j.csr.2019.03.007

Ansell, A., Gibson, R., Barnes, M. & Press, U. (1998). Ecological impact of green macroalgal blooms. *Oceanography and Marine Biology: an annual review*, *36*, 97–125.

Anthony, A., Atwood, J., August, P., Byron, C., Cobb, S. & Foster, C. (2009). Coastal lagoons and climate change: ecological and social ramifications in U. S. Atlantic and Gulf coast ecosystems. *Ecology and Society*, *14*(1).

Antonioli, F., Anzidei, M., Amorosi, A., Presti, V. L., Mastronuzzi, G., Deiana, G., Falco, G. D., Fontana, A., Fontolan, G., Lisco, S., Marsico, A., Moretti, M., Orrù, P. E., Sannino, G. M., Serpelloni, E. & Vecchio, A. (2017). Sea-level rise and potential drowning of the Italian coastal plains: flooding risk scenarios for 2100. *Quaternary Science Reviews*, *158*, 29–43. https://doi.org/10.1016/j.quascirev.2016.12.021

APHA (American Public Health Association). (1992). *Standard methods for the examination of water and wastewaters* (APHA, Ed.; 18th).

Arbačiauskas, K., rate Lesutiene, J. & Gasiunaite, Z. R. (2013). Feeding strategies and elemental composition in Ponto-Caspian peracaridans from contrasting environments: can stoichiometric plasticity promote invasion success? *Freshwater Biology*, *58*(5), 1052–1068. https://doi.org/10.1111/fwb.12108

Ascott, M., Gooddy, D., Wang, L., Stuart, M., Lewis, M., Ward, R. & Binley, A. (2017). Global patterns of nitrate storage in the vadose zone. *Nature Communications*, *8*(1), 1–7. https://doi.org/10.1038/s41467-017-01321-w

Asmala, E., Carstensen, J., Conley, D. J., Slomp, C. P., Stadmark, J. & Voss, M. (2017). Efficiency of the coastal filter: nitrogen and phosphorus removal in the Baltic Sea. *Limnology and Oceanography*, *62*, S222–S238. https://doi.org/10.1002/lno.10644

Asmus, H. & Helgoland, B. A. (1982). Field measurements on respiration and secondary production of a benthic community in the Northern Wadden Sea. *Netherlands Journal of Sea Research*, *16*, 403–413.

Azzoni, R., Giordani, G. & Viaroli, P. (2005). Iron-sulphur-phosphorus interactions: implications for sediment buffering capacity in a mediterranean eutrophic lagoon (Sacca di Goro, Italy). *Hydrobiologia*, *550*(1), 131–148. https://doi.org/10.1007/s10750-005-4369-x

Baird, D., Luczkovich, J. & Christian, R. R. (1998). Assessment of spatial and temporal variaility in ecosystem attributes of the St Marks National Wildlife Refuge, Apalachee Bay, Florida. *Estuarine Coastal and Shelf Science*, *47*, 329–349.

Baird, D., Ulanowicz, R. E. & Boynton, W. R. (1995). Seasonal nitrogen dynamics in Chesapeake Bay: a network approach. *Estuarine Coastal and Shelf Science*, *41*(2), 137–162. https://doi.org/10.1006/ecss.1995.0058

Baird, D., Asmus, H. & Asmus, R. (2008). Nutrient dynamics in the Sylt-Rømø Bight ecosystem, German Wadden Sea: an ecological network analysis approach. *Estuarine, Coastal and Shelf Science*, *80*(3), 339–356. https://doi.org/10.1016/j.ecss.2008.08.012

Baird, D., Asmus, H. & Asmus, R. (2011). Carbon, nitrogen and phosphorus dynamics in nine sub-systems of the Sylt-Rømø Bight ecosystem, German Wadden Sea. *Estuarine, Coastal and Shelf Science*, *91*(1), 51–68. https://doi.org/10.1016/j.ecss.2010.10.004

Baird, D. & Ulanowicz, R. E. (1989). The seasonal dynamics of the Chesapeake Bay ecosystem. *Ecological Monographs*, *59*(4), 329–364.

Bartoli, M., Longhi, D., Nizzoli, D., Como, S., Magni, P. & Viaroli, P. (2009). Short term effects of hypoxia and bioturbation on solute fluxes, denitrification and buffering capacity in a shallow dystrophic pond. *Journal of Experimental Marine Biology and Ecology*, *381*(2), 105–113. https://doi.org/10.1016/j.jembe.2009.09.018

Bartoli, M., Racchetti, E., Delconte, C. A., Sacchi, E., Soana, E., Laini, A., Longhi, D. & Viaroli, P. (2012). Nitrogen balance and fate in a heavily impacted watershed (Oglio River , Northern Italy): in quest of the missing sources and sinks. *Biogeosciences*, *9*, 361–373. https://doi.org/10.5194/bg-9-361-2012

Bartoli, M., Benelli, S., Lauro, M., Magri, M., Vybernaite-Lubiene, I. & Petkuviene, J. (2020). Variable oxygen levels lead to variable stoichiometry of benthic nutrient fluxes in a hypertrophic estuary. *Estuaries and Coasts*, 1–15. https://doi.org/10.1007/s12237-020-00786-1

Bartoli, M., Castaldelli, G., Nizzoli, D., Fano, E. A. & Viaroli, P. (2016). Manila clam introduction in the Sacca di Goro Lagoon (Northern Italy): ecological implications. *Bull. Jap. Fish. Res. Edu. Agen.*, *42*, 43–52.

Bartoli, M., Castaldelli, G., Nizzoli, D. & Viaroli, P. (2012). Benthic primary production and bacterial denitrification in a Mediterranean eutrophic coastal lagoon. *Journal of Experimental Marine Biology and Ecology*, *438*, 41–51. https://doi.org/10.1016/j.jembe.2012.09.011

Bartoli, M., Cattadori, M., Giordani, G. & Viaroli, P. (1996). Benthic oxygen respiration, ammonium and phosphorus regeneration in surficial sediments of the Sacca di Goro (Northern Italy) and two French coastal lagoons: a comparative study. *Hydrobiologia*, *329*(1-3), 143–159. https://doi.org/10.1007/BF00034554

Bartoli, M., Naldi, M., Nizzoli, D., Roubaix, V. & Viaroli, P. (2003). Influence of clam farming on macroalgal growth: a microcosm experiment. *Chemistry and Ecology*, *19*(2-3), 147–160. https://doi.org/10.1080/0275754031000119906

Bartoli, M., Nizzoli, D., Pusceddu, A., Bianchelli, S. & Sundbäck, K. (2021). Denitrification, nitrogen uptake, and organic matter quality undergo different seasonality in sandy and muddy sediments of a turbid estuary. *Frontiers in Microbiology*, *11*. https://doi.org/10.3389/fmicb.2020.612700

Bartoli, M., Nizzoli, D., Viaroli, P., Turolla, E., Castaldelli, G., Fano, E. A. & Rossi, R. (2001). Impact of *Tapes philippinarum* farming on nutrient dynamics and benthic respiration in the Sacca di Goro. *Hydrobiologia*, *455*, 203–212. https://doi.org/10.1023/A:1011910422400

Bartoli, M., Zilius, M., Bresciani, M., Vaiciute, D., Vybernaite-Lubiene, I., Petkuviene, J., Giordani, G., Daunys, D., Ruginis, T., Benelli, S., Giardino, C., Bukaveckas, P. A., Zemlys, P., Griniene, E., Gasiunaite, Z. R., Lesutiene, J., Pilkaitytė, R. & Baziukas-Razinkovas, A. (2018). Drivers of cyanobacterial blooms in a hypertrophic lagoon. *Frontiers in Marine Science*, *5*, 1–12. https://doi.org/10.3389/fmars.2018.00434

Beintema, A. T. (1997). European Black Terns (*Chlidonias niger*) in trouble: examples of dietary problems. *Colonial Waterbirds*, *20*(3), 558–565.

Benelli, S., Bartoli, M., Racchetti, E., Carpintero, P., Mindaugas, M., Lubiene, I. & Anna, E. (2017). Rare but large bivalves alter benthic respiration and nutrient recycling in riverine sediments. *Aquatic Ecology*, *51*(1), 1–16. https://doi.org/10.1007/s10452-016-9590-3

Benelli, S., Bartoli, M., Ribaudo, C. & Fano, E. A. (2019). Contrasting effects of an alienworm on benthic N cycling in muddy and sandy sediments. *Water*, *11*(3), 1–12. https://doi.org/10.3390/w11030465

Benelli, S., Bartoli, M., Zilius, M., Vybernaite-Lubiene, I., Ruginis, T., Petkuviene, J. & Fano, E. A. (2018). Microphytobenthos and chironomid larvae attenuate nutrient recycling in shallow-water sediments. *Freshwater Biology*, *63*(2), 187–201. https://doi.org/10.1111/fwb.13052

Berezina, N. A., Razinkovas-Baziukas, A. & Tiunov, A. V. (2017). Non-indigenous amphipods and mysids in coastal food webs of eastern Baltic Sea estuaries. *Journal of Marine Biological Association of the United Kingdom*, *97*(3), 581–590.

Bernot, M. J. & Dodds, W. K. (2005). Nitrogen retention, removal, and saturation in lotic ecosystems. *Ecosystems*, *8*(4), 442–453. https://doi.org/10.1007/s10021-003-0143-y

Bianchini, G., Natali, C., Forgli, R. & Antisari, L. (2015). Preliminary notes on C-N pools in subacqueous soils from the Sacca di Goro Coastal lagoon (Po delta, Northern Italy). *Environmental Quality*, *19*, 45–54. https://doi.org/10.6092/issn.2281-4485/5800

Blackburn, T. H. & Henriksen, K. (1983). Nitrogen cycling in different types of sediments from Danish waters. *Limnology and Oceanography*, *28*(3), 477–493. https://doi.org/10.4319/lo.1983.28.3.0477

Blackburn, T. H. & Sorensen, J. (1988). *Nitrogen cycling in coastal marine environment*. John Wiley & Sons, New York.

Boesch, D. F. (2002). Challenges and opportunities for science in reducing nutrient overenrichment of coastal ecosystems. *Archivos Argentinos de Pediatria*, *25*(4), 886–900.

Bonaglia, S., Bartoli, M., Gunnarsson, J. S., Rahm, L., Raymond, C., Svensson, O., Yekta, S. S. & Brüchert, V. (2013). Effect of reoxygenation and *Marenzelleria*

spp. bioturbation on Baltic Sea sediment metabolism. *Marine Ecology Progress Series*, *482*, 43–55. https://doi.org/10.3354/meps10232

Bonaglia, S., Klawonn, I., De Brabandere, L., Deutsch, B., Thamdrup, B. & Brüchert, V. (2016). Denitrification and DNRA at the Baltic Sea oxic–anoxic interface: substrate spectrum and kinetics. *Limnology and Oceanography*, *61*(5), 1900–1915. https://doi.org/10.1002/lno.10343

Borrett, S. R., Carter, M. & Hines, D. E. (2016). Six general ecosystem properties are more intense in biogeochemical cycling networks than food webs. *Journal of Complex Networks*, (4), 575–603.

Borrett, S. R. & Lau, M. K. (2014). enaR: an R package for Ecosystem Network Analysis. *Methods in Ecology and Evolution*, *5*(11), 1206–1213. https://doi.org/10.1111/2041-210X.12282

Borrett, S. R., Sheble, L., Moody, J. & Anway, E. C. (2018). Bibliometric review of ecological network analysis : 2010 – 2016. *Ecological Modelling*, *382*(April), 63–82. https://doi.org/10.1016/j.ecolmodel.2018.04.020

Borrett, S. R., Whipple, S. J., Patten, B. C. & Christian, R. R. (2006). Indirect effects and distributed control in ecosystems: temporal variation of indirect effects in a seven-compartment model of nitrogen flow in the Neuse River Estuary , USA — Time series analysis. *Ecological Modelling*, *4*, 178–188. https://doi.org/10.1016/j.ecolmodel.2005.10.011

Bouraoui, F. & Grizzetti, B. (2011). Long term change of nutrient concentrations of rivers discharging in European seas. *Science of the Total Environment*, *409*(23), 4899–4916. https://doi.org/10.1016/j.scitotenv.2011.08.015

Bower, C. E. & Holm-Hansen, T. (1980). A salicylate-hypochlorite method for determining ammonia in seawater. *Canadian Journal of Fisheries and Aquatic Sciences*, *37*(5), 794–798.

Boynton, W. R., Kemp, W. M. & Osborne, C. G. (1980). Nutrient fluxes across the sediment-water interface in the turbid zone of a coastal plain estuary. In W. S. Kennedy (Ed.), *Estuarine perspective* (pp. 93–109). Academis Press, New york.

Braeckman, U., Provoost, P., Gribsholt, B., Gansbeke, D. V., Middelburg, J. J., Soetaert, K., Vincx, M. & Vanaverbeke, J. (2010). Role of macrofauna functional traits and density in biogeochemical fluxes and bioturbation. *Marine Ecology Progress Series*, *399*, 173–186. https://doi.org/10.3354/meps08336

Bresciani, M., Adamo, M., De Carolis, G., Matta, E., Pasquariello, G., Vaičiute, D. & Giardino, C. (2014). Monitoring blooms and surface accumulation of cyanobacteria in the Curonian Lagoon by combining MERIS and ASAR data. *Remote Sensing of Environment*, *146*, 124–135. https://doi.org/10.1016/j.rse.2013.07.040

Bresciani, M., Giardino, C., Stroppiana, D., Pilkaityte, R., Zilius, M., Bartoli, M. & Razinkovas, A. (2012). Retrospective analysis of spatial and temporal variability of chlorophyll-a in the Curonian Lagoon. *Journal of Coastal Conservation*, *16*(4), 511–519. https://doi.org/10.1007/s11852-012-0192-5

Breukelaar, A. W., Lammens, E., Breteler, J. & Tatrai, I. (1994). Effects of benthivorous bream (*Abramis brama*) and carp (*Cyprinus carpio*) on sediment resuspension

and concentrations of nutrients and chlorophyll a. *Freshwater Biology*, *32*(1), 113–121. https://doi.org/10.1111/j.1365-2427.1994.tb00871.x

Broman, E., Zilius, M., Samuiloviene, A., Vybernaite-lubiene, I., Politi, T., Klawonn, I., Voss, M., Nascimento, F. J. A. & Bonaglia, S. (2021). Active DNRA and denitrification in oxic hypereutrophic waters. *Water Research*, *194*, 116954. https://doi.org/10.1016/j.watres.2021.116954

Bruesewitz, D. A., Gardner, W. S., Mooney, R. F., Pollard, L. & Buskey, E. J. (2013). Estuarine ecosystem function response to flood and drought in a shallow, semi-arid estuary: nitrogen cycling and ecosystem metabolism. *Limnology and Oceanography*, *58*(6), 2293–2309. https://doi.org/10.4319/10.2013.58.6.2293

Brunet, R. C. & Garcia-Gil, L. J. (1996). Sulfide-induced dissimilatory nitrate reduction to ammonia in anaerobic freshwater sediments. *FEMS Microbiology Ecology*, *21*(2), 131–138. https://doi.org/10.1016/0168-6496(96)00051-7

Brunetti, M., Maugeri, M., Monti, F. & Nanni, T. (2006). Temperature and precipitation variability in Italy in the last two centuries from homogenised instrumental time series. *International Journal of Climatology*, *26*(3), 345–381. https://doi.org/10.1002/joc.1251

BSAP. (2007). *Baltic Sea Action Plan. Presented at HELCOM Ministerial Meeting.*

Bubinas, A. & Ložys, L. (2000). The nutrition of fish in the Curonian Lagoon and the coastal zone of the Baltic Sea. *Acta Zoologica Lituanica*, *10*(4), 56–67. https://doi.org/10.1080/13921657.2000.10512346

Bubinas, A. & Vaitonis, G. (2005). The structure and seasonal dynamics of zoobenthic communities in the northern and central parts of the Curonian Lagoon. *Acta Zoologica Lituanica*, *15*(4), 297–304. https://doi.org/10.1080/13921657.2005.10512694

Bukaveckas, P. A., Katarzyte, M., Schlegel, A., Spuriene, R., Egerton, T. & Vaiciute, D. (2019). Composition and settling properties of suspended particulate matter in estuaries of the Chesapeake Bay and Baltic Sea regions. *Journal of Soils and Sediments*, *19*(5), 2580–2593. https://doi.org/10.1007/s11368-018-02224-z

Bukaveckas, P. A., Olenina, I. & Pilkaityt, R. (2017). Microcystin in aquatic food webs of the Baltic and Chesapeake Bay regions. *Estuarine Coastal and Shelf Science*, *191*, 50–59. https://doi.org/10.1016/j.ecss.2017.04.016

Burgin, A. J. & Hamilton, S. K. (2007). Have we overemphasized the role of denitrification in aquatic ecosystems? A review of nitrate removal pathways. *Frontiers in Ecology and the Environment*, *5*(2), 89–96. https://doi.org/10.1890/1540-9295(2007)5[89:HWOTRO]2.0.CO;2

Burnham, K. P. & Anderson, D. R. (2002). Model selection and multimodel inference: A practical information-theoretic approach. https://doi.org/10.1016/b978-0-12-801370-0.00011-3

Cabrita, M. T. & Brotas, V. (2000). Seasonal variation in denitrification and dissolved nitrogen fluxes in intertidal sediments of the Tagus estuary, Portugal. *Marine Ecology Progress Series*, *202*, 51–65. https://doi.org/10.3354/meps202051

Caffrey, J. M., Bonaglia, S. & Conley, D. J. (2019). Short exposure to oxygen and sulfide alter nitrification, denitrification, and DNRA activity in seasonally hypoxic estuarine sediments. *FEMS Microbiology Letters*, *366*, 1–10. https://doi.org/10.1093/femsle/fny288

Cammen, L. M. (1980). Ingestion rate: an empirical model for aquatic deposit feeders and detritivores. *Oecologia*, *44*(3), 303–310.

Canfield, D. E. (1994). Factors influencing organic carbon preservation in marine sediments. *Chemical Geology*, *114*(3-4), 315–329. https://doi.org/10.1016/0009-2541(94)90061-2

Canfield, D. E., Kristensen, E. & Thamdrup, B. (2005). *Aquatic geomicrobiology*. Academic Press, New York.

Canfield, D. E., Thamdrup, B. & Hansen, J. W. (1993). The anaerobic degradation of organic matter in Danish coastal sediments: iron reduction, manganese reduction, and sulfate reduction. *Geochimica et Cosmochimica Acta*, *57*(16), 3867–3883. https://doi.org/10.1016/0016-7037(93)90340-3

Cardoso, P. G., Raffaelli, D., Lillebø, A. I., Verdelhos, T. & Pardal, M. A. (2008). The impact of extreme flooding events and anthropogenic stressors on the macrobenthic communities' dynamics. *Estuarine Coastal and Shelf Science*, *76*, 553–565. https://doi.org/10.1016/j.ecss.2007.07.026

Carpenter, S. R., Caraco, N. F., Correll, D. L., Howarth, R. W., Sharpley, A. N. & Smith, V. H. (1998). Non point pollution of surface waters with phosphorus and nitrogen. *Ecological Applications*, *8*(3), 559–568.

Carpenter, S. R., Booth, E. G. & Kucharik, C. J. (2018). Extreme precipitation and phosphorus loads from two agricultural watersheds. *Limnology and Oceanography*, *63*(3), 1221–1233. https://doi.org/10.1002/lno.10767

Carstensen, J., Conley, D. J., Almroth-Rosell, E., Asmala, E., Bonsdorff, E., Fleming-Lehtinen, V., Gustafsson, B. G., Gustafsson, C., Heiskanen, A.-s., Janas, U., Norkko, A., Slomp, C., Villnas, A., Voss, M. & Zilius, M. (2020). Factors regulating the coastal nutrient filter in the Baltic Sea. *Ambio*, *49*, 1194–1210. https://doi.org/10.1007/s13280-019-01282-y

Castaldelli, G., Soana, E., Racchetti, E., Pierobon, E., Mastrocicco, M., Tesini, E., Fano, E. A. & Bartoli, M. (2013). Nitrogen budget in a lowland coastal area within the Po River Basin (Northern Italy): multiple evidences of equilibrium between sources and internal sinks. *Environmental Management*, *52*(3), 567–580. https://doi.org/10.1007/s00267-013-0052-6

Castaldelli, G., Vincenzi, F., Fano, E. A. & Soana, E. (2020). In search for the missing nitrogen: closing the budget to assess the role of denitrification in agricultural watersheds. *Applied Sciences*, *10*(6). https://doi.org/10.3390/app10062136

Cattaneo, E., Zaldívar, J. M., Murray, C. N., Viaroli, P. & Giordani, G. (2001). Application of LOICZ methodology to a Mediterranean coastal lagoon: Sacca di Goro (Italy). *European Communities Report*.

Cerkasova, N. & Umgiesser, G. (2021). Modelling framework for flow, sediments and nutrient loads in a large transboundary river watershed: a climate change impact assessment of the Nemunas River watershed. *Journal of Hydrology*, *598*, 126422.

Chen, N., Krom, M. D., Wu, Y., Yu, D. & Hong, H. (2018). Storm induced estuarine turbidity maxima and controls on nutrient fluxes across river-estuary-coast continuum. *Science of the Total Environment*, *628-629*, 1108–1120. https://doi.org/10.1016/j.scitotenv.2018.02.060

Christensen, V., Walters, C. J. & Pauly, D. (2005). *Ecopath with Ecosim: a user's guide*. Fisheries Centre, University of British Columbia.

Christian, R. R., Camacho-Ibar, V. F., Piehler, M. F. & Smyth, a. R. (2012). Understanding the nitrogen cycle through Network Models in coastal ecosystems. *Treatise on estuarine and coastal science* (pp. 383–396). Elsevier Inc. https://doi.org/10.1016/B978-0-12-374711-2.00916-5

Christian, R. R. & Thomas, C. R. (2003). Network analysis of nitrogen inputs and cycling in the Neuse River Estuary, North Carolina, USA. *Estuaries*, *26*(3), 815–828.

Christian, R. R., Forés, E., Comin, F., Viaroli, P., Naldi, M. & Ferrari, I. (1996). Nitrogen cycling networks of coastal ecosystems: influence of trophic status and primary producer form. *Ecological Modelling*, *87*(1-3), 111–129. https://doi.org/10.1016/0304-3800(95)00019-4

Christian, R. R., Voss, C. M., Bondavalli, C., Viaroli, P., Naldi, M., Tyler, A. C., Anderson, I. C., McGlathery, K. J., Ulanowicz, R. E. & Camacho-Ibar, V. (2010). Ecosystem health indexed through networks of nitrogen cycling. *Coastal Lagoons: Critical Habitats of Environmental Change*, 73–99. https://doi.org/10.1201/EBK1420088304

Cline, J. D. (1969). Spectrophotometric determination of hydrogen sulfide in natural waters. *Limnology and Oceanography*, *14*(3), 454–458. https://doi.org/https://doi.org/10.4319/lo.1969.14.3.0454

Cloern, J. E. (2001). Our evolving conceptual model of the coastal eutrophication problem. *Marine Ecology Progress Series*, *210*, 223–253. https://doi.org/10.3354/meps210223

Colman, A. S. & Holland, H. D. (2000). The global diagenetic flux of phosphorus from marine sediments to the oceans: redox sensitivity and the control of atmospheric oxygen levels. *Marine authigenesis: From global to microbial* (pp. 53–75). SEPM (Society for Sedimentary Geology), Tulsa.

Conley, D. J., Cartensen, J., Aertebjrg, G., Christensen, P. B., Dalsgaard, T., Hansen, J. L. S. & Josefson, A. B. (2007). Long-term changes and impacts of hypoxia in Danish Coastal Waters. *Ecological Applications*, *17*(5), 165–184. https://doi.org/10.1890/05-0766.1

Conley, D. J., Quigley, M. A. & Schelske, C. L. (1988). Silica and phosphorus flux from sediments: importance of internal recycling in Lake Michigan. *Canadian Journal of Fisheries and Aquatic Sciences*, *45*, 1030–1035. https://doi.org/10.1139/f88-126

Coppola, E. & Giorgi, F. (2010). An assessment of temperature and precipitation change projections over Italy from recent globaland regional climate model simulations. *International Journal of Climatology*, *30*, 11–32. https://doi.org/10.1002/joc

Coppola, E., Verdecchia, M., Giorgi, F., Colaiuda, V., Tomassetti, B. & Lombardi, A. (2014). Changing hydrological conditions in the Po basin under global warming. *Science of the Total Environment*, *493*, 1183–1196. https://doi.org/10.1016/j.scitotenv.2014.03.003

Corbau, C., Munari, C., Mistri, M., Lovo, S. & Simeoni, U. (2016). Application of the Principles of ICZM for Restoring the Goro Lagoon. *Coastal Management*, *44*(4), 350–365. https://doi.org/10.1080/08920753.2016.1155040

Cornwell, J. C., Kemp, W. M. & Kana, T. M. (1999). Denitrification in coastal ecosystems: Methods, environmental controls, and ecosystem level controls, a review. *Aquatic Ecology*, *33*(1), 41–54. https://doi.org/10.1023/A:1009921414151

Correll, D. L., Jordan, T. E. & Weller, D. E. (1999). Transport of nitrogen and phosphorus from Rhode River watersheds during storm events. *Water Resources Research*, *35*(8), 2513–2521. https://doi.org/10.1029/1999WR900058

Costa, J. L., Assis, C. A., Almeida, P. R., Moreira, F. M. & Costa, M. J. (1992). On the food of the European eel, *Anguilla anguilla* (L.), in the upper zone of the Tagus estuary, Portugal. *Journal of Fish Biology*, *41*(5), 841–850. https://doi.org/10.1111/j.1095-8649.1992.tb02712.x

Cozzi, S. & Giani, M. (2011). River water and nutrient discharges in the Northern Adriatic Sea: current importance and long term changes. *Continental Shelf Research*, *31*(18), 1881–1893. https://doi.org/10.1016/j.csr.2011.08.010

Czamanski, M., Nugraha, A., Pondaven, P., Lasbleiz, M., Masson, A., Caroff, N., Bellail, R. & Tréguer, P. (2011). Carbon, nitrogen and phosphorus elemental stoichiometry in aquacultured and wild-caught fish and consequences for pelagic nutrient dynamics. *Marine Biology*, *158*(12), 2847–2862. https://doi.org/10.1007/s00227-011-1783-7

Dailidiene, I., Baudler, H., Chubarenko, B. & Navrotskaya, S. (2011). Long term water level and surface temperature changes in the lagoons of the southern and eastern Baltic. *Oceanologia*, *53*(1), 293–308. https://doi.org/10.5697/oc.53-1-TI.293

Dalsgaard, T., Nielsen, L. P., Brotas, V., Viaroli, P., Underwood, G. J. C., Nedwell, D. B., Sundbäck, K., Rysgaard, S., Miles, A., Bartoli, M., Dong, L., Thornton, D. C. O., Ottosen, L. D. M., Castaldelli, G. & Risgaard-Petersen, N. (2000). *Protocol handbook for NICE-Nitrogen Cycling in Estuaries: a project under the EU research programme: Marine Science and Technology (MAST III)*. Ministry of Environment; Energy National Environmental Research Institute, Denmark© Department of Lake; Estuarine Ecology.

Daunys, D. (2001). Patterns of bottom macrofauna variability and its role in the shallow coastal lagoon - Ph.D. Thesis Summary.

De Backer, A. D., Coillie, F. V., Provoost, P., Colen, C. V., Vincx, M. & Degraer, S. (2011). Bioturbation effects of *Corophium volutator*: importance of density and

behavioural activity. *Estuarine, Coastal and Shelf Science*, *91*(2), 306–313. https://doi.org/10.1016/j.ecss.2010.10.031

de la Vega, C., Horn, S., Baird, D., Hines, D., Borrett, S., Jensen, L. F., Schwemmer, P., Asmus, R., Siebert, U. & Asmus, H. (2018). Seasonal dynamics and functioning of the Sylt-Rømø Bight, northern Wadden Sea. *Estuarine, Coastal and Shelf Science*, *203*, 100–118. https://doi.org/10.1016/j.ecss.2018.01.021

de la Vega, C., Schückel, U., Horn, S., Kröncke, I., Asmus, R. & Asmus, H. (2018). How to include ecological network analysis results in management? A case study of three tidal basins of the Wadden Sea, south-eastern North Sea. *Ocean and Coastal Management*, *163*(May), 401–416. https://doi.org/10.1016/j.ocecoaman.2018.07.019

De Vicente, I., Amores, V., Guerrero, F. & Cruz-Pizarro, L. (2010). Contrasting factors controlling microbial respiratory activity in the sediment of two adjacent Mediterranean wetlands. *Naturwissenschaften*, *97*(7), 627–635. https://doi.org/10.1007/s00114-010-0678-7

Demars, B. O. L. & Edwards, A. C. (2007). Tissue nutrient concentrations in freshwater aquatic macrophytes: high inter-taxon differences and low phenotypic response to nutrient supply. *Freshwater Biology*, *52*, 2073–2086. https://doi.org/10.1111/j.1365-2427.2007.01817.x

Demars, B. O. L. & Edwards, A. C. (2008). Tissue nutrient concentrations in aquatic macrophytes: comparison across biophysical zones, surface water habitats and plant life forms. *Chemistry and Ecology*, *24*(6), 412–422. https://doi.org/10.1080/02757540802534533

Dettmann, E. H. (2001). Effect of water residence time on annual export and denitrification of nitrogen in estuaries: a model analysis. *Estuaries*, *24*(4), 481–490. https://doi.org/10.2307/1353250

Diaz, R. J. & Rosenberg, R. (1995). Marine benthic hypoxia: a review of its ecological effects and the behavioural responses of benthic macrofauna. *Oceanography and Marine Biology: an annual review*, *33*, 245–303. https://doi.org/10.1016/S0022-0981(01)00355-0

Diaz, R. J. & Rosenberg, R. (2008). Spreading dead zones and consequences for marine ecosystems. *Science*, *321*, 926–929. https://doi.org/10.1126/science.1156401

Ding, S., Chen, M., Gong, M., Fan, X., Qin, B., Xu, H., Gao, S. S., Jin, Z., Tsang, D. C. & Zhang, C. (2018). Internal phosphorus loading from sediments causes seasonal nitrogen limitation for harmful algal blooms. *Science of the Total Environment*, *625*, 872–884. https://doi.org/10.1016/j.scitotenv.2017.12.348

Dixit, S. & Van Cappellen, P. (2002). Surface chemistry and reactivity of biogenic silica. *Geochimica et Cosmochimica Acta*, *66*(14), 2559–2568. https://doi.org/10.1016/S0016-7037(02)00854-2

Dmitrieva, O. A. & Semenova, A. S. (2012). Seasonal dynamics of phyto- and zooplankton and their interactions in the hypereutrophic reservoir. *Inland Water Biology*, *4*(3), 308–315. https://doi.org/10.1134/s1995082911030059

Dodson, S. (1990). Predicting diel vertical migration of zooplankton. *Limnology and Oceanography*, *35*(5), 1195–1200. https://doi.org/10.4319/lo.1990.35.5.1195

Dolman, A. M., Rücker, J., Pick, F. R., Fastner, J., Rohrlack, T., Mischke, U. & Wiedner, C. (2012). Cyanobacteria and cyanotoxins: the influence of nitrogen versus phosphorus. *PLoS ONE*, *7*(6). https://doi.org/10.1371/journal.pone.0038757

Dong, L. F., Thornton, D. C., Nedwell, D. B. & Underwood, G. J. (2000). Denitrification in sediments of the River Colne estuary, England. *Marine Ecology Progress Series*, *203*, 109–122. https://doi.org/10.3354/meps203109

Du, J., Shen, J., Park, K., Wang, Y. P. & Yu, X. (2018). Worsened physical condition due to climate change contributes to the increasing hypoxia in Chesapeake Bay. *Science of the Total Environment*, *630*, 707–717. https://doi.org/10.1016/j.scitotenv.2018.02.265

Duarte, C. M. (1992). Nutrient concentration of aquatic plants: patterns across species. *Limnology*, *37*(4), 882–889.

Duarte, C. M. (2009). Coastal eutrophication research: A new awareness. *Hydrobiologia*, *629*(1), 263–269. https://doi.org/10.1007/s10750-009-9795-8

Duarte, C. M., Conley, D. J., Carstensen, J. & Sánchez-Camacho, M. (2009). Return to neverland: shifting baselines affect eutrophication restoration targets. *Estuaries and Coasts*, *32*(1), 29–36. https://doi.org/10.1007/s12237-008-9111-2

Dunning, J. B. (2008). *CRC Hanbook of avian body masses Second Edition*. CRC Press: Boca Raton.

Egertson, C. J., Kopaska, J. A. & Downing, J. A. (2004). A century of change in macrophyte abundance and composition in response to agricultural eutrophication. *Hydrobiologia*, *524*(1), 145–156. https://doi.org/10.1023/B:HYDR.0000036129.40386.ce

Ejsmont-Karabin, J. (1984). Phosphorus and nitrogen excretion by lake zooplankton (rotifers and crustaceans) in relationship to individual body weights of the animals, ambient temperature and presence or absence of food. *Ekologia Polska*, *32*(1), 3–42.

Ellis, J., Cummings, V., Hewitt, J., Thrush, S. & Norkko, A. (2002). Determining effects of suspended sediment on condition of a suspension feeding bivalve (*Atrina zelandica*): results of a survey, a laboratory experiment and a field transplant experiment. *Journal of Experimental Marine Biology and Ecology*, *267*, 147–174.

Engström, P., Dalsgaard, T., Hulth, S. & Caller, R. C. (2005). Anaerobic ammonium oxidation by nitrite (anammox): implications for N_2 production in coastal marine sediments. *Geochimica et Cosmochimica Acta*, *69*(8), 2057–2065. https://doi.org/10.1016/j.gca.2004.09.032

Eyre, B. D. & Ferguson, A. J. P. (2009). Denitrification efficiency for defining critical loads of carbon in shallow coastal ecosystems. *Hydrobiologia*, *629*, 137–146. https://doi.org/10.1007/s10750-009-9765-1

FAOSTAT. (2005). *Statistical database of the Food and Agricultural Organization of the United Nations*.

Fath, B. D. & Patten, B. C. (1999). Review of the Foundations of Network Environ Analysis. *Ecosystems*, *2*, 167–179.

Fath, B. D., Scharler, U. M., Ulanowicz, R. E. & Hannon, B. (2007). Ecological network analysis: network construction. *Ecological Modelling*, *208*(1), 49–55. https://doi.org/10.1016/j.ecolmodel.2007.04.029

Ferrarin, C., Razinkovas, A., Gulbinskas, S., Umgiesser, G. & Bliudžiute, L. (2008). Hydraulic regime-based zonation scheme of the Curonian Lagoon. *Hydrobiologia*, *611*(1), 133–146. https://doi.org/10.1007/s10750-008-9454-5

Ferrarin, C., Bajo, M., Bellafiore, D., Cucco, A., Pascalis, F. D., Ghezzo, M. & Umgiesser, G. (2014). Toward homogenization of Mediterranean lagoons and their loss of hydrodiversity. *Geophysical Research Letters*, *41*, 5935–5941. https://doi.org/10.1002/2014GL060843

Ferro, I., Van Nugteren, P., Middelburg, J. J., Herman, P. M. & Heip, C. H. (2003). Effect of macrofauna, oxygen exchange and particle reworking on iron and manganese sediment biogeochemistry: a laboratory experiment. *Vie et Milieu/Life & Environment, Observatoire Oceanologique*, *53*(4), 211–220.

Feyen, L. & Dankers, R. (2009). Impact of global warming on streamflow drought in Europe. *Journal of Geophysical Research*, *114*(17), 1–17. https://doi.org/10.1029/2008JD011438

Fieszl, J., Bogacka-Kapusta, E., Kapusta, A., Szymańska, U. & Martyniak, A. (2011). Feeding ecology of sterlet *Acipenser ruthenus* L. in the Hungarian section of the Danube River. *Archives of Polish Fisheries*, *19*(2), 105–111. https://doi.org/10.2478/v10086-011-0012-9

Filippelli, G. M. (2008). The global phosphorus cycle: past, present, and future. *Elements*, *4*(2), 89–95. https://doi.org/10.2113/GSELEMENTS.4.2.89

Finn, J. T. (1976). Measures of ecosystem structure and function derived from analysis of flows. *Journal of Theoretical Biology*, *56*(2), 363–380. https://doi.org/10.1016/S0022-5193(76)80080-X

Finn, J. T. (1980). Flow analysis of models of the Hubbard Brook ecosystem. *Ecology*, *61*(3), 562–571. http://www.jstor.org/stable/1937422

Finn, J. T. & Leschine, T. M. (1980). Does salt marsh fertilization enhance shellfish production? An application of Flow Analysis. *Environmental Management*, *4*(3), 193–203.

Fisher, T. R., Carlson, P. R. & Barber, R. T. (1982). Sediment nutrient regeneration in three North Carolina estuaries. *Estuarine, Coastal and Shelf Science*, *14*(1), 101–116. https://doi.org/10.1016/S0302-3524(82)80069-8

Friedl, G., Dinkel, C. & Wehrli, B. (1998). Benthic fluxes of nutrients in the northwestern Black Sea. *Marine Chemistry*, *62*(1-2), 77–88. https://doi.org/10.1016/S0304-4203(98)00029-2

Gallagher, C. P. & Dick, T. A. (2015). Winter feeding ecology and the importance of cannibalism in juvenile and adult burbot (*Lota lota*) from the Mackenzie Delta, Canada. *Hydrobiologia*, *757*(1), 73–88. https://doi.org/10.1007/s10750-015-2227-z

Galloway, J. N., Dentener, F. J., Capone, D. G., Boyer, E. W., Howarth, R. W., Seitzinger, S. P., Asner, G. P., Cleveland, C. C., Green, P. A., Holland, E. A., Karl, D. M., Michaels, A. F., Porter, J. H., Townsend, A. R. & Vo, C. J. (2004). Nitrogen cycles: past, present, and future. *Biogeochemistry*, *70*, 153–226.

Galloway, J. N., Townsend, A. R., Erisman, J. W., Bekunda, M., Cai, Z., Freney, J. R., Martinelli, L. A., Seitzinger, S. P. & Sutton, M. A. (2008). Transformation of the nitrogen cycle: recent trends, questions, and potential solutions. *Science*, *320*, 889–892.

Gameiro, C., Cartaxana, P., Cabrita, M. T. & Brotas, V. (2004). Variability in chlorophyll and phytoplankton composition in an estuarine system. *Hydrobiologia*, *525*(1-3), 113–124. https://doi.org/10.1023/B:HYDR.0000038858.29164.31

Gao, Y., Zhu, B., Yu, G., Chen, W., He, N., Wang, T. & Miao, C. (2014). Coupled effects of biogeochemical and hydrological processes on C, N, and P export during extreme rainfall events in a purple soil watershed in southwestern China. *Journal of Hydrology*, *511*, 692–702. https://doi.org/10.1016/j.jhydrol.2014.02.005

García-Oliva, M., Marcos, C., Umgiesser, G., Mckiver, W., Ghezzo, M., Pascalis, F. D. & Pérez-ruzafa, A. (2019). Modelling the impact of dredging inlets on the salinity and temperature regimes in coastal lagoons. *Ocean and Coastal Management*, *180*, 104913. https://doi.org/10.1016/j.ocecoaman.2019.104913

García-Oliva, M., Perez-Ruzafa, A., Umgiesser, G., Mckiver, W., Ghezzo, M., De Pascalis, F. & Marcos, C. (2018). Assessing the hydrodynamic response of the Mar Menor Lagoon to dredging inlets interventions through numerical modelling. *Water*, *10*, 959. https://doi.org/10.3390/w10070959

Garcia-Ruiz, R., Patttinson, S. N. & Whitton, B. A. (1998). Kinetic parameters of denitrification in a river continuum. *Applied and Environmental Microbiology*, *64*(7), 2533–2538.

Gardner, W. S. & McCarthy, M. J. (2009). Nitrogen dynamics at the sediment-water interface in shallow, sub-tropical Florida Bay: why denitrification efficiency may decrease with increased eutrophication. *Biogeochemistry*, *95*(2), 185–198. https://doi.org/10.1007/s10533-009-9329-5

Gardner, W. S., McCarthy, M. J., An, S., Sobolev, D., Sell, K. S. & Brock, D. (2006). Nitrogen fixation and dissimilatory nitrate reduction to ammonium (DNRA) support nitrogen dynamics in Texas estuaries. *Limnology and Oceanography*, *51*(1), 558–568. https://doi.org/10.4319/lo.2006.51.1_part_2.0558

Gasiunaite, Z. R. & Razinkovas-Baziukas, A. (2004). Temporal and spatial patterns of crustacean zooplankton dynamics in a transitional lagoon ecosystem. *Hydrobiologia*, *514*, 139–149.

Gasiūnaitė, Z. R., Daunys, D., Olenin, S. & Razinkovas-Baziukas, A. (2006). The Curonian Lagoon. In U. Schiewer (Ed.), *Ecology of baltic coastal waters*. Springer Heidelberg.

Gasiūnaitė, Z. R., Razinkovas-baziukas, A., Grinienė, E., Gulbinskas, S., Pilkaitytė, R. & Žaromskis, R. (2012). Pelagic patterns along the Nemunas River–Curonian

Lagoon transition, south–eastern Baltic Sea. *Baltica*, *25*(1), 77–86. https://doi.org/10.5200/baltica.2012.25.07

Ger, K. A., Urrutia-cordero, P., Frost, P. C., Hansson, L.-a., Sarnelle, O., Wilson, A. E. & Lu, M. (2016). The interaction between cyanobacteria and zooplankton in a more eutrophic world. *Harmful Algae*, *54*, 128–144. https://doi.org/10.1016/j.hal.2015.12.005

Gergs, R., Rinke, K. & Rothhaupt, K. O. (2009). Zebra mussels mediate benthic – pelagic coupling by biodeposition and changing detrital stoichiometry. *Freshwater Biology*, 1379–1391. https://doi.org/10.1111/j.1365-2427.2009.02188.x

Ghaisas, N. A., Maiti, K. & White, J. R. (2019). Coupled iron and phosphorus release from seasonally hypoxic Louisiana shelf sediment. *Estuarine, Coastal and Shelf Science*, *219*, 81–89. https://doi.org/10.1016/j.ecss.2019.01.019

Giblin, A. E., Weston, N. B., Banta, G. T., Tucker, J. & Hopkinson, C. S. (2010). The effects of salinity on nitrogen losses from an oligohaline estuarine sediment. *Estuaries and Coasts*, *33*, 1054–1068. https://doi.org/10.1007/s12237-010-9280-7

Gilbert, A. T. & Servello, F. A. (2005). Insectivory versus piscivory in Black Terns: implications for food provisioning and growth of chicks. *Waterbirds*, *28*(4), 436–444. https://doi.org/https://doi.org/10.1675/1524-4695(2005)28[436:IVPIBT]2.0.CO;2

Giordani, G., Azzoni, R., Bartoli, M. & Viaroli, P. (1997). Seasonla variations of sulphate reduction rates, sulphur pools and iron availability in the sediment of a dystrophic lagoon (Sacca di Goro, Italy). *Water, Air and Soil Pollution*, *99*, 363–371.

Giordani, G., Bartoli, M., Cattadori, M. & Viaroli, P. (1996). Sulphide release from anoxic sediments in relation to iron availability and organic matter recalcitrance and its effects on inorganic phosphorus recycling. *Hydrobiologia*, *329*(1-3), 211–222. https://doi.org/10.1007/BF00034559

Glibert, P. M. (2012). Ecological stoichiometry and its implications for aquatic ecosystem sustainability. *Current Opinion in Environmental Sustainability*, *4*(3), 272–277. https://doi.org/10.1016/j.cosust.2012.05.009

Glibert, P. M. (2017). Eutrophication, harmful algae and biodiversity - Challenging paradigms in a world of complex nutrient changes. *Marine Pollution Bulletin*, *124*(2), 591–606. https://doi.org/10.1016/j.marpolbul.2017.04.027

Glud, R. N. (2008). Oxygen dynamics of marine sediments. *Marine Biology Research*, *4*, 243–289. https://doi.org/10.1080/17451000801888726

Goc, M., Iliszko, L. & Stempniewicz, L. (2005). The largest European colony of the Great Cormorant on the Vistula Spit (N Poland) - an impact on the forest ecosystem. *Ecological Questions*, *6*, 93–103.

Golterman, H., Clymo, L. & Ohnstand, M. (1978). Methods for physical anc chemical analysis of freshwaters. In I.B.P. (Ed.), *Handbook nr. 8* (Blackwell).

Gómez, R., Arce, I. M., Sánchez, J. J. & del Mar Sánchez-Montoya, M. (2012). The effects of drying on sediment nitrogen content in a Mediterranean intermittent stream: a microcosms study. *Hydrobiologia*, *679*(1), 43–59. https://doi.org/10.1007/s10750-011-0854-6

Grasshoff, K., Kremling, K. & Ehrhardt, M. (1983). *Methods of seawater analysis*. Chemie: Verlag.

Grinienė, E., Šulčius, S. & Kuosa, H. (2016). Size-selective microzooplankton grazing on the phytoplankton in the Curonian Lagoon (SE Baltic Sea). *Oceanologia*, *58*(4), 292–301. https://doi.org/10.1016/j.oceano.2016.05.002

Gwiazda, R., Jarocha, K. & Szarek-Gwiazda, E. (2010). Impact of a small cormorant (*Phalacrocorax carbo sinensis*) roost on nutrients and phytoplankton assemblages in the littoral regions of a submontane reservoir. *Biologia*, *65*(4), 742–748. https://doi.org/10.2478/s11756-010-0072-0

Hahn, S., Bauer, S. & Klaassen, M. (2007). Estimating the contribution of carnivorous waterbirds to nutrient loading in freshwater habitats. *Freshwater Biology*, *52*(12), 2421–2433. https://doi.org/10.1111/j.1365-2427.2007.01838.x

Hallett, C. S., Hobday, A. J., Tweedley, J. R., Thompson, P. A., McMahon, K. & Valesini, F. J. (2018). Observed and predicted impacts of climate change on the estuaries of south-western Australia, a Mediterranean climate region. *Regional Environmental Change*, *18*(5), 1357–1373. https://doi.org/10.1007/s10113-017-1264-8

Han, H. & Allan, J. D. (2012). Uneven rise in N inputs to the Lake Michigan Basin over the 20th century corresponds to agricultural and societal transitions. *Biogeochemistry*, *109*(1-3), 175–187. https://doi.org/10.1007/s10533-011-9618-7

Hannon, B. (1973). The structure of ecosystems. *J. theor. Biol.*, *41*(41), 535–546. https://doi.org/10.1016/0022-5193(73)90060-X

Hansen, B., Thorling, L., Schullehner, J. & Termansen, M. (2017). Groundwater nitrate response to sustainable nitrogen management. *Scientific Reports*, *7*(1), 1–12. https://doi.org/10.1038/s41598-017-07147-2

Harrison, J. A., Caraco, N. & Seitzinger, S. P. (2005). Global patterns and sources of dissolved organic matter export to the coastal zone: results from a spatially explicit, global model. *Global Biogeochemical Cycles*, *19*(4). https://doi.org/10.1029/2005GB002480

Hatano, T., Murakami, K., Ishii, H., Kadowaki, A., Kuwae, T. & Nakase, K. (2013). Characteristic of nitrogen and phosphorus budgets at a tidal flat in Tokyo Port Wild Bird Park. *Journal of JSCE*, *1*, 145–161. https://doi.org/10.2208/jscejb.66.419

Herbert, R. A. (1999). Nitrogen cycling in coastal marine ecosystems. *FEMS Microbiology Reviews*, *23*(5), 563–590. https://doi.org/10.1016/S0168-6445(99)00022-4

Heymans, J. J., Coll, M., Libralato, S., Morissette, L. & Christensen, V. (2014). Global patterns in ecological indicators of marine food webs: a modelling approach. *PLoS ONE*, *9*(4). https://doi.org/10.1371/journal.pone.0095845

Hietanen, S. & Lukkari, K. (2007). Effects of short-term anoxia on benthic denitrification, nutrient fluxes and phosphorus forms in coastal Baltic sediment. *Aquatic Microbial Ecology*, *49*(3), 293–302. https://doi.org/10.3354/ame01146

Hines, D. E., Lisa, J. a., Song, B., Tobias, C. R. & Borrett, S. R. (2012). A network model shows the importance of coupled processes in the microbial N cycle in

the Cape Fear River Estuary. *Estuarine, Coastal and Shelf Science*, *106*, 45–57. https://doi.org/10.1016/j.ecss.2012.04.018

Hines, D. E., Ray, S. & Borrett, S. R. (2018). Uncertainty analyses for Ecological Network Analysis enable stronger inferences. *Environmental Modelling and Software*, *101*, 117–127. https://doi.org/10.1016/j.envsoft.2017.12.011

Hölker, F., Vanni, M. J., Kuiper, J. J., Christof, M., Grossart, H.-P., Stief, P., Adrian, R., Lorke, A., Dellwig, O., Brand, A., Hupfer, M., Mooij, W. M., Nutzmann, G. & Lewandowski, J. (2015). Tube-dwelling invertebrates: tiny ecosystem engineers have large effects in lake ecosystems. *Ecological Monographs*, *85*(3), 333–351.

Howarth, R. W., Swaney, D. P., Boyer, E. W., Marino, R., Jaworski, N. & Goodale, C. (2006). The influence of climate on average nitrogen export from large watersheds in the Northeastern United States. *Biogeochemistry*, *79*(1-2), 163–186. https://doi.org/10.1007/s10533-006-9010-1

Howarth, R. W., Swaney, D. P., Buthler, T. J. & Marino, R. (2000). Climatic control on eutrophication of the Hudson River estuary. *Ecosystems*, *3*(2), 210–215. https://doi.org/10.1007/s100210000020

Howarth, R. W., Swaney, D., Billen, G., Garnier, J., Hong, B., Humborg, C., Johnes, P., Mörth, C. M. & Marino, R. (2012). Nitrogen fluxes from the landscape are controlled by net anthropogenic nitrogen inputs and by climate. *Frontiers in Ecology and the Environment*, *10*(1), 37–43. https://doi.org/10.1890/100178

Idzelyte, R., Kozlov, I. E. & Umgiesser, G. (2019). Remote sensing of ice phenology and dynamics of Europe' s largest coastal lagoon (the Curonian Lagoon). *Remote Sensing*, *11*(17), 2059.

IPCC. (2021). *IPCC, 2021: Climate Change 2021: The Physical Science Basis. Contribution of Working Group I to the Sixth Assessment Report of the Intergovernmental Panel on Climate Change*. Cambridge University Press.

Jacobson, P., Bergström, U. & Eklöf, J. (2019). Size-dependent diet composition and feeding of eurasian perch (*Perca fluviatilis*) and northern pike (*Esox lucius*) in the Baltic Sea. *Boreal Environment Research*, *24*, 137–153.

Jensen, H. S., Mortensen, P. B., Andersen, F. 0., Rasmussen, E. & Jensen, A. (1995). Phosphorus cycling in a coastal marine sediment, Aarhus Bay, Denmark. *Limnology and Oceanography*, *40*(5), 908–917. https://doi.org/10.4319/lo.1995.40.5.0908

Jiang, T., Yu, Z., Song, X., Cao, X. & Yuan, Y. (2010). Long-term ecological interactions between nutrient and phytoplankton community in the Changjiang estuary. *Chinese Journal of Oceanology and Limnology*, *28*(4), 887–898. https://doi.org/10.1007/s00343-010-9059-5

Jickells, T. D. & Weston, K. (2012). *Nitrogen Cycle - External Cycling: Losses and Gains* (Vol. 5). Elsevier Inc. https://doi.org/10.1016/B978-0-12-374711-2.00509-X

Jones, J. G. (1979). *A guide to methods for estimating microbial numbers and biomass in fresh water*. Scientific Publication N.39. Freshwater Biological Association.

Jorgensen, B. B. (1996). Material flux in the sediment. In B. B. Jorgensen & K. Richardson (Eds.), *Eutrophication in coastal marine ecosystems* (pp. 115–135). American Geophysical Union.

Jørgensen, B. B. & Nelson, D. C. (2004). Sulfide oxidation in marine sediments: Geochemistry meets microbiology. *Geological Society of America*, *379*, 63–81. https://doi.org/10.1130/0-8137-2379-5.63

Joye, S. B., Smith, S. V., Hollibaugh, J. T. & Paerl, H. W. (1996). Estimating denitrification rates in estuarine sediments: a comparison of stoichiometric and acetylene based methods. *Biogeochemistry*, *33*, 197–215.

Kahlert, M. (1998). C:N:P ratios of freshwater benthic algae. *Advances in Limnology*, *51*, 105–114.

Kallio-Nyberg, I., Saloniemi, I., Jutila, E. & Saura, A. (2007). Effects of marine conditions, fishing, and smolt traits on the survival of tagged, hatchery-reared sea trout (*Salmo trutta trutta*) in the Baltic Sea. *Canadian Journal of Fisheries and Aquatic Sciences*, *64*(9), 1183–1198. https://doi.org/10.1139/F07-084

Kana, T. M., Darkangelo, C., Hunt, M. D., Oldham, J. B., Bennett, G. E. & Cornwell, J. C. (1994). Membrane Inlet Mass Spectometer for rapid high-precision determination of N_2, O_2, and Ar in environment water samples. *Analytical Chemistry*, *66*, 4166–4170.

Karlson, K., Bonsdorff, E. & Rosenberg, R. (2007). The Impact of Benthic Macrofauna for Nutrient Fluxes from Baltic Sea Sediments. *Ambio*, *36*(2), 161–167.

Karpowicz, M., Zielin, P., Joanna, J. E.-k. & Irina, K. (2020). Effect of eutrophication and humification on nutrient cycles and transfer efficiency of matter in freshwater food webs. *Hydrobiologia*, *5*, 2521–2540. https://doi.org/10.1007/s10750-020-04271-5

Kaufman, A. G. & Borrett, S. R. (2010). Ecosystem network analysis indicators are generally robust to parameter uncertainty in a phosphorus model of Lake Sidney Lanier, USA. *Ecological Modelling*, *221*(8), 1230–1238. https://doi.org/10.1016/j.ecolmodel.2009.12.018

Kauppi, L., Bernard, G., Bastrop, R., Norkko, A. & Norkko, J. (2018). Increasing densities of an invasive polychaete enhance bioturbation with variable effects on solute fluxes. *Scientific Reports*, *65*, 1–12. https://doi.org/10.1038/s41598-018-25989-2

Kay, J. J., Graham, L. A. & Ulanowicz, R. E. (1989). A detaile guide to Network Analysis. In F. Wulff, J. G. Field & K. H. Mann (Eds.), *Network analysis in marine ecology: Methods and applications* (pp. 15–61). Springer, Berlin, Heidelberg.

Kelly, F. L. & King, J. J. (2001). A review of the ecology and distribution of three lamprey species, *Lampetra fluviatilis* (L.), *Lampetra planeri* (Bloch) and *Petromyzon marinus* (L.): a context for conservation and biodiversity considerations in Ireland. *Biology and Environment*, *101*(3), 165–185.

Kelly, P. T., Renwick, W. H., Knoll, L. & Vanni, M. J. (2019). Stream nitrogen and phosphorus loads are differentially affected by storm events and the difference may be exacerbated by conservation tillage. *Environmental Science and Technology*, *53*(10), 5613–5621. https://doi.org/10.1021/acs.est.8b05152

Kemp, W. M., Boynton, W. R., Adolf, J. E., Boesch, D. F., Boicourt, W. C., Brush, G., Cornwell, J. C., Fisher, T. R., Glibert, P. M., Hagy, J. D., Harding, L. W., Houde, E. D., Kimmel, D. G., Miller, W. D., Newell, R. I., Roman, M. R., Smith, E. M. & Stevenson, J. C. (2005). Eutrophication of Chesapeake Bay: historical trends and ecological interactions. *Marine Ecology Progress Series*, *303*, 1–29. https://doi.org/10.3354/meps303001

Kessler, A. J. (2018). Biogeochemical controls on the relative importance of denitrification and dissimilatory nitrate reduction to ammonium in estuaries. *Global Biogeochemical Cycles*, *1*, 1045–1057. https://doi.org/10.1029/2018GB005908

Klaus, V. H., Friedritz, L., Hamer, U. & Kleinebecker, T. (2020). Drought boosts risk of nitrate leaching from grassland fertilisation. *Science of the Total Environment*, *726*, 137877. https://doi.org/10.1016/j.scitotenv.2020.137877

Klausmeier, C. A., Litchman, E., Daufresne, T. & Levin, S. A. (2008). Phytoplankton stoichiometry. *Ecological Research*, *23*(3), 479–485. https://doi.org/10.1007/s11284-008-0470-8

Klausmeier, C. A., Litchman, E. & Levin, S. A. (2004). Phytoplankton growth and stoichiometry under multiple nutrient limitation. *Limnology and Oceanography*, *49*(4), 1463–1470. https://doi.org/10.4319/lo.2004.49.4_part_2.1463

Koli, L. & Soikkeli, M. (1974). Fish prey of breeding Caspian terns in Finland. *Finnish Zoological and Botanical Publishing Board*, *4*, 304–308.

Kotta, J., Torn, K., Paalme, T., Rätsep, M., Kaljurand, K., Teeveer, M. & Kotta, I. (2021). Scale-specific patterns of the production of the charophyte Chara aspera in the brackish Baltic Sea: linking individual and community production and biomass growth. *Frontiers in Marine Science*, *8*, 1–13. https://doi.org/10.3389/fmars.2021.674014

Krevs, A., Koreiviene, J., Paskauskas, R. & Sulijiene, R. (2007). Phytoplankton production and community respiration in different zones of the Curonian lagoon during the midsummer vegetation period. *Transitional Waters Bulletin*, *1*(1), 17–26. https://doi.org/10.1285/i1825229Xv1n1p17

Kristensen, E. & Kostka, J. E. (2005). Macrofaunal burrows and irrigation in marine sediment: microbiological and biogeochemical interactions. In K. J. Kristensen E, Haese RR (Ed.), *Interactions between macro- and microorganisms in marine sediments* (pp. 125–158). American Geophysical Union.

Kristensen, E. (2000). Organic matter diagenesis at the oxic/anoxic interface in coastal marine sediments, with emphasis on the role of burrowing animals. *Hydrobiologia*, *426*(1-3), 1–24. https://doi.org/10.1023/A:1003980226194

Krpo-Ćetković, J., Hegediš, A. & Lenhardt, M. (2010). Diet and growth of asp, *Aspius aspius* (Linnaeus, 1758), in the Danube River near the confluence with the Sava River (Serbia). *Journal of Applied Ichthyology*, *26*(4), 513–521. https://doi.org/10.1111/j.1439-0426.2010.01456.x

Kruopiene, J. (2007). Distribution of heavy metals in sediments of the Nemunas River (Lithuania). *Polish Journal of Environmental Studies*, *16*(5), 715–722.

Kubetzki, U. & Garthe, S. (2003). Distribution, diet and habitat selection by four sympatrically breeding gull species in the south-eastern North Sea. *Marine Biology*, *143*(1), 199–207. https://doi.org/10.1007/s00227-003-1036-5

Lamb, A. L., Wilson, G. P. & Leng, M. J. (2006). A review of coastal palaeoclimate and relative sea-level reconstructions using $\delta^1$3C and C/N ratios in organic material. *Earth-Science Reviews*, *75*, 29–57. https://doi.org/10.1016/j.earscirev.2005.10.003

Laverman, A. M., Cappellen, P. V., Rotterdam-los, D. V. & Abell, J. (2006). Potential rates and pathways of microbial nitrate reduction in coastal sediments. *FEMS Microbiology Ecology*, *58*, 179–192. https://doi.org/10.1111/j.1574-6941.2006.00155.x

Laverock, B., Gilbert, J. A., Tait, K., Osborn, A. M. & Widdicombe, S. (2011). Bioturbation: impact on the marine nitrogen cycle. *Biochemical Society Transactions*, *39*(1), 315–320. https://doi.org/10.1042/BST0390315

Lehner, B., Döll, P., Alcamo, J., Henrichs, T. & Kaspar, F. (2006). Estimating the impact of global change on flood and drought risks in Europe: a continental, integrated analysis. *Climatic Change*, *75*(3), 273–299. https://doi.org/10.1007/s10584-006-6338-4

Lemmetyinen, R. (1973). Feeding ecology of Sterna paradisaea Pontopp. and S. hirundo L. in the archipelago of southwestern Finland. *Annales Zoologici Fennici*, *10*(4), 507–525.

Lesutiene, J., Bukaveckas, P. A., Gasiunaite, Z. R., Pilkaityte, R. & Razinkovas-Baziukas, A. (2014). Tracing the isotopic signal of a cyanobacteria bloom through the food web of a Baltic Sea coastal lagoon. *Estuarine, Coastal and Shelf Science*, *138*, 47–56. https://doi.org/10.1016/j.ecss.2013.12.017

Lesutienė, J., Semenova, A., Grinienė, E., Gasiūnaitė, Z. R., Savickytė, V. & Dmitrieva, O. (2012). Abundance dynamics and functional role of predaceous *Leptodora kindtii* in the Curonian Lagoon. *Central European Journal of Biology*, *7*(1). https://doi.org/10.2478/s11535-011-0098-5

Lewandowski, J. & Hupfer, M. (2005). Effect of macrozoobenthos on two-dimensional small-scale heterogeneity of pore water phosphorus concentrations in lake sediments: a laboratory study. *Limnology and Oceanography*, *50*(4), 1106–1118.

Li, J. & Reardon, P. (2017). Water column particulate matter: A key contributor to phosphorus regeneration in a coastal eutrophic environment, the Chesapeake Bay. *Journal of Geophysical Research*, 737–752. https://doi.org/10.1002/2016JG003572

Li, S. (2006). *Ecology of Baltic Coastal Waters* (Vol. 131). Springer
Cap. 9: the Curonian Lagoon.

Lin, J. T. & Stewart, V. (1997). Nitrate assimilation by bacteria. *Advances in Microbial physiology*, *39*, 1–30.

Liu, M. (2006). Organic carbon and nitrogen stable isotopes in the intertidal sediments from the Yangtze Estuary , China. *Marine Pollution Bulletin*, *52*, 1625–1633. https://doi.org/10.1016/j.marpolbul.2006.06.008

Lloret, J., Marín, A. & Marín-Guirao, L. (2008). Is coastal lagoon eutrophication likely to be aggravated by global climate change? *Estuarine, Coastal and Shelf Science*, *78*(2), 403–412. https://doi.org/10.1016/j.ecss.2008.01.003

Lovley, D. R. & Phillips, E. J. (1987). Rapid assay for microbially reducible ferric iron in aquatic sediments. *Applied and Environmental Microbiology*, *53*(7), 1536–1540.

Luque-Almagro, V. M., Gates, A. J., Moreno-Vivián, C., Ferguson, S. J., Richardson, D. J. & Roldán, M. D. (2011). Bacterial nitrate assimilation: gene distribution and regulation. *Biochemical Society Transactions*, *39*(6), 1838–1843. https://doi.org/10.1042/BST20110688

Magni, P., Micheletti, S., Casu, D., Floris, A., Giordani, G., Petrov, A. N., Falco, G. D. & Castelli, A. (2005). Relationships between chemical characteristics of sediments and macrofaunal communities in the Cabras lagoon (Western Mediterranean, Italy). *Hydrobiologia*, *550*, 105–119. https://doi.org/10.1007/s10750-005-4367-z

Magri, M., Benelli, S., Bondavalli, C. & Bartoli, M. (2018). Benthic N pathways in illuminated and bioturbated sediments studied with network analysis. *Limnology and Oceanography*, *63*, S68–S84. https://doi.org/10.1002/lno.10724

Maicu, F., Alessandri, J., Pinardi, N., Verri, G., Umgiesser, G., Lovo, S., Turolla, S., Paccagnella, T. & Valentini, A. (2021). Downscaling with an unstructured coastal-ocean model to the Goro Lagoon and the Po River Delta branches. *Frontiers in Marine Science*, *8*, 647781. https://doi.org/10.3389/fmars.2021.647781

Malbrouck, C., Mergen, P. & Micha, J. C. (2006). Growth and diet of introduced coregonid fish *Coregonus peled* (Gmelin) and *Coregonus lavaretus* (L.) in two Belgian reservoir lakes. *Applied Ecology and Environmental Research*, *4*(1), 27–44. https://doi.org/10.15666/aeer/0401_027044

Marinov, D., Zaldívar, J. M., Norro, A., Giordani, G. & Viaroli, P. (2008). Integrated modelling in coastal lagoons: Sacca di Goro case study. *Hydrobiologia*, *611*(1), 147–165. https://doi.org/10.1007/s10750-008-9451-8

Marinov, D., Norro, A. & Zaldivar, J. M. (2006). Application of COHERENS model for hydrodynamic investigation of Sacca di Goro coastal lagoon (Italian Adriatic Sea shore). *Ecological Modelling*, *193*, 52–68. https://doi.org/10.1016/j.ecolmodel.2005.07.042

Marion, L., Clergeau, P., Brient, L. & Bertru, G. (1994). The importance of avian-contributed nitrogen (N) and phosphorus (P) to Lake Grand-Lieu, France. *Hydrobiologia*, *279-280*(1), 133–147. https://doi.org/10.1007/BF00027848

Marshall, E. & Randhir, T. (2008). Effect of climate change on watershed system: a regional analysis. *Climatic Change*, *89*, 263–280. https://doi.org/10.1007/s10584-007-9389-2

Marzocchi, U., Trojan, D., Larsen, S., Meyer, R. L., Revsbech, N. P., Schramm, A., Nielsen, L. P. & Risgaard-petersen, N. (2014). Electric coupling between distant nitrate reduction and sulfide oxidation in marine sediment. *The ISME Journal*, *8*(8), 1682–1690. https://doi.org/10.1038/ismej.2014.19

Mazzola, A. & Sarà, G. (2001). The effect of fish farming organic waste on food availability for bivalve molluscs (Gaeta Gulf, Central Tyrrhenian, MED): stable carbon isotopic analysis. *Aquaculture*, *192*, 361–379.

Mccarthy, M. J., Gardner, W. S., Lehmann, M. F. & Bird, D. F. (2013). Implications of water column ammonium uptake and regeneration for the nitrogen budget in temperate, eutrophic Missisquoi Bay, Lake Champlain (Canada/USA). *Hydrobiologia*, *718*, 173–188. https://doi.org/10.1007/s10750-013-1614-6

Mccarthy, M. J., Gardner, W. S., Lehmann, M. F., Guindon, A. & Bird, D. F. (2016). Benthic nitrogen regeneration, fixation, and denitrification in a temperate, eutrophic lake: effects on the nitrogen budget and cyanobacteria blooms. *Limnology and Oceanography*, *2*, 1406–1423. https://doi.org/10.1002/lno.10306

Mermillod-Blondin, F., Rosenberg, R., Francois-Carcaillet, F., Norling, K. & Mauclaire, L. (2004). Influence of bioturbation by three benthic infaunal species on microbial communities and biogeochemical processes in marine sediment. *Aquatic Microbial Ecology*, *36*, 271–284.

Milardi, M., Soana, E., Chapman, D., Fano, E. A. & Castaldelli, G. (2020). Could a freshwater fish be at the root of dystrophic crises in a coastal lagoon? *Science of the Total Environment*, *711*, 135093. https://doi.org/10.1016/j.scitotenv.2019.135093

Moraes, P. C., Zilius, M., Benelli, S. & Bartoli, M. (2018). Nitrification and denitrification in estuarine sediments with tube-dwelling benthic animals. *Hydrobiologia*, *819*(1), 217–230. https://doi.org/10.1007/s10750-018-3639-3

Morkune, R., Petkuviene, J., Bružas, M., Morkunas, J. & Bartoli, M. (2020). Monthly abundance patterns and the potential role of waterbirds as phosphorus sources to a hypertrophic baltic lagoon. *Water*, *12*(5). https://doi.org/10.3390/W12051392

Mulholland, P. J., Helton, A. M., Poole, G. C., Hall, R. O., Hamilton, S. K., Peterson, B. J., Tank, J. L., Ashkenas, L. R., Cooper, L. W., Dahm, C. N., Dodds, W. K., Findlay, S. E., Gregory, S. V., Grimm, N. B., Johnson, S. L., McDowell, W. H., Meyer, J. L., Valett, H. M., Webster, J. R., … Thomas, S. M. (2008). Stream denitrification across biomes and its response to anthropogenic nitrate loading. *Nature*, *452*, 202–205. https://doi.org/10.1038/nature06686

Murphy, A. E., Nizzoli, D., Bartoli, M., Smyth, A. R., Castaldelli, G. & Anderson, I. C. (2018). Variation in benthic metabolism and nitrogen cycling across clam aquaculture sites. *Marine Pollution Bulletin*, *127*, 524–535. https://doi.org/10.1016/j.marpolbul.2017.12.003

Murphy, A. E. & Reidenbach, M. A. (2016). Oxygen transport in periodically ventilated polychaete burrows. *Marine Biology*, *163*, 1–14. https://doi.org/10.1007/s00227-016-2983-y

Murray, R. E., Parsons, L. L. & Smith, M. S. (1989). Kinetics of nitrate utilization by mixed populations of denitrifying bacteria. *Applied and Environmental Microbiology*, *55*(3), 717–721.

Mußmann, M., Schulz, H. N., Strotmann, B., Kjær, T., Nielsen, L. P., Rosselló-Mora, R. A., Amann, R. I. & Jørgensen, B. B. (2003). Phylogeny and distribution of

nitrate-storing *Beggiatoa* spp. in coastal marine sediments. *Environmental Microbiology*, *5*(6), 523–533. https://doi.org/10.1046/j.1462-2920.2003.00440.x

Nagy, K. A. (2001). Food requirements of wild animals: predictive equations for free-living mammals, reptiles, and birds. *Nutrition Abstracts and Reviews*.

Najjar, R. G., Pyke, C. R., Beth, M., Breitburg, D., Hershner, C., Kemp, M., Howarth, R., Mulholland, M. R., Paolisso, M., Secor, D., Sellner, K., Wardrop, D. & Wood, R. (2010). Potential climate-change impacts on the Chesapeake Bay. *Estuarine, Coastal and Shelf Science*, *86*(1), 1–20. https://doi.org/10.1016/j.ecss.2009.09.026

Naldi, M., Nizzoli, D., Bartoli, M., Viaroli, P. & Viaroli, P. (2020). Effect of filter-feeding mollusks on growth of green macroalgae and nutrient cycling in a heavily exploited coastal lagoon. *Estuarine, Coastal and Shelf Science*, *239*, 106679. https://doi.org/10.1016/j.ecss.2020.106679

Naldi, M., Pierobon, E., Tornatore, F. & Viaroli, P. (2010). Relationships between flood events and formation and variability of nitrogen and phosphorus loads in the Po river. *Biologia Ambientale*, *24*(1), 59–69 (Italian).

Naldi, M. & Viaroli, P. (2002). Nitrate uptake and storage in the seaweed *Ulva rigida* C. Agardh in relation to nitrate availability and thallus nitrate content in a eutrophic coastal lagoon (Sacca di Goro, Po River Delta, Italy). *Journal of Experimental Marine Biology and Ecology*, *269*(1), 65–83. https://doi.org/10.1016/S0022-0981(01)00387-2

Neubacher, E. C., Parker, R. E. & Trimmer, M. (2011). Short-term hypoxia alters the balance of the nitrogen cycle in coastal sediments. *Limnology and Oceanography*, *56*(2), 651–665. https://doi.org/10.4319/lo.2011.56.2.0651

Newton, A., Icely, J., Cristina, S., Brito, A., Cardoso, A. C., Colijn, F., Riva, S. D., Gertz, F., Hansen, J. W., Holmer, M., Ivanova, K., Leppäkoski, E., Canu, D. M., Mocenni, C., Mudge, S., Murray, N., Pejrup, M., Razinkovas, A., Reizopoulou, S., ... Zaldívar, J. M. (2014). An overview of ecological status, vulnerability and future perspectives of European large shallow, semi-enclosed coastal systems, lagoons and transitional waters. *Estuarine, Coastal and Shelf Science*, *140*, 95–122. https://doi.org/10.1016/j.ecss.2013.05.023

Nielsen, L. P. (1992). Denitrification in sediment determined from nitrogen isotope pairing. *FEMS Microbiology Letters*, *86*(4), 357–362. https://doi.org/10.1111/j.1574-6968.1992.tb04828.x

Niemistö, J. & Lund-Hanses, L. C. (2019). Instantaneous effects of sediment resuspension on inorganic and organic benthic nutrient fluxes at a shallow water coastal site in the Gulf of Finland , Baltic Sea. *Estuaries and Coasts*, *42*, 2054–2071.

Nilsson, L. (2005). Wintering swans Cygnus spp. and Coot Fulica atra in the Öresund, South Sweden, in relation to available food recources. *Ornis Svecica*, *15*(1), 13–21.

Nixon, S. W., Ammerman, J. W., Atkinson, L. P., Berounsky, V. M., Billen, G., Boicourt, W. C., Boynton, W. R., Church, T. M., Ditoro, D. M., Pilson, M. E. Q. &

Seitzinger, S. P. (1996). The fate of nitrogen and phosphorus at the land-sea margin of the North Atlantic Ocean. *Biogeochemistry*, *35*, 141–180.

Nixon, S. W. (1995). Coastal marine eutrophication: a definition, social causes, and future concerns. *Ophelia*, *41*(1), 199–219. https://doi.org/10.1080/00785236.1995.10422044

Nixon, S. W. (2009). Eutrophication and the macroscope. *Hydrobiologia*, *629*(1), 5–19. https://doi.org/10.1007/s10750-009-9759-z

Nizzoli, D., Bartoli, M., Cooper, M., Welsh, D. T., Underwood, G. J. & Viaroli, P. (2007). Implications for oxygen, nutrient fluxes and denitrification rates during the early stage of sediment colonisation by the polychaete *Nereis* spp. in four estuaries. *Estuarine, Coastal and Shelf Science*, *75*(1-2), 125–134. https://doi.org/10.1016/j.ecss.2007.03.035

Nizzoli, D., Bartoli, M. & Viaroli, P. (2006). Nitrogen and phosphorous budgets during a farming cycle of the Manila clam *Ruditapes philippinarum*: an *in situ* experiment. *Aquaculture*, *261*(1), 98–108. https://doi.org/10.1016/j.aquaculture.2006.06.042

Nizzoli, D., Carraro, E., Nigro, V. & Viaroli, P. (2010). Effect of organic enrichment and thermal regime on denitrification and dissimilatory nitrate reduction to ammonium (DNRA) in hypolimnetic sediments of two lowland lakes. *Water Research*, *44*(9), 2715–2724. https://doi.org/10.1016/j.watres.2010.02.002

Nizzoli, D., Castaldelli, G., Bartoli, M., Welsh, D. T., Gomez, P. A., Fano, A. E. & Viaroli, P. (2002). Benthic fluxes of dissolved inorganic Nitrogen in a coastal lagoon of the Northern Adriatic Sea: an interpretation of spatial variability based on sediment features and infauna activity. *Marine Ecology*, *23*(SUPPL. 1), 297–306. https://doi.org/10.1111/j.1439-0485.2002.tb00028.x

Nizzoli, D., Welsh, D. T., Fano, E. A. & Viaroli, P. (2006). Impact of clam and mussel farming on benthic metabolism and nitrogen cycling, with emphasis on nitrate reduction pathways. *Marine Ecology Progress Series*, *315*, 151–165. https://doi.org/10.3354/meps315151

Nizzoli, D., Welsh, D. T. & Viaroli, P. (2011). Seasonal nitrogen and phosphorus dynamics during benthic clam and suspended mussel cultivation. *Marine Pollution Bulletin*, *62*(6), 1276–1287. https://doi.org/10.1016/j.marpolbul.2011.03.009

Nogaro, G. & Burgin, A. J. (2014). Influence of bioturbation on denitrification and dissimilatory nitrate reduction to ammonium (DNRA) in freshwater sediments. *Biogeochemistry*, *120*(1-3), 279–294. https://doi.org/10.1007/s10533-014-9995-9

Nõges, T., Luup, H. & Feldmann, T. (2010). Primary production of aquatic macrophytes and their epiphytes in two shallow lakes (Peipsi and Võrtsjärv) in Estonia. *Aquatic Ecology*, *44*(1), 83–92. https://doi.org/10.1007/s10452-009-9249-4

Odum, H. T. (1957). Trophic structure and productivity of Silver Springs, Florida. *Ecological Monographs*, *27*(1), 55–112.

Ogilvie, B., Nedwell, D. B., Harrison, R. M., Robinson, A. & Sage, A. (1997). High nitrate, muddy estuaries as nitrogen sinks: the nitrogen budget of the River Colne estuary (United Kingdom). *Marine Ecology Progress Series*, *150*, 217–228.

Paerl, H. W., Havens, K. E., Xu, H., Zhu, G., Mccarthy, M. J., Newell, S. E., Scott, J. T., Hall, N. S., Otten, T. G. & Qin, H. (2020). Mitigating eutrophication and toxic cyanobacterial blooms in large lakes: The evolution of a dual nutrient (N and P) reduction paradigm. *Hydrobiologia*, *847*(21), 4359–4375. https://doi.org/10.1007/s10750-019-04087-y

Paerl, H. W. (2009). Controlling eutrophication along the freshwater-marine continuum: dual nutrient (N and P) reductions are essential. *Estuaries and Coasts*, *32*(4), 593–601. https://doi.org/10.1007/s12237-009-9158-8

Paerl, H. W., Gardner, W. S., Havens, K. E., Joyner, A. R., Mccarthy, M. J., Newell, S. E., Qin, B. & Scott, J. T. (2016). Mitigating cyanobacterial harmful algal blooms in aquatic ecosystems impacted by climate change and anthropogenic nutrients. *Harmful Algae*, *54*, 213–222. https://doi.org/10.1016/j.hal.2015.09.009

Paerl, H. W., Hall, N. S. & Calandrino, E. S. (2011). Controlling harmful cyanobacterial blooms in a world experiencing anthropogenic and climatic-induced change. *Science of the Total Environment*, *409*(10), 1739–1745. https://doi.org/10.1016/j.scitotenv.2011.02.001

Pakhomova, S. V., Hall, P. O., Kononets, M. Y., Rozanov, A. G., Tengberg, A. & Vershinin, A. V. (2007). Fluxes of iron and manganese across the sediment-water interface under various redox conditions. *Marine Chemistry*, *107*(3), 319–331. https://doi.org/10.1016/j.marchem.2007.06.001

Palomares, M. L. D. & Pauly, D. (1998). Predicting food consumption of fish populations as functions of mortality, food type, morphometrics, temperature and salinity. *Marine and Freshwater Research*, *49*(5), 447–453. https://doi.org/10.1071/MF98015

Patten, B. C., Bosserman, R. W., Finn, J. T. & Cale, W. G. (1976). Systems analysis and simulations in ecology. Vol IV. Academis Press.

Pauly, D. (1989). A multiple regression model for predicting the food consumption of marine fish populations. *Marine and Freshwater Research*, *40*(3), 259–273. https://doi.org/10.1071/MF9890259

Pelegri, S. P. & Blackburn, T. H. (1995a). Effect of bioturbation by *Nereis* sp., *Mya Arenaria* and *Cerastoderma* sp. on nitrification and denitrification in estuarine sediments. *Ophelia*, *42*, 289–299.

Pelegri, S. P. & Blackburn, T. H. (1995b). Effects of Tubifex tubifex (oligochaeta: tubificidae) on N-mineralization in freshwater sediments, measured with 15N isotopes. *Aquatic Microbial Ecology*, *9*(3), 289–294. https://doi.org/10.3354/ame009289

Pelegrì, S. P. & Blackburn, T. H. (1994). Bioturbation effects of the amphipod Corophium volutator on microbial nitrogen transformations in marine sediments. *Marine Biology*, *121*, 253–258.

Pérez-Ruzafa, A., Fernández, A. I., Marcos, C., Gilabert, J., Quispe, J. I. & García-Charton, J. A. (2005). Spatial and temporal variations of hydrological conditions, nutrients and Chl-*a* in a Mediterranean coastal lagoon (Mar Menor, Spain). *Hydrobiologia*, *550*(1), 11–27. https://doi.org/10.1007/s10750-005-4356-2

Petkuviene, J., Vaiciute, D., Katarzyte, M., Gecaite, I., Rossato, G., Vybernaite-Lubiene, I. & Bartoli, M. (2019). Feces from piscivorous and herbivorous birds stimulate differentially phytoplankton growth. *Water*, *11*(12), 1–17. https://doi.org/10.3390/w11122567

Petkuviene, J., Zilius, M., Lubiene, I., Ruginis, T., Giordani, G., Razinkovas-Baziukas, A. & Bartoli, M. (2016). Phosphorus cycling in a freshwater estuary impacted by cyanobacterial blooms. *Estuaries and Coasts*, *39*(5), 1386–1402. https://doi.org/10.1007/s12237-016-0078-0

Phlips, E. J., Badylak, S., Nelson, N. G. & Havens, K. E. (2020). Hurricanes, El Niño and harmful algal blooms in two sub-tropical Florida estuaries: direct and indirect impacts. *Scientific Reports*, *10*(1), 1–12. https://doi.org/10.1038/s41598-020-58771-4

Pilati, A. & Vanni, M. J. (2007). Ontogeny, diet shifts, and nutrient stoichiometry in fish. *Oikos*, *116*(10), 1663–1674. https://doi.org/10.1111/j.2007.0030-1299.15970.x

Pilkaityte, R. (2007a). Seasonal changes in phytoplankton composition and nutrient limitation in a shallow Baltic lagoon. *Boreal Environment Research*, *12*, 551–559.

Pilkaityte, R. (2007b). Spring-summer transition in the curonian lagoon (SE Baltic Sea) phytoplankton community. *Transitional Waters Bulletin*, *1*(1), 39–47. https://doi.org/10.1285/i1825229Xv1n1p39

Pimenov, N. V., Ul'yanova, M. O., Kanapatskii, T. A., Mitskevich, I. N., Rusanov, I. I., Sigalevich, P. A., Nemirovskaya, I. A. & Sivkov, V. V. (2013). Sulfate reduction, methanogenesis, and methane oxidation in the upper sediments of the Vistula and Curonian Lagoons, Baltic Sea. *Microbiology*, *82*(2), 224–233.

Pina-Ochoa, E. & M., A. C. (2006). Denitrification in aquatic environments: a cross-system analysis. *Biogeochemistry*, *81*, 111–130. https://doi.org/10.1007/s10533-006-9033-7

Pitacco, V., Mistri, M. & Munari, C. (2018). Long-term variability of macrobenthic community in a shallow coastal lagoon (Valli di Comacchio, northern Adriatic): is community resistant to climate change? *Marine Environmental Research*, *137*, 73–87. https://doi.org/10.1016/j.marenvres.2018.02.026

Politi, T., Zilius, M., Bartoli, M. & Bučas, M. (2021). Amphipods' grazing and excretion loop facilitates *Chara contraria* persistence in a eutrophic lagoon. *Aquatic Botany*, *171*, 103378. https://doi.org/10.1016/j.aquabot.2021.103378

Politi, T., Zilius, M., Castaldelli, G., Bartoli, M. & Daunys, D. (2019). Estuarine macrofauna affects benthic biogeochemistry in a hypertrophic lagoon. *Water*, *11*(6), 1186. https://doi.org/10.3390/w11061186

Postgate, J. R. (1987). *Nitrogen fixation studies in biology*. Edward Arnold, London.

Pratt, D. R., Pilditch, C. A., Lohrer, A. M. & Thrush, S. F. (2014). The effects of short-term increases in turbidity on sandflat microphytobenthic productivity and nutrient fluxes. *Journal of Sea Research*, *92*, 170–177. https://doi.org/10.1016/j.seares.2013.07.009

Pusceddu, A., Anno, A. D., Fabiano, M. & Danovaro, R. (2009). Quantity and bioavailability of sediment organic matter as signatures of benthic trophic status. *Marine Ecology Progress Series*, *375*, 41–52. https://doi.org/10.3354/meps07735

Putys, Ž. & Zarankaite, J. (2010). Diet of the great cormorant (*Phalacrocorax carbo sinensis*) at the Juodkrantė colony, Lithuania. *Acta Zoologica Lituanica*, *20*(3), 179–189. https://doi.org/10.2478/v10043-010-0031-6

Pyrzanowski, K., Zięba, G., Dukowska, M., Smith, C. & Przybylski, M. (2019). The role of detritivory as a feeding tactic in a harsh environment – a case study of weatherfish (*Misgurnus fossilis*). *Scientific Reports*, *9*(1), 1–9. https://doi.org/10.1038/s41598-019-44911-y

R Core Team. (2018). R: A Language and Environment for Statistical Computing. http://www.r-project.org/

Rabalais, N. N., Turner, R. E., Gupta, B. S. & Boesch, D. F. (2007). Characterization and longterm trends of hypoxia in the northern Gulf of Mexico: does the science support the Action Plan? *Estuaries and Coasts*, *30*(5), 753–772.

Rabalais, N. N., Turner, R. E., Díaz, R. J. & Justić, D. (2009). Global change and eutrophication of coastal waters. *ICES Journal of Marine Science*, *66*(7), 1528–1537. https://doi.org/10.1093/icesjms/fsp047

Radach, G., Berg, J. & Hagmeier, E. (1990). Long-term changes of the annual cycles of meteorological, hydrographic, nutrient and phytoplankton time series at Helgoland and at LV ELBE 1 in the German Bight. *Continental Shelf Research*, *10*(4), 305–328. https://doi.org/10.1016/0278-4343(90)90054-P

Rakauskas, V. (2020). Invasive Neogobius melanostomus in the Lithuanian Baltic Sea coast: trophic role and impact on the diet of piscivorous fish. *Journal of Great Lakes Research*, *46*, 597–608. https://doi.org/10.1016/j.jglr.2020.03.005

Rakauskas, V., Putys, Ž., Dainys, J., Lesutiene, J., Ložys, L. & Arbačiauskas, K. (2013). Increasing population of the invader round goby, *Neogobius melanostomus* (Actinopterygii: Perciformes: Gobiidae), and its trophic role in the Curonian Lagoon, SE Baltic Sea. *Acta Ichthyologica et Piscatoria*, *43*(2), 95–108. https://doi.org/10.3750/AIP2013.43.2.02

Randall, M. C., Carling, G. T., Dastrup, D. B., Miller, T., Nelson, S. T., Rey, K. A., Hansen, N. C., Bickmore, B. R. & Aanderud, Z. T. (2019). Sediment potentially controls in-lake phosphorus cycling and harmful cyanobacteria in shallow, eutrophic Utah Lake. *PLoS ONE*, *14*(2), 1–17. https://doi.org/10.1371/journal.pone.0212238

Reddy, K. R., Wetzel, R. G. & Kadlec, R. H. (2005). Biogeochemistry of phosphorus in wetlands. *Agronomy*, *46*, 263–316.

Redfield, A. C. (1958). The biological control of chemical factors in the environment. *American Scientist*, *46*(3), 230–221.

Relexans, J. C., Etcheber, H., Castel, J., Escaravage, V. & Auby, I. (1992). Benthic respiratory potential with relation to sedimentary carbon quality in seagrass beds and oyster parks in the tidal flats of Arcachon Bay, France. *Estuarine, Coastal and Shelf Science*, *34*(2), 157–170. https://doi.org/10.1016/S0272-7714(05)80102-7

Remeikaitė-Nikienė, N., Lujanienė, G., Malejevas, V., Barisevičiūtė, R., Zilius, M., Vybernaitė-Lubienė, I., Garnaga-Budrė, G. & Stankevičius, A. (2017). Assessing nature and dynamics of POM in transitional environment (the Curonian Lagoon, SE Baltic Sea) using a stable isotope approach. *Ecological Indicators*, *82*, 217–226. https://doi.org/10.1016/j.ecolind.2017.06.035

Repečka, R. (2003). The species composition of the ichthyofauna in the Lithuanian Economic Zone of the Baltic Sea and the Curonian Lagoon and its changes in recent years. *Acta Zoologica Lituanica*, *13*(2), 149–157. https://doi.org/10.1080/13921657.2003.10512558

Repečka, R. (2008). Kuršių Marių žuvų išteklių racionalaus naudojimo tyrimai.

Repečka, R. (2009). Ichtiofaunos tyrimai bei ekologinös būklöspagal žuvų rodiklius įvertinimas Kuršių Mariose ir Baltijos Jūroje.

Revsbech, N. P., Jacobsen, J. P. & Nielsen, L. P. (2005). Nitrogen transformations in microenvironments of river beds and riparian zones. *Ecological Engineering*, *24*, 447–455. https://doi.org/https://doi.org/10.1016/j.ecoleng.2005.02.002

Ricciardi, A. & Bourget, E. (1998). Weight-to-weight conversion factors for marine benthic macroinvertebrates. *Marine Ecology Progress Series*, *163*, 245–251.

Risgaard-Petersen, N. (2003). Coupled nitrification–denitrification in autotrophic and heterotrophic estuarine sediments: on the influence of benthic microalgae. *Limnology and Oceanography*, *48*(1), 93–105. https://doi.org/10.4319/lo.2003.48.1.0093

Risgaard-Petersen, N. & Rysgaard, S. (1995). Nitrate reduction in sediments and waterlogged soil measured by ^{15}N techniques. *Anaerobic Microbial Activity in Soil*, 287–295.

Risgaard-Petersen, N., Rysgaard, S., Nielsen, L. P. & Revsbech, N. P. (1994). Diurnal variation of denitrification and nitrification in sediments colonized by benthic microphytes. *Limnology and Oceanography*, *39*(3), 573–579. https://doi.org/10.4319/lo.1994.39.3.0573

Roberts, K. L., Eate, V. M., Eyre, B. D., Holland, D. P. & Cook, P. L. (2012). Hypoxic events stimulate nitrogen recycling in a shallow salt-wedge estuary: the Yarra River estuary, Australia. *Limnology and Oceanography*, *57*(5), 1427–1442. https://doi.org/10.4319/lo.2012.57.5.1427

Roberts, K. L., Kessler, A. J., Grace, M. R. & Cook, P. L. M. (2014). Increased rates of dissimilatory nitrate reduction to ammonium (DNRA) under oxic conditions in a periodically hypoxic estuary. *Geochimica et Cosmochimica Acta*, *133*, 313–324. https://doi.org/10.1016/j.gca.2014.02.042

Robertson, E. K., Bartoli, M., Brüchert, V., Dalsgaard, T., Hall, P. O. J., Hellemann, D., Hietanen, S., Zilius, M. & Conley, D. J. (2019). Application of the isotope pairing technique in sediments: use, challenges, and new directions. *Limnology and Oceanography*, *17*, 112–136. https://doi.org/10.1002/lom3.10303

Robertson, E. K., Roberts, K. L., Burdorf, L. D., Cook, P. & Thamdrup, B. (2016). Dissimilatory nitrate reduction to ammonium coupled to Fe(II) oxidation in sediments of a periodically hypoxic estuary. *Limnology and Oceanography*, *61*(1), 365–381. https://doi.org/10.1002/lno.10220

Roden, E. E. & Edmonds, J. W. (1997). Phosphate mobilization in iron-rich anaerobic sediments: microbial Fe(III) oxide reduction versus iron-sulfide formation. *Archiv für Hydrobiologie*, *139*(3), 347–378.

Rojo, C., Sánchez-carrillo, S., Rodrigo, M. A., Puche, E., Cirujano, S. & Álvarez-cobelas, M. (2020). Charophyte stoichiometry in temperate waters. *Aquatic Botany*, *161*, 103182. https://doi.org/10.1016/j.aquabot.2019.103182

Romero, E., Garnier, J., Lassaletta, L., Billen, G., Le, R., Philippe, G. & Cugier, P. (2013). Large-scale patterns of river inputs in southwestern Europe: seasonal and interannual variations and potential eutrophication effects at the coastal zone. *Biogeochemistry*, *113*, 481–505. https://doi.org/10.1007/s10533-012-9778-0

Roselli, L., Cañedo-Argüelles, M., Costa Goela, P., Cristina, S., Rieradevall, M., D'Adamo, R. & Newton, A. (2013). Do physiography and hydrology determine the physico-chemical properties and trophic status of coastal lagoons? A comparative approach. *Estuarine, Coastal and Shelf Science*, *117*, 29–36. https://doi.org/10.1016/j.ecss.2012.09.014

Rossetti, G., Viaroli, P. & Ferrari, I. (2009). Role of abiotic and biotic factors in structuring the metazoan plankton community in a lowland river. *River Research and Applications*, *25*, 814–835. https://doi.org/10.1002/rra.1170

Ruttenberg, K. C. (2004). *The Global Phosphorus Cycle. Tratise on Geochemistry*. HD Holland, KK Turekian; WH. Schlesinger.

Ruttenberg, K. C. (1992). Development of a sequential extraction method for different forms of phosphorus in marine sediments. *Limnology and Oceanography*, *37*(7), 1460–1482. https://doi.org/10.4319/lo.1992.37.7.1460

Rysgaard, S., Christensen, P. B. & Nielsen, L. P. (1995). Seasonal variation in nitrification and denitrification in estuarine sediment colonized by benthic microalgae and bioturbating infauna. *Marine Ecology Progress Series*, *126*(1-3), 111–121. https://doi.org/10.3354/meps126111

Rysgaard, S., Thastum, P., Dalsgaard, T., Christensen, P. B. & Sloth, N. P. (1999). Effects of salinity on NH_4^+ adsorption capacity, nitrification, and denitrification in Danish estuarine sediments. *Estuaries*, *22*(1), 21–30.

Ryther, J. H. & Dunstan, W. M. (1971). Nitrogen, phosphorus and eutrophication in the coastal marine environment. *Science*, *171*, 1008–1013.

Sathyendranath, S., Stuart, V., Nair, A., Oka, K., Nakane, T., Bouman, H., Forget, M. H., Maass, H. & Platt, T. (2009). Carbon-to-chlorophyll ratio and growth rate of phytoplankton in the sea. *Marine Ecology Progress Series*, *383*, 73–84. https://doi.org/10.3354/meps07998

Scavia, D., Field, J. C., Boesch, D. F., Buddemeier, R. W., Burkett, V., Cayan, D. R., Fogarty, M., Harwell, M. A., Howarth, R. W., Mason, C., Reed, D. J., Royer, T. C., Sallenger, A. H. & Titus, J. G. (2002). Climate change impacts on U.S. coastal and marine ecosystems. *Estuaries*, *25*(2), 149–164.

Scharler, U. M. & Borrett, S. R. (2021). Network construction, evaluation and documentation: a guideline. *Environmental Modelling and Software*, *140*. https://doi.org/10.1016/j.envsoft.2021.105020

Scharler, U. M., Ulanowicz, R. E., Fogel, M. L., Wooller, M. J., Jacobson-Meyers, M. E., Lovelock, C. E., Feller, I., Frischer, M., Lee, R., McKee, K., Romero, I. C., Schmit, J. P. & Shearer, C. (2015). Variable nutrient stoichiometry (carbon:nitrogen:phosphorus) across trophic levels determines community and ecosystem properties in an oligotrophic mangrove system. *Oecologia*, *179*, 863–876. https://doi.org/10.1007/s00442-015-3379-2

Scharler, U. M. & Ayers, M. J. (2019). Stoichiometric multitrophic networks reveal significance of land-sea interaction to ecosystem function in a subtropical nutrient-poor bight, South Africa. *PLoS ONE*, 1–20. https://doi.org/10.1371/journal.pone.0210295

Schindler, D. E. & Eby, L. A. (1997). Stoichiometry of fishes and their prey: implications for nutrient recycling. *Ecology*, *78*(6), 1816–1831.

Schramski, J. R., Gattie, D. K., Patten, B. C., Borrett, S. R., Fath, B. D., Thomas, C. R. & Whipple, S. J. (2006). Indirect effects and distributed control in ecosystems: Distributed control in the environ networks of a seven-compartment model of nitrogen flow in the Neuse River Estuary, USA - Steady-state analysis. *Ecological Modelling*, *194*, 189–201. https://doi.org/10.1016/j.ecolmodel.2005.10.012

Schratzberger, M. & Ingels, J. (2018). Meiofauna matters: the roles of meiofauna in benthic ecosystems. *Journal of Experimental Marine Biology and Ecology*, *502*, 12–25. https://doi.org/10.1016/j.jembe.2017.01.007

Seitzinger, S. P. (1988). Denitrification in freshwater and coastal marine ecosystems: ecological and geochemical significance. *Limnology and Oceanography*, *33*(4), 702–724. https://doi.org/10.4319/lo.1988.33.4part2.0702

Seitzinger, S. P. (1990). Denitrification in aquatic sediments. In N. P. Revsbech & J. Sørensen (Eds.), *Denitrification in soil and sediment* (pp. 301–322). MA:Springer.

Seitzinger, S. P., Harrison, J. A., Böhlke, J. K., Bouwman, A. F., Lowrance, R., Peterson, B., Tobias, C. & Van Drecht, G. (2006). Denitrification across landscapes and waterscapes: a synthesis. *Ecological Applications*, *16*(6), 2064–2090.

Seitzinger, S. P., Harrison, J. A. & Dumont, E. (2005). Sources and delivery of carbon, nitrogen, and phosphorus to the coastal zone: an overview of global nutrient export from Watersheds (NEWS) models and their application. *Global Biogeochemical Cycles*, *19*, 1–11. https://doi.org/10.1029/2005GB002606

Semenova, A. S. (2011). Quantitative characteristics of zooplankton of the Curonian Lagoon taken by different sampling methods. *Hydrobiological Journal*, *47*(3), 112–120.

Semenova, A. S. & Aleksandrov, S. V. (2009). The zooplankton consumption of primary production and an assessment of the waterbody trophic state on the basis of its structural and functional characteristics. *Inland Water Biology*, *2*(4), 348–354. https://doi.org/10.1134/S1995082909040099

Sharples, J., Middelburg, J. J., Fennel, K. & Jickells, T. D. (2017). What proportion of riverine nutrients reaches the open ocean? *Global Biogeochemical Cycles*, *31*, 39–58. https://doi.org/10.1002/2016GB005483

Siipola, V., Lehtimäki, M. & Tallberg, P. (2016). The effects of anoxia on Si dynamics in sediments. *Journal of Soils and Sediments*, *16*(1), 266–279. https://doi.org/10.1007/s11368-015-1220-5

Silvennoinen, H., Liikanen, A., Torssonen, J., Florian Stange, C. & Martikainen, P. J. (2008). Denitrification and nitrous oxide effluxes in boreal, eutrophic river sediments under increasing nitrate load: a laboratory microcosm study. *Biogeochemistry*, *91*(2-3), 105–116. https://doi.org/10.1007/s10533-008-9262-z

Skóra, M. E., Bogacka-Kapusta, E., Morzuch, J., Kulikowski, M., Rolbiecki, L., Kozłowski, K. & Kapusta, A. (2018). Exotic sturgeons in the Vistula Lagoon in 2011, their occurrence, diet and parasites, with notes on the fishery background. *Journal of Applied Ichthyology*, *34*(1), 33–38. https://doi.org/10.1111/jai.13577

Slomp, C. P., Malschaert, J. F. P. & Raaphorst, W. V. (1997). The role of adsorption in sediment-water exchange of phosphate in North Sea continental margin sediments. *Limnology and Oceanography*, *43*(5), 832–846.

Slomp, C. (2012). Phosphorus cycling in the estuarine and coastal zones. *Treatise on estuarine and coastal science* (pp. 201–229). Elsevier Inc. https://doi.org/10.1016/b978-0-12-374711-2.00506-4

Small, G. E., Sterner, R. W. & Finlay, J. C. (2014). An Ecological Network Analysis of nitrogen cycling in the Laurentian Great Lakes. *Ecological Modelling*, *293*(3), 150–160. https://doi.org/10.1016/j.ecolmodel.2014.02.001

Somura, H., Masunaga, T., Mori, Y., Takeda, I., Ide, J. & Sato, H. (2015). Estimation of nutrient input by a migratory bird, the Tundra Swan (*Cygnus columbianus*), to winter-flooded paddy fields. *Agriculture, Ecosystems and Environment*, *199*, 1–9. https://doi.org/10.1016/j.agee.2014.07.018

Sondergaard, M., Kristensen, P. & Jeppesen, E. (1992). Phosphorus release from resuspended sediment in the shallow and wind- exposed Lake Arreso, Denmark. *Hydrobiologia*, *228*, 91–99.

Stal, L. J., Albertano, P., Bergman, B., Von Bröckel, K., Gallon, J. R., Hayes, P. K., Sivonen, K. & Walsby, A. E. (2003). BASIC: Baltic Sea cyanobacteria. An investigation of the structure and dynamics of water blooms of cyanobacteria in the Baltic Sea - Responses to a changing environment. *Continental Shelf Research*, *23*(17-19), 1695–1714. https://doi.org/10.1016/j.csr.2003.06.001

Statham, P. J. (2012). Nutrients in estuaries - an overview and the potential impacts of climate change. *Science of the Total Environment*, *434*, 213–227. https://doi.org/10.1016/j.scitotenv.2011.09.088

Stempniewicz, L., Meissner & W. (2012). Assessment of the zoobenthos biomass consumed yearly by diving ducks wintering in the Gulf of Gdansk (southern Baltic Sea). *Ornis Svecica*, *9*, 143–154.

Stief, P. (2013). Stimulation of microbial nitrogen cycling in aquatic ecosystems by benthic macrofauna: mechanisms and environmental implications. *Biogeosciences*, *10*(12), 7829–7846. https://doi.org/10.5194/bg-10-7829-2013

Stocum, E. T. & Plante, C. J. (2006). The effect of artificial defaunation on bacterial assemblages of intertidal sediments. *Journal of Experimental Marine Biology and Ecology*, *337*, 147–158. https://doi.org/10.1016/j.jembe.2006.06.012

Stookey, L. L. (1970). Ferrozine: a new spectrophotometric reagent for iron. *Analytical Chemistry*, *42*(7), 779–781.

Störmer, O. (2011). Climate change impacts on coastal waters of the Baltic Sea. *Global change and baltic coastal zones* (pp. 51–69). Springer. https://doi.org/10.1007/978-94-007-0400-8_4

Stott, P. (2016). How climate change affects extreme weather events. *Science*, *352*(6293), 1517–1518. https://doi.org/10.1126/science.aaf7271

Sundbäck, K., Miles, A. & Göransson, E. (2000). Nitrogen fluxes, denitrification and the role of microphytobenthos in microtidal shallow-water sediments: an annual study. *Marine Ecology Progress Series*, *200*, 59–76. https://doi.org/10.3354/meps200059

Sundby, B., Gobeil, C., Silverberg, N. & Mucci, A. (1992). The phosphorus cycle in coastal marine sediments. *Limnology and Oceanography*, *37*(6), 1129–1145. http://www.jstor.org/stable/30001658

Švažas, S., Chukalova, N., Grishanov, G., Žilvinas, P., Sruoga, A. & Regione, K. Ų. M. Ų. (2011). The role of great cormorant (*Phalacrocorax carbo sinensis*) for fish stock and dispersal of helmintes parasites in the Curonian Lagoon area. *Veterinarija Ir Zootechnika*, *55*(77), 79–85.

Švažas, S., Meissner, W. & Nehls, H. (1994). Wintering Populations of Goosander (*Mergus merganser*) And Smew (*Mergellus albellus*) At the South Eastern Baltic Coast. *Acta Ornithologica Lituanica*, *9*, 56–69.

Svenja Oncken, N., Lange, T., Kristensen, E., Quintana, C. O., Steinfurth, R. C. & Flindt, M. R. (2022). Sand-capping – A large-scale approach to restore organic-enriched estuarine sediments. *Marine Environmental Research*, *173*, 105534. https://doi.org/10.1016/j.marenvres.2021.105534

Svensson, J., Enrich-Prast, A. & Leonardson, L. (2001). Nitrification and dentrification in a eutrophic lake sediment bioturbated by oligochaetes. *Aquatic Microbial Ecology*, *23*, 177–186. https://doi.org/10.3354/ame023177

Swanberg, I. L. (1991). The influence of the filter-feeding bivalve Cerastoderma edule L. on microphytobenthos: a laboratory study. *Journal of Experimental Marine Biology and Ecology*, *151*, 93–111.

Syväranta, J., Cucherousset, J., Kopp, D., Crivelli, A., Céréghino, R. & Santoul, F. (2009). Dietary breadth and trophic position of introduced European catfish *Silurus glanis* in the River Tarn (Garonne River basin), Southwest France. *Aquatic Biology*, *8*(2), 137–144. https://doi.org/10.3354/ab00220

Szydłowski, M., Kolerski, T. & Zima, P. (2019). Impact of the artificial strait in the Vistula Spit on the hydrodynamics of the Vistula Lagoon (Baltic Sea). *Water*, *11*, 990.

Szyrmer, J. & Ulanowicz, R. E. (1987). Total flows in ecosystems. *Ecological Modelling*, *35*(1-2), 123–136. https://doi.org/10.1016/0304-3800(87)90094-9

Tanner, D. K., Brazner, J. C. & Brady, V. J. (2000). Factors influencing carbon, nitrogen, and phosphorus content of fish from a Lake Superior coastal wetland. *Canadian Journal of Fisheries and Aquatic Sciences*, *57*(6), 1243–1251. https://doi.org/10.1139/f00-062

Tarvainen, M., Ventelä, A. M., Helminen, H. & Sarvala, J. (2005). Nutrient release and resuspension generated by ruffe (*Gymnocephalus cernuus*) and chironomids. *Freshwater Biology*, *50*(3), 447–458. https://doi.org/10.1111/j.1365-2427.2005.01331.x

Tennenbaum, S. & Ulanowicz, R. E. (2006). Growth and Development: Ecosystems Phenomenology. https://doi.org/10.2307/1351721

Thamdrup, B., Fossing, H. & Jorgensen, B. B. (1994). Manganese, iron, and sulfur cycling in a coastal marine sediment, Aarhus Bay, Denmark. *Geochimica et Cosmochimica Acta*, *58*(23), 5115–5129. https://doi.org/https://doi.org/10.1016/0016-7037(94)90298-4

Thamdrup, B. (2000). Bacterial manganese and iron reduction in aquatic sediments. *Advances in Microbial Ecology*, 41–84.

Thomas, C. R. & Christian, R. R. (2001). Comparison of nitrogen cycling in salt marsh zones related to sea-level rise. *Marine Ecology Progress Series*, *221*, 1–16. https://doi.org/10.3354/meps221001

Tiedje, J. M. (1988). Ecology of denitrification and dissimilatory nitrate reduction to ammonium. In A. J. B. Zehnder (Ed.), *Environmental microbiology of anaerobes* (pp. 179–244). John Wiley & Sons, N.Y.

Tilly, L. J. (1968). The structure and dynamics of Cone Spring. *Ecological Monographs*, *38*(2), 169–197.

Tobias, C., Giblin, A., Mcclelland, J., Tucker, J. & Peterson, B. (2003). Sediment DIN fluxes and preferential recycling of benthic microalgal nitrogen in a shallow macrotidal estuary. *Marine Ecology Progress Series*, *257*, 25–36.

Tomczak, M. T., Müller-Karulis, B., Järv, L., Kotta, J., Martin, G., Minde, A., Põllumäe, A., Razinkovas, A., Strake, S., Bucas, M. & Blenckner, T. (2009). Analysis of trophic networks and carbon flows in south-eastern Baltic coastal ecosystems. *Progress in Oceanography*, *81*(1-4), 111–131. https://doi.org/10.1016/j.pocean.2009.04.017

Torn, K., Martin, G. & Paalme, T. (2006). Seasonal changes in biomass, elongation growth and primary production rate of *Chara tomentosa* in the NE Baltic Sea. *Annales Botanici Fennici*, *43*(4), 276–283.

Trenberth, K. E. (2005). The impact of climate change and variability on heavy precipitation, floods, and droughts. *Encyclopedia of Hydrological Sciences*, 1–11. https://doi.org/10.1002/0470848944.hsa211

Trimmer, M., Nedwell, D. B., Sivyer, D. B. & Malcolm, S. J. (1998). Nitrogen fluxes through the lower estuary of the river Great Ouse, England: the role of the bottom sediments. *Marine Ecology Progress Series*, *163*, 109–124. https://doi.org/10.3354/meps163109

Ulanowicz, R. E. (2012). *Quantitative methods for Ecological Network Analysis and its application to coastal ecosystems* (Vol. 9). Elsevier Inc. https://doi.org/10.1016/B978-0-12-374711-2.00904-9

Ulanowicz, R. E. (1983). Identifying the structure of cycling in ecosystems. *Mathematical Biosciences*, *65*(2), 219–237. https://doi.org/10.1016/0025-5564(83)90063-9

Ulanowicz, R. E. (2004). Quantitative methods for ecological network analysis. *Computational Biology and Chemistry*, *28*, 321–339. https://doi.org/10.1016/j.compbiolchem.2004.09.001

Ulanowicz, R. E. & Baird, D. (1999). Nutrient controls on ecosystem dynamics: the Chesapeake mesohaline community. *Journal of Marine Systems*, *19*, 159–172.

Ulanowicz, R. E. & Kemp, W. M. (1979). Toward canonical trophic aggregations. https://doi.org/10.1086/283534

Ulyanova, M., Sivkov, V., Kanapatskij, T. & Pimenov, N. (2014). Seasonal variations in methane concentrations and diffusive fluxes in the Curonian and Vistula lagoons, Baltic Sea. *Geo-Marine Letters*, *34*(2-3), 231–240. https://doi.org/10.1007/s00367-013-0352-0

Umgiesser, G., Zemlys, P., Erturk, A., Razinkova-Baziukas, A., Mezine, J. & Ferrarin, C. (2016). Seasonal renewal time variability in the Curonian Lagoon caused by atmospheric and hydrographical forcing. *Ocean Science*, *12*(2), 391–402. https://doi.org/10.5194/os-12-391-2016

Vahtera, E., Conley, D. J., Gustafsson, B. G., Kuosa, H., Pitkänen, H., Oleg, P., Tamminen, T., Viitasalo, M., Voss, M., Wasmund, N. & Wulff, F. (2007). Internal ecosystem feedbacks enhance Nitrogen-fixing cyanobacteria blooms and complicate management in the Baltic Sea. *Ambio*, *36*(2), 186–194.

Vaičiūtė, D., Bresciani, M., Bartoli, M., Giardino, C. & Bučas, M. (2015). Spatial and temporal distribution of coloured dissolved organic matter in a hypertrophic freshwater lagoon. *Journal of Limnology*, *74*(3), 572–583. https://doi.org/10.4081/jlimnol.2015.1176

Vaičiūtė, D., Bucas, M., Bresciani, M., Dabulevicienė, T., Gintauskas, J., Mezine, J., Tiskus, E., Umgiesser, G., Morkunas, J., De Santi, F. & Bartoli, M. (2021). Hot moments and hotspots of cyanobacteria hyperblooms in the Curonian Lagoon (SE Baltic Sea) revealed via remote sensing-based retrospective analysis. *Science of the Total Environment*, *769*. https://doi.org/10.1016/j.scitotenv.2021.145053

Van Der Zee, C., Slomp, C. P. & Raaphorst, W. V. (2002). Authigenic P formation and reactive P burial in sediments of canyon on the Iberian margin (NE Atlantic) the Nazare. *Marine Geology*, *185*, 379–392.

van der Winden, J. & Nesterenko, M. (2003). A postnuptial staging site for the Black Tern (*Chlidonias niger*) and White-winged Tern (*C. leucopterus*) in the Sivash, Ukraine. *Journal fur Ornithologie*, *144*(3), 330–344. https://doi.org/10.1046/j.1439-0361.2003.03010.x

Van Meter, K. J., Basu, N. B., Veenstra, J. J. & Burras, C. L. (2016). The nitrogen legacy: emerging evidence of nitrogen accumulation in anthropogenic landscapes. *Environmental Research Letters*, *11*(3), 035014.

Vanni, M. J., Boros, G. & McIntyre, P. B. (2013). When are fish sources vs. sinks of nutrients in lake ecosystems? *Ecology*, *94*(10), 2195–2206.

Vanni, M. J. (2002). Nutrient cycling by animals in freshwater ecosystems. *Annual Review of Ecology and Systematics*, *33*(1), 341–370. https://doi.org/10.1146/annurev.ecolsys.33.010802.150519

Vanni, M. J. & McIntyre, P. B. (2016). Predicting nutrient excretion of aquatic animals with metabolic ecology and ecological stoichiometry: a global synthesis. *Ecology*, *97*(12), 3460–3471.

Vaughn, C. C. & Hakenkamp, C. C. (2001). The functional role of burrowing bivalves in freshwater ecosystems. *Freshwater Biology*, 1431–1446.

Ventura, M. (2006). Linking biochemical and elemental composition in freshwater and marine crustacean zooplankton. *Marine Ecology Progress Series*, *327*, 233–246. https://doi.org/10.3354/meps327233

Vezzoli, R., Mercogliano, P., Pecora, S., Zollo, A. L. & Cacciamani, C. (2015). Hydrological simulation of Po river (North Italy) discharge under climate change scenarios using the RCM COSMO-CLM. *Science of the Total Environment*, *521-522*, 346–358. https://doi.org/10.1016/j.scitotenv.2015.03.096

Viaroli, P., Azzoni, R., Bartoli, M., Giordani, G. & Taje, L. (2001). Evolution of the trophic conditions and dystrophic outbreaks in the Sacca di Goro Lagoon (Northern Adriatic Sea). *Mediterranean ecosystems* (pp. 467–475). Springer.

Viaroli, P., Bartoli, M., Giordani, G., Azzoni, R. & Nizzoli, D. (2003). Short term changes of benthic fluxes during clam harvesting in a coastal lagoon (Sacca di Goro, Po River Delta). *Chemistry and Ecology*, *19*(2-3), 189–206. https://doi.org/10.1080/0275754031000119933

Viaroli, P., Giordani, G., Bartoli, M., Naldi, M., Azzoni, R., Nizzoli, D., Ferrari, I., Comenges, J. M. Z., Bencivelli, S., Castaldelli, G. & Fano, E. A. (2006). The Sacca di Goro lagoon and an arm of the Po River. *Estuaries* (pp. 197–232). Springer, Berlin, Heidelberg. https://doi.org/10.1007/698_5_030

Viaroli, P., Bartoli, M., Bondavalli, C. & Naldi, M. (1995). Oxygen fluxes and dystrophy in a coastal lagoon colonized by *Ulva rigida* (Sacca di Goro, Po River Delta, northern Italy). *Fresenius Environmental Bullettin*, *4*(6), 381–386.

Viaroli, P., Bartoli, M., Castaldelli, G., Naldi, M., Nizzoli, D. & Rossetti, G. (2013). Recent evolution and expected changes of nutrient loads in a heavily exploited watershed: the Po River, Italy. *Understanding Freshwater Quality Problems in a Changing World*, *4*, 175–182.

Viaroli, P., Bartoli, M., Giordani, G. & Naldi, M. (2008). Community shifts, alternative stable states, biogeochemical controls and feedbacks in eutrophic coastal lagoons: a brief overview. *Aquatic Conservation: Marine and Freshwater Ecosystems*, *18*, 105–117. https://doi.org/10.1002/aqc

Viaroli, P., Naldi, M., Bondavalli, C. & Bencivelli, S. (1996). Growth of the seaweed *Ulva rigida* C. Agardh in relation to biomass densities, internal nutrient pools and external nutrient supply in the Sacca di Goro lagoon (Northern Italy). *Hydrobiologia*, *329*(1-3), 93–103. https://doi.org/10.1007/BF00034550

Viaroli, P., Soana, E., Pecora, S., Laini, A., Naldi, M., Anna, E. & Nizzoli, D. (2018). Space and time variations of watershed N and P budgets and their relationships with reactive N and P loadings in a heavily impacted river basin (Po river , Northern Italy). *Science of the Total Environment*, *639*, 1574–1587. https://doi.org/10.1016/j.scitotenv.2018.05.233

Vidal, M., Morguì, J.-A., Latasa, M., Romero, J. & Camp, J. (1997). Factors controlling seasonal variability of benthic ammonium release and oxygen uptake in Alfacs Bay (Ebro Delta , NW Mediterranean). *Hydrobiologia*, *350*, 169–178.

Vidal-Durà, A., Burke, I. T., Stewart, D. I. & Mortimer, R. J. G. (2018). Reoxidation of estuarine sediments during simulated resuspension events: effects on nutrient and trace metal mobilisation. *Estuarine Coastal and Shelf Science*, *207*, 40–55. https://doi.org/10.1016/j.ecss.2018.03.024

Viktorsson, L., Ekeroth, N., Nilsson, M., Kononets, M. & Hall, P. O. (2013). Phosphorus recycling in sediments of the central Baltic Sea. *Biogeosciences*, *10*(6), 3901–3916. https://doi.org/10.5194/bg-10-3901-2013

Vitousek, P. M., Cassman, K., Cleveland, C., Crews, T., Field, C. B., Grimm, N. B., Howarth, R. W., Marino, R., Martinelli, L., Rastetter, E. B. & Sprent, J. I. (2002). Towards an ecological understanding of biological nitrogen fixation. *Biogeochemistry*, *57-58*, 1–45. https://doi.org/10.1023/A:1015798428743

Volkenborn, N., Woodin, S. A., Wethey, D. S. & Polerecky, L. (2016). Bioirrigation in Marine Sediments. In S. Elias (Ed.), *Reference module in earth systems and environmental sciences* (pp. 1–9). Elsevier Inc. https://doi.org/10.1016/B978-0-12-409548-9.09525-7

Voss, M., Wannicke, N., Deutsch, B., Bronk, D., Sipler, R., Purvaja, R., Ramesh, R. & Rixen, T. (2012). *Internal Cycling of Nitrogen and Nitrogen Transformations* (Vol. 5). Elsevier Inc. https://doi.org/10.1016/B978-0-12-374711-2.00508-8

Voss, M., Baker, A., Bange, H. W., Conley, D., Cornell, S., Deutsch, B., Engel, A., Ganeshram, R., Garnier, J., Heiskanen, A. S., Jickells, T., Lancelot, C., Mcquattersgollop, A., Middelburg, J., Schiedek, D., Slomp, C. P. & Conley, D. P. (2011). Nitrogen processes in coastal and marine ecosystems. Cambridge University Press.

Vybernaite-Lubiene, I., Zilius, M., Giordani, G., Petkuviene, J., Vaiciute, D., Bukaveckas, P. A. & Bartoli, M. (2017). Effect of algal blooms on retention of N, Si and P in Europe's largest coastal lagoon. *Estuarine, Coastal and Shelf Science*, *194*, 217–228. https://doi.org/10.1016/j.ecss.2017.06.020

Vybernaite-Lubiene, I., Zilius, M. & Bartoli, M. (2018). Recent trends (2012-2016) of N, Si and P export from the Nemunas River watershed: loads, unbalanced stoichiometry and threats for downstream acquatic ecosystems. *Water*, *10*, 1178. https://doi.org/10.3390/w10091178

Vybernaitė-Lubienė, I., Zilius, M., Bartoli, M., Petkuviene, J., Zemlys, P., Magri, M. & Giordani, G. (2022). Biogeochemical budgets of nutrients and metabolism in the Curonian Lagoon (South East Baltic Sea): spatial and temporal variations. *Water*, *14*, 144. https://doi.org/https://doi.org/10.3390/w14020164

Wagele, J. W. (1981). Study of the Anthuridae (Crustacea: Isopoda: Anthuridea) from the Mediterranean and the Red Sea. *Israel Journal of Zoology*, *30*, 113–159.

Wagena, M. B., Collick, A. S., Ross, A. C., Najjar, R. G., Rau, B., Sommerlot, A. R., Fuka, D. R., Kleinman, P. J. A. & Easton, Z. M. (2018). Impact of climate change and climate anomalies on hydrologic and biogeochemical processes in an agricultural catchment of the Chesapeake Bay watershed, USA. *Science of the Total Environment*, *637-638*, 1443–1454. https://doi.org/10.1016/j.scitotenv.2018.05.116

Ward, B. B. (2011). Nitrification: an introduction and overview of the state of the field. In B. B. Ward, D. J. Arp & K. M. G (Eds.), *Nitrification* (pp. 1–8). https://doi.org/https://doi.org/10.1128/9781555817145.ch1

Warembourg, F. R. (1993). *Nitrogen fixation in soil and plant systems*. Academis Press. https://doi.org/10.1016/b978-0-08-092407-6.50010-9

Warnken, K. W., Gill, G. A., Griffin, L. L. & Santschi, P. H. (2001). Sediment-water exchange of Mn, Fe, Ni and Zn in Galveston Bay, texas. *Marine Chemistry*, *73*(3-4), 215–231. https://doi.org/10.1016/S0304-4203(00)00108-0

Warwick, R. M., Joint, I. R. & Radford, P. J. (1979). *Secondary production of the benthos in an estuarine environment*. Blackwell Scientific.

Webb, A. P. & Eyre, B. D. (2004). Effect of natural populations of burrowing thalassinidean shrimp on sediment irrigation, benthic metabolism, nutrient fluxes and denitrification. *Marine Ecology Progress Series*, *268*, 205–220. https://doi.org/10.3354/meps268205

Welsh, D. T. (2003). It's a dirty job but someone has to do it: the role of marine benthic macrofauna in organic matter turnover and nutrient recycling to the water column. *Chemistry and Ecology*, *19*(5), 321–342. https://doi.org/10.1080/0275754031000155474

Welsh, D. T., Nizzoli, D., Fano, E. A. & Viaroli, P. (2015). Direct contribution of clams (Ruditapes philippinarum) to benthic fluxes, nitrification, denitrification and nitrous oxide emission in a farmed sediment. *Estuarine, Coastal and Shelf Science*, *154*, 84–93. https://doi.org/10.1016/j.ecss.2014.12.021

Whipple, S. J., Borrett, S. R., Patten, B. C., Gattie, D. K., Schramski, J. R. & Bata, S. A. (2007). Indirect effects and distributed control in ecosystems: comparative network environ analysis of a seven-compartment model of nitrogen flow in the Neuse River estuary, USA — Time series analysis. *Ecological Modelling*, *6*, 1–17. https://doi.org/10.1016/j.ecolmodel.2007.03.002

Whipple, S. J., Patten, B. C. & Borrett, S. R. (2014). Indirect effects and distributed control in ecosystems. *Ecological Modelling*, *293*, 161–186. https://doi.org/10.1016/j.ecolmodel.2014.08.025

Winkler, L. (1988). Die Bestimmung des in Wasser Gelösten Sauerstoffes. *Ber Dtsch Chem Ges*, *21*, 2843–2855.

Wulff, F., Field, J. G. & H, M. K. (2012). *Network analysis in marine ecology: methods and applications. Vol. 32*. Springer Science & Business Media.

Yamada, S. S. & D'Elia, C. F. (1984). Silicic acid regeneration from estuarine sediment cores. *Marine Ecology Progress Series*, *18*, 113–118.

Yamamuro, M. (2000). Chemical tracers of sediment organic matter origins in two coastal lagoons. *Journal of Marine Systems*, *26*, 127–134.

Zaiko, A., Păskauskas, R. & Krevš, A. (2010). Biogeochemical alteration of the benthic environment by the zebra mussel *Dreissena polymorpha* (Pallas). *Oceanologia*, *52*(4), 649–667. https://doi.org/10.5697/oc.52-4.649

Zaldivar, J. M., Cattaneo, E., Plus, M., Murray, C. N., Giordani, G. & Viaroli, P. (2003). Long-term simulation of main biogeochemical events in a coastal lagoon: Sacca Di Goro (Northern Adriatic Coast , Italy). *Continental Shelf Research*, *23*, 1847–1875. https://doi.org/10.1016/j.csr.2003.01.001

Zaromskis, R. (2002). Macrophytes of the Curonian Lagoon and lithodynamic conditions of their habitats (in Lithuanian). *Geografija*, *38*(2), 35–41.

Zemlys, P., Ferrarin, C., Umgiesser, G., Gulbinskas, S. & Bellafiore, D. (2013). Investigation of saline water intrusions into the Curonian Lagoon (Lithuania) and two-layer flow in the Klaipeda Strait using finite element hydrodynamic model. *Ocean Science*, *9*(3), 573–584. https://doi.org/10.5194/os-9-573-2013

Zettler, M. L. & Daunys, D. (2007). Long-term macrozoobenthos changes in a shallow boreal lagoon: comparison of a recent biodiversity inventory with historical data. *Limnologica*, *37*(2), 170–185. https://doi.org/10.1016/j.limno.2006.12.004

Zhang, Y., Wang, Y., Chen, Y., Liang, F. & Liu, H. (2019). Assessment of future flash flood inundations in coastal regions under climate change scenarios-a case study of Hadahe River basin in northeastern China. *Science of the Total Environment*, *693*, 133550. https://doi.org/10.1016/j.scitotenv.2019.07.356

Zheng, W., Wang, S., Tan, K. & Lei, Y. (2020). Nitrate accumulation and leaching potential is controlled by land-use and extreme precipitation in a headwater catchment in the North China Plain. *Science of the Total Environment*, *707*, 136168. https://doi.org/10.1016/j.scitotenv.2019.136168

Zilius, M., Bartoli, M., Daunys, D., Pilkaityte, R. & Razinkovas, A. (2012). Patterns of benthic oxygen uptake in a hypertrophic lagoon: spatial variability and controlling factors. *Hydrobiologia*, *699*(1), 85–98. https://doi.org/10.1007/s10750-012-1155-4

Zilius, M., Daunys, D., Petkuviene, J. & Bartoli, M. (2012). Sediment-water oxygen, ammonium and soluble reactive phosphorus fluxes in a turbid freshwater estuary (Curonian lagoon, Lithuania): evidences of benthic microalgal activity. *Journal of Limnology*, *71*(2), 309–319. https://doi.org/10.4081/jlimnol.2012.e33

Zilius, M., Giordani, G., Petkuviene, J., Lubiene, I., Ruginis, T. & Bartoli, M. (2015). Phosphorus mobility under short-term anoxic conditions in two shallow eutrophic coastal systems (Curonian and Sacca di Goro lagoons). *Estuarine, Coastal and Shelf Science*, *164*, 134–146. https://doi.org/10.1016/j.ecss.2015.07.004

Zilius, M., Vybernaite-Lubiene, I., Vaiciute, D., Petkuviene, J., Zemlys, P., Liskow, I., Voss, M., Bartoli, M. & Bukaveckas, P. A. (2018). The influence of cyanobacteria

blooms on the attenuation of nitrogen throughputs in a Baltic coastal lagoon. *Biogeochemistry*, *141*(2), 143–165. https://doi.org/10.1007/s10533-018-0508-0

Zilius, M. (2016). Response of sedimentary processes to cyanobacterial processes. *Journal of Limnology*, *75*(2), 236–247. https://doi.org/10.4081/jlimnol.2015.1296

Zilius, M., Bartoli, M., Bresciani, M., Katarzyte, M., Ruginis, T., Petkuviene, J., Lubiene, I., Giardino, C., Bukaveckas, P. A., de Wit, R. & Razinkovas-Baziukas, A. (2014). Feedback mechanisms between cyanobacterial blooms, transient hypoxia, and benthic phosphorus regeneration in shallow coastal environments. *Estuaries and Coasts*, *37*(3), 680–694. https://doi.org/10.1007/s12237-013-9717-x

Zilius, M., Daunys, D., Bartoli, M., Marzocchi, U., Bonaglia, S., Cardini, U. & Castaldelli, G. (2021). Partitioning benthic nitrogen cycle processes among three common macrofauna holobionts. *Biogeochemistry*, *8*, 1–21. https://doi.org/10.1007/s10533-021-00867-8

Žydelis, R. & Kontautas, A. (2008). Piscivorous birds as top predators and fishery competitors in the lagoon ecosystem. *Hydrobiologia*, *611*(1), 45–54. https://doi.org/10.1007/s10750-008-9460-7

Acknowledgements

This study would not be done without support of all my colleagues and family.
I would like to thank my supervisors for the time and knowledge they gave me. Prof. Marco Bartoli, since my bachelor degree, introduced me to the fascinating and diversified world of the biogeochemistry. I am grateful to him above all for the passion, enthusiasm, and curiosity, that he communicates every day. I thank Prof. Antonio Bodini for the chance he gave me and the trust he placed in me and Prof. Artūras Razinkovas-Baziukas for welcoming me at the Klaipeda University.
I deeply thank the Prof. Pierluigi Viaroli and the Dr. Jūrate Lesutiene for giving me the chance to attend the double degree.
Special thanks to Sara for the first scientific and experimental lessons and long scientific discussions, and to Cristina for the precious support in the networks construction. I would like to thank my sampling colleagues during all the experimental activities that I carried out in these 3 years: Samuele, Claudio, Tobia, Mindaugas, Ugo, Stefano, Ulisse, Marta, Maria Pia, Valeria, Alessandra, Floriana.
I would like to thank my colleagues in Parma, Beatrice, Alice, Gemma, Rossano, Monica, Erica, Edoardo, Alex for the time spent together and their continuous support.
Thanks go also to Lithuanian colleagues, that besides share with me data and precious explanations, they welcomed me during my stay in Klaipeda. I thank Irma, Jolita, Evelina, Rasa, Diana, Martynas, Paola, Rudy, Greta, and again Mindaugas and Tobia.
My deepest thanks go to my dear family and my boyfriend for their continuous and tireless support.